Fluorous Mixture Synthesis (FMS) of Four Isomers of 4,8,12,-Trimethylnonadecanol and the Development of an NMR-based Method for Determining the Configurations of Polyisoprenoid Structures

by

An-Hung Edmund Yeh

Bsc, Queen's University, Kingston, Canada, 2004

MA, CCNY, New York, 2006

Submitted to the Graduate Faculty of

the Kenneth P. Dietrich School of Arts and Sciences in partial fulfillment

of the requirements for the degree of

Doctor of Philosophy

University of Pittsburgh

2011

UNIVERSITY OF PITTSBURGH

KENNETH P. DIETRICH SCHOOL OF ARTS AND SCIENCES

This dissertation was presented

by

An-Hung Edmund Yeh

It was defended on

November 22, 2011

and approved by

Professor Paul E. Floreancig, Department of Chemistry

Professor Scott G. Nelson, Department of Chemistry

Professor Billy W. Day, Department of Pharmaceutical Sciences

Dissertation Advisor: Professor Dennis P. Curran, Department of Chemistry

Fluorous Mixture Synthesis (FMS) of Four Isomers of 4,8,12,-Trimethylnonadecanol and the Development of an NMR-based Method for Determining the Configurations in Polyisoprenoid Structures

An-Hung Edmund Yeh, PhD

University of Pittsburgh, 2011

Copyright © by An-Hung Edmund Yeh

2011

Fluorous Mixture Synthesis (FMS) of Four Isomers of 4,8,12,-Trimethylnonadecanol and the Development of an NMR-based Method for Determining the Configurations in Polyisoprenoid Structures

An-Hung Edmund Yeh, PhD

University of Pittsburgh, 2011

The chiral polyisoprenoid motif has been identified in various natural products such as vitamin E, chlorophyll-d, and *β*-mannosyl phosphomycoketide. This motif features stereocenters bearing branched methyl groups at every fourth carbon of a long alkyl chain. Due to the lack of function group, assigning the configurations of these structures is difficult.

Herein, we describe the fluorous mixture synthesis (FMS) of the 4*S*,8*S*,12*S*-, 4*S*,8*R*,12*S*-, 4*R*,8*S*,12*S*-, and 4*R*,8*R*,12*S*-trimethylnonadecanol isomers. The FMS features a new family of ultra-light fluorous *O*-phenyl thionocarbonate tags and employees the most efficient fluorous tagging strategy to date. The analyses of these four isomers were found to exhibit small but reliable differences in ^{1}H and ^{13}C NMR spectra. Furthermore, these chemical shifts of the branched methyl groups were diagnostic of relative configurations. By deducing the relative relationship between configuration and chemical shift, we developed predictions of 4,8,12,16-tetramethyltricoanol, and 4,8,12,16,20-pentamethyl-heptacosanol.

TABLE OF CONTENTS

LIST OF TABLES

LIST OF FIGURES

LIST OF SCHEMES

LIST OF ABBREVIATIONS

APC	antigen presenter cell
Boc	*t*-butyl carbamate
CBz	carboxybenzyl
CD1c	cluster of differentiation 1c
DIABAL-*H*	diisobutylaluminum hydride
Equiv	equivalent
Fmoc	fluorenylmethoxycarbonyl
FMS	fluorous mixture synthesis
HMQC	heteronuclear multiple quantum coherence
HPLC	high pressure liquid chromatography
HRMS	high resolution mass spectrometry
MPM	β-mannosyl phosphomycoketide
MTPA	α-methoxytrifluorophenylacetic acid
NMR	nuclear magnetic resonance
OEG	oligoethylene glycol tags
PF-C8	perfluorooctyl ethyl silyl HPLC column
PFP	perfluorophenyl HPLC column
ph	phenyl

PMB	*p*-methoxybenzyl
py	pyridine
RP-3	reverse phase n-propyl silyl HPLC column
RP-10	reverse phase decyl silyl HPLC column
rt	room temperature (25 °C)
THF	tetrahydrofuran
TIPS	triisopropylsilyl
TOCSY	total correlation spectroscopy

PREFACE

There is a saying that "it takes a village to raise a child." In my opinion, it also takes a village to raise a Ph.D. I would like to take a moment here to acknowledge those who have made an impact in my scientific career so far.

First and foremost, I'd like to thank my Ph.D thesis advisor Dr. Dennis Curran, who has tirelessly guided me through my research in the past five years. The lessons I learned will forever be my guide as I journey further into the scientific jungle. I would also like to thank my Master's thesis advisor Dr. Mahesh Lakshman, who took me under his wings during a difficult period of my life and re-ignited my passion for science during my tenure at The City College of New York.

Second, I want to acknowledge all the Curran group members, past and present, for their supports, academically and otherwise. I would like to thank especially Dr. Bin Sui, Dr. David Guthrie, and Dr. Mantosh Sinha, who have helped me at different stages of my graduate school career. I am also very grateful to have an esteemed panel of professors, Dr. Billy Day, Dr. Paul Floreancig, and Dr. Scott Nelson on my committee. Special thanks also go out to Dr. Ted Cohen for serving as my proposal mentor, and Dr. Damodaran Krishnan for helping me with all my NMR related problems.

Last, but definitely not least, I would like to dedicate this thesis to my family. To my lovely fiancée, Christine Killmeyer, thank you for keeping me grounded and being there for me

in everything I do. To my brother, Dr. An-Chou Yeh, thank you for setting a great example for me to follow. I will probably never achieve the academic heights you did, but I will keep trying. To my dad and mom, Sui-Chung Yeh and Cheng-Wu Lu, thank you both for allowing me to pursue my dreams and passions. I am forever indebted to you for everything you have sacrificed to get me here.

This thesis belongs to all of you, and I thank you all for being in my village!

1.0 INTRODUCTION

1.1 FLUOROUS MIXTURE SYNTHESIS (FMS)

Fluorous mixture synthesis (FMS) is a solution-phase technique that was introduced by Curran and coworkers in 2001.[1] FMS relies on the ability of fluorous stationary phases to separate molecules by fluorine content during fluorous HPLC experiments.[1]

A typical FMS takes place in four stages, 1) pre-mixing; 2) mixture synthesis; 3) demixing; 4) and detagging (Scheme 1.1).[1] During the pre-mixing stage, individual reactions are carried out in parallel, and each member of a series of substrate (S^1–S^n) is tagged with a specific fluorous tag (F^1–F^n). The tagged molecules (S^1F^1–S^nF^n) are then mixed together (M1) and carried through a sequence of reactions in the mixture synthesis stage. During this stage, each encoded molecule (S^1F^1–S^nF^n) within a mixture (M1) undergoes transformations to arrive at the final mixture (M2). M2 is then separated by fluorous HPLC (F-HPLC) into the constituent components (P^1F^1–P^nF^n) based on the fluorine content of the tag(s) in the demixing stage. The fluorous tag from each component is removed during the detagging stage to access the target molecules (P^1–P^n).

Scheme 1.1. Schematic flowchart of FMS

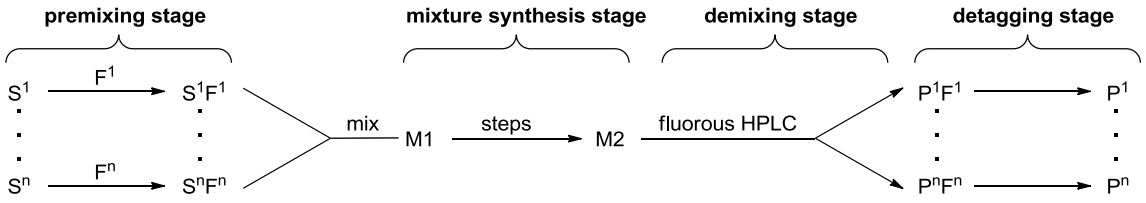

Similar to other mixture synthesis techniques such as solid phase mixture synthesis, FMS has often been used in library synthesis. Unlike the solid phase mixture synthesis, however, FMS is compatible with all solution-phase synthetic and analytical methods.[2]

1.1.1 Fluorous Separation by Fluorous-HPLC

At the heart of FMS is the fluorous demixing, which is defined as the separation and isolation of individual fluorinated molecule based on its fluorine content using silica gel with a fluorocarbon stationary phase.[1] This process is usually carried out by HPLC with a fluorous column. Fluorous separation is different from normal phase or reverse phase separation because of the C-F bonds in the stationary phase contain significant dipole character, which interact strongly with halogenated molecules.[3]

The strong fluorine-fluorine interaction between a fluorinated molecule and a florous column was first observed by de Galan and coworkers in 1980, when previously inseparable benzene and monofluorobenzene (by reverse phase columns RP-3 and RP-10) were separated by heptadecafluorodecyl dimethylsilyl bounded (RP-F10) column (Figure 1.1).[4] In a follow-up study, de Galan and coworkers further demonstrated the characteristic of strong fluorine-fluorine interactions between mobile and stationary phases with the sequential separation of five different fluorobenzenes by fluorine content (Figure 1.2).[5]

Figure 1.1. Stationary phase of the heptadecafluorodecyl dimethylsilyl (RP-F10) column

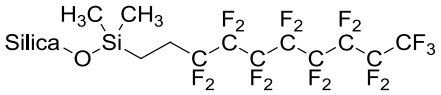

Figure 1.2. Fluorous separation of fluorinated benzene by RP-F10 column[5]

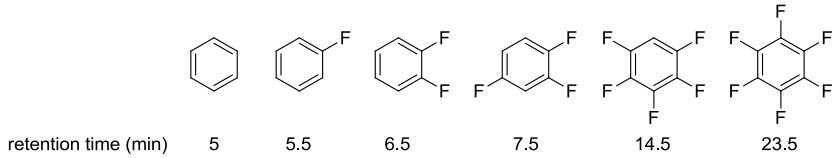

The first use of F-HPLC in FMS was reported by Curran and coworkers in 2001 to separate a mixture (M-**3**) of the two mappicine quasiisomers (*R*)-**3** and (*S*)-**3** with TIPS tags (TIPS^{F13}and TIPS^{F17}, respectively) by a fluorous column (Scheme 1.2). The superscripts F13 and F17 refer to the corresponding fluorine content in the perfluoroalkyl chain. Upon subjecting M-**3** to F-HPLC with a Fluofix^{TM} column, (*R*)-**3**, which had the lower fluorine content, was eluted first. This was followed by (*S*)-**3** with the higher fluorine content. Removal of the fluorous TIPS tag on each molecule by desilylation after demixing gave the two enantiomers of mappicine.[6]

Scheme 1.2. The first application of fluorous HPLC in FMS

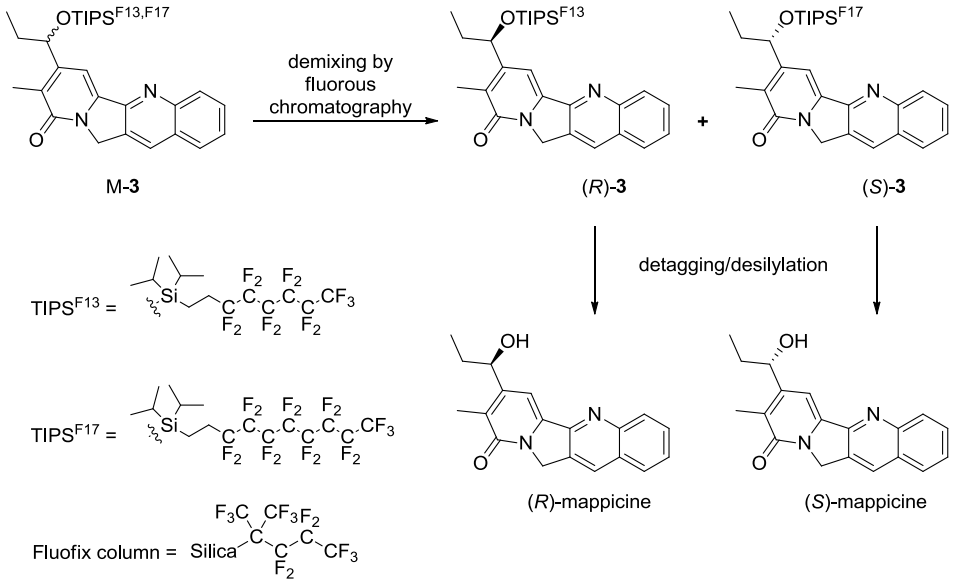

1.1.2 Uses of FMS in Natural Product Synthesis

One of the most popular uses of FMS is in natural product library synthesis. In particular, molecules with structures that are difficult to assign have been targeted.[7] For example, in order to assign the stereocenters in murisolin A, 28 of the 64 possible stereoisomers were synthesized through FMS by Dr. Q. Zhang and coworkers in 2005 (Figure 1.3).[7c] A synthetic effort of this magnitude by conventional parallel synthesis would take a substantially longer time to accomplish.

Figure 1.3. Two-dimentional structure of murisolin A

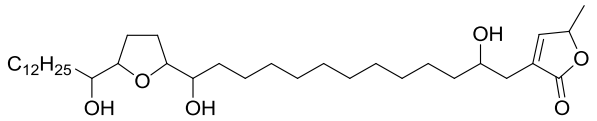

The fluorous tags in FMS of natural products have so far been based on protecting groups of alcohols or amines. Figure 1.4 shows some of the most common fluorous tags, including F-TIPS, F-PMB, F-Fmoc, F-Cbz, and F-Boc.[2] These fluorous tags function not only as protecting groups, but also encode the specific configurations of the molecules as well as assist in F-HPLC separations.

Figure 1.4. Common fluorous tags

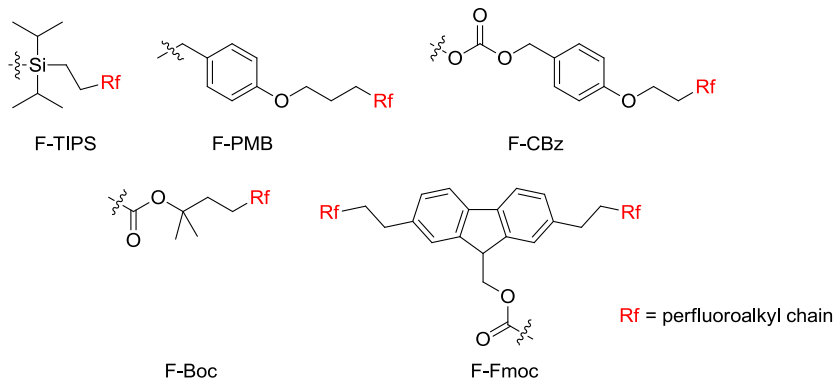

1.1.3 Fluorous Tagging Strategies

The tagging strategy of each FMS often depends on the individual target structure and synthetic design, but in general there are three different types of tagging strategies to date: 1) single tagging; 2) double tagging; 3) and orthogonal double tagging.

The single tagging strategy uses a single tagging site on the molecule to encode the specific configurations of all target isomers in a FMS. Two examples of this tagging strategy are FMS of murisolin A and pinesaw fly sex pheromone.[7c,8] In the FMS of murisolin A, tagging of the C20 hydroxy group with four different ^{F}PMB groups encoded the four quasiisomers of protected murisolin A as a mixture M-**4**. In the FMS of the pinesaw fly sex pheromone, tagging of the C2 hydroxy group with four different ^{F}PMB groups encoded for the four quasiisomers of protected pinesaw fly sex pheromone as a mixture M-**5** (Figure 1.5). The mixtures (M-**4** and M-**5**) were subjected to F-HPLC to separate the constituting quasiisomers based on fluorine content. The respective isomers of the natural products were obtained after the deprotection/detagging of the protected quasiisomers by Pd/C catalyzed hydrogenolysis.

Figure 1.5. Examples of single tagging FMS strategy

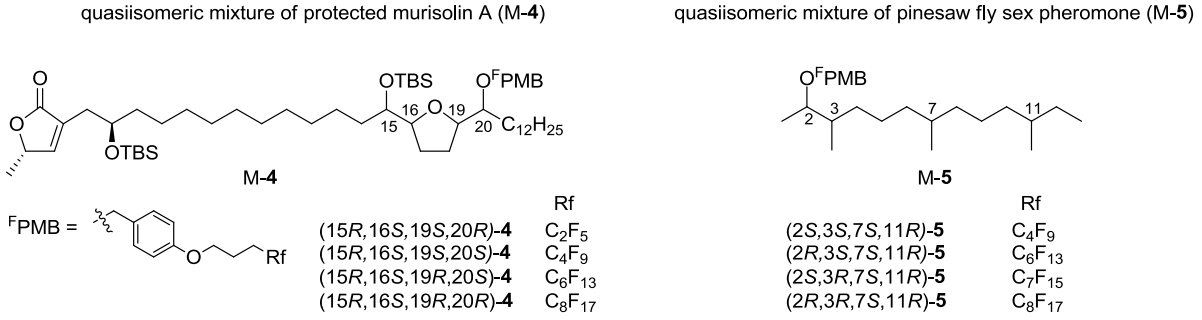

The double tagging strategy uses two different tagging sites to encode the specific configurations of the target isomers in a given FMS.[7b,7d,9] For example, in the FMS of passifloricin the hydroxy groups at C7 and C9 positions were tagged with three different fluorous

tags (TIPS^{F0}, TIPS^{F7}, and TIPS^{F9}) to encode the four quasiisomers of protected passifloricin in M-**6**. Each TIPS^{F} tagged quasiisomer contained a different number of fluorine atoms for F-HPLC demixing. Depending on the complexity and synthetic design of the target molecule, the number of fluorous tag in a double tagging FMS can vary from two to four. For instance, the FMS of SCH725674 only used two different fluorous tags (TIPS^{F0} and TIPS^{F5}) to encode four quasiisomers of protected SCH725674 in M-**7**,[9c] while the FMS of cytostatin used four different fluorous tags (TIPS^{F0}, TIPS^{F9}, TIPS^{F13}, and TIPS^{17}) to encode four quasiisomers of protected cytostatin precursor in M-**8** (Figure 1.6).[10] The double tagging strategy typically allows for re-use of the same fluorous tag as seen in the FMS of passifloricin with TIPS^{F7} tag and the FMS of SCH725674 with the TIPS^{F5} tag, as long as each quasiisomer is encoded with a unique number of fluorine atoms.

Figure 1.6. Examples of double tagging FMS strategy

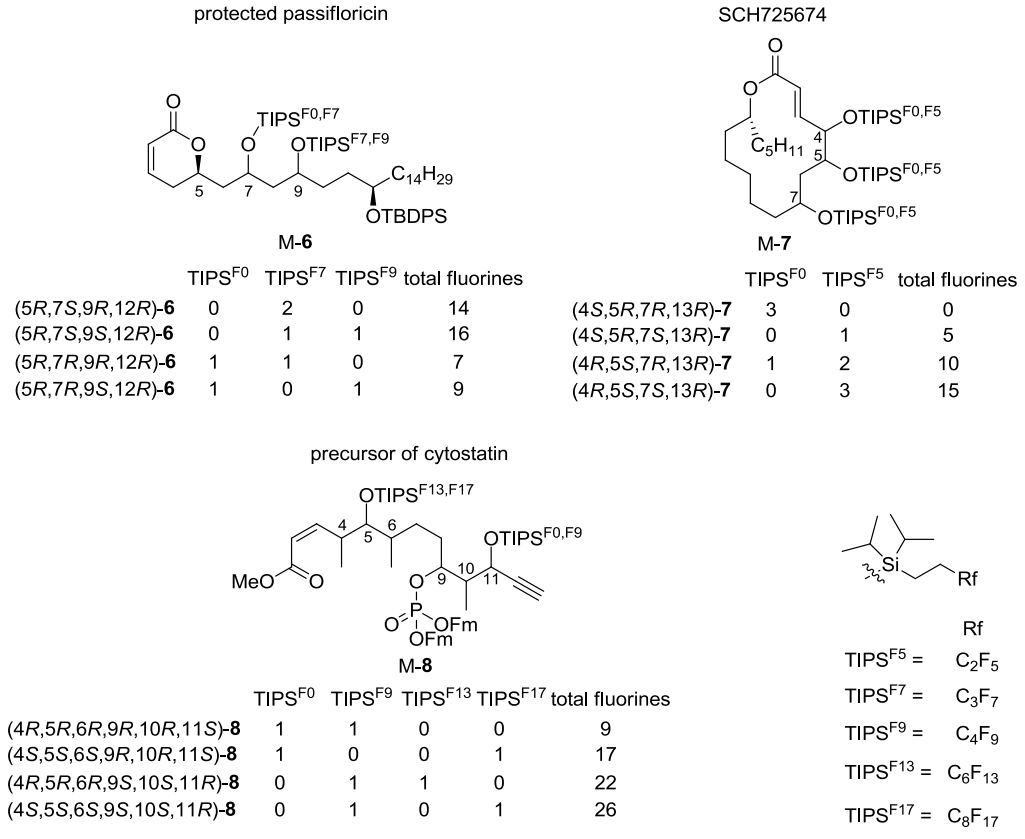

	TIPS^{F0}	TIPS^{F7}	TIPS^{F9}	total fluorines
(5*R*,7*S*,9*R*,12*R*)-**6**	0	2	0	14
(5*R*,7*S*,9*S*,12*R*)-**6**	0	1	1	16
(5*R*,7*R*,9*R*,12*R*)-**6**	1	1	0	7
(5*R*,7*R*,9*S*,12*R*)-**6**	1	0	1	9

	TIPS^{F0}	TIPS^{F5}	total fluorines
(4*S*,5*R*,7*R*,13*R*)-**7**	3	0	0
(4*S*,5*R*,7*S*,13*R*)-**7**	0	1	5
(4*R*,5*S*,7*R*,13*R*)-**7**	1	2	10
(4*R*,5*S*,7*S*,13*R*)-**7**	0	3	15

	TIPS^{F0}	TIPS^{F9}	TIPS^{F13}	TIPS^{F17}	total fluorines
(4*R*,5*R*,6*R*,9*R*,10*R*,11*S*)-**8**	1	1	0	0	9
(4*S*,5*S*,6*S*,9*R*,10*R*,11*S*)-**8**	1	0	0	1	17
(4*R*,5*R*,6*R*,9*S*,10*S*,11*R*)-**8**	0	1	1	0	22
(4*S*,5*S*,6*S*,9*S*,10*S*,11*R*)-**8**	0	1	0	1	26

The orthogonal double tagging strategy also uses two different tagging sites to encode the stereo-information of the isomers, but instead of using only one class of tag, two different classes of tags are used. For example, in the second generation FMS of murisolin A,[7b,9a] fluorous and oligoethylene glycol OEG tags were used. OEG tags are a class of polarity-based solution phase mixture synthesis tag developed by Wilcox and coworkers.[11] In this synthesis, the PMB^F tags were used to code for four quasiisomers at C20 position in fragment M-**9** and the OEG tags were used to code for four quasiisomers at the C4 position in fragment M-**10**. After connecting the two fragments via Julia-Kolcienski olefination followed by hydrogenation, the final mixture M-**11** contained 16 quasiisomers of protected murisolin A (Scheme 1.3). The mixture M-**11** was first subjected to flash chromatography to separate four fractions based on polarity of the OEG tags from OEG1 (least polar) to OEG4 (most polar). Each fraction was then subjected to F-HPLC to separate each quasiisomer based on the number of fluorine atom. Following detagging, a total of 16 isomers were obtained from the FMS.

Scheme 1.3. Example of the orthogonal double tagging FMS strategy

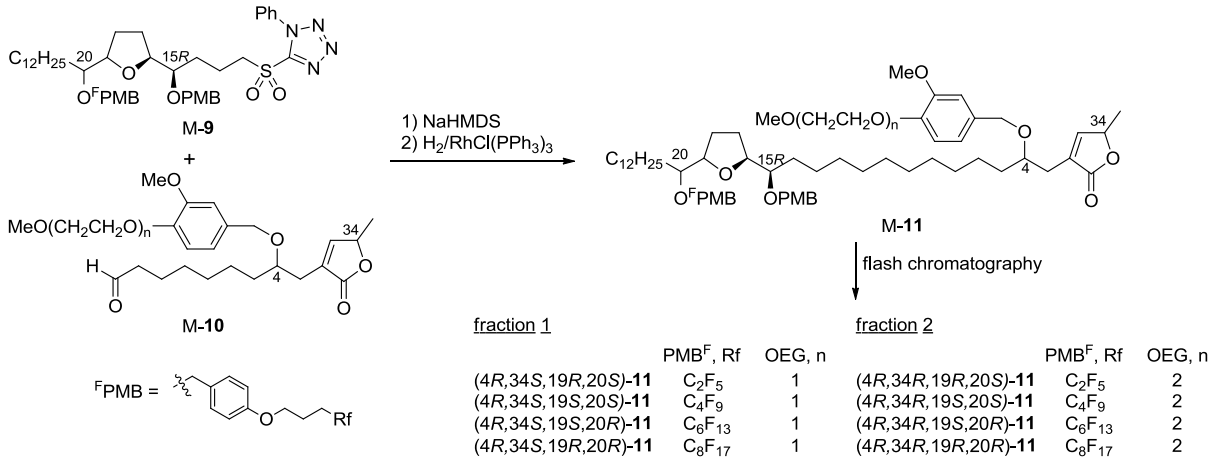

fraction 1

	PMB^F, Rf	OEG, n
(4*R*,34*S*,19*R*,20*S*)-**11**	C_2F_5	1
(4*R*,34*S*,19*S*,20*S*)-**11**	C_4F_9	1
(4*R*,34*S*,19*S*,20*R*)-**11**	C_6F_{13}	1
(4*R*,34*S*,19*R*,20*R*)-**11**	C_8F_{17}	1

fraction 2

	PMB^F, Rf	OEG, n
(4*R*,34*R*,19*R*,20*S*)-**11**	C_2F_5	2
(4*R*,34*R*,19*S*,20*S*)-**11**	C_4F_9	2
(4*R*,34*R*,19*S*,20*R*)-**11**	C_6F_{13}	2
(4*R*,34*R*,19*R*,20*R*)-**11**	C_8F_{17}	2

fraction 3

	PMB^F, Rf	OEG, n
(4*S*,34*S*,19*R*,20*S*)-**11**	C_2F_5	3
(4*S*,34*S*,19*S*,20*S*)-**11**	C_4F_9	3
(4*S*,34*S*,19*S*,20*R*)-**11**	C_6F_{13}	3
(4*S*,34*S*,19*R*,20*R*)-**11**	C_8F_{17}	3

fraction 4

	PMB^F, Rf	OEG, n
(4*S*,34*R*,19*R*,20*S*)-**11**	C_2F_5	4
(4*S*,34*R*,19*S*,20*S*)-**11**	C_4F_9	4
(4*S*,34*R*,19*S*,20*R*)-**11**	C_6F_{13}	4
(4*S*,34*R*,19*R*,20*R*)-**11**	C_8F_{17}	4

One way to judge the efficiency of an FMS is by the total number of fluorine atoms used to encode a library of isomers. The fewer fluorines used, the more efficient the route. To date, the most efficient FMS was the library synthesis of SCH725674 by Dr. Moretti and coworkers, which used a total of 30 fluorine atoms to encode four stereoisomers.[9c] In contrast, typical use of four different single tags such as the FMS of murisolin needed 44 fluorine atoms. Double tagging strategy used in the FMS of passifloricin and cytostatin needed 46 and 72 fluorine atoms respectively.

1.1.4 Current Limitations of FMS

Despite the convenience and efficiency of FMS in natural product library syntheses, there are at least two current limitations. The first limitation is the large number of fluorine atoms introduced by the perfluoroalkyl tags. Each increase in perfluoroalkyl chain length adds two additional fluorine atoms to the tag. As the number of fluorine atom increases, the molecular weight and the F-HPLC demixing time also increase. This causes isolation problems because of the prolonged retention time on the fluorous column. Additionally, the solubility of highly fluorinated molecules in non-fluorinated organic solvents decreases with increasing fluorine contents. Typically, 60% fluorine by weight is considered the threshold for good solubility.[12] Currently, perfluoroalkyl groups are the only class of tag in FMS. It would be desirable to develop other class of fluorous tags, especially ones with fewer fluorine atoms.

The second limitation is regarding the type of natural products that usually can be targeted. Because all current fluorous tags are based on protecting groups of hydroxy and amino groups, to date the molecules targeted by FMS all contained either functionality for fluorous tagging (Figure 1.7). It would be advantageous to develop non-protecting group based tags, such

as traceless tags, to expand the scope of FMS into natural products without convenient handles for tagging.

Figure 1.7. Recently completed FMS targets based on hydroxy group tagging

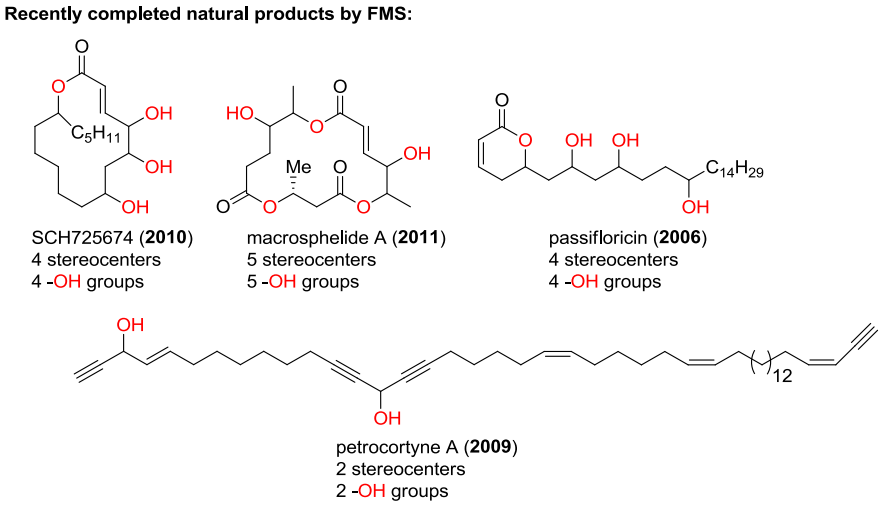

1.2 NATURAL PRODUCTS CONTAINING CHIRAL SATURATED POLYISOPRENOID MOTIFS

One of the most common types of chiral isoprenoid motifs is a long alkyl chain with asymmetric methyl branching at every fourth carbon. This substructure can be found in a variety of natural products including vitamins K and E, chlorophyll, β-mannosyl phosphomycoketide, and pinesaw fly pheromones (Figure 1.8).[13] Despite the structural similarities between the polyisoprenoid side chains, the biosynthetic pathways of these natural products are very different. The side chains in vitamin K and E, and chlorophyll come from the non-mevalonate pathway, and the side chain of β-mannosyl phosphomycoketide comes from a polyketide synthase pathway.[13d,14]

Figure 1.8. Natural products with polyisoprenoid motif highlighted in red

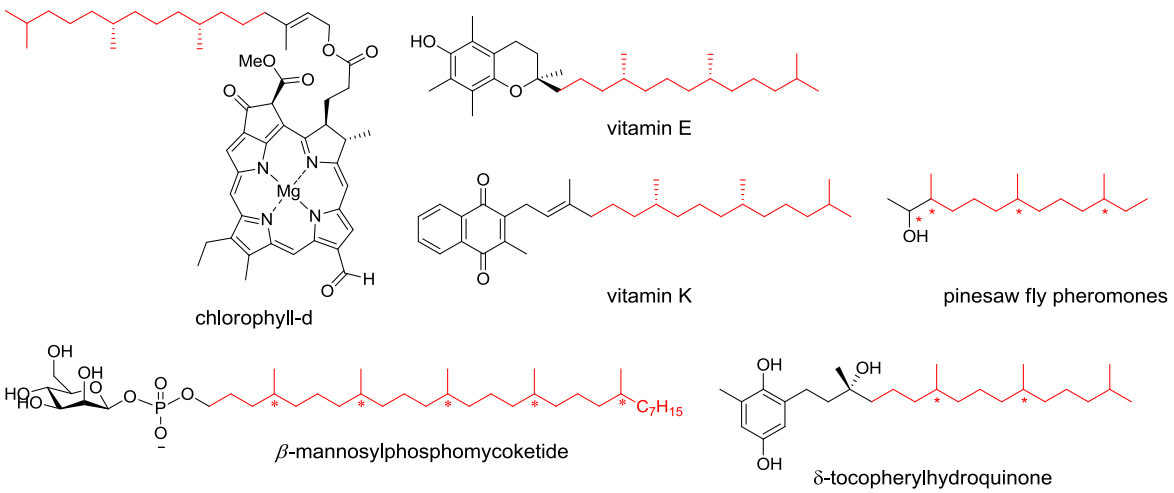

Because of the lack of functionality on the alkyl chain, the asymmetric synthesis and the identification of the methyl branch configurations are challenging.[15] While methods to efficiently synthesize these asymmetric polyisoprenoid structures have advanced considerably since the early 1980s,[13a,13c,13e,15-16] to date, there is no established method for determining the methyl branch configurations directly by spectroscopic means. The standard way to identify the methyl branch configurations in a natural product is by a combination of optical rotation comparison with a library of synthetic isomers.[17]

1.2.1 Vitamin E

α-Tocopherol **12** (vitamin E) is a common natural product first isolated from vegetable oil in 1922.[13e] It is an antioxidant best known to protect polyunsaturated fatty acids and cell membranes from radical damage.[13b] The structure of α-tocopherol consists of a shikimate-derived aromatic ring connected to a chiral saturated polyisoprenoid side chain with 2*R*,4'*R* and 8'*R* stereocenters (Figure 1.9). Although the natural vitamin E is found to contain only the

2*R*,4'*R*,8'*R*-α-tocopherol,[17] tests have shown that the 2*R*,4'*RS*,8'*RS*-α-tocopherol mixture exhibits comparable bioactivity,[18] i.e. the 4' and 8' methyl configurations on the side chain do not affect the bioactivity.

Figure 1.9. Structure of α-tocopherol (vitamin E)

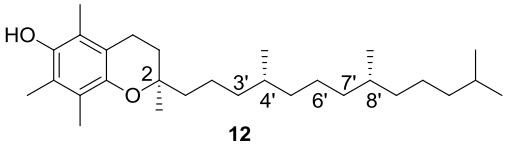

12

The determination of the methyl branch configurations of the natural α-tocopherol was highly sought after between 1980 and 1990.[5,16b,17,19] In 1981, Cohen and coworkers reported combined GC analysis with optical rotation to confirm the methyl branch configurations of the natural α-tocopherol to be exclusively 2*R*,4'*R*,8'*R*.[16b] In the same year, Bremser and coworkers showed that the natural (2*R*,4'*R*,8'*R*)-**12** and the synthetic (2*S*,4'*R*,8'*S*)-**12** could be distinguished by the C2', C3', C5', C6', C7', and C8' signals in ^{13}C NMR spectra (Figure 1.10).[20]

Figure 1.10. Selected ^{13}C NMR spectra of (2*R*,4'*R*,8'*R*)-**12**, (2*S*,4'*R*,8'*S*)-**12**, and stereorandom **12**

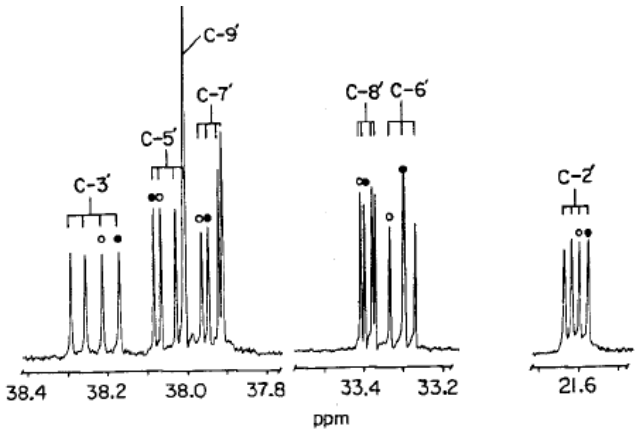

Figure 1. 100.655 MHz ^{13}C NMR spectrum of **1** in acetone-d_6 (10 mm tube). 12 000 scans were accumulated on a Bruker WH 400 with a digital resolution of 1.4 Hz. The signals of (2*R*, 4'*R*, 8'*R*) + (2*S*, 4'*S*, 8'*S*) − **1** are marked with ●, those of (2*S*, 4'*R*, 8'*R*) + (2*R*, 4'*S*, 8'*S*) − **1** with ○.

(taken from ref. 20 with permission)

In 1988 Ingold and coworkers published an in-depth ^{13}C NMR study detailing how the methyl branch configurations in α-tocopherol and related molecules influence chemical shifts in the rest of the molecule.[19a] They observed the maximum differences in chemical shift per bond at the carbon signals one, three, and five bonds away from the stereocenters (C2, C4', and C8'). Based on this observation, they postulated that "at a low energy, chain extended conformers, the interaction between two nearest asymmetric carbons is likely to occur by a relay type mechanism" through interactions between the methyl branch carbons and the hydrogen atoms of the middle carbon.[19a] For example, the interaction between the 4' and 8' carbons is likely to involve primarily the methyl groups attached to the 4' and 8' carbons relay by the hydrogen atoms on the 6' carbon (Figure 1.11). This thorough analysis of vitamin E provides some insights into how chirality may propagate through the bonds in a polyisoprenoid system and provided the basis for future analyses of polyisoprenoid natural products.[21]

Figure 1.11. Illustration of the "relay" type mechanism discussed by Ingold and coworkers

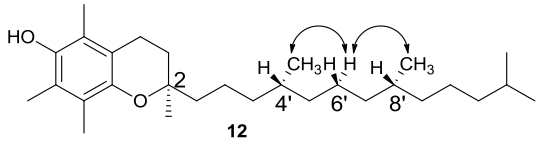

1.2.2 β–Manosyl Phosphomycoketide (MPM)

β-D-Mannosyl phosphomycoketides (MPMs) **1** and **2** (Figure 1.12) are potent mycobacterial antigens isolated by Moody and coworkers in 2000 from the cell walls of *Mycobacterium tuberculosis* and *Mycobacterium avium*.[13d] Similar to the structure of vitamin E, the structure of MPM-**1** and MPM-**2** contain a polyisoprenoid motifs of five isoprenoid units connected to a phosphate sugar of β-mannosyl linkage. In 2002, Crich and coworkers confirmed

the β-mannosyl linkage by comparing the MS fragmentation patterns of β-MPM-**2** with a stereorandom isoprenoid side chain and the natural β-MPM-**2**.[22]

Figure 1.12. Structure of β-mannosyl phosphomycoketide (MPM) **1** and **2**

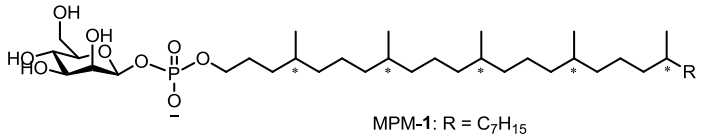

The exceptional potency of MPMs comes from the strong binding of their hydrophobic tails with the deep hydrophobic pocket of the CD1c antigen presenting protein on the antigen presenter cell (APC), which leaves the hydrophilic phosphate sugar group free to interact with the T-cell receptor protein on T-cell (Figure 1.13).[23]

Figure 1.13. CD1–glycolipid antigen–T-cell receptor interactions binding model

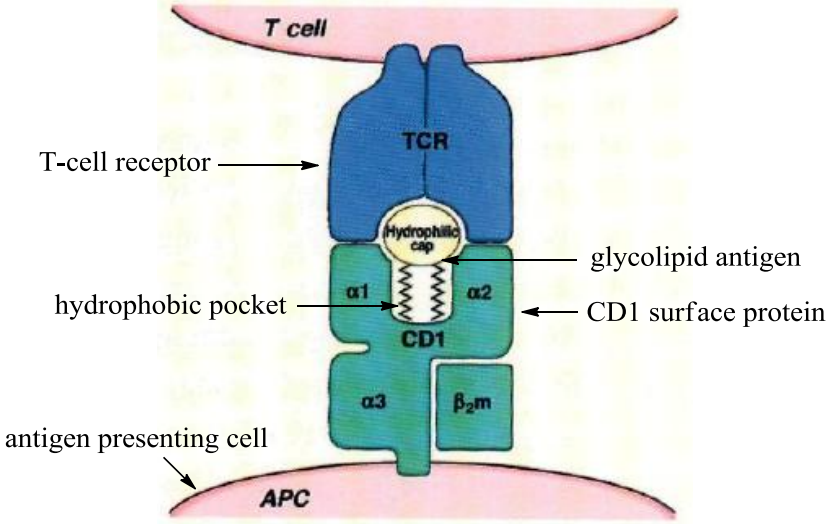

(taken from ref. 23 with permission)

In 2006, Feringa and coworkers postulated that all the methyl stereocenters have the same configuration because they are introduced by the same polyketide synthase through an iterative action.[24] Feringa and coworkers then accomplished a stereoselective total synthesis of the all-*S* isomer of MPM-**1** by using a highly convergent approach with four chiral building blocks **13**, **14**, **15**, and **16**.[25] Aside from **16**, all other building blocks contained branched methyl groups

introduced by an asymmetric conjugate addition reaction developed by Feringa and coworkers.[26] Each of the building blocks were connected by Julia-Kocienski olefination[27] followed by Pd/C catalyzed hydrogenation to give the all-*S* isoprenoid alcohol **17**. Coupling of **17** with the mannosyl phosphate building block **16** followed by deacetylation to complete the synthesis of the all-*S* MPM-**1** (Scheme 1.4).

Scheme 1.4. Total synthesis of all-*S* MPM-**1** by Feringa and coworkers

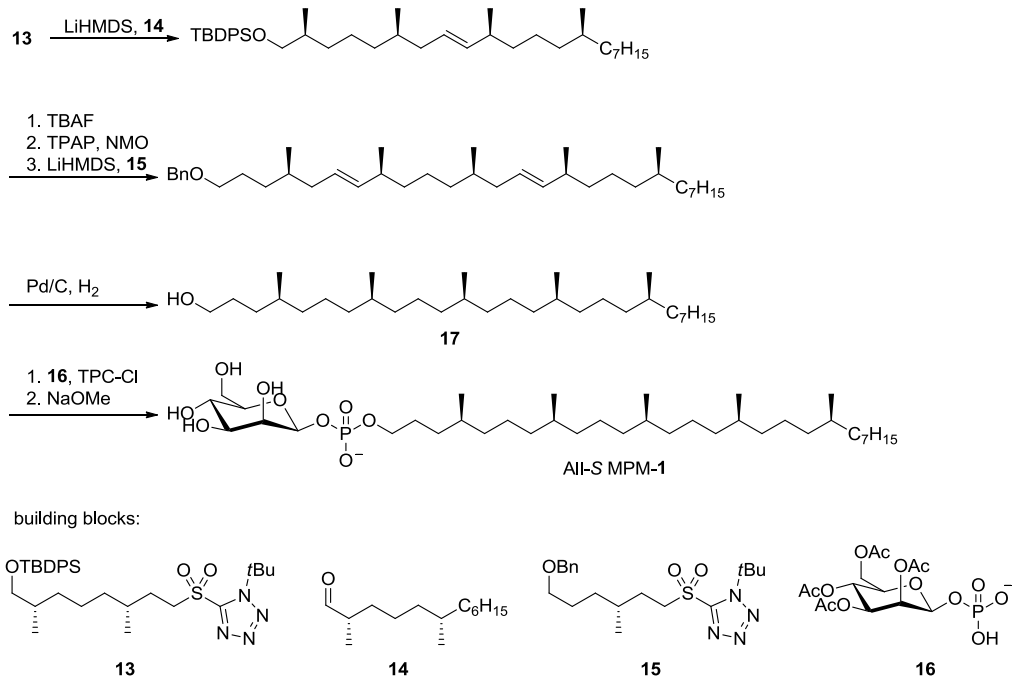

The synthetic all-*S* MPM-**1** was shown to elicit similar level of T-cell response as the natural MPM-**1**, while the stereorandom MPM-**2** showed 20–40 folds lower response than the natural MPM-**2**. Additionally, a crystal structure of CD1c in complex with MPM was recently reported by Scharf and coworkers to show the synthetic all-*S* MPM binding deeply inside the hydrophobic groove of the CD1c protein.[28] Based on the above evidence, the natural product was assigned to have the all-*S* branch methyl configuration.[25,29] To date, however, only one isomer has been tested. Could there be other isomers that have similar activity to the natural

product? Ideally, it would be better to develop analytical or spectroscopic tools for the assignment.

1.2.3 Project Design and Overview: Identifying Branched Methyl Group Configurations in Polyisoprenoid Systems by NMR Spectroscopy

While structurally simpler polyisoprenoid molecules like vitamin E and its isomers can now be differentiated spectroscopically, more complex molecules like MPM have not been fully studied. In vitamin E, the repeating isoprenoid unit $CH_2CH_2CH(CH_3)CH_2$ occurs only twice, whereas in MPM it occurs five times. Will the stereoisomers of MPM side chain have different spectra or not? Can the structures be assigned from spectra?

To begin answering these questions, a study of how the relative methyl configuration affects chemical shift in a shorter polyisoprenoid system such as 4,8,12-trimethyl-nonadecanol was carried out because it is structurally similar to the side chain of MPM-**1**, yet it only contains three repeating isoprenoid units. As shown in Figure 1.14, the structures of the MPM-**1** side chain and 4,8,12-trimethylnonadecanol both contain two end methyl groups (end-1 and end-2), the only difference between the two molecules is the number of saturated isoprene units in the middle. It was hypothesized that one could develop a tool to identify the branched methyl group configurations of the isomers of 4,8,12-trimethylnonadecanol spectroscopically, we may be able to extend the method towards more complex systems such as the side chain of MPM-**1**.

Figure 1.14. A 2D comparison of the side chain of MPM-**1** and 4,8,12-trimethylnonadecanol

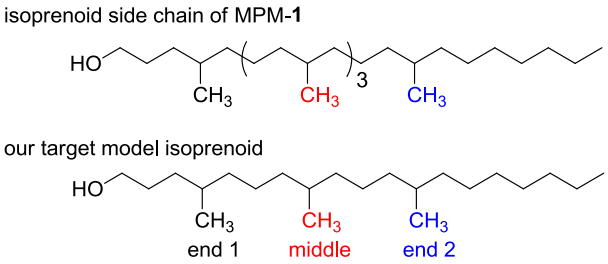

1.3 INITIAL ITERATIVE FMS APPROACH TOWARDS FOUR ISOMERS OF 4,8,12-TRIMETHYLNONADECANOL

The primary objectives of this project were to first synthesize four isomers of 4,8,12-trimethylnonadecanol and then develop spectroscopic tools to characterize the branched methyl group configurations of these polyisoprenoids. The plan was to utilize FMS to rapidly access the 4*S*,8*S*,12*S*-, 4*S*,8*R*,12*S*-, 4*R*,8*S*,12*S*-, and 4*R*,8*R*,12*S*-trimethylnonadecanols (Figure 1.15), then thoroughly characterize them by ^{1}H and ^{13}C NMR spectroscopy. Would the spectra of these four isomers be different? Would there be a decipherable relationship between the branched methyl group configurations and their respective chemical shifts? Could an NMR-based method be developed to identify the configurations of these branched methyl groups, and can it be applied to higher order polyisoprenoid molecules?

Figure 1.15. The four target isomers of 4,8,12-trimethylnonadecanol

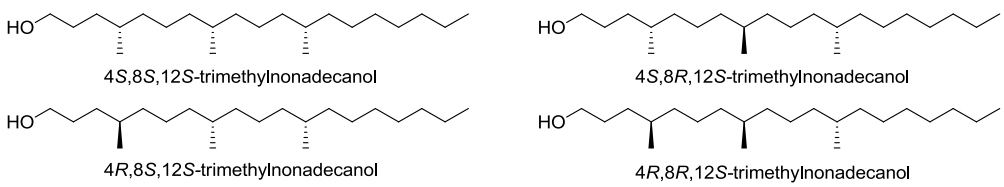

1.3.1 Synthetic Design

The initial synthetic effort towards FMS of 4,8,12-trimethylnonadecanol was started by Dr. Eveline Kumli,[30] and her first challenge was to design an FMS synthesis of a target molecule without any functional group for fluorous tagging. Dr. Kumli proposed the use of "auxiliary functional groups", which are hydroxy groups that are used to append different fluorous tags during the FMS and cleaved off at the end of the synthesis by global deoxygenation (Scheme 1.5).

Scheme 1.5. The utility of auxiliary hydroxy for the FMS of 4,8,12-trimethylnonadecanol

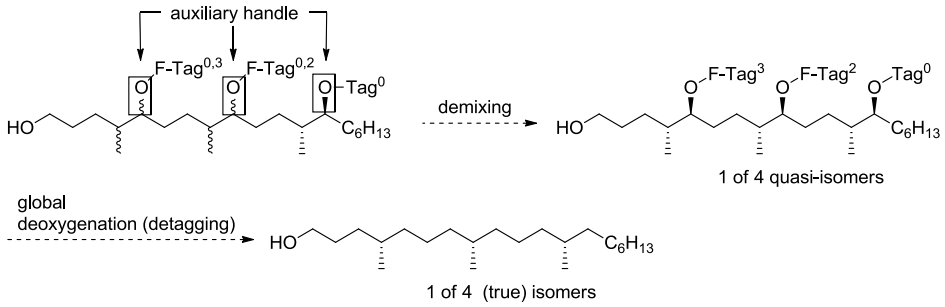

The initial FMS approach of 4,8,12-trimethylnonadecanol contained an *en route* double tagging strategy of three iterations of Brown crotylation,[31] fluorous xanthate tagging, cross-metathesis,[32] and hydrogenation followed by global deoxygention. This approach was abandoned when cross-metathesis of **18** and **19** did not give the desired product **20**, but instead gave diene **20'** through a Chugeav elimination (Scheme 1.6).[33] Apparently the cross-metathesis reaction worked in the presence of xanthate functionality, but the product was not stable.

Scheme 1.6. Observed Chugeav elimination during cross-metathesis by Dr. Kumli

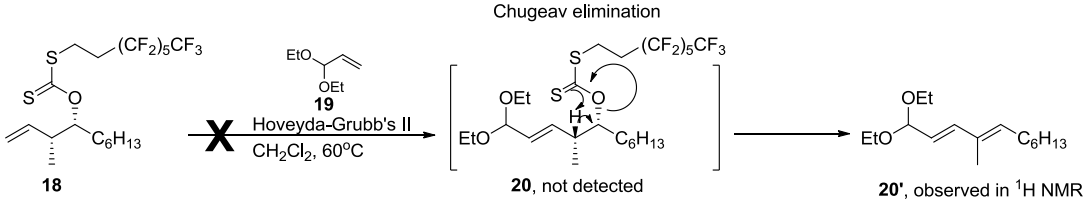

To circumvent this unwanted elimination reaction, Dr. Kumli changed from the fluorous xanthate tag to the more stable fluorous TIPS ($TIPS^F$) to complete the FMS. This new approach also added two extra steps (desilylation and hydroxy activation) to the synthesis at the end. The fluorous TIPS tags are herein represented in $TIPS^{Fn}$ form, the superscript F indicates it contains a fluorous tag, and n indicates the number of fluorine atoms on the tag. In case of a fluorous mixture, the tags are represented in $TIPS^{Fn,Fm}$ form, the two different tags are separated by a comma.

1.3.2 Initial FMS of 4,8,12-Trimethylnonadecanol with $TIPS^F$ tags

The first cycle of the FMS of 4,8,12-trimethylnonadecanol started with Brown crotylation of heptanal with (–)-(*Z*)-crotyldiisopino-campheylborane (Brown reagent)[31] followed by TIPS protection to give alkene **21** in 74% over 2 steps. Cross-metathesis of **21** with crotonaldehyde gave *α,β*-unsaturated aldehyde **22** in 66% yield. This was subjected to Pd-C catalyzed hydrogenation to form aldehyde **23**. The overall yield of the first iteration was 47% (Scheme 1.7).

Scheme 1.7. First cycle of the initial approach by Dr. Kumli

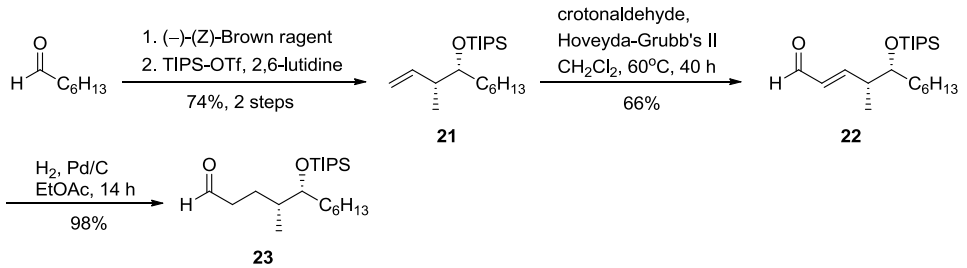

At the start of the second cycle of the FMS, aldehyde **23** was split into two portions and reacted with either (–)- or (+)- (*Z*)-Brown reagent in the crotylation step. The resulting allylic

alcohols were tagged with $TIPS^{F0}$ and $TIPS^{F9}$ tag respectively. The fluorous-tagged allylic alcohols were then mixed and subjected to cross-metathesis then hydrogenation to afford mixture aldehyde M-**24**. The overall yield of the second cycle was 36%. The third cycle was completed in the same fashion as the second cycle by splitting followed by separate crotylations. The resulting allylic alcohols were tagged with $TIPS^{F0}$ and $TIPS^{F13}$ respectively. At the end of the third cycle, aldehyde M-**25** was reduced to alcohol M-**26** with DIBAL-*H*. Alcohol M-**26** could not be demixed, because it lacked UV absorption for detection. Dr. Kumli then converted the primary alcohol to a benzoate ester to provide UV-absorbance for HPLC detection. Fluorous HPLC demixing of benzoate protected alcohol M-**27** with a FluoroFlash^{TM} (PF-C8) columan successfully yielded four quasiisomers (Scheme 1.8).

Scheme 1.8. Second and third FMS cycles by Dr. Kumli

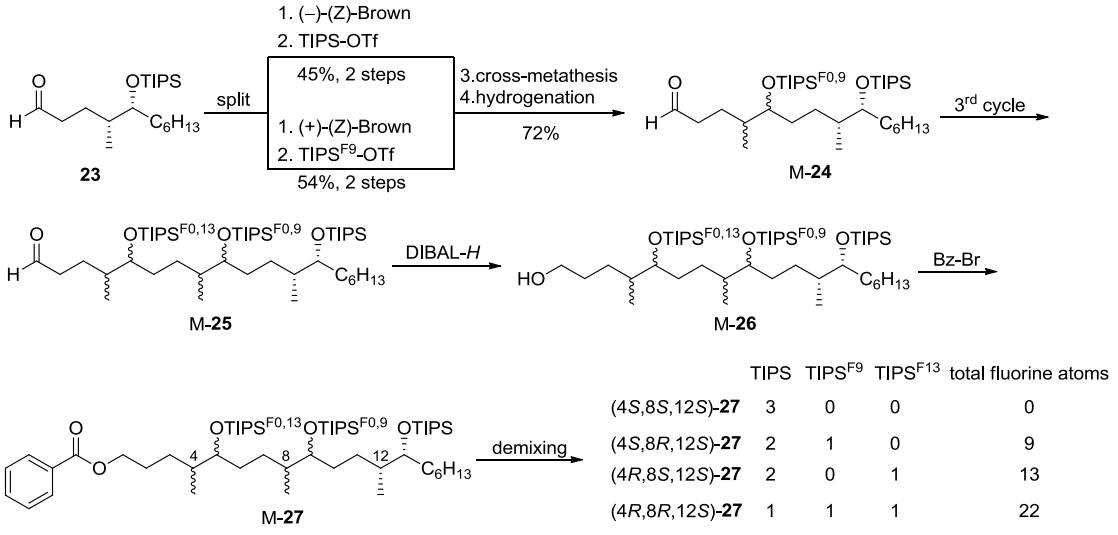

	TIPS	$TIPS^{F9}$	$TIPS^{F13}$	total fluorine atoms
(4*S*,8*S*,12*S*)-**27**	3	0	0	0
(4*S*,8*R*,12*S*)-**27**	2	1	0	9
(4*R*,8*S*,12*S*)-**27**	2	0	1	13
(4*R*,8*R*,12*S*)-**27**	1	1	1	22

The final deoxygenation was first evaluated on the mixture M-**27**. Desilylation of M-**27** gave triol M-**28** in 99% yield. However, hydroxy activation of triol M-**28** could not be achieved in good yield by tosylation, thionocarbonate or xanthate formation.[34,35,36] The subsequent global deoxygenation step was never successfully performed (Scheme 1.9).

Scheme 1.9. Simultaneous hydroxy activation of M-**26**

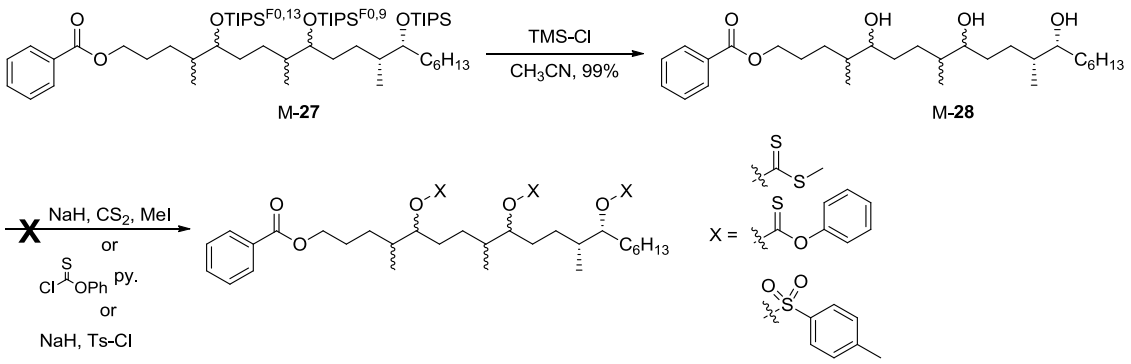

1.3.3 Conclusions from The Initial Synthesis

Dr. Kumli was able to demonstrate the utility of FMS by rapidly synthesizing a mixture of four TIPS^F-protected quasiisomers M-**27** through three cycles of Brown crotylation, TIPS tagging, cross-metathesis and hydrogenation. This FMS highlighted the first use of auxiliary hydroxy groups for fluorous tagging in a molecule lacking either hydroxyl or amino groups. The overall yields per cycle varied from 38% to 48%.

The work also identified two major problems that needed to be resolved before a stereoisomer library of 4,8,12-trimethylnonadecanol could be made. First, the yields per cycle (38% to 48%) were not consistently high. Second, the simultaneous activation of multiple hydroxy groups was not accomplished, so the subsequent global deoxygenation steps were unsolved problems.

2.0 NEW ITERATIVE APPROACH TOWARDS FMS OF FOUR ISOMERS OF 4,8,12-TRIMETHYLNONADECANOL

2.1 THE REVISED ITERATIVE APPROACH

This new approach was developed to address two main problems: 1) to improve the yields and consistency per cycle, and 2) to circumvent the global deoxygenation problems. Since the global deoxygenation problems began at the multiple hydroxy groups activation, the auxiliary hydroxy groups were tagged with radical labile fluorous tags *en route* during each cycle. This new approach would avoid the activation all hydroxy groups at once and also allow for global deoxygenation directly after the last cycle ends. *O*-Phenyl thionocarbonate[35] based fluorous tags were chosen because they can be conveniently appended to a hydroxy group by a simple (thiono)acylation reaction and can be readily cleaved (Scheme 2.1). Additionally, they also possess UV-absorbance, which aids in fluorous HPLC demixing. To ensure the success of this new approach, all reactions per cycle (crotylation and carbonylation) were first examined for compatibility with the *O*-phenyl thionocarbonate functionality (Scheme 2.2).

Scheme 2.1. *O*-phenyl thionocarbonate tag

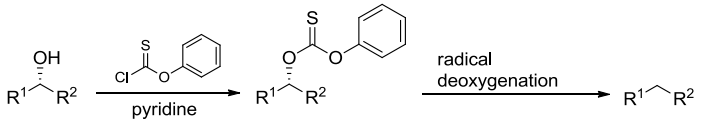

Scheme 2.2. The new approach with *O*-phenyl thionocarbonate tags

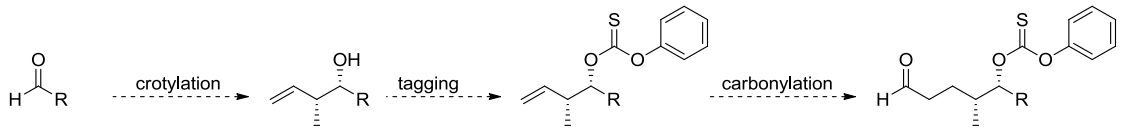

2.2 CROTYLATION REACTIONS

The first goal of the synthesis was to identify a suitable crotylation reaction with high yields and high stereoselectivity. Common crotylation reactions Brown crotylation[31] and Roush crotylation[37] were assessed with commercially available heptanal as starting aldehyde.

2.2.1 Brown Crotylation

The (–)-(*Z*)-Brown reagent[31] was prepared *in situ* before each reaction according to literature procedure: KO*t*Bu was added to a stirring solution of *cis*-butene in THF over 10 min, followed by addition of *n*-BuLi at –78 °C. The resulting mixture was stirred for 45 min before the addition of (–)-Ipc_2BOMe and then $BF_3{\cdot}OEt_2$. The corresponding aldehyde was added to this crude mixture of (–)-(*Z*)-Brown reagent **29** in THF at –78 °C to begin the crotylation reaction (Scheme 2.3).[31]

Scheme 2.3. Preparation of (–)-(*Z*)-Brown reagent **29**

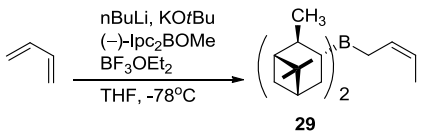

29

Heptanal was added directly to the (–)-Brown reagent **29** (1.5 equiv) in THF at –78 °C and the resulting mixture stirred for 16 h. After complete consumption of heptanal by TLC, the

reaction was quenched by addition of 3N NaOH and 30% H_2O_2 then slowly warmed to room temperature over 3 h. The target allylic alcohol (3*R*,4*R*)-**30** was isolated in 75% yield by column chromatography. The enantioselectivity of Brown crotylation was determined by analysis of Mosher esters **31** and **32**. The esters were made from reactions of (+)- or (–)-Mosher acid with allylic alcohol (3*R*,4*R*)-**30** in the presence of DCC and DMAP (Scheme 2.4).[38] The crude ^{19}F NMR spectra showed 93/7 enantioselectivity was achieved (Figure 2.1).

Scheme 2.4. Brown crotylation of heptanal and Mosher ester derivatization

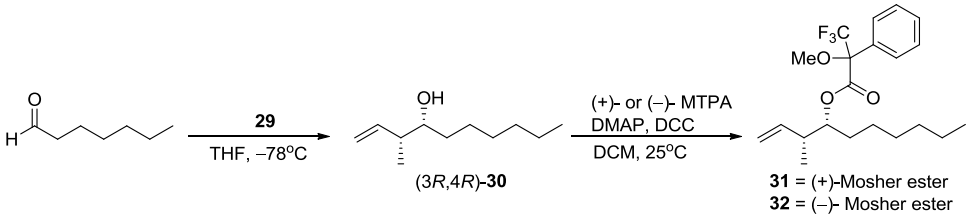

Figure 2.1. ^{19}F NMR spectra of (+)- and (–)-Mosher ester derivatives of **31** and **32**

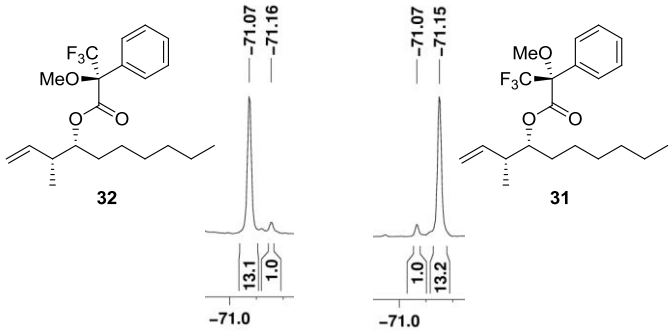

2.2.2 Roush Crotylation

The two Roush reagents (–)-diisopropyl-D-tartrate-(*E*)-crotylborate **33** and (+)-diisopropyl-L-tartrate-(*E*)-crotylborate **34** were used in the initial screening process. The reagents were prepared from literature procedures:[37] KO*t*Bu was added to a solution of *trans*-butene in THF over 10 min, followed by slow addition of *n*-BuLi at –78 °C. To the resulting mixture was added

triisopropyl borate and the resulting mixture was poured into 1 N HCl. Followed by addition of either diisopropyl-D-tartrate in ether to form **33** or a solution of diisopropyl-L-tartrate in ether to form **34** (Scheme 2.5). The organic layer was concentrated and then diluted with toluene to be stored at –20 °C. The concentration of each reagent in toluene was determined by measuring the yield of a crotylation reaction with 1 equiv of heptanal. The **33** solution was 1.0 M and the **34** solution was 0.53 M (see experimental section for details).

Scheme 2.5. Syntheses of Roush reagents **33** and **34**

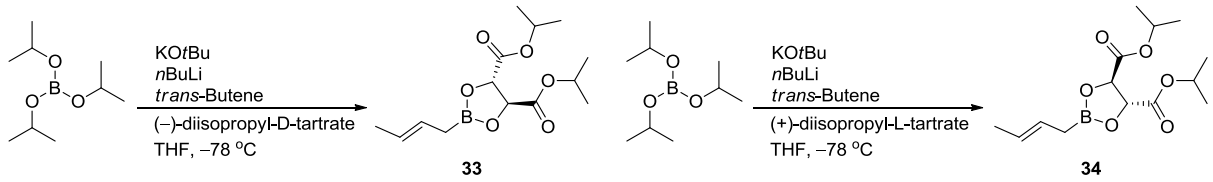

Heptanal (10 g, 88 mmol) and 15 mg of powdered 4 Å molecular sieves were treated with 1.5 equiv of (–)-(Z)-Roush reagent **33** in toluene (1.0 M) at –78 °C. The reaction was completed after 3 h. After aq NaOH workup, 87% of allylic alcohol (3*R*,4*S*)-**30** was isolated by column chromatography. The enantioselectivity of Roush crotylation was determined by analyses of Mosher esters **36** and **37** made from reactions of allylic alcohol (3*R*,4*S*)-**30** with (+)-or (–)-Mosher acids in the presence of DCC and DMAP (Scheme 2.6.).[38] The crude ^{19}F NMR spectra showed that 89/11 enantioselectivity was achieved (Figure 2.2).

Scheme 2.6. Roush crotylation of heptanal

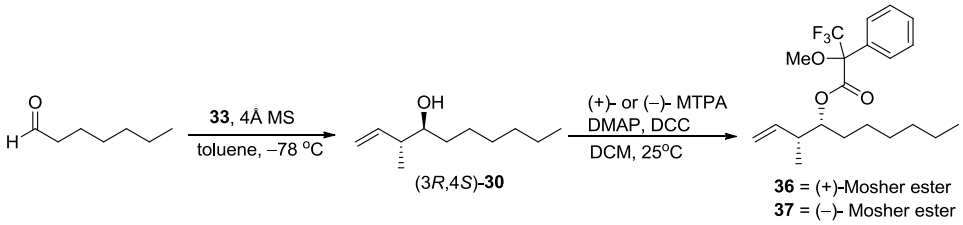

Figure 2.2. ^{19}F NMR spectra of (+)- and (–)-Mosher ester **36** and **37**

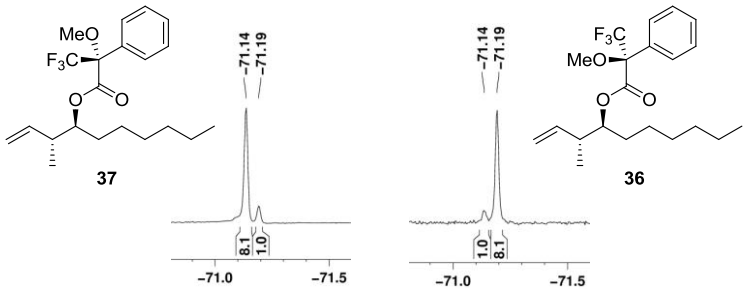

The *syn*/*anti* diastereoselectivity of both Brown and Roush crotylation was determined by ^{13}C NMR comparison of the C3 and C5 signals between allylic alcohols (3*R*,4*R*)-**30**, (3*R*,4*S*)-**30**, and *rac*-**30**. The allylic alcohol *rac*-**30** was synthesized by reaction of heptanal with 1-methyl-2-propenyl magnesium bromide at 0 °C. The ^{13}C NMR spectra comparisons of signals at C3 and C5 positions of **30** showed excellent reagent-controlled diastereoselectivities. The Brown crotylation gave exclusively *syn* product (3*R*,4*R*)-**30**, and the Roush crotylation gave exclusively *anti* product (3*R*,4*S*)-**30** (Figure 2.3).

Figure 2.3. ^{13}C NMR spectra comparisons of allylic alcohols **30** at C3 and C5 position

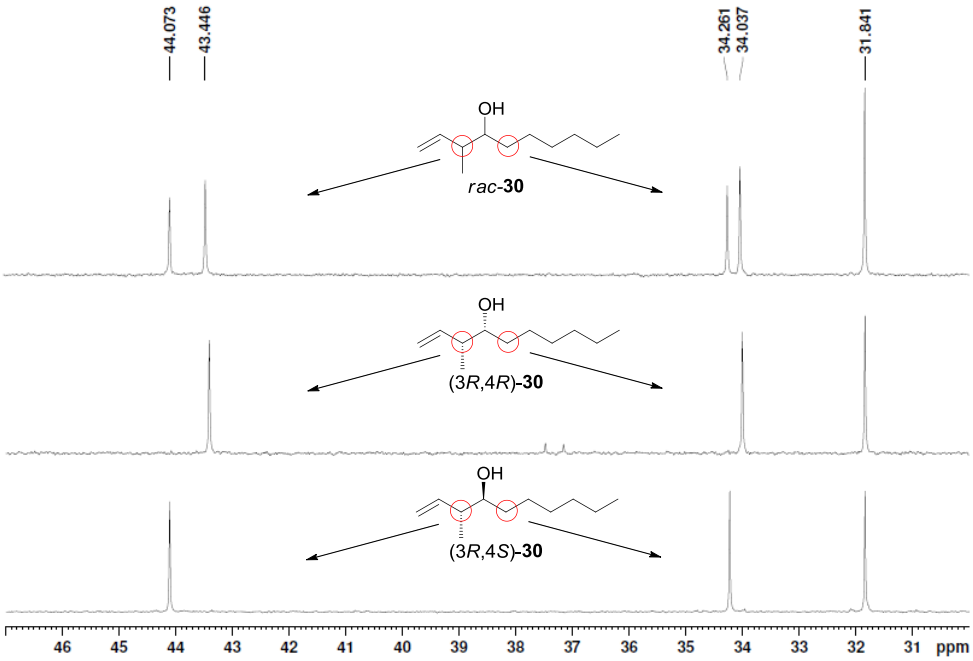

2.3 HYDROFORMYLATION IN THE PRESENCE OF *O*-PHENYL THIONOCARBONATE

In the initial approach by Dr. Kumli, the transformation from terminal alkene **21** to aldehyde **23** was accomplished by a two-step cross-metathesis and then hydrogenation sequence (Section 1.3.1). A new reaction was sought because, 1) the cross-metathesis reaction took over 48 h and the yields were inconsistent, varying from 56% to 80%; and 2) the cross-metathesis reaction was reported to be incompatible with the xanthate functionality (Section 1.3.1), which is an analog of the *O*-phenyl thionocarbonate.

Because of the mild conditions reported, the Rh-catalyzed reaction by Breit and coworkers was chosen as a potential candidate for the hydroformylation step.[39] It was reported that under 1 atm syngas (1:1 v/v, CO/H_2) at room temp, 1-bromo-6-hexene was converted to 6-bromo-hexanal in 91% yield using $Rh(CO)_2acac$ and the 6-diphenylphosphino-2-pyridone ligand **41** (Scheme 2.8).

Scheme 2.7. Mild Rh-catalyzed hydroformylation using diphenylphosphinopyridone ligand **41**

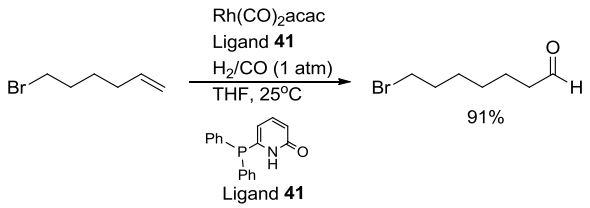

The 6-diphenylphosphino-2-pyridone ligand **41** used in this hydroformylation reaction was synthesized from reaction of 2,6-dichloropyridine with KO*t*Bu to give **39** in 89% yield. Treatment of **39** in liquid ammonia, sodium, and triphenylphosphine afforded **40** in 86% yield. Hydrolysis of **40** afforded the target pyridone **41** in 77% yield (Scheme 2.9).

Scheme 2.8. Synthesis of diphenylphosphinopyridone ligand **41**

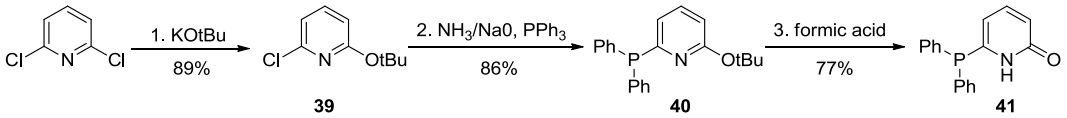

2.3.1 Rh-Catalyzed Hydroformylation in the Presence of *O*-Phenyl Thionocarbonate

The compatibility of the *O*-phenyl thionocarbonate functionality with this hydroformylation was evaluated with alkene **42**, which was synthesized in two steps (63% yield) from commercially available heptanal. In the initial experiment, alkene (3*R*,4*R*)-**42** was added to a mixture of 7 mol% $Rh(CO_2)acac$, 35 mol% pyridone ligand **41** in THF. The resulting mixture was subjected to 1 atm (15 psi) of 1:1 mixture of CO/H_2 at 25 °C.[39] The CO and H_2 gases in this initial experiment were introduced to the reaction vessel by two separate balloons via a T-shape connector (Appendix A, Figure 1). After 48 h, target aldehyde (4*R*,5*R*)-**43** was isolated by flash chromatography in 43% yield, but 50% of starting alkene **42** was also recovered (Scheme 2.10).

Scheme 2.9. Synthesis of *O*-phenyl thionocarbonate containing alkene **42**

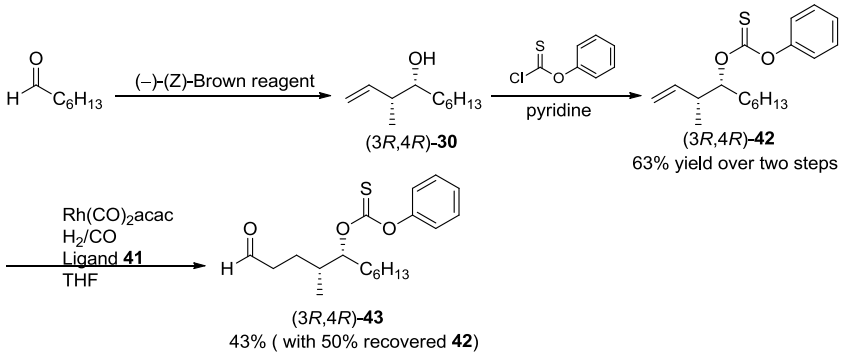

Prolonging the reaction time to 72 h, only improved the yield marginally to 65%, and 30% of starting alkene (3*R*,4*R*)-**42** was recovered (entry 2, Table 2.1). Next, the experiment was conducted in a Parr© EA apparatus (Appendix A, Figure 2) and syngas (1:1 v/v mixture of

CO/H_2) was used instead of separate CO and H_2 balloons. At a pressure of 70 psi, the desired aldehyde **43** was isolated in 65% yield after only 48 h (entry 3, Table 2.1). Increase in temperature from 25 to 45 °C at 70 psi further increased the speed of the reaction. The starting material disappeared after 48 h and aldehyde (4*R*,5*R*)-**43** was isolated in 87% yield (entry 4, Table 2.1). The next sets of experiments were conducted in a pressure reactor (Appendix A, Figure 3) to allow for higher operating pressure. At 45 °C and 100 psi, the starting material was completely consumed after only 30 h and aldehyde (4*R*,5*R*)-**43** was isolated in 86% yield (entry 5, Table 2.1). Increasing the pressure and temperature to 120 psi and 60 °C sped up the reaction further to give 89% yield of (4*R*,5*R*)-**43** in just 20 h (entry 6, Table 2.1). All the crude products were found to contain trace amount (~1–2%) of branched aldehyde product **44**, but this byproduct could easily be separated by column chromatography. Based on the results, the conditions listed in entry 6 were chosen for the iterative cycle, because they gave the maximum yield in the shortest time.

Table 2.1. Rh-catalyzed hydroformylation of model substrate **42**

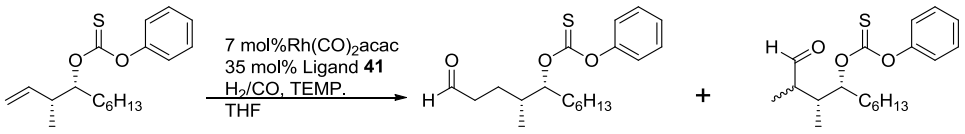

entry	pressure	temperature	reaction time	%yield	% recovered
1	15 psi	25 °C	48 h	43%	50%
2	15 psi	25 °C	72 h	65%	30%
3	70 psi	25 °C	48 h	65%	30%
4	70 psi	45 °C	45 h	87%	-
5	100 psi	45 °C	30 h	86%	-
6	120 psi	60 °C	20 h	89%	-

-all reactions conducted at 0.1 M in THF

2.4 CROTYLATION REACTIONS IN THE PRESENCE OF *O*-PHENYL THIONOCARBONATE

The next goal was to determine the compatibility of Brown and Roush crotylation reactions with the new synthetic route using *O*-phenyl thionocarbonate containing aldehyde (4*R*,5*R*)-**43** and (4*R*,5*S*)-**43**. The starting aldehydes was prepared by Rh-catalyzed hydroformylation of alkene (3*R*,4*R*)-**42** and (3*R*,4*S*)-**42** (See Section 2.3.1).

2.4.1 Brown Crotylation of Aldehyde (4*R*,5*R*)-43

The (–)-(*Z*)-Brown reagent was prepared *in situ* as described in Section 2.2.1. Several Brown crotylation reactions of aldehyde (4*R*,5*R*)-**43** were conducted using 1.6 to 2 equiv of Brown reagent, but the isolated yields varied from 51% to 65%. Furthermore, when 3 equiv of Brown reagent was used, only 35% of allylic alcohol (3*R*,4*R*,7*R*,8*R*)-**45** was isolated. There were substantial difficulties associated with the purification of allylic alcohol (3*R*,4*R*,7*R*,8*R*)-**45** because it co-eluted with the isopinol by-product **46**. The low, variable yields were probably due to the multiple flash chromatographies that took place to purify the crude product (Scheme 2.12).

Scheme 2.10. Brown crotylation of aldehyde (4*R*,5*R*)-**43**

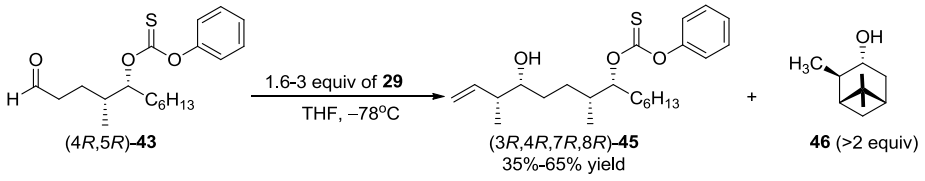

(4*R*,5*R*)-**43**

(3*R*,4*R*,7*R*,8*R*)-**45**
35%-65% yield

46 (>2 equiv)

The Brown crotylation selectivity in the second cycle was determined by integration of the carbinol carbon signals in the ^{13}C NMR spectrum of target allylic alcohol (3*R*,4*R*,7*R*,8*R*)-**45**. As shown in Figure 2.4, the ratio of major to minor peaks was determined to be roughly 86/14

dr. This ratio was consistent with two cycles of Brown crotylation with 93/7 enantioselectivity plus its minor enantiomer (0.93*0.93 + 0.07*0.07 = 0.869). Therefore the enantioselectivity of the second Brown crotylation reaction appeared to also be 93/7 with no apparent erosion of selectivity (Figure 2.4).

Figure 2.4. Determination of enantioselectivity of Brown crotylation of (4*R*,5*R*)-**43** by ^{13}C NMR spectrum

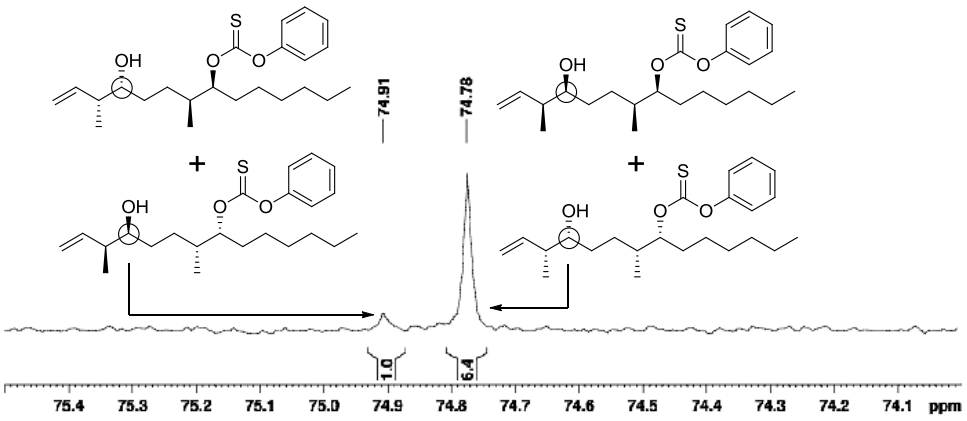

2.4.2 Roush Crotylation of Aldehyde (4*R*,5*S*)-43

The compatibility of *O*-phenyl thionocarbonate functionality with the Roush crotylation reaction was assessed by treating aldehyde (4*R*,5*S*)-**43** (made in two steps from (3R,4S)-**30**) with 2 equiv of a 1.0 M solution of Roush reagent **33** and 4 Å MS in toluene at –78 °C (Scheme 2.13). The initial experiment showed complete consumption of aldehyde (4*R*,5*S*)-**43** after 3 h by TLC. After aq NaOH workup, 87% of the desired allylic alcohol (3*R*,4*S*,7*R*,8*S*)-**45** was isolated by column chromatography. This experiment was repeated several times and consistent yields (83%–87%) were obtained.

Scheme 2.11. Crotylation of aldehyde (4*R*,5*S*)-**43** with Roush reagent **33**

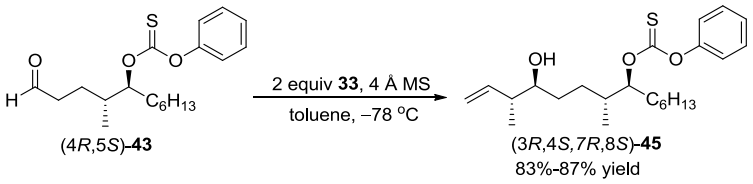

Roush crotylation diastereoselectivity for the second cycle was determined by the integration of carbinol carbon signals of allylic alcohols (3*R*,4*S*,7*R*,8*S*)-**45**. The integrations the carbinol carbon signals in ^{13}C NMR spectra showed an 83/17 ratio of major and minor peaks (Figure 2.5). This ratio was consistent with the two cycles of Roush crotylation of 89/11 enantioselectivity. No erosion of selectivity was observed during the second cycle.

Figure 2.5. Determination of enantioselectivity of Roush crotylation of (4*R*,5*S*)-**43** by ^{13}C NMR spectrum

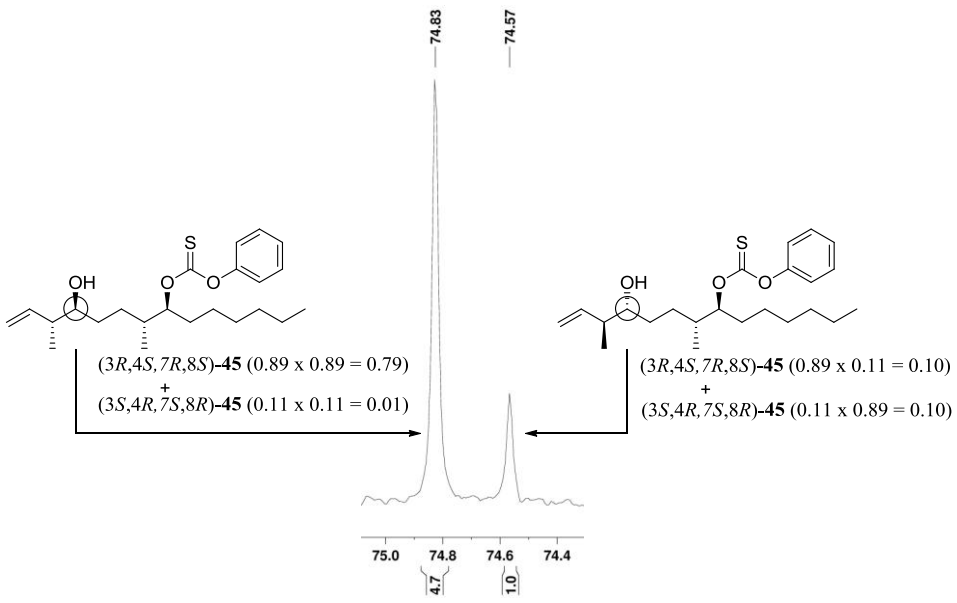

2.4.3 *O*-Phenyl Thionocarbonate Compatibility with Crotylation Reaction Summary

Although the Brown crotylation gave slightly better enantioselectivity, the difficult isolation process resulted in only 35%–63% yield of the target allylic alcohol (3*R*,4*R*,7*R*,8*R*)-**45**. On the other hand, the Roush crotylation gave only moderate enantioselectivity, but it consistently gave 85%–87% yields of target allylic alcohol (3*R*,4*S*,7*R*,8*S*)-**45**. The Roush crotylation was chosen in the new approach because the consistent yields and easy isolation were better suited for the iterative approach.

2.5 FLUOROUS *O*-PHENYL THIONOCARBONATE TAGS

Two different ways to introduce fluorine into the *O*-phenyl thionocarbonate functionality were explored next, either by appending a perfluoroalkyl chain or by substituting fluorine atom(s) directly onto the phenyl ring.

2.5.1 4-Perfluoroalkyl-*O*-Phenyl Thionocarbonate Tags

The first focus was on synthesizing *O*-phenyl thionocarbonate with perfluoroalkyl chains. It was envisioned that these fluorous analogs could be synthesized from 4-perfluoroalkylphenyl chlorothionoformate **51**, which could be accessed from the corresponding 4-perfluoroalkyl phenol **50** in one step (Scheme 2.14).

Scheme 2.12. Synthesis of *O*-4-perfluoroalkylphenyl chlorothionoformate **51**

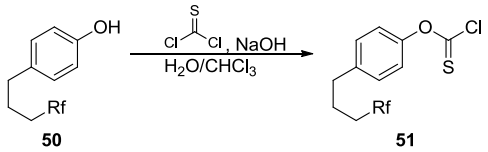

4-(4,4,5,5,6,6,7,7,7-Nonafluorohexyl)phenol **50** was synthesized in three steps from 4-hydroxybenzaldehyde (Scheme 2.15).[40] Benzyl protection of 4-hydroxybenzaldehyde followed by Wittig reaction with iodo(3,3,4,4,5,5,6,6,6-nonafluorohexyl)triphenylphosphorane **48** furnished the benzyl-protected perfluoroalkylphenol **49** in 32% yield over two steps. Hydrogenation of **49** gave the target perfluoroalkylphenol **50** in 97% yield.[40]

Scheme 2.13. Synthesis of 4-(4,4,5,5,6,6,7,7,7-nonafluorohexyl)phenol **50**

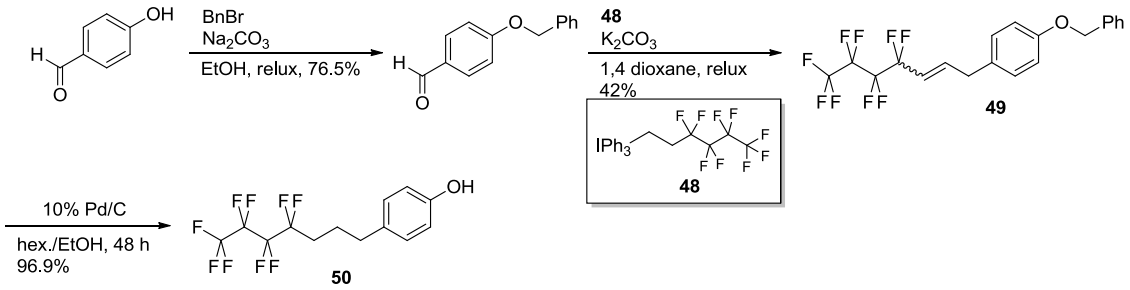

4-(4,4,5,5,6,6,7,7,7-Nonafluorohexyl)phenol **50** was converted to the (*O*-4-(4,4,5,5,6,6,7,7,7-nonafluorohexyl)phenyl)chlorothionoformate **51** upon treatment with thiophosgene in the presence of aq NaOH. The crude product **51** was used directly in the thionoacylation step without further purification. The structure of **51** was confirmed by a reaction with ethanol to give the corresponding ethyl(*O*-4-(4,4,5,5,6,6,7,7,7-nonafluorohexyl)-phenyl)chlorothionoformate **52** in 80% yield (Scheme 2.16).

Scheme 2.14. Verification of formation of **51** by reaction with ethanol

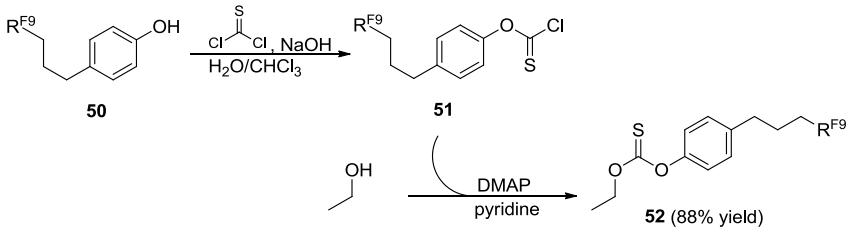

Reaction of model allylic alcohol (3*R*,4*R*,7*R*,8*R*)-**45** with **52** in the presence of 5 equiv of pyridine in CH_2Cl_2 did not give the desired *bis*-*O*-phenyl thionocarbonate containing product. Instead, 95% of starting alcohol (3*R*,4*R*,7*R*,8*R*)-**45** was recovered. Other acylation attempts with stronger bases such as NaH or NaHMDS resulted in decomposition of (3*R*,4*R*,7*R*,8*R*)-**45**.

As a control experiment, allylic alcohol (3*R*,4*R*,7*R*,8*R*)-**45** was also reacted with *O*-phenyl chlorothionoformate in CH_2Cl_2 in the presence of pyridine (5 equiv), and this successfully furnished the desired *bis*-*O*-phenyl thionocarbonated product (3*R*,4*R*,7*R*,8*R*)-**53** in 90% yield (Scheme 2.17). This experiment shows that it is possible to attach a second *O*-phenyl thionocarbonate group to the allylic alcohol (3*R*,4*R*,7*R*,8*R*)-**45**. Because the perfluoroalkyl analog of *O*-phenyl chlorothiono-formate could not be attached to model allylic alcohol (3*R*,4*R*,7*R*,8*R*)-**45**. Therefore the second strategy in which the fluorine atoms were attached directly on the phenyl ring was explored.

Scheme 2.15. Synthesis of **53** as control experiment

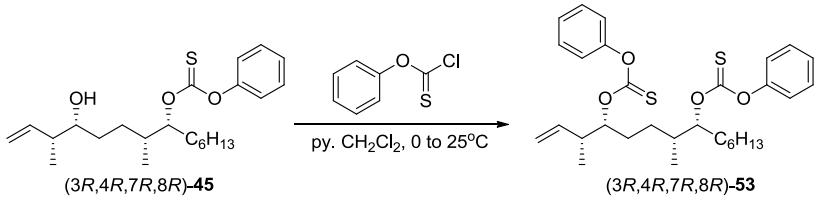

2.5.2 Ultra-Light Fluorous *O*-Phenyl Thionocarbonate Tags

The syntheses of fluorine-substituted *O*-phenyl thionoformates were examined. The *O*-phenyl chlorothionoformates **56** and **59** were commercially available. The other *O*-phenyl thionocarbonates **54**, **55**, **56**, **57**, **58**, and **59** were synthesized by reaction the corresponding fluorinated phenol with thiophosgene in the presence of aq NaOH (Scheme 2.18).

Scheme 2.16. Syntheses of "fluorous" *O*-phenyl chlorothionoformate **54** to **59**

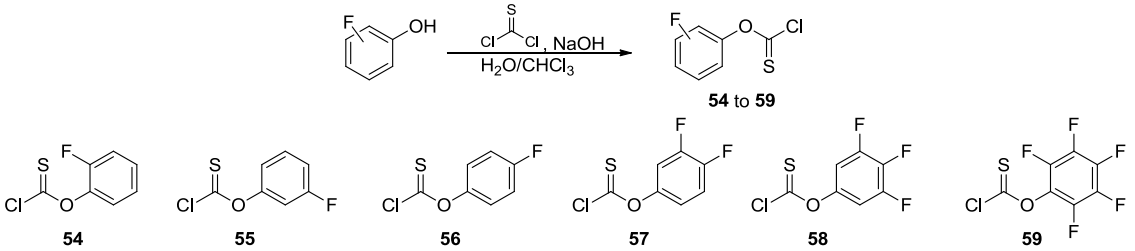

Reactions of fluorous *O*-phenyl chlorothionoformates **54**, **55**, **56**, **57**, **58** and **59** with allylic alcohol (3*R*,4*R*,7*R*,8*R*)-**45** in the presence of pyridine (5 equiv) in CH_2Cl_2 successfully furnished the corresponding fluorinated analogs of the *bis*-*O*-phenyl thionocarbonate tagged olefins **60**, **61**, **62**, **63**, and **64** (Scheme 2.19). The only exception was the reaction of alcohol (3*R*,4*R*,7*R*,8*R*)-**45** with **59** which resulted in decomposition.

Scheme 2.17. Syntheses of model "fluorous" *bis*-*O*-phenyl thionocabonate tagged olefins

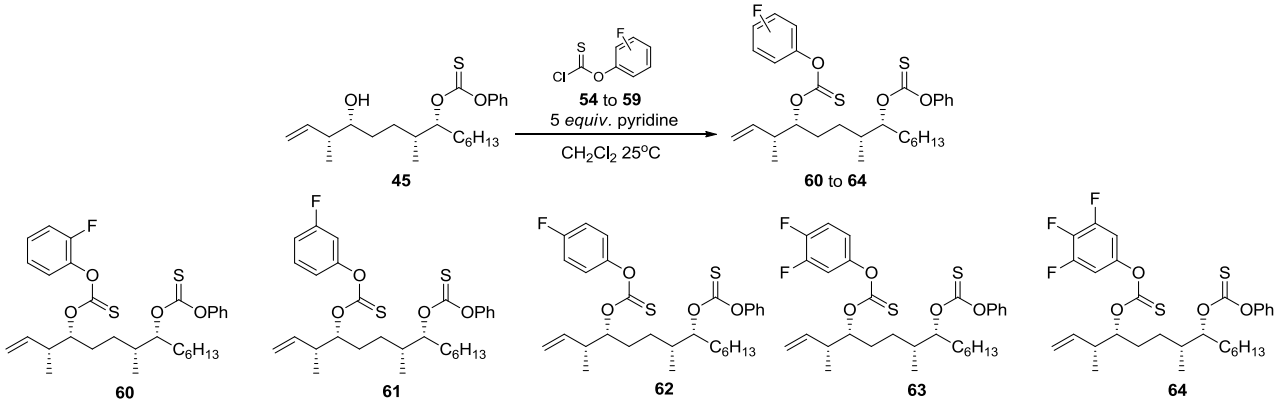

The F-HPLC separation of these fluorous *bis*-*O*-phenyl thionocarbonate molecules **53**, **60**, **61**, **62**, **63**, and **64** was examined using a FluoroFlash^{TM} (PF-C8) column. The elution time of each fluorous analog was established first by individual injections before co-injection of all six compounds. The HPLC trace of the co-injection shows five separate peaks based on increasing fluorine content with one overlapping peak that contained mono-fluorinated analogs **61** and **62** (Figure 2.6). The F-HPLC with a PFP column gave a similar separation pattern except the **53** and **60** fractions, which overlapped on a PFP column (Appenix B, Figure 1).

Figure 2.6. Fluorous HPLC trace of **53**, **60**, **61**, **62**, **63**, and **64** mixture by PF-C8 column[a)]

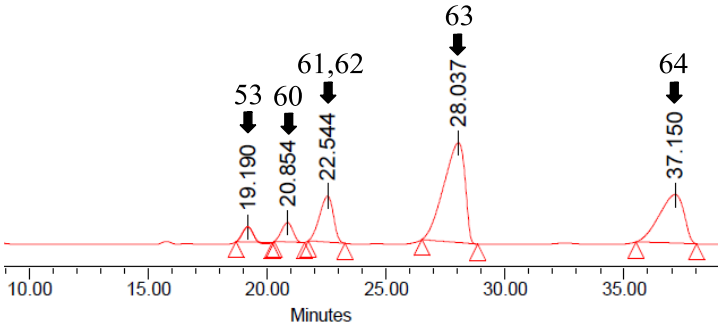

a. conditions: isocratic 75/25 acetonitrile: H_2O, 1 mL/min

2.5.3 *O*-Phenyl Thionocarbonate Fluorous Tag Summary

Two different analogs of *O*-phenyl chlorothionoformate, one with a perfluoroalkyl chain, and the other with direct fluorine substitution on the phenyl rings were synthesized. The acylation reactions to append the analog with perfluoroalkyl chain to model allylic alcohol (3*R*,4*R*,7*R*,8*R*)-**45** were unsuccessful. The acylation reactions of (3*R*,4*R*,7*R*,8*R*)-**45** with fluorinated phenyl analogs of *O*-phenyl chlorothionoformate were successful. The resulting *bis*-*O*-phenyl thionocarbonate molecules **53**, **60**, **61** (or **62**), **63**, and **64** were separable by F-HPLC.

3.0 THE FMS OF FOUR ISOMERS OF 4,8,12-TRIMETHYLNONADECANOL USING ULTRA-LIGHT FLUOROUS *O*-PHENYL THIONOCARBONATE TAGS

After developing a high yielding route that is compatible with the use of *O*-phenyl thionocarbonate group tags and successfully validating the fluorous separations of model compounds containing the new tags, the FMS of 4,8,12-trimethylnonadecanol could commence.

The new synthetic plan involved three cycles of Roush crotylation, tagging, and Rh-catalyzed hydroformylation followed by aldehyde reduction, demixing, and finally global deoxygenation to furnish the (4*S*,8*S*,12*S*)-, (4*S*,8*R*,12*S*)-, (4*R*,8*S*,12*S*)-, and (4*R*,8*R*,12*S*)-trimethylnonadecanol isomers (Scheme 3.1).

Scheme 3.1. Synthetic plan of FMS of four isomers of 4,8,12-trimethylnonadecanol

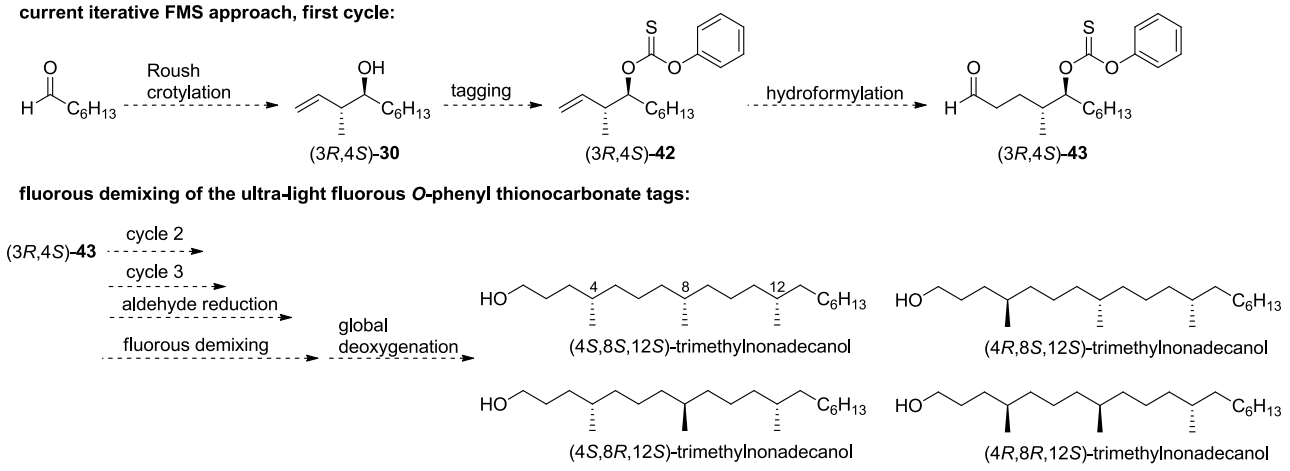

3.1 THE NEW APPROACH WITH *O*-PHENYL, *O*-2-FLUOROPHENYL, AND *O*-4-FLUOROPHENYL THIONOCARBONATE TAGS

3.1.1 Tagging Scheme

This FMS follows an *en route* double tagging strategy using three different ultra-light *O*-phenyl thionocarbonate tags. In this first attempt of the new route, the hope was that the lowest possible number of fluorine atoms to encode the four isomers could be used. As shown in Section 2.5.2, the three lowest separable tags were the *O*-phenyl thionocarbonate (F^0), the *O*-2-fluorophenyl (F^1) and the *O*-4-fluorophenyl thionocarbonate ($F^{1'}$) tags.

After the tags were chosen, the tagging was devised. During the first cycle, the hydroxy group adjacent to the methyl stereocenter fixed at the *R* configuration would be tagged with the F^0 tag. During the second cycle, the hydroxy group adjacent to the *R* methyl stereocenter would be tagged with the F^0 tag, and the hydroxy group adjacent to the *S* methyl stereocenter would be tagged with a F^1 tag. During the third cycle, the hydroxy group adjacent to the *R* methyl stereocenter would be tagged the F^0 tag and the hydroxy group adjacent to the *S* methyl stereocenter would be tagged with a $F^{1'}$tag. This tagging scheme would result in the use of only two fluorine atoms to encode for four quasiisomers (Scheme 3.2).

Scheme 3.2. Tagging scheme of the first attempt of the new approach

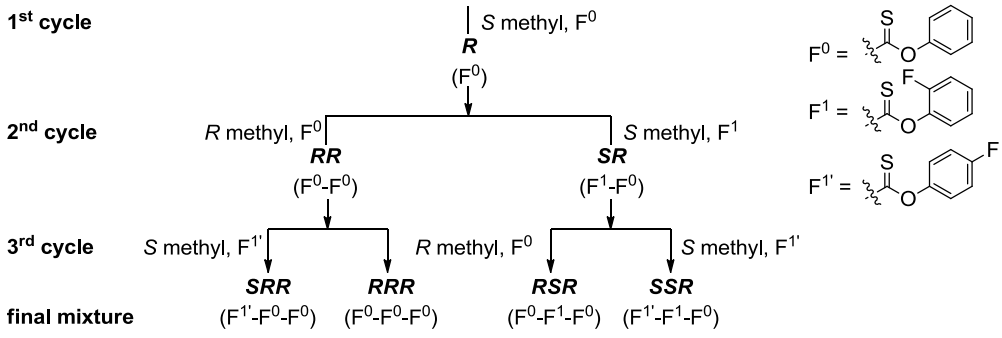

3.1.2 First Cycle

The first cycle started with Roush crotylation of heptanal with diisopropyl-D-tartrate-(*E*)-crotylborate **33** in toluene at –78 °C. This furnished (3*R*,4*S*)-3-methyldec-1-en-4-ol **30** in 88% yield with 89/11 enantioselectivity (Section 2.2.2.). Allylic alcohol (3*R*,4*S*)-**30** in CH_2Cl_2 was then treated with *O*-phenyl chlorothionoformate (1.5 equiv) in the presence of pyridine (5 equiv) at 25 °C to give the F^0-tagged alkene (3*R*,4*S*)-**42** in 85% yield. Hydroformylation of (3*R*,4*S*)-**42** in the presence of 7 mol% $Rh(CO)_2$acac and 35 mol% pyridone ligand **41** under 120 psi of syngas at 60 °C afforded aldehyde (3*R*,4*S*)-**43** in 80% yield. The overall yield for the first cycle was 60% over 3 steps (Scheme 3.3).

Scheme 3.3. First cycle of the initial second generation approach

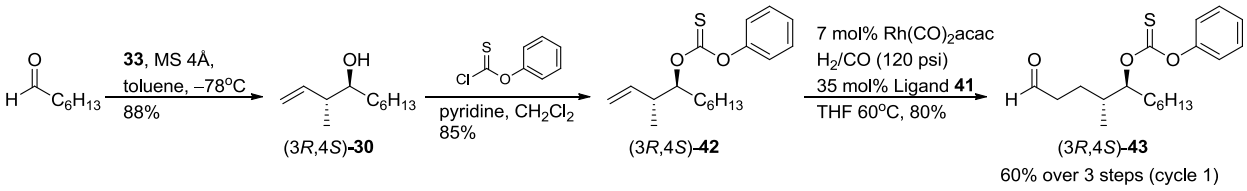

3.1.3 Second Cycle

To start the second cycle, aldehyde (3*R*,4*S*)-**43** was split into two half-portions. One half portion was reacted with diisopropyl-D-tartrate-(*E*)-crotylborate **33** to give allylic alcohol (3*R*,4*S*,7*R*,8*S*)-**45** in 83% yield with 82/18 dr, and the other half portion was reacted with diisopropyl-L-tartrate-(*E*)-crotylborate **34** to give allylic alcohol (3*S*,4*R*,7*R*,8*S*)-**45** in 83% yield with 83/17 dr (see Section 2.4.2). Allylic alcohol (3*R*,4*S*,7*R*,8*S*)-**45** in CH_2Cl_2 was treated with *O*-phenyl chlorothionoformate in the presence of pyridine (5 equiv) at 25 °C to furnish *bis*-(F^0,F^0)-tagged alkene (3*R*,4*S*,7*R*,8*S*)-**53** in 81% yield. Allylic alcohol (3*S*,4*R*,7*R*,8*S*)-**45** in

CH_2Cl_2 was treated with *O*-2-fluorophenyl chlorothionoformate **54** in the presence of pyridine (5 equiv) at 25 °C to give the *bis*-(F^0,F^1)-tagged alkene (3*S*,4*R*,7*R*,8*S*)-**60** in 84% yield. A 1:1 mixture of (3*R*,4*S*,7*R*,8*S*)-**53** and (3*S*,4*R*,7*R*,8*S*)-**60** was then subjected to the Rh-catalyzed hydroformylation afford mixture aldehyde M-**65** in 82% yield. The overall yield for the second cycle was 56% over 3 steps (Scheme 3.4).

Scheme 3.4. Second cycle of the initial second generation approach

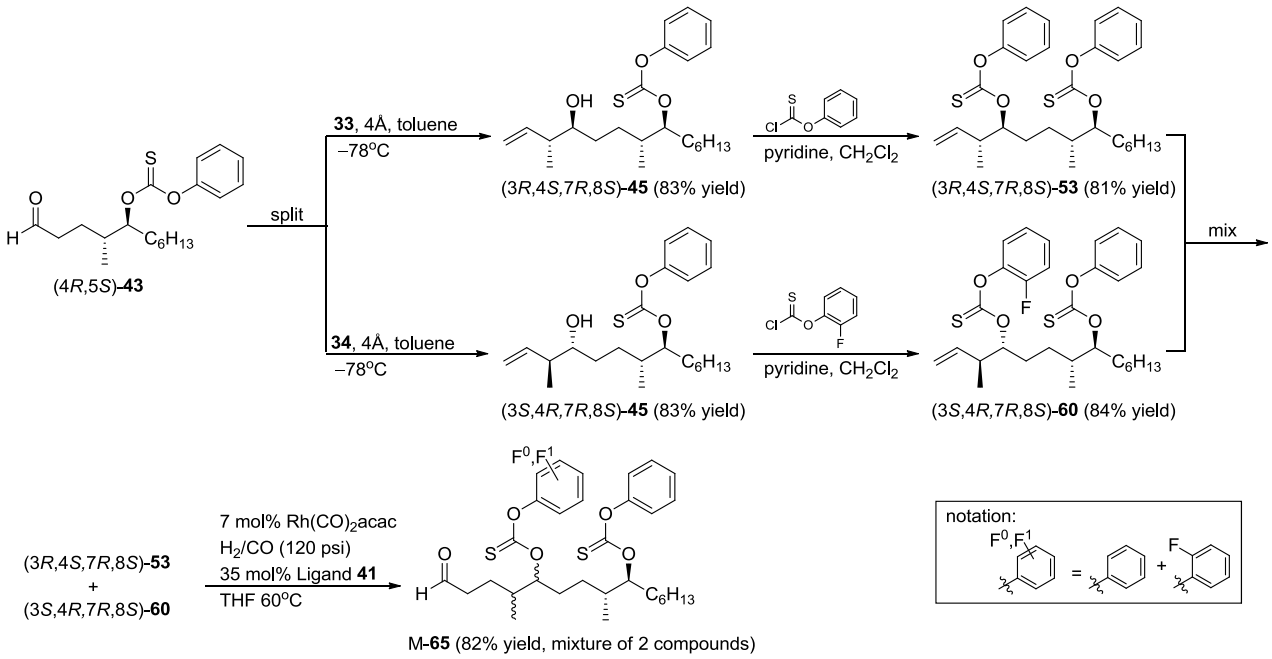

3.1.4 Third Cycle

To start the third cycle, aldehyde M-**65** was again split into two half portions. One half was reacted with diisopropyl-D-tartrate-(*E*)-crotylborate **33** to give mixture allylic alcohol M-**66** in 80% yield, and the other half was reacted with diisopropyl-L-tartrate-(*E*)-crotylborate **34** to give mixture allylic alcohol M-**67** in 83% yield. Allylic alcohol M-**66** in CH_2Cl_2 was treated with *O*-phenyl chlorothionoformate in the presence of pyridine (5 equiv) at 25 °C to give alkene

M-**68** in 87% yield. Allylic alcohol M-**67** in CH_2Cl_2 was treated with *O*-4-fluorophenyl chlorothionoformate **56** in the presence of pyridine (5 equiv) at 25 °C to give alkene M-**69** in 84% yield. Following fluorous tagging, a 1:1 mixture of M-**68** and M-**69** was subjected to Rh-catalyzed hydroformylation reaction to afford mixture aldehyde M-**70** in 83% yield. The third cycle gave the overall yield of 58% yield over three steps. Mixture aldehyde M-**70** was reduced by DIBAL-*H* at 0 °C to furnish the mixture of four fluorous-tagged quasiisomers of 4,8,12-trimethylnonadecanol M-**71** in 87% yield (Scheme 3.5). The overall yield was 17% yield over 16 steps, and 140 mg of M-**71** was obtained at the end of the synthesis.

Scheme 3.5. Third cycle of the initial second generation approach

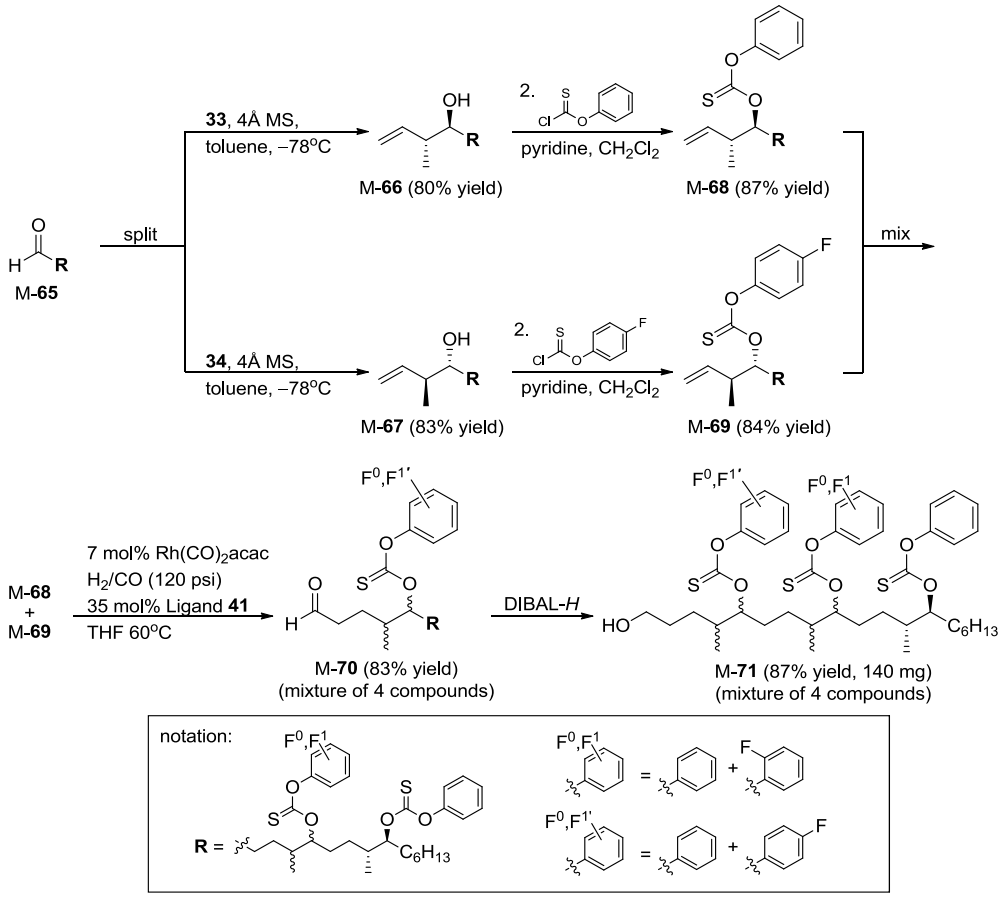

3.1.5 Characterizations and Fluorous Demixing of Mixture M-71

The ^{19}F NMR spectrum of M-**71** showed the presence of both the *O*-2-fluorophenyl and the *O*-4-fluorophenyl thionocarbonate tags, and the ^{1}H NMR spectrum of M-**71** at 700 MHz showed the presence of a triplet signal at 3.64 ppm, which is consistent with the carbinol signal of a primary alcohol, and a multiplet signal at 5.39 ppm, which is consistent with the secondary carbinol proton signals. A triplet signal at 0.89 ppm, which was consistent with the terminal methyl group was identified. The HRMS of M-**71** confirmed the presence of all four quasiisomers.

The mixture M-**71** was first injected into F-HPLC with a FluoroFlash^{TM} (PF-C8) column and eluted with isocratic 65:35 acetonitrile/H_2O system (Figure 3.1). Four different fluorous quasiisomers were observed but they eluted too closely to be isolated individually. M-**71** was also analyzed by a Discovery® HS F5 PFP column on F-HPLC, but the trace gave even less separation between each fluorous quasiisomers than the analysis on a FluoroFlash^{TM} (Appendix.B, Figure 2). Although four peaks could be observed using the FluoroFlash^{TM} PF-C8 column, baseline resolution was only achieved between peaks 2 and 3. It was concluded that preparative demixing on a larger scale would not succeed.

Figure 3.1. Fluorous HPLC trace of mixture M-**71** by PF-C8 column

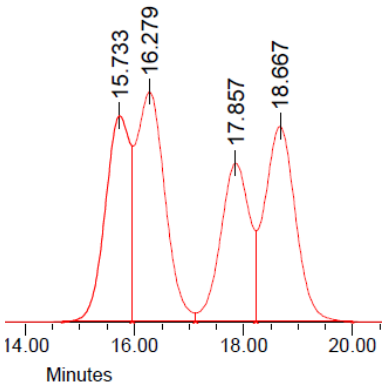

3.2 THE NEW APPROACH WITH *O*-PHENYL, *O*-4-FLUOROPHENYL, AND *O*-3,4-DIFLUOROPHENYL THIONOCARBONATE TAGS

3.2.1 Tagging Scheme

It was hypothesized that the tight separations between peaks 1 and 2, and peaks 3 and 4 in the previous attempt were due to the use of the *O*-2-fluorophenyl thionocarbonate (F^1) tag (Figure 3.1). To circumvent this problem, the F^1 tag was substituted with the *O*-3,4-difluorophenyl thionocarbonate (F^2) tag in the second attempt. The three tags used in this second attempt were *O*-phenyl (F^0), *O*-4-fluorophenyl ($F^{1'}$) and *O*-3,4-difluorophenyl (F^2) thionocarbonate tags. This new attempt would start from the second cycle because the first cycle was identical to the first attempt.

During the second cycle, it was planned to tag the hydroxy group adjacent to the *R* methyl with the F^0 tag, and tag the hydroxy group adjacent to the *S* methyl with the $F^{1'}$tag. During the third cycle, it was planned to tag the hydroxy group adjacent to the *R* methyl with the F^0 tag, and tag the hydroxy group adjacent to the *S* methyl with the F^2 tag (Scheme 3.6). This tagging scheme would result in the use of six fluorine atoms to encode for four isomers.

Scheme 3.6. Tagging scheme of the new second generation approach

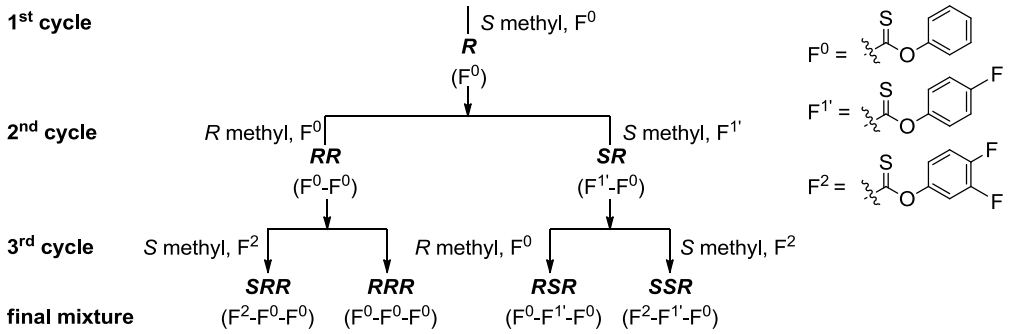

3.2.2 Second Cycle

The product of the first cycle, aldehyde (3*R*,4*S*)-**43** was split into two half portions. The first half portion was reacted with diisopropyl-D-tartrate-(*E*)-crotylborate **33** to give allylic alcohol (3*R*,4*S*,7*R*,8*S*)-**45** in 88% yield. The second half portion was reacted with diisopropyl-L-tartrate-(*E*)-crotylborate **34** to give allylic alcohol (3*S*,4*R*,7*R*,8*S*)-**45** in 84% yield. Allylic alcohol (3*R*,4*S*,7*R*,8*S*)-**45** was treated with *O*-phenyl chlorothionoformate in the presence of pyridine (5 equiv) at 25 °C to give *bis*-(F^0-F^0)-tagged alkene (3*R*,4*S*,7*R*,8*S*)-**53** in 84% yield. Allylic alcohol (3*S*,4*R*,7*R*,8*S*)-**45** in CH_2Cl_2 was treated with *O*-4-fluorophenyl chlorothionoformate **56** in the presence of pyridine (5 equiv) at 25 °C to give *bis*-(F^0-$F^{1'}$)-tagged alkene (3*S*,4*R*,7*R*,8*S*)-**62** in 84% yield. After fluorous tagging, a 1:1 mixture of (3*R*,4*S*,7*R*,8*S*)-**53** and (3*S*,4*R*,7*R*,8*S*)-**62** was subjected to the Rh-catalyzed hydroformylation reaction to afford aldehyde M-**72** in 82% yield. The overall yield for the second cycle was 59.4% over 3 steps (Scheme 3.7).

Scheme 3.7. Second cycle of the second attempt of the new FMS approach

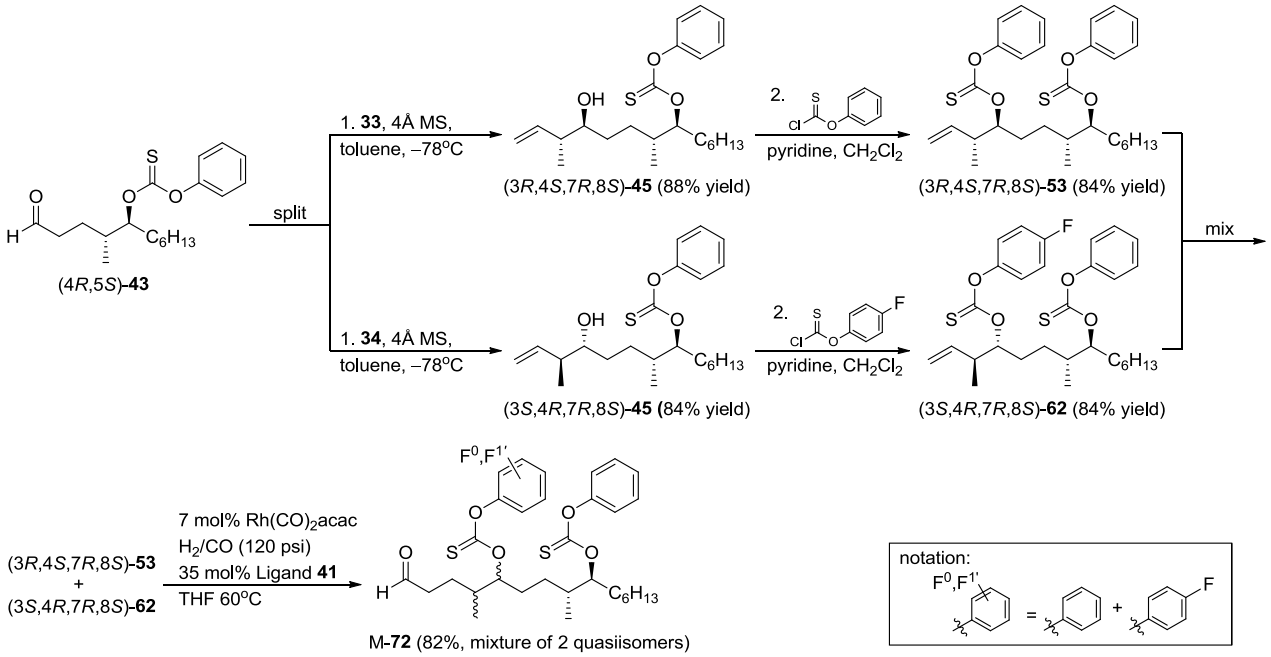

3.2.3 Third Cycle

The third cycle started with splitting of aldehyde M-**72** in two half portions. The first half portion was reacted with diisopropyl-D-tartrate-(*E*)-crotylborate **33** to give mixture allylic alcohol M-**73** in 84% yield. The second half portion was reacted with diisopropyl-L-tartrate-(*E*)-crotylborate **34** to give mixture allylic alcohol M-**74** in 84% yield. Mixture allylic alcohol M-**73** was reacted with *O*-phenyl chlorothionoformate in the presence of pyridine (5 equiv) to give alkene M-**75** in 86% yield. Mixture allylic alcohol M-**74** was reacted with *O*-3,4-difluorophenyl chlorothionoformate **57** in the presence of pyridine (5 equiv) to give alkene M-**76** in 88% yield. A 1:1 mixture of M-**75** and M-**76** was subjected to the Rh-catalyzed hydroformylation to afford mixture aldehyde M-**77** in 80% yield. Aldehyde M-**77** was reduced by DIBAL-*H* at 0 °C to give 880 mg of a mixture of four fluorous tagged 4,8,12-nonadecanols M-**78** in 88% yield (Scheme 3.8). The yield for the third cycle was 56% over 3 steps. The overall yield for the synthesis of M-**78** was 18% over 16 steps. The yields per cycle were reliably between 56% and 60%.

Scheme 3.8. Third cycle of the second attempt of the new FMS approach

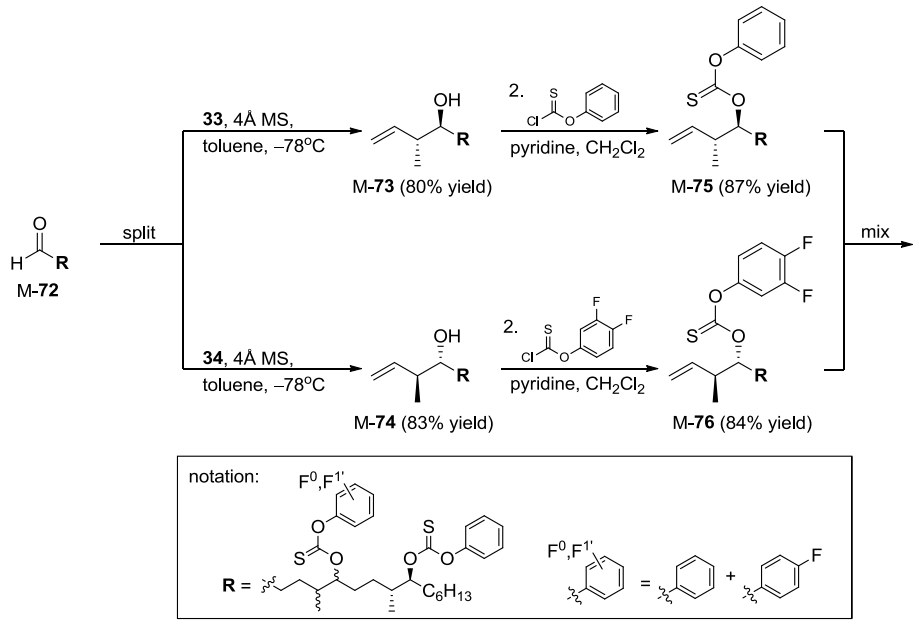

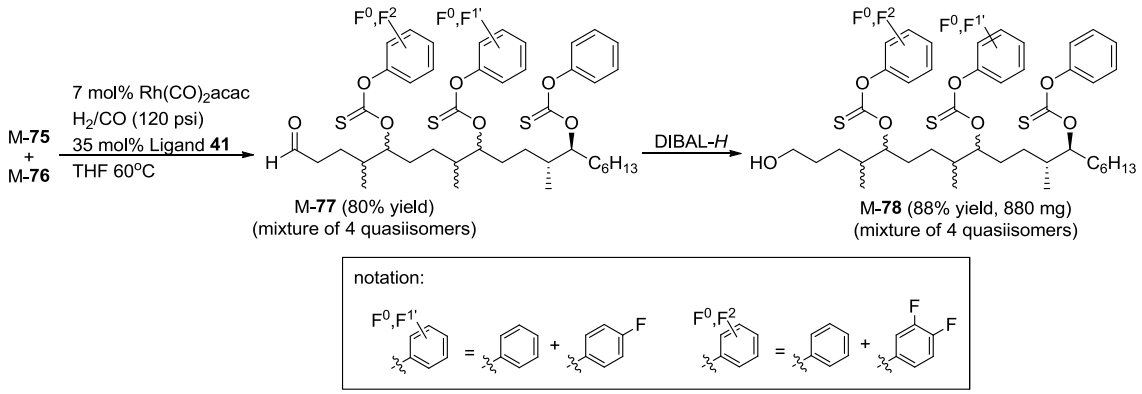

3.2.4 Characterizations and Fluorous Demixing of Mixture M-78

The ^{19}F NMR spectrum of M-**78** showed the presence of both the *O*-4-fluorophenyl and the *O*-3,4-difluorophenyl thionocarbonate tags, and the ^{1}H NMR spectrum of M-**78** showed the presence of a triplet at 3.65 ppm which is consistent with the carbinol signal of a primary alcohol and a multiplet at 5.33 ppm, which is consistent with the secondary carbinol proton signal. A triplet signal at 0.892 ppm, which is consistent with the terminal methyl group was also identified. The HRMS of M-**78** confirmed the presence of all four quasiisomers.

Injection of M-**78** into F-HPLC with a Fluoro*Flash*^{TM} PF-C8 column eluting with isocratic 65:35 (acetonitrile/H_2O) gave baseline separation of all four quasiisomers (Figure 3.2). Analysis of M-**78** on Discovery® HS F5 PFP column gave a similar separation, but the analysis of M-**78** on the reverse phase RP-C18 column gave only one large unresolved peak (Appendix B, Figure 3).

Figure 3.2. Fluorous HPLC trace of mixture M-**78** by PFC-8 column[a)]

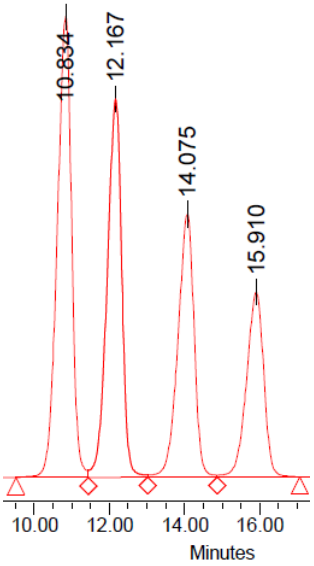

a) conditions: isocratic 70/30 acetonitrile: H_2O, 1 mL/min

The semi-prep scale F-HPLC demixing of alcohol M-**78** was achieved on the PF-C8 column (Fluoro*Flash*® 100 Å, 5 µm) by eluting with a gradient of 60:40 CH_3CN/H_2O to 100% CH_3CN over 1 h (Figure 3.3). Because of the close elution of the four peaks, the demixing was accomplished by several 1 mL injections of 10 mg/mL of M-**78** in CH_3CN. The four different peaks were collected and the products were identified by ^{19}F NMR. The first peak, which did not give any signal in the ^{19}F NMR spectrum, was identified as the (4*R*,5*S*,8*R*,9*S*,12*R*,13*S*)-**78** quasiisomer; the second peak, which gave 1 fluorine signal at –115.89 ppm in the ^{19}F NMR spectrum, was identified as the (4*R*,5*S*,8*S*,9*R*,12*R*,13*S*)-**78** quasiisomer; the third peak, which gave 2 fluorine signals at –134.14 and –139.75 ppm, was identified as the (4*S*,5*R*,8*R*,9*S*,12*R*,13*S*)-**78** quasiisomer; and the fourth peak, which gave 3 fluorine signals at –115.77, –134.14 and –139.63 ppm, was identified as the (4*S*,5*R*,8*S*,9*R*,12*R*13*S*)-**78** quasiisomer.

Figure 3.3. Semi-prep fluorous HPLC trace of mixture M-**78** by PF-C8 column[a)]

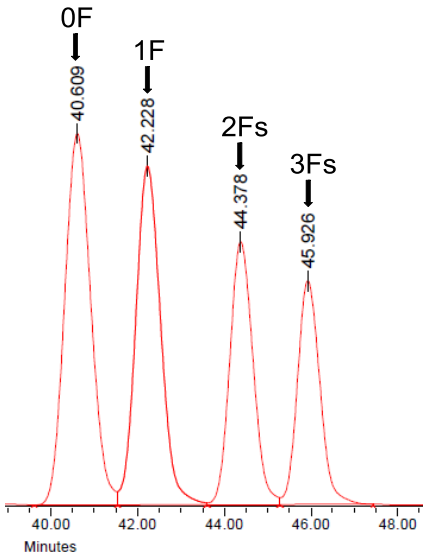

conditions: gradient 60:40 to 100:0 acetonitrile: H_2O, 5 mL/min

Overall, 107 mg of M-**78** was subjected to semi-prep HPLC, the recovery of each isomer is summarized in Table 3.1. The overall % recovery was calculated to be ~70%. To confirm the purity of each quasiisomer, each fraction was re-injected to the HPLC under analytical conditions. The F-HPLC traces showed that the first quasiisomer was pure, but that the following three quasiisomers were contaminated with 1–3% of the previous isomer (Figure 3.4). Since the samples were expected to have ~35% of true isomer contaminants from the Roush crotylations, the 1–3% of quasiisomer contaminants were not significant in comparison. So the samples were detagged without further purification.

Table 3.1. Recovery of each isomer after demixing

	recovered (mg)	% recovery
(4*S*,8*S*,12*S*)-**78**	20	74%
(4*S*,8*R*,12*S*)-**78**	19	71%
(4*R*,8*S*,12*S*)-**78**	16	68%
(4*R*,8*R*,12*S*)-**78**	20	67%

Figure 3.4. F-HPLC trace of each quasiisomer by PF-C8 column

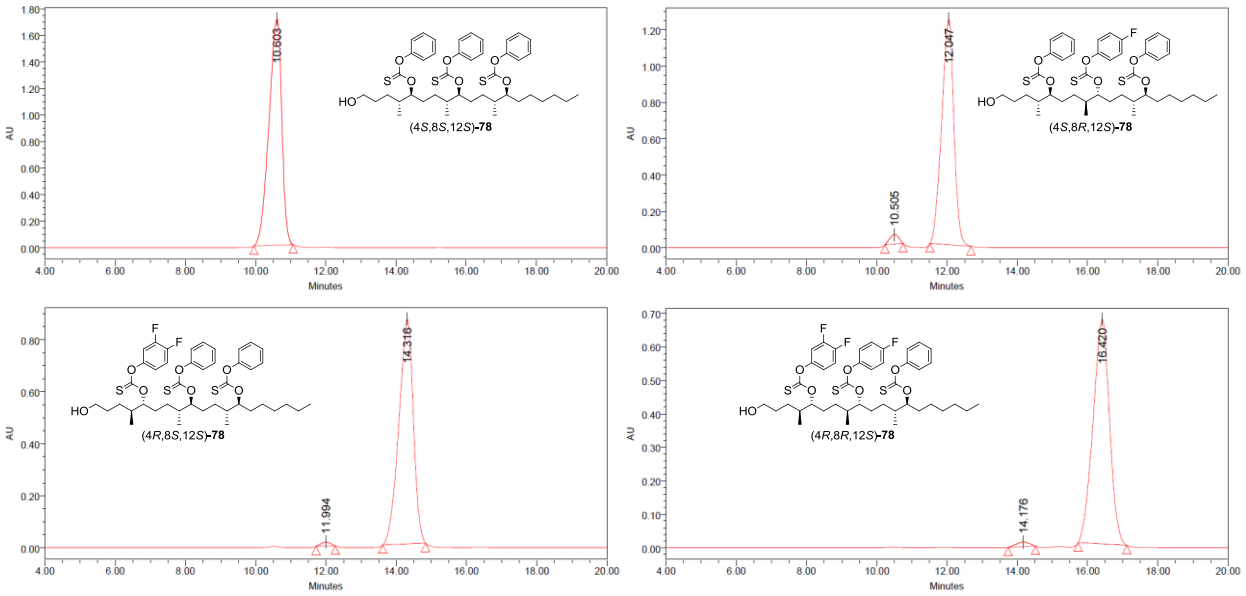

3.2.5 Global Radical Deoxygenation (Detagging) of F-*O*-Phenyl Thionocarbonate

The global radical deoxygenation step was first evaluated with mixture M-**78** using dimethylimidazolium carbene borane (diMe-Imd-BH_3) at room temp and with heating conditions.[41] In the room temp experiment, 5 equiv of both diMe-Imd-BH_3 and Et_3B were added to a solution of M-**78** in benzene-d_6. The mixture was initially stirred in open air for 3 h, TLC analysis showed that staring alcohol M-**78** remained, so an additional 5 equiv of Et_3B was added. After 3 h more, the solvent was removed. The ^{1}H NMR spectrum of the crude product showed a large signal at 5.33 ppm, indicating the presence of the secondary *O*-phenyl thionocarbonate and showing that incomplete deoxygenation. In the heated condition, 5 equiv of both diMe-Imd-BH_3 and AIBN were added to a solution of M-**78**, and the mixture was heated to 80 °C. After 3 h, TLC analysis showed the complete consumption of alcohol M-**78**. The mixture 4,8,12-trimethylnonadecanol M-**79** was isolated in 75% yield after flash chromatography (Scheme 3.9).

The ^{19}F NMR spectrum of M-**79** showed no signals, indicating that no fluorous tags remained. This sample served as the standard for spectroscopic characterization of the mixed products. It should contain four different isomers in a ratio of 1/1/1/1.

Scheme 3.9. Model radical global deoxygenation of mixture M-**78**

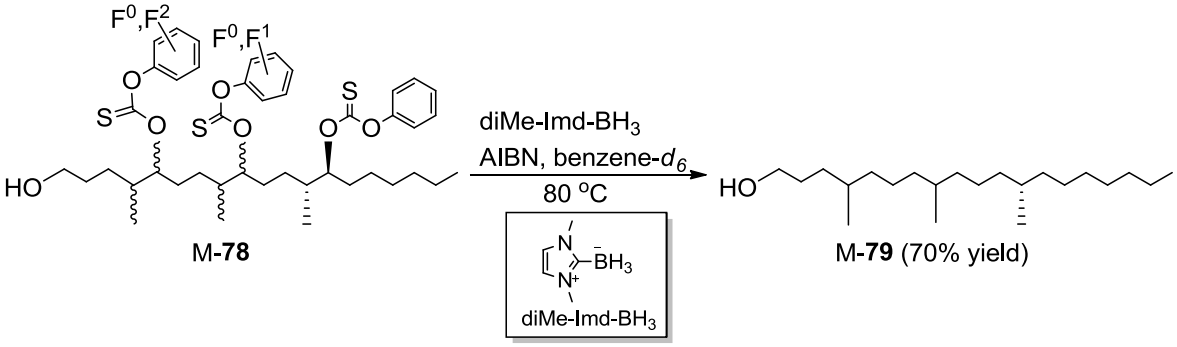

The global deoxygenation of quasiisomers (4*R*,5*S*,8*R*,9*S*,12*R*,13*S*)-**78**, (4*R*,5*S*,8*S*,9*R*,12*R*,13*S*)-**78**, (4*S*,5*R*,8*R*,9*S*,12*R*,13*S*)-**78**, and (4*S*,5*R*,8*S*,9*R*,12*R*,13*S*)-**78** were accomplished by heating with diMe-Imd-BH_3/AIBN to afford (4*S*,8*S*,12*S*)-**79**, (4*S*,8*R*,12*S*)-**79**, (4*S*,8*R*,12*S*)-**79**, and (4*R*,8*R*,12*S*)-**79** in 67%, 52%, 65%, and 63% yields, respectively after purification by column chromatography (Scheme 3.10).

Scheme 3.10. Global radical deoxygenation of four quasiisomers

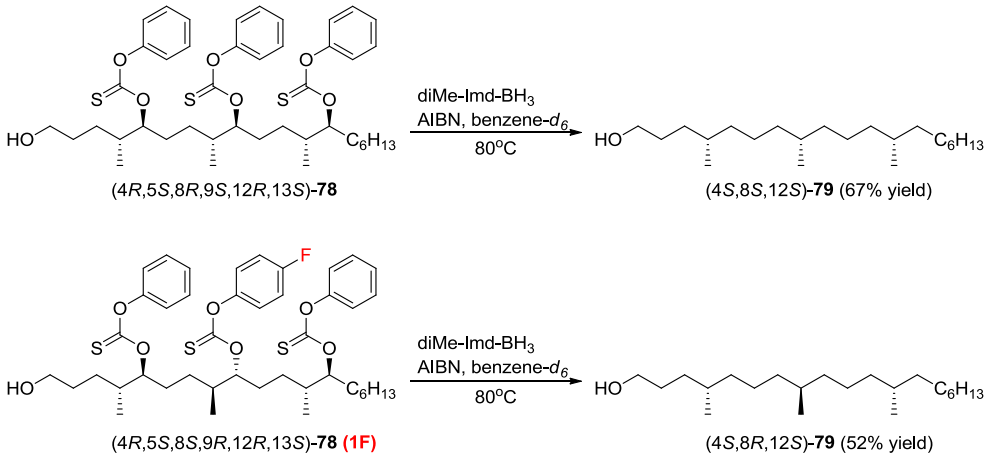

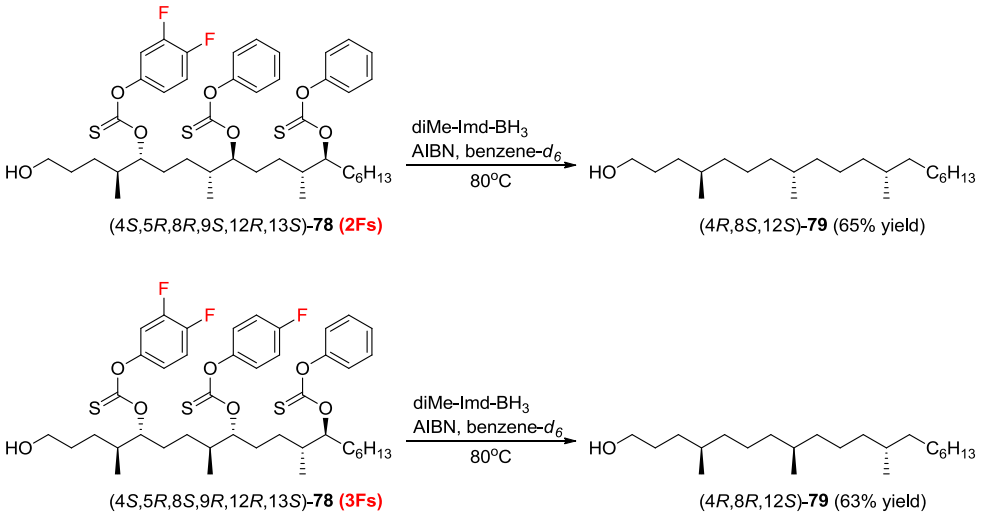

3.2.6 FMS Summary

The FMS of four isomers of 4,8,12-trimethylnonadecanol was accomplished in 16 steps (including F-HPLC recovery, and the global deoxygenation steps) with an average of 7.8% overall yield. This FMS was accomplished by using the new ultra-light fluorous *O*-phenyl thionocabonate tags. These new fluorous tags were used to successfully encode four stereoisomers with only six fluorine atoms, making it the most efficient FMS to date. This is a dramatic improvement over the previously most efficient FMS (FMS of SCH725674),[9c] which used 30 fluorine atoms to code for four isomers.

3.3 SPECTROSCOPIC ANALYSES OF FOUR ISOMERS OF 4,8,12-TRIMETHYLNONADECANOL

3.3.1 Analyses of ^{1}H NMR Spectra of M-79 and Four Isomers of 4,8,12-Trimethyl-nonadecanol

The ^{1}H NMR spectra of the mixture M-**79** and the four individual isomers were recorded in $CDCl_3$ at 700 MHz, and the complete ^{1}H NMR spectra are shown in Appendix E. The five spectra were similar in all respects except for the methyl region (0.82–0.90 ppm). To simplify the labeling of the branched methyl groups, the terminal methyl is herein designated as 19, C4-methyl as 20, the C8-methyl as 21, and the C12-methyl as 22 (Figure 3.5).

Figure 3.5. Designations of the methyl groups in 4,8,12-trimethylnonadecanol **79**

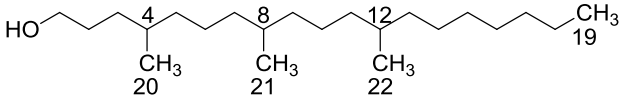

Upon expanding the methyl region (0.82–0.90 ppm) of the four spectra of single isomers, we learned that all the branched methyl group protons (H20, H21, and H22) signals are distinguishable in all four isomers. Furthermore, each spectrum showed a unique combination of chemical shifts for the major H20, H21, and H22 signals, and the terminal methyl group H19 signal remained the same in all four spectra. The ^{1}H NMR spectra from standard processing did not give good enough resolution to show all the signals, however, because they are so close. Therefore, each spectrum was subjected to additional processing by using the Traficante algorithm followed by forward linear prediction to improve the resolution.[42] Figure 3.6 shows the overlay of the methyl region of (4*S*,8*S*,12*S*)-**79** spectrum of the before and after additional processing. The red spectrum was generated with standard processing and the black spectrum

was generated with the Traficante processing. The black spectrum clearly resolves the two overlapping doublets of 0.844 and 0.840 ppm (right group of peaks), and the overlapping doublet and triplet of 0.882 and 0.874 ppm (left group of peaks). Small peaks of expected stereoisomer impurities are also clearly visible.

Figure 3.6. ^{1}H NMR spectra between regular and the Traficante algorithm processing

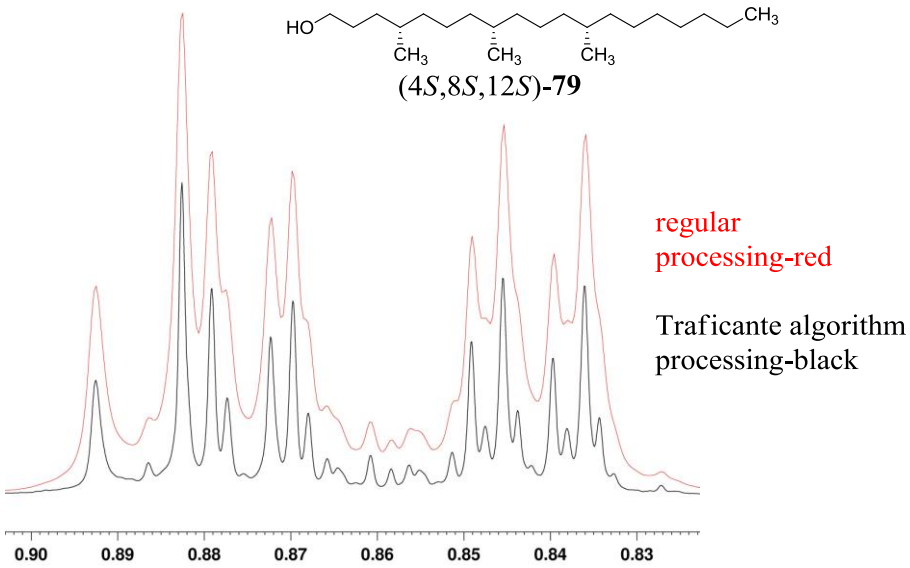

By lining up the methyl regions of the four ^{1}H NMR spectra (Figure 3.7), it was learned that both (4*S*,8*S*,12*S*)-**79** (spectrum 2) and (4*R*,8*R*,12*S*)-**79** (spectrum 5) contained a doublet at 0.874 ppm, but the other two signals differed. These two isomers also both have the C20 in a *syn* relationship to the C21. It was deduced that the 0.874 ppm signal must belong to the H20 in both (4*S*,8*S*,12*S*)-**79** and (4*R*,8*R*,12*S*)-**79**. Likewise, both (4*S*,8*R*,12*S*)-**79** and (4*R*,8*S*,12*S*)-**79**, which have the C20 in a *anti* relationship to the C21, contained a doublet signal at 0.872 ppm in their ^{1}H NMR spectra. Therefore, we assigned this doublet signal to the H20 for (4*S*,8*R*,12*S*)-**79** and (4*R*,8*S*,12*S*)-**79**. By a similar process of deduction, we were able to assign all the methyl signals in all four isomers (Table 3.3). The complete assignments of the methyl group region are listed under the corresponding methyl group in Figure 3.7. There are a total of seven different doublets

found in the methyl region, H20-*syn* (0.874 ppm), H20-*anti* (0.872 ppm), *syn*-H21-*syn* (0.844 ppm), *syn*-H21-*anti* or *anti*-H21-*syn* (0.842 ppm), *anti*-H21-*anti* (0.841 ppm), H22-*syn* (0.840 ppm), H22-*anti* (0.839 ppm) (Table 3.3). The 0.841 and 0.840 ppm signals overlapped in the ^{1}H NMR of M-**79** as one larger signal (spectrum 1, Figure 3.7). These seven signals correspond to the seven different types of methyl groups as indicated in Table 3.3. Five of the methyl group types appear twice, and two appear once, for the total of seven.

Figure 3.7. ^{1}H NMR of methyl region expansion of the four isomers

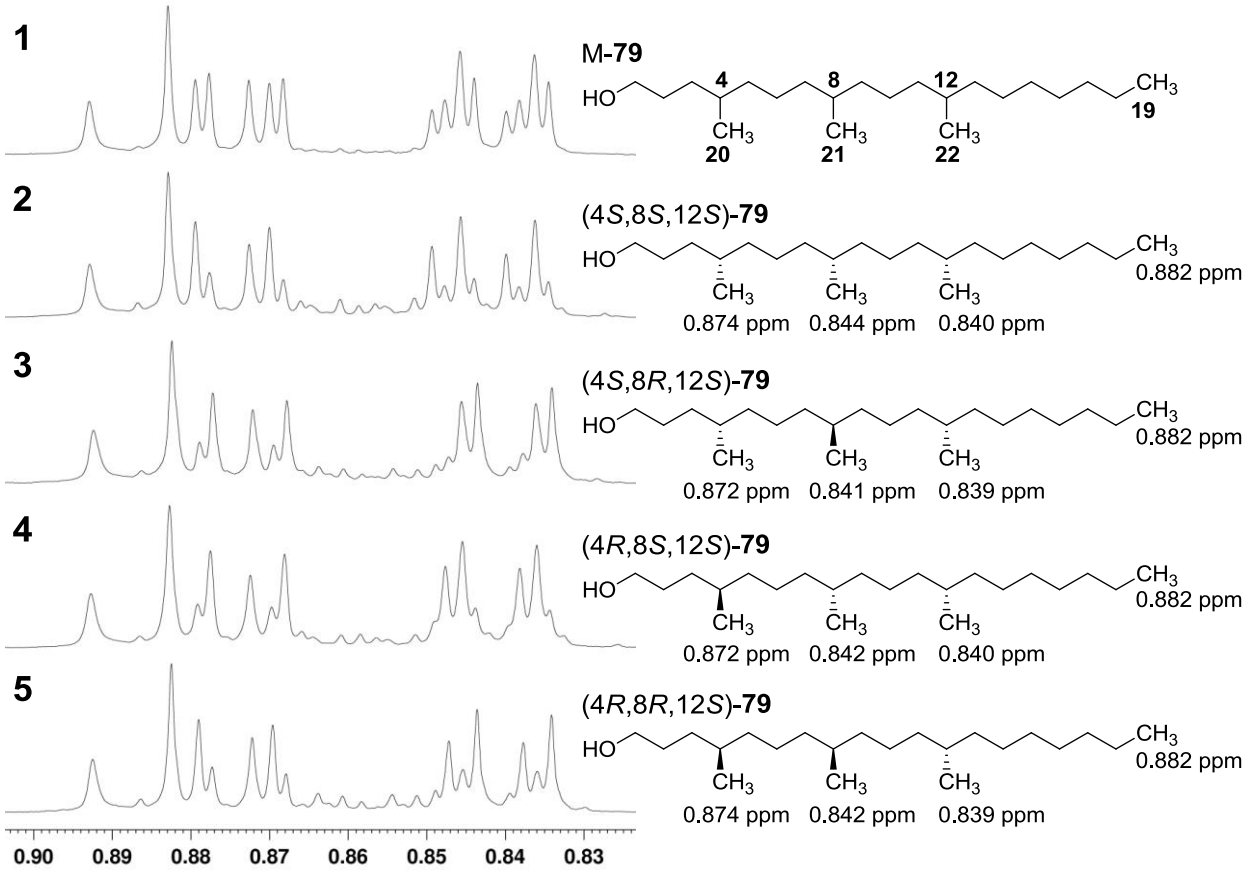

Table 3.2. Relationship table for methyl group matching in 4,8,12-trimethylnonadecanol **79**

spectrum	2	3	4	5
2	—	no match	H22-*syn*	H20-*syn*
3	no match	—	H20-*anti*	H22-*anti*
4	H22-*syn*	H20-*anti*	—	*anti*-H21-*syn*
5	H20-*syn*	H22-*anti*	*syn*-H21-*anti*	—

Table 3.3. The complete assignments of the 7 different methyl proton signals in ^{1}H NMR spectra

type of methyl proton	chemical shift (δ, ppm)
H20-*syn*	0.874
H20-*anti*	0.872
syn-H21-*syn*	0.844
syn-H21-*anti* and *anti*-H21-*syn*	0.842
anti-H21-*anti*	0.841*
H22-*syn*	0.840*
H22-*anti*	0.839

* -shows up as an overlapping signal in ^{1}H NMR spectrum of M-**89**

The purity of each isomer was not estimated due to the large number of possible peaks ($3 + 2 \times 7 = 17$) found in a small region. The isomeric purity of each sample becomes clearer in the subsequent ^{13}C NMR spectroscopic analysis due to fewer numbers of possible peaks.

The H20, H21, and H22 assignments in ^{1}H NMR were verified by 1D TOCSY experiments conducted by Dr. D. Krishnan. In each experiment, the carbinol proton signal were first excited, followed by a recording of the spectrum after a 0.3 sec delay, and then a second recording after a 0.5 sec delay. During the delay, the initial magnetization was gradually transferred to the methyl groups depending on their distance from the carbinol protons.

An example of the results from the 1D TOCSY experiment of (4*S*,8*S*,12*S*)-**79** is shown in Figure 3.8. The carbinol proton signal at 3.634 ppm was irradiated. After 0.3 sec the spectrum showed an increase in the doublet at 0.874 ppm. This signal was assigned to the closest H20. After 0.5 sec, the spectrum showed an increase of a second doublet at 0.844 ppm. This was assigned to the second closest H21. The remaining unaffected doublet at 0.840 ppm was assigned to the furthest away H22. Likewise, the methyl groups of the other three isomers were assigned. The assignments from the 1D TOCSY experiments agreed with the previous assignments made by the direct comparative method. The 1D TOCSY spectra of (4*S*,8*R*,12*S*)-**79**, (4*R*,8*S*,12*S*)-**79**, and (4*R*,8*R*,12*S*)-**79** are shown in Appendix C.

Figure 3.8. 1D TOCSY of (4*S*,8*S*,12*S*)-trimethylnonadecanol **79**

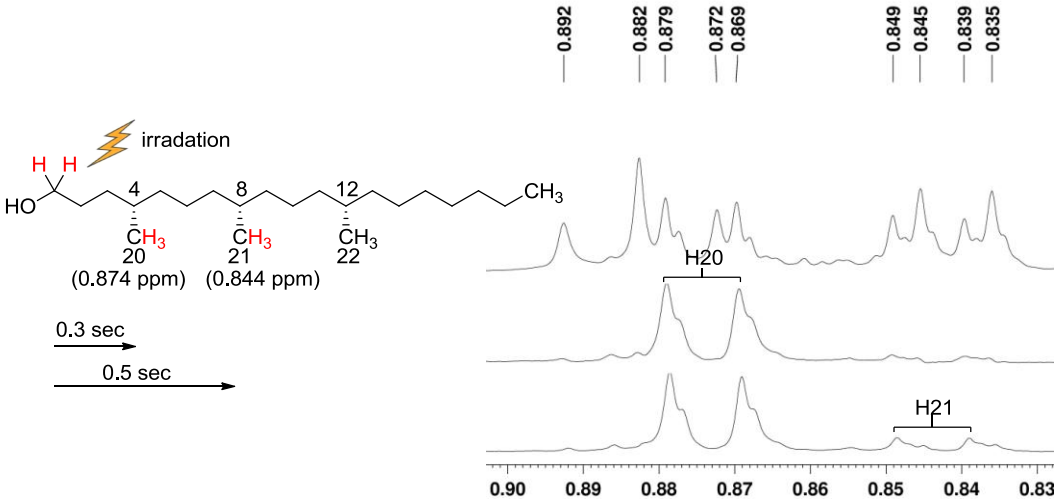

3.3.2 Analysis of ^{13}C NMR Spectra of M-79 and Four isomers of 4,8,12-Trimethylnonadecanol

The ^{13}C NMR spectra of the mixture M-**79** and the four isomers were recorded in $CDCl_3$ at 150 MHz. The ^{13}C NMR spectra of the four isomers were slightly different in three regions, 19.5–20.0 ppm, 32.0–33.5 ppm, and 37.0–37.5 ppm. Based on the ^{13}C NMR assignments of α-tocopherol by Ingold and coworkers,[19a] these three regions were identified as the C20, C21, and C22 methyl region at 19.5–19.9 ppm, the C4, C8, and C12 methine region at 32.6–33.1 ppm, and the C3, C5, C7, C9, C11, and C13 methylene region at 37.0–37.5 ppm (Figure 3.9).

Figure 3.9. The three regions in ^{13}C NMR spectra with differentiable signals

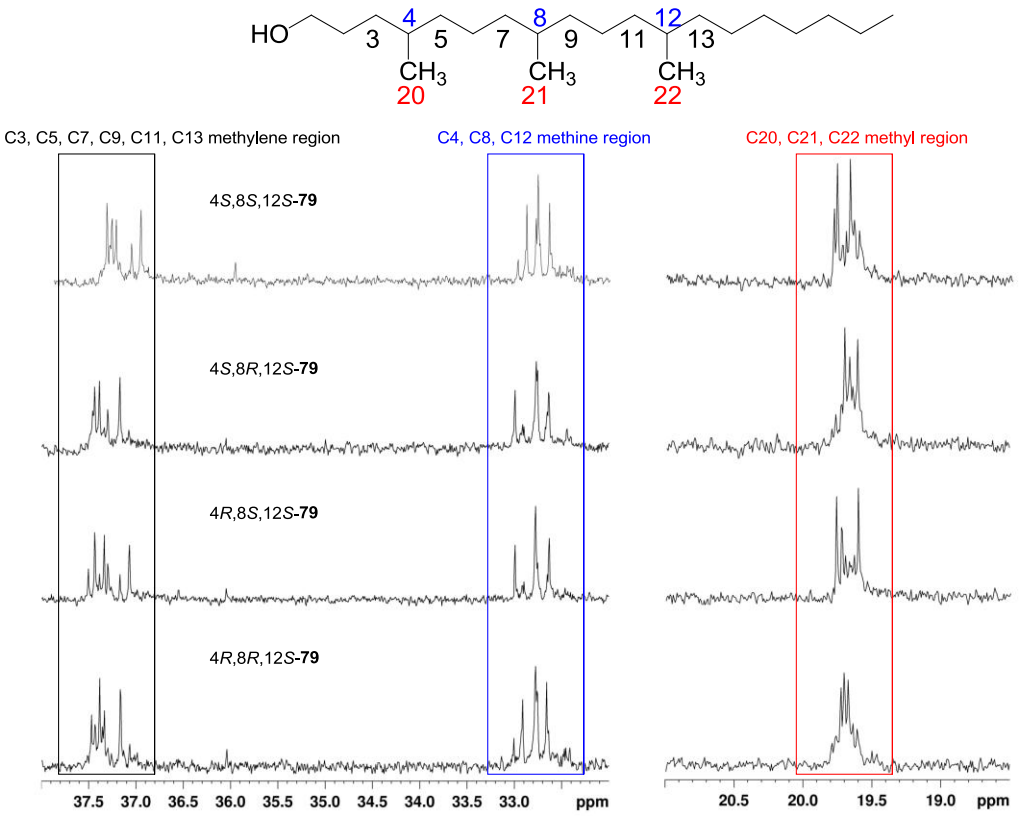

The most downfield region is difficult to analyze because it contains six closely spaced resonances with some overlapping one another. Both the methane and branched methyl regions have three resonances. We chose to analyze the later region (19.0–20.5 ppm) further to see if the methyl configurations to chemical shifts correlations observed in ^{1}H NMR spectra also exist in the ^{13}C NMR spectra. To improve the resolution of the ^{13}C NMR spectra, the five samples (M-**79**, 4*S*,8*S*,12*S*-**79**, 4*S*,8*R*,12*S*-**79**, 4*R*,8*S*,12*S*-**79**, 4*R*,8*R*,12*S*-**79**) were first subjected to ^{13}C NMR experiments with a narrower scanning range between 19.0–20.5 ppm. The resulting spectra were then processed with the Traficante algorithm processing.[42] Figure 3.10 shows the improvement in resolution by overlaying the 19.50–19.90 ppm expansion of the (4*S*,8*S*,12*S*)-**79** ^{13}C NMR spectrum. The red spectrum was generated from standard processing and the black spectrum

was generated from the additional Traficante algorithm processing. The black spectrum clearly shows three major peaks and several minor peaks.

Figure 3.10. ^{13}C NMR spectra between regular processing and Traficante algorithm processing

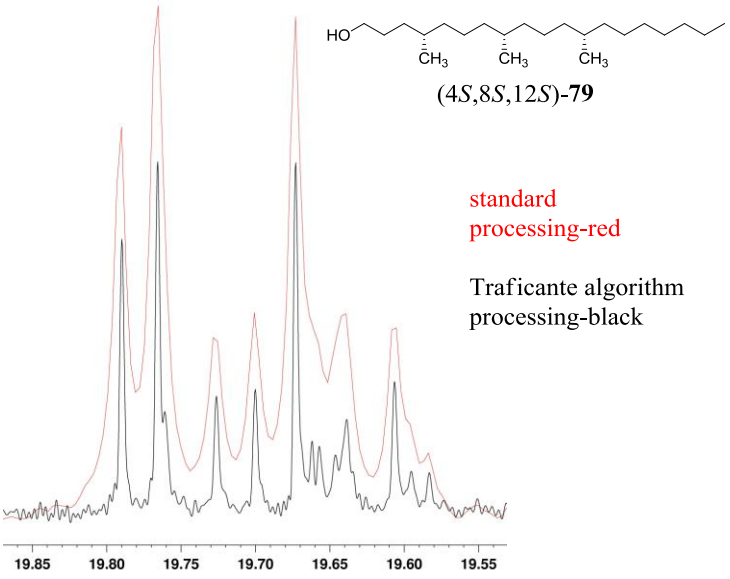

The ^{13}C NMR spectrum expansion of the C20, C21, C22 methyl region (19.0–20.5 ppm) in the mixture M-**79** showed seven distinct carbon signals in roughly equal heights, indicating the presence of seven different configurations (types) of the methyl group in the four isomers. After lining up the five ^{13}C NMR spectra, we learned that each spectrum contained 7 peaks, 3 major peaks and four minor peaks, and all seven peaks aligned with the seven peaks found in the ^{13}C NMR spectrum of the mixture M-**79** (Figure 3.11). We were able to assign the three major peaks and four minor peaks in each spectrum by the same comparative method introduced earlier. To illustrate this method, in Figure 3.11 we color-code the methyl group with *syn* relationship(s) with its neighboring methyl group(s) in red; the methyl group with *anti* relationship(s) with its neighboring methyl group(s) in blue; and the methyl group with a *syn* relationship on one side and an *anti* relationship on the other in black (Figure 3.11). The complete assignments of the

seven methyl carbon signals are summarized in Table 3.4. It is important to note that all seven signals appear within a 0.18 ppm span.

Figure 3.11. ^{13}C NMR methyl branch expansion of the mixture M-**79** and four isomers

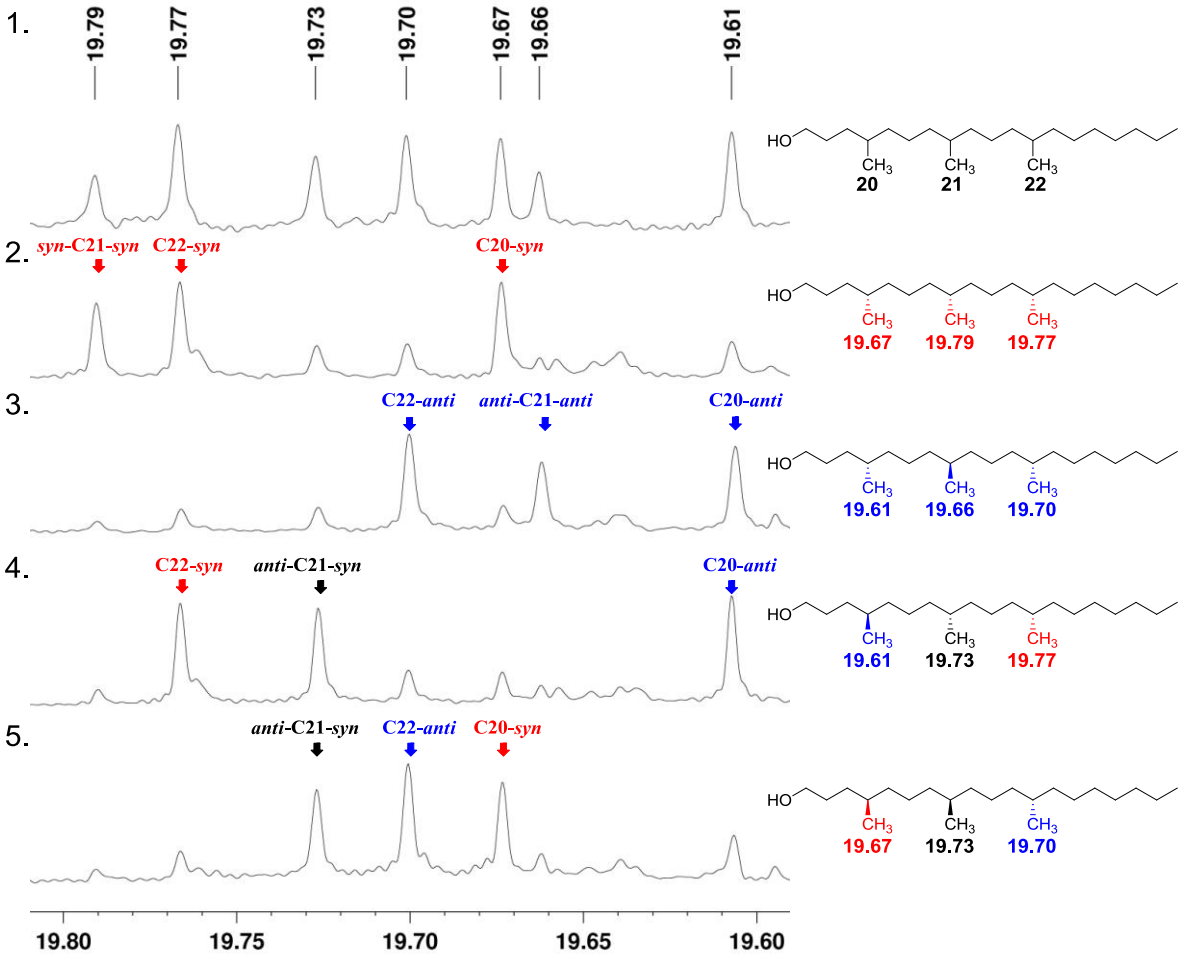

Table 3.4. The complete assignments of the seven different methyl carbon signals in ^{13}C NMR spectra

type of methyl carbon	chemical shift (δ, ppm)
C20-*syn*	19.67
C20-*anti*	19.61
syn-C21-*syn*	19.79
syn-C21-*anti* and *anti*-C21-*syn*	19.73
anti-C21-*anti*	19.66
C22-*syn*	19.77
C22-*anti*	19.70

The methyl group carbon assignments were verified by correlating the methyl carbon signals with their corresponding proton signals in inverse 2D HMQC experiments conducted by Dr. D. Krishnan. For example, in the methyl region expansion of the 2D HMQC spectrum of (4*S*,8*S*,12*S*)-**79** shown in Figure 3.12., the 19.79 ppm signal was correlated to the C21 methyl proton doublet signal at 0.844 ppm; the 19.77 ppm signal was correlated to the C22 methyl proton doublet signal at 0.840 ppm; and the 19.67 ppm signal was correlated to the C20 methyl proton doublet signal at 0.874 ppm. These 2D HMQC assignments agreed with the assignments made by the comparative method. The methyl group assignments of remaining three isomers were verified by similar 2D HMQC experiments (Appendix D).

Figure 3.12. Expansion of the branched methyl region of the inverse 2D HMQC of (4*S*,8*R*,12*S*)-**79**

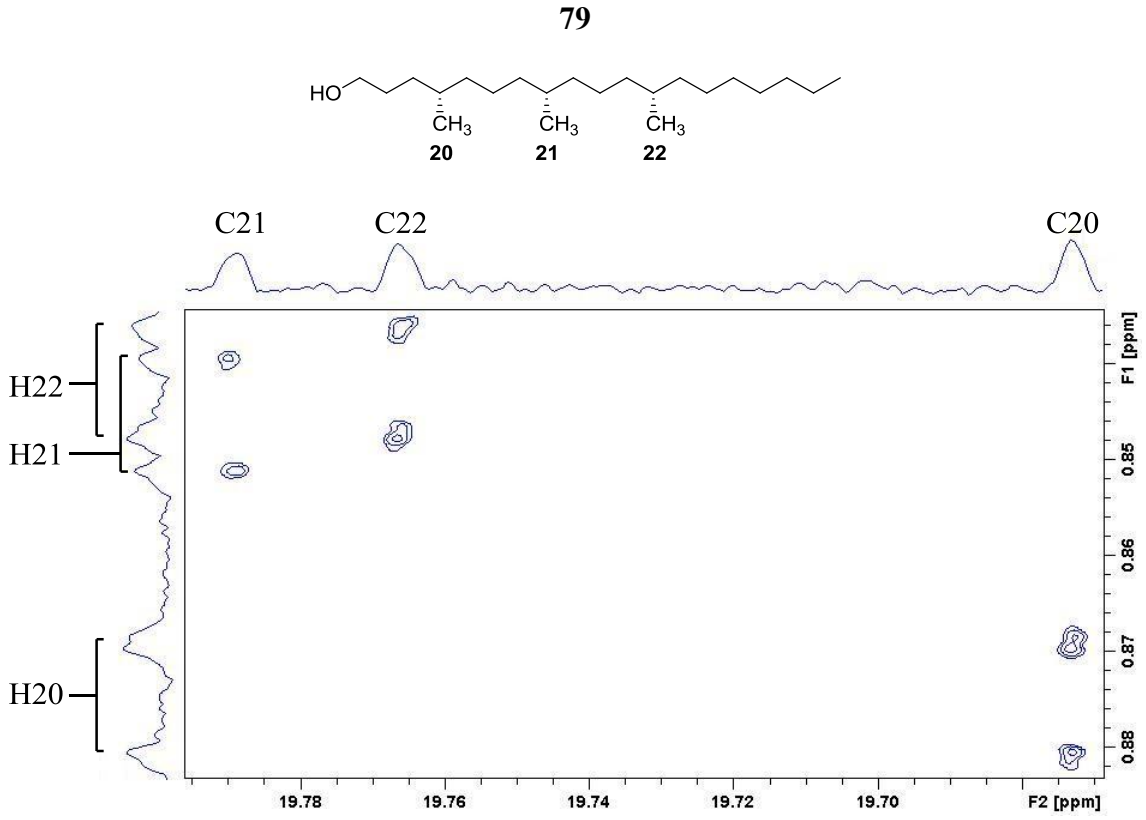

3.3.3 Isomeric Purity Estimation in Each Sample

Due to the different isomeric impurities present in each sample, we decided to estimate the purity of each sample by comparing the ^{13}C NMR spectra to the simulated ^{13}C NMR spectra of each final product based on 89/11 Roush crotylation selectivity per cycle (for three cycles). To simulate these four ^{13}C NMR spectra, we first constructed a table of percentage compositions for each isomer in a given sample (Table 3.5). For example, sample 1 contains ~70% of (4*S*,8*S*,12*S*)-**79** isomer (0.89*0.89*0.89 = 0.70), ~9% of the (4*S*,8*R*,12*S*)-**79** isomer (0.89*0.11*0.89 = 0.09), ~9% of the (4*R*,8*S*,12*S*)-**79** isomer, ~9% of the (4*S*,8*S*,12*R*)-**79** isomer, ~1% of the (4*R*,8*R*,12*S*)-**79** isomer (0.11*0.11*0.89 = 0.01), ~1% of the (4*R*,8*S*,12*R*)-**79** isomer, ~1% of the (4*R*,8*R*,12*S*)-**79** isomer, and ~0.1% of the (4*R*,8*R*,12*R*)-**79** isomer.

Based on Table 3.5, we then calculated the percentage intensity of each carbon signal. For example, for the sample 1, the percentage of *syn*-C20 (19.67 ppm) was calculated to be ~0.80. This was calculated by adding the percentage composition of the main isomer (4*S*,8*S*,12*S*)-**79**, and impurities (4*S*,8*S*,12*R*)-**79**, (4*R*,8*R*,12*S*)-**79**, and (4*R*,8*R*,12*R*)-**79** isomers, which all contain a *syn*-C20 signal (0.70 + 0.09 +0.01 + 0.001 = 0.80). The percentage intensity of the *anti*-C20 (19.61 ppm) signal was calculated to be ~20% by adding the impurities (4*S*,8*R*,12*S*)-**79**, (4*S*,8*R*,12*R*)-**79**, (4*R*,8*S*,12*S*)-**79**, and (4*R*,8*S*,12*R*)-**79** isomers (0.09 + 0.01 + 0.09 + 0.01 = 0.20). Together, *syn*-C20 and *anti*-C20 makes up to 100% of all C20 signals. The percentage intensity of each type of C21 and C22 are calculated in the same way using Table 3.5, and summarized in Table 3.6.

The four simulated ^{13}C NMR spectra with 89/11 selectivity at each cycle were created using Table 3.6 with an NMR spectra simulator-WINDNMR©. These spectra are shown in Figure 3.13.

Table 3.5. The percentage composition of each isomer in the four samples

	sample (%)			
	1	2	3	4
(4*S*,8*S*,12*S*)-**79**	70	9	9	1
(4*S*,8*S*,12*R*)-**79**	9	1	1	0.1
(4*S*,8*R*,12*S*)-**79**	9	70	1	9
(4*S*,8*R*,12*R*)-**79**	1	9	0.1	1
(4*R*,8*S*,12*S*)-**79**	9	1	70	9
(4*R*,8*S*,12*R*)-**79**	1	0.1	9	1
(4*R*,8*R*,12*S*)-**79**	1	9	9	70
(4*R*,8*R*,12*R*)-**79**	0.1	1	1	9

sample 1 contains (4*S*,8*S*,12*S*)-**89** as the major isomer; sample 2 contains (4*S*,8*R*,12*S*)-**89** as the major isomer; sample 3 contains (4*R*,8*S*,12*S*)-**89** as the major isomer; sample 4 contains (4*R*,8*R*,12*S*)-**89** as the major isomer.

Table 3.6. The estimated percentage C20, C21, and C22 intensities in ^{13}C NMR spectra

	sample (%)			
	1	2	3	4
syn-C20 (19.67 ppm)	80	20	20	80
anti-C20 (19.61 ppm)	20	80	80	20
syn-C21-*syn* (19.79 ppm)	71	10	10	10
syn-C21-*anti* (19.73 ppm)	20	20	80	80
anti-C21-*anti* (19.66 ppm)	10	71	10	10
syn-C22 (19.77 ppm)	80	20	80	20
anti-C22 (19.70 ppm)	20	80	20	80

Figure 3.13. Spectral comparison between actual and simulated ^{13}C NMR spectra

a). sample 1: (4*S*,8*S*,12*S*)-**79**

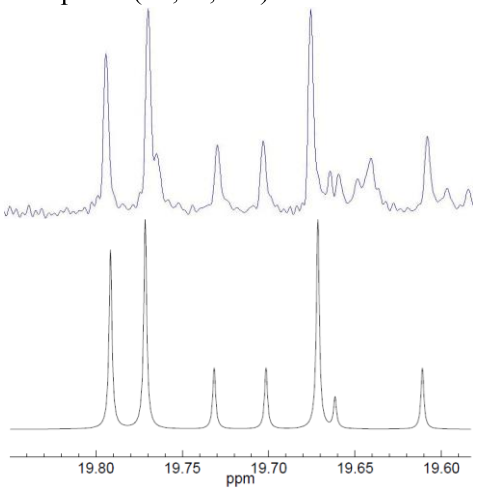

b). sample 2: (4*S*,8*R*,12*S*)-**79**

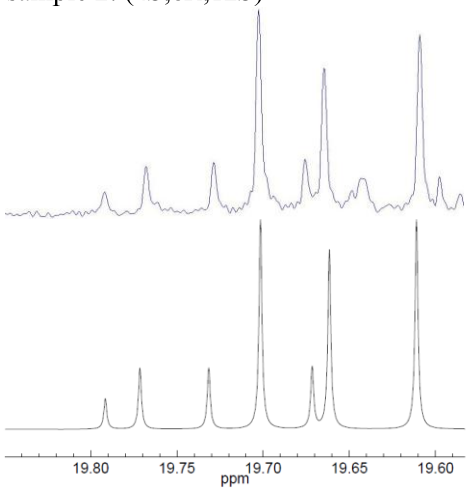

c). sample 3: (4*R*,8*S*,12*S*)-**79**

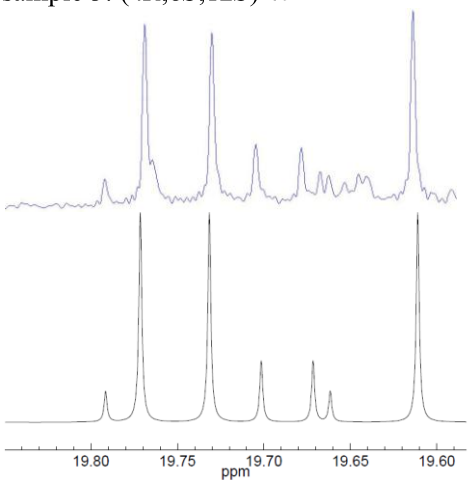

d). sample 4: (4*R*,8*R*,12*S*)-**79**

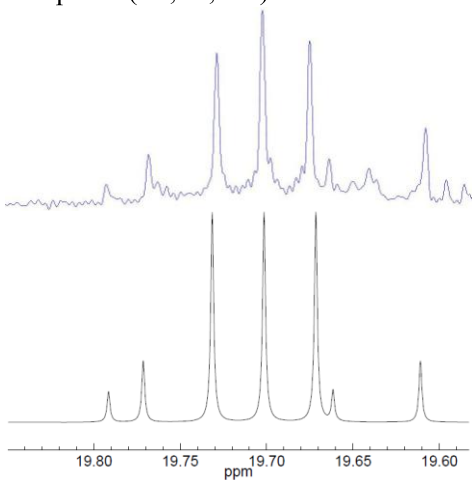

As shown in Figure 3.13, the simulated ^{13}C NMR spectra closely resemble the actual ^{13}C NMR spectra in all four samples. Therefore, it can be conclude that the isomeric purities in each sample are ~70% as a result of three cycles of Roush crotylation at about 89% for each cycle. No apparent erosion in enantioselectivity for Roush crotylation between the second and third cycle was observed.

3.3.4 Development of an NMR-Based Method for Assigning the Methyl Group Configurations in a Polyisoprenoid System

The spectroscopic analyses of isoprenoids M-**79**, 4*S*,8*S*,12*S*-**79**, 4*S*,8*R*,12*S*-**79**, 4*R*,8*S*,12*S*-**79**, and 4*R*,8*R*,12*S*-**79** showed that the methyl groups at the same position with the same relative configuration with neighboring methyl group(s) would share identical ^{1}H and ^{13}C NMR chemical shifts. This phenomenon is further evident by the fact that only seven, instead of 12, different signals were observed in both the ^{1}H and the ^{13}C NMR spectra of the mixture M-**79**. These seven principle signals were identified as C20-*syn*, C20-*anti*, *syn*-C21-*syn*, *syn*-C21-*anti* (or *anti*-

C21-*syn*), *anti*-C21-*anti*, C22-*syn*, and C22-*anti* methyl configurations. Table 3.7 lists the ^{1}H and ^{13}C NMR chemical shifts for the 7 principle methyl configurations.

Table 3.7. Chemical shifts of the seven principle types of methyl configuration in ^{1}H and ^{13}C NMR

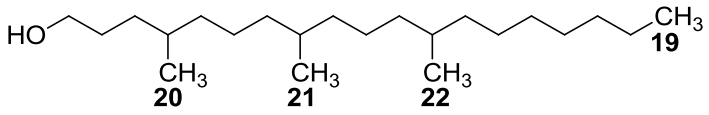

type of methyl group	^{1}H NMR chemical shift (δ, ppm)	^{13}C NMR chemical shift (δ, ppm)
C20-*syn*	0.874 (d)	19.67
C20-*anti*	0.872 (d)	19.61
syn-C21-*syn*	0.844 (d)	19.79
syn-C21-*anti*	0.842 (d)	19.73
anti-C21-*anti*	0.841 (d)	19.66
C22-*syn*	0.840 (d)	19.77
C22-*anti*	0.839 (d)	19.70

d- doublet; t- triplet

Based on these observations, it was postulated that the methyl group chemical shifts in repeating isoprenoid system will be dictated predominantly by the 1,5-methyl-methyl interaction(s). Based on this, it can be predicted that the appearance of branched methyl group ^{1}H and ^{13}C NMR region of any isoprenoid molecule by applying the appropriate chemical shifts and multiplicities from Table 3.4. If these values are inputted into an NMR simulator such as WINDNMR©, the resulted predicted spectra can be visualized and compared with the spectra of synthetic or natural products for the purpose of structural identification or purity assessments.

4.0 SPECTROSCOPIC PREDICTIONS

The first step in predicting the appearance of the branched methyl region of ^{1}H and ^{13}C NMR spectra of a given polyisoprenoid is to set up a characterization table that includes the quantity and type of branched methyl within the given polyisoprenoid. The ^{1}H and ^{13}C NMR spectra can then be simulated by inputting these values into WINDNMR©.

To generalize the labeling of the branched methyl groups, we will herein refer to the C20 or the left-most methyl carbon as the end1, the C21 or the middle methyl carbon(s) as middle, and C22 or the right-most methyl carbon as end2. In any polyisoprenoid system there will be one end1 methyl group, and one end2 methyl group, but depending on the number of repeating units there can be many middle methyl groups (Figure 4.1).

Figure 4.1. Branched methyl group designations for isoprenoid structures

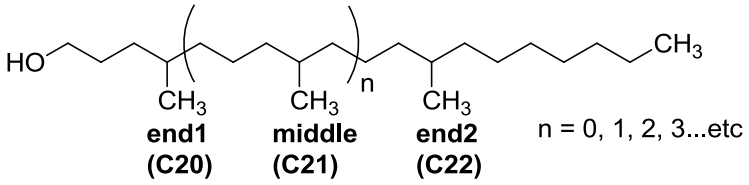

4.1 SPECTROSCOPIC PREDICTIONS OF EIGHT ISOMERS OF 4,8,12,16-TETRAMETHYLTRICOSANOL

To predict the ^{1}H and ^{13}C NMR spectra of 4,8,12,16-tetramethyltricosanol, the characterization table for each isomer was setup. As shown in Figure 4.2, 4,8,12,16-tetramethyltricosanol **80** contains four branched methyl groups: one end-1 methyl group, one end-2 methyl group and two middle methyl groups. The methyl group characterization table (Table 4.1) is set up with the 8 diastereomers on vertical axis and the seven principle type of methyl on the horizontal axis. The numbers correspond to the quantity of each type of methyl group in a given isomer.

Figure 4.2. The structure of 4,8,12,16-tetramethyltricosanol **80**

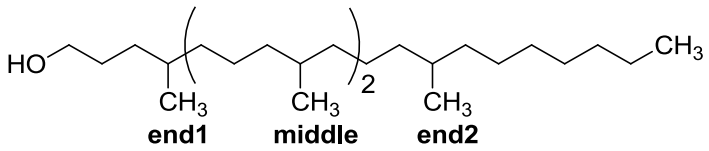

Table 4.1. Characterization table for 4,8,12,16-tetramethyltricosanol **80**

	syn-**e1**	*anti*-**e1**	*syn*-**m**-*syn*	*syn*-**m**-*anti*	*anti*-**m**-*anti*	*syn*-**e2**	*anti*-**e2**
4*S*,8*S*,12*S*,16*S*	1	—	2	—	—	1	—
4*S*,8*S*,12*S*,16*R*	1	—	1	1	—	—	1
4*S*,8*S*,12*R*,16*S*	1	—	—	1	1	—	1
4*S*,8*R*,12*S*,16*S*	—	1	—	1	1	1	—
4*S*,8*S*,12*R*,16*R*	1	—	—	2	—	1	—
4*S*,8*R*,12*R*,16*S*	—	1	—	2	—	—	1
4*S*,8*R*,12*S*,16*R*	—	1	—	—	2	—	1
4*S*,8*R*,12*R*,16*R*	—	1	1	1	—	1	—

e1 = end1; **m** = middle; **e2** = end2

The spectra can then be simulated using WINDNMR© by referencing chemical shifts and multiplicities of each corresponding methyl group from Table 3.4. The ^{1}H NMR spectra are simulated at 700 MHz and the ^{13}C NMR are simulated at 150 MHz. The predicted ^{1}H NMR spectra are shown in Figure 4.3 and the predicted ^{13}C NMR spectra are shown in Figure 4.4.

Figure 4.3. ^{1}H NMR spectra prediction of 8 isomers of 4,8,12,16-tetramethyltricosanol **80**

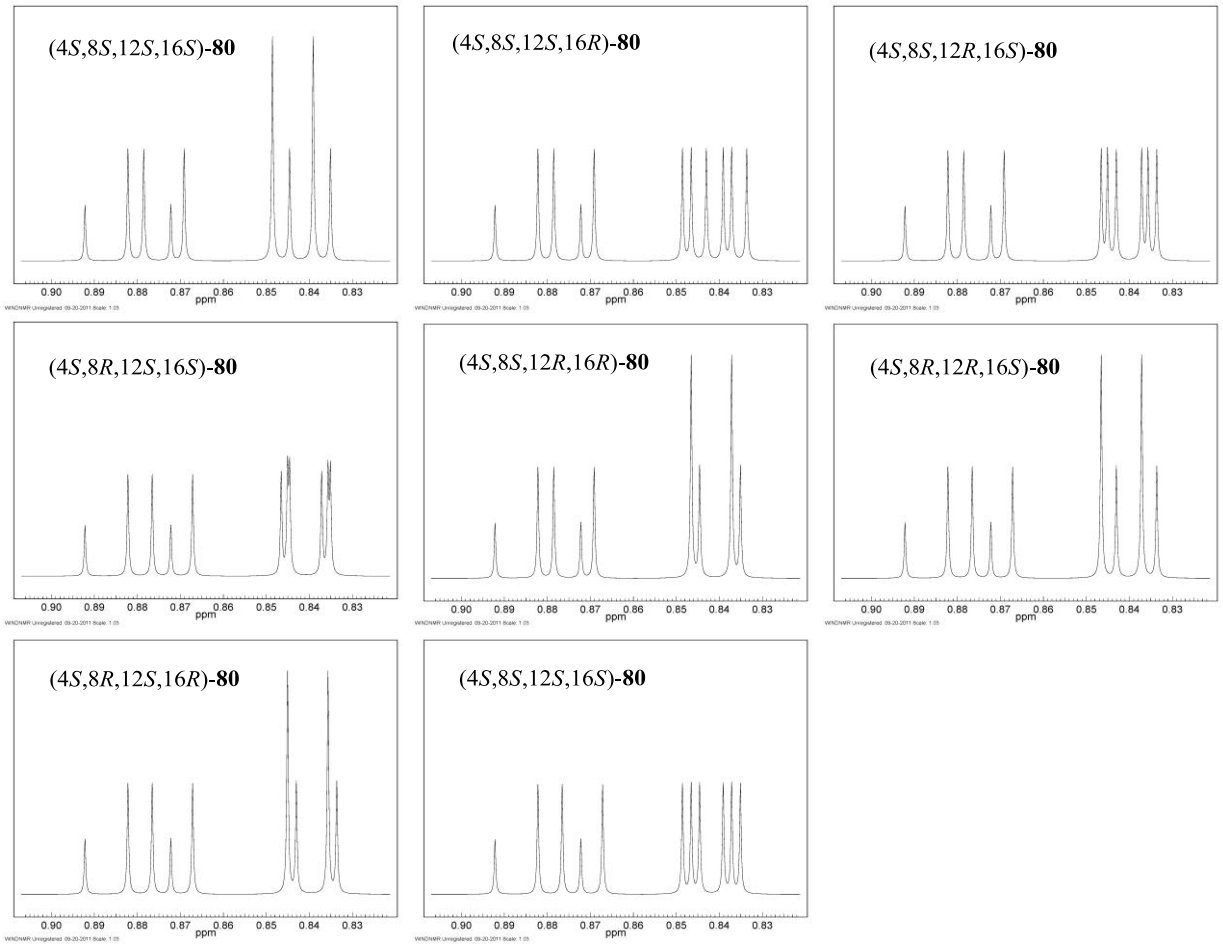

Figure 4.4. ^{13}C NMR spectra prediction of 8 isomers of 4,8,12,16-tetramethyltricosanol **80**

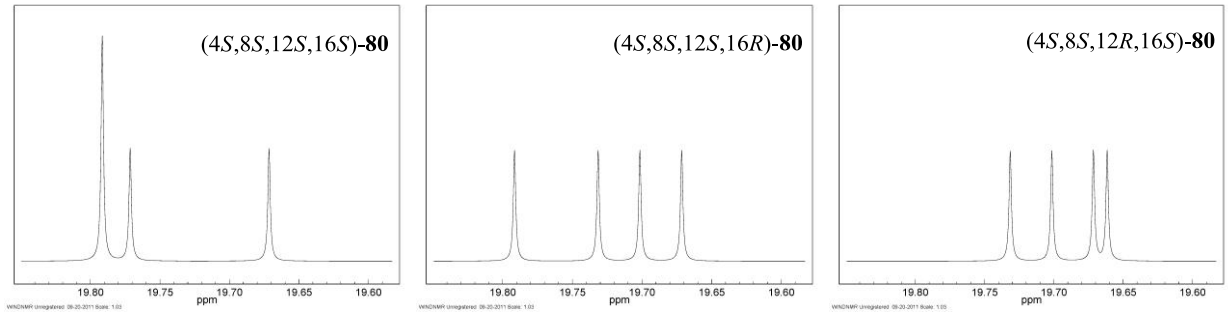

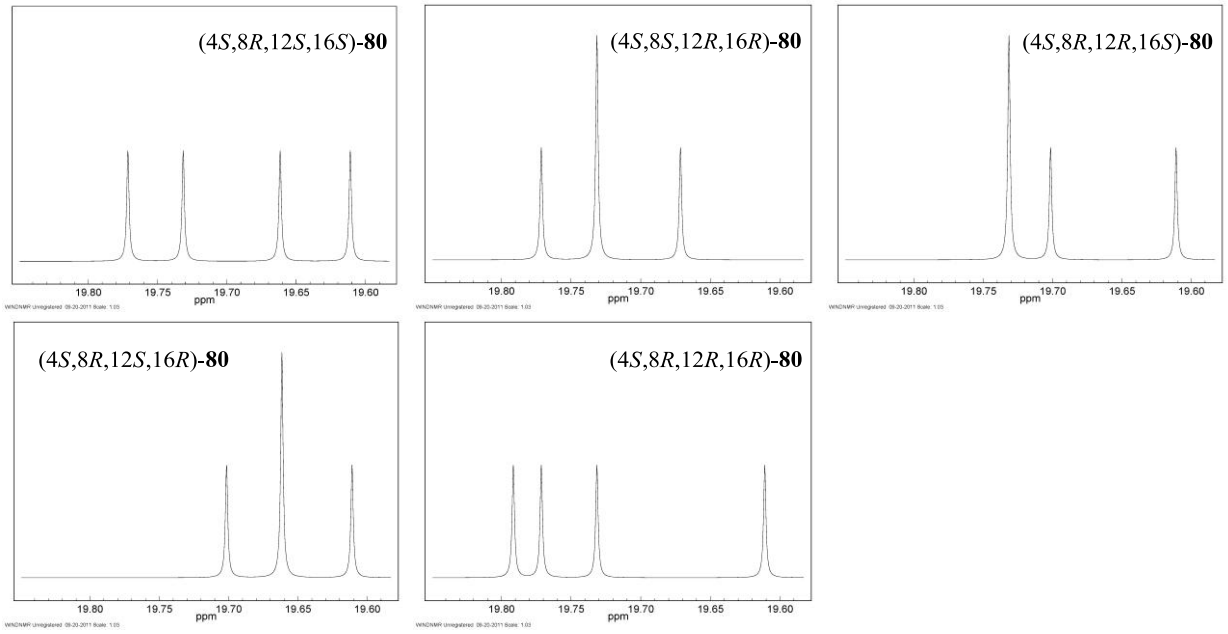

From the predicted ^{1}H and ^{13}C NMR spectra of 4,8,12,16-tetramethyltrocosanol, it can be seen that the spectra of all eight isomers are different. The ^{1}H NMR spectra contain either 9 (one triplet and three doublets) or 11 (one triplet and four doublets) signals and the ^{13}C NMR spectra contain either 3 or 4 signals. Since the terminal methyl always appear as a triplet at 0.882 ppm in the ^{1}H NMR spectra, and the two end methyl groups (end1 and end2) appear as two doublets in the ^{1}H NMR spectra and as two signals in the ^{13}C NMR spectra. The only factor that determines whether a spectrum would have nine or 11 signals in the ^{1}H NMR spectra and three or four signals in the ^{13}C NMR spectra is the type of middle methyl groups. If the two middle methyl groups are the same type, then their signals would overlap to give only nine signals (one triplet and three doublets) in the ^{1}H NMR spectra and three signals in the ^{13}C NMR spectra with the overlapping signals having double intensities [e.g., (4*S*,8*S*,12*S*,16*S*)-, (4*S*,8*S*,12*R*,16*R*)-, (4*S*,8*R*,12*R*,16*S*)-, and (4S,8R,12S,16R)-**80**]. On the other hand, if the two middle methyl groups are different types, then there would be a total of 11 signals in the ^{1}H NMR spectra, and 4 signals

in the ^{13}C NMR spectra with all signals in equal intensities [e.g. (4*S*,8*S*,12*S*,16*R*)-, (4*S*,8*S*,12*R*,16*S*)-, (4*S*,8*R*,12*S*,16*S*)-, and (4*S*,8*R*,12*R*,16*R*)-**80**].

4.2 SPECTROSCOPIC PREDICTIONS OF SIXTEEN ISOMERS OF 4,8,12,16,20-PENTAMETHYLHEPTACOSANOL

The 4,8,12,16,20-pentamethylheptacosanol **81**, which was identified as the polyisoprenoid side chain of the natural product MPM-**1**, contains five branched methyl groups: one end1 methyl group; one end2 methyl group; and three middle methyl groups (Figure 4.5).

Figure 4.5. The structure of 4,8,12,16,20-pentamethylheptacosanol **81**

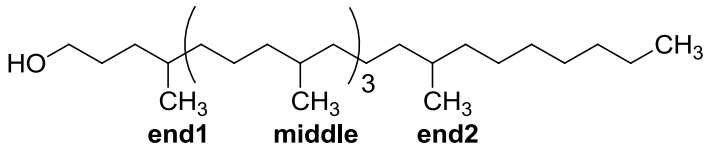

To predict the ^{1}H and ^{13}C NMR spectra of 4,8,12,16,20-pentamethylheptacosanol **81**, the characterization table (Table 4.2) was setup. Although there are sixteen diastereomers, Table 4.2 shows that there are only fourteen unique methyl group profiles. Two sets of isomers share the same methyl group characterizations. Therefore, each of the two sets of isomers would have the same ^{1}H and ^{13}C NMR spectra and the remaining 12 isomers would have unique spectra. The isomers that share the same methyl group profiles are (4*S*,8*S*,12*S*,16*R*,20*R*)- and the (4*S*,8*S*,12*R*,16*R*,20*R*)-**81** isomers (highlighted in yellow), which have one *syn*-**e1**, one *syn*-**e2**, one *syn*-**m**-*syn*, and two *syn*-**m**-*anti* methyl groups, and the (4*S*,8*R*,12*S*,16*S*,20*R*)- and the (4*S*,8*R*,12*R*,16*S*,20*R*)-**81** isomers (highlighted in red), which have one *anti*-**e1**, one *anti*-**e2**, two *syn*-**m**-*anti*, and one *anti*-**m**-*anti* methyl groups.

Table 4.2. Methyl group characterization table for 4,8,12,16,20-pentamethylheptacosanol **81**

	syn-**e1**	*anti*-**e1**	*syn*-**m**-*syn*	*syn*-**m**-*anti*	*anti*-**m**-*anti*	*syn*-**e2**	*anti*-**e2**
4*S*,8*S*,12*S*,16*S*,20*S*	1	—	3	—	—	1	—
4*S*,8*S*,12*S*,16*S*,20*R*	1	—	2	1	—	—	1
4*S*,8*S*,12*S*,16*R*,20*S*	1	—	1	1	1	—	1
4*S*,8*S*,12*R*,16*S*,20*S*	1	—	—	2	1	1	—
4*S*,8*R*,12*S*,16*S*,20*S*	—	1	1	1	1	1	—
4*S*,8*S*,12*S*,16*R*,20*R*	1	—	1	2	—	1	—
4*S*,8*S*,12*R*,16*R*,20*S*	1	—	—	3	—	—	1
4*S*,8*R*,12*R*,16*S*,20*S*	—	1	—	3	—	1	—
4*S*,8*S*,12*R*,16*S*,20*R*	1	—	—	1	2	—	1
4*S*,8*R*,12*S*,16*S*,20*R*	—	1	—	2	1	—	1
4*S*,8*R*,12*S*,16*R*,20*S*	—	1	—	—	3	—	1
4*S*,8*S*,12*R*,16*R*,20*R*	1	—	1	2	—	1	—
4*S*,8*R*,12*R*,16*R*,20*S*	—	1	1	2	—	—	1
4*S*,8*R*,12*R*,16*S*,20*R*	—	1	—	2	1	—	1
4*S*,8*R*,12*S*,16*R*,20*R*	—	1	—	1	2	1	—
4*S*,8*R*,12*R*,16*R*,20*R*	—	1	2	1	—	1	—

After Table 4.2 was set up, the branched methyl region of the fourteen ^{1}H and ^{13}C NMR spectra of 4,8,12,16,20-pentamethylheptacosanol were predicted based on the same method described in Section 4.1. The predicted ^{1}H NMR spectra are shown in Figure 4.6, and the predicted ^{13}C NMR spectra are shown in Figure 4.7.

Figure 4.6. ^{1}H NMR spectra prediction of 16 isomers of 4,8,12,16,20-pentamethylheptacosanol **81**

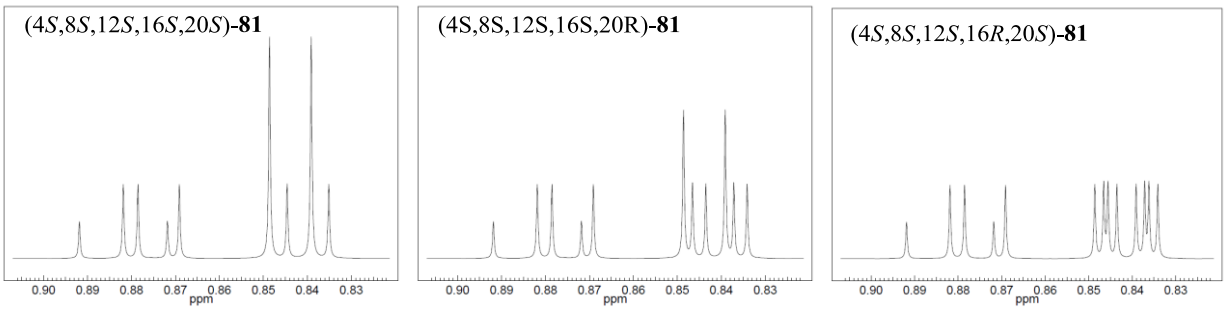

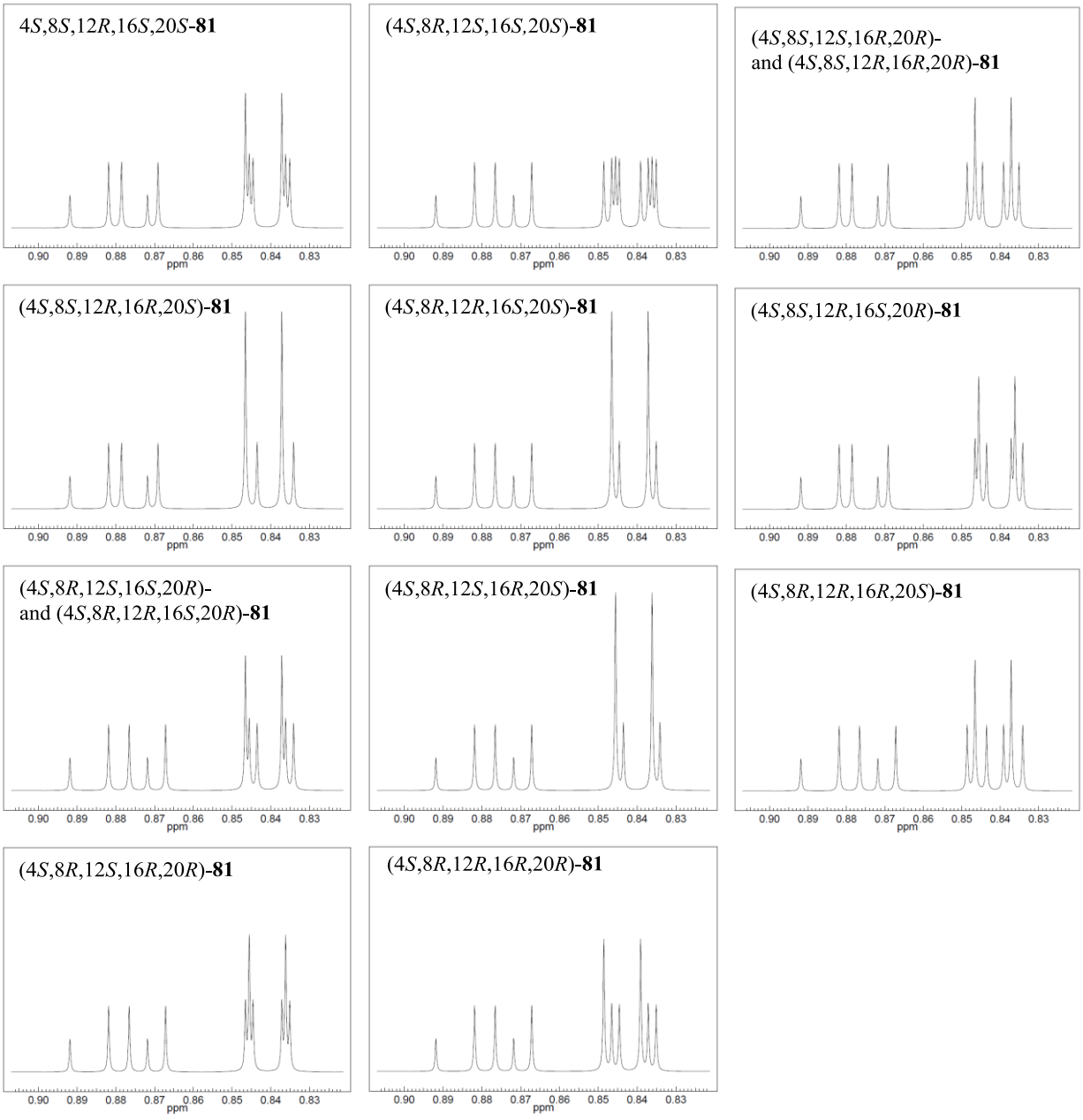

Figure 4.7. ^{13}C NMR spectra prediction of 16 isomers of 4,8,12,16,20-pentamethylheptacosanol

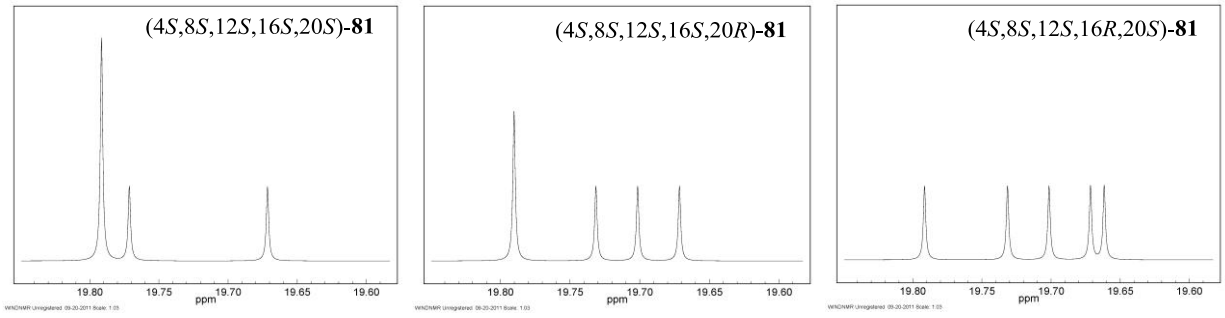

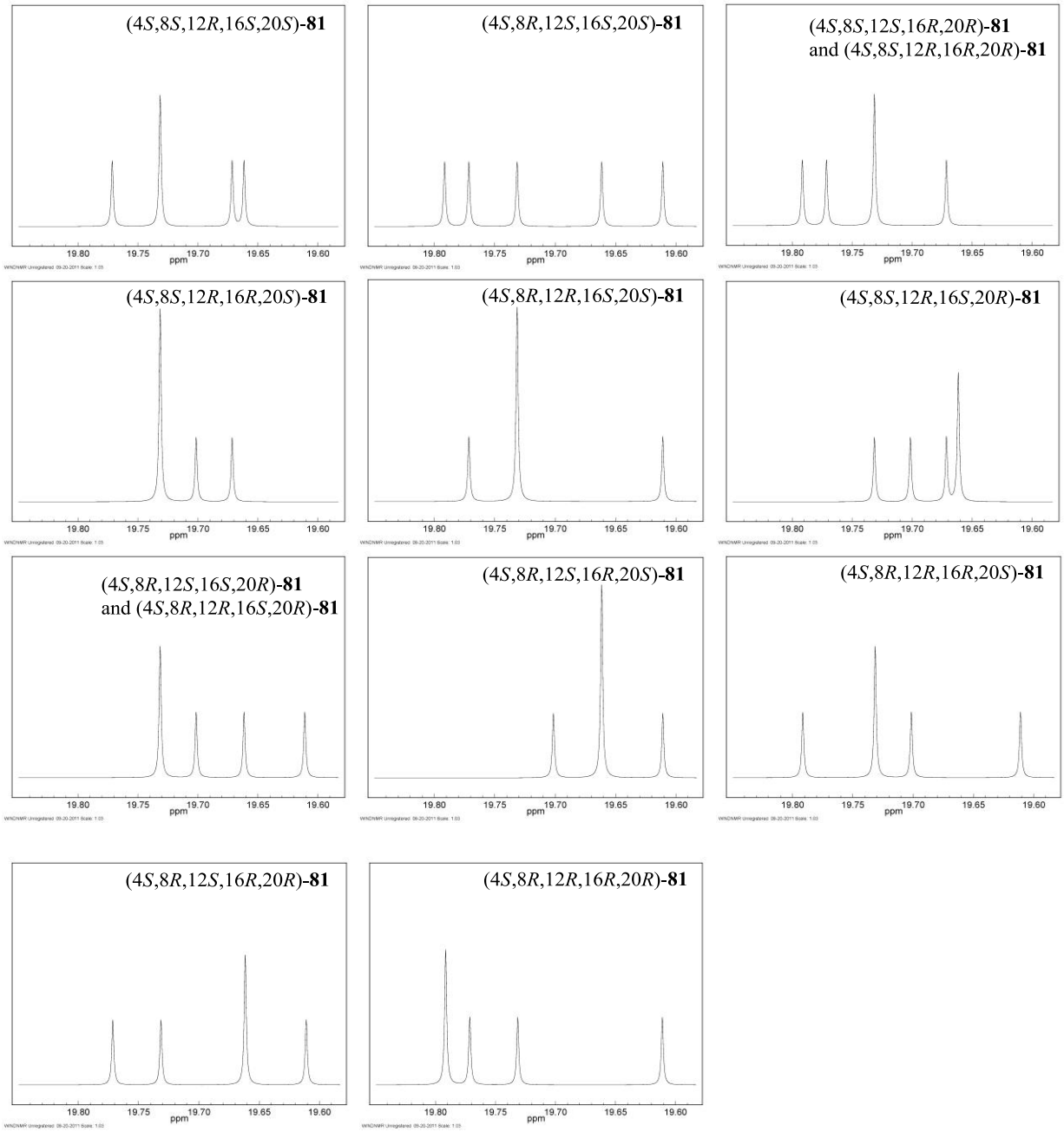

As shown in the predicted ^{1}H NMR spectra, there are four spectra that contain nine signals (one triplet and three doublets), eight spectra that contain 11 signals (one triplet and four doublets), and two spectra that contain 13 signals (one triplet and five doublets) signals. And from the predicted ^{13}C NMR spectra, there are four spectra that contain three signals, eight spectra that contain 4 signals, and two spectra that contain five signals. For the same reason

discussed in Section 4.1, the types of the three middle methyl groups determines how many signals appear in both ^{1}H and ^{13}C NMR spectra. If all three middle methyl groups are the same type, they would all overlap to give nine signals (one triplet and three doublets) in the ^{1}H NMR spectra, and three signals in the ^{13}C NMR with the overlapping signals giving triple intensities [e.g., (4*S*,8*S*,12*S*,16*S*,20*S*)-, (4*S*,8*S*,12*R*,16*R*,20*S*)-, (4*S*,8*R*,12*R*,16*S*,20*S*)-, and (4*S*,8*R*,12*S*,16*R*,20*S*)-**81**]. If the two middle methyl groups are the same type and one middle methyl group is a different type, the same type of methyl group would overlap to give 11 signals (one triplet and four doublets) in the ^{1}H NMR spectra, and 4 signals in the ^{13}C NMR spectra with the overlapping signals giving double intensities [e.g., (4*S*,8*S*,12*S*,16*S*,20*R*)-, (4*S*,8*S*,12*R*,16*S*,20*S*)-, (4*S*,8*S*,12*R*,16*R*,20*R*)-, (4*S*,8*S*,12*S*,16*R*,20*R*)-, (4*S*,8*S*,12*R*,16*S*,20*R*)-, (4*S*,8*R*,12*S*,16*S*,20*R*)-, (4*S*,8*R*,12*R*,16*S*,20*R*)-, (4*S*,8*R*,12*R*,16*R*,20*S*)-, and (4*S*,8*R*,12*R*,16*R*,20*R*)-**81**]. Furthermore, if all three middle methyl groups are different types, then there would be 13 signals (one triplet and five doublets) in the ^{1}H NMR spectra, and 5 signals in the ^{13}C NMR with all the signals in equal intensities [e.g., (4*S*,8*S*,12*S*,16*R*,20*S*)- and (4*S*,8*R*,12*S*,16*S*,20*S*)-**81**].

5.0 SUMMARY AND CONCLUSION

In summary, we successfully synthesized four isomers of 4,8,12-trimethylnonadecanol by FMS of three iterations of Roush crotylation, *O*-phenyl thionocarbonate formation (tagging), and Rh-catalyzed hydroformylation. DIBAL-*H* reduction and fluorous demixing gave four quasiisomers. Global deoxygenation/detagging of each quasiisomer afforded the four target 4,8,12-trimethylnonadecanols (Scheme 3.10). The average yield per cycle (three steps) was 59% and the overall yield before fluorous demixing was 17.6% over 14 steps. This FMS showcased the first utility of the fluorous *O*-phenyl thionocarbonate tags and the first successful demixing of quasiisomers with tags that only differ in one fluorine atom. The global deoxygenation step was accomplished cleanly using the new diMe-Imd-BH_3 reagent. Overall, this FMS used only six fluorine atoms to encode for four quasiisomers, making this synthesis by far the most efficient FMS to date.

The spectroscopic analyses of the ^{1}H and ^{13}C NMR spectra of the four isomers of 4,8,12-trimethylnonadecanol revealed there are seven principle methyl types in a repeating polyisoprenoid system. A way to predict the appearance of the branched methyl group region ^{1}H and ^{13}C NMR of 4,8,12,16-tetramethyltricosanol (four branched methyl groups) and 4,8,12,16,20-pentamethyl-heptacosanol (five branched methyl groups) by identifying the number and nature of the branched methyl group, then applying the appropriate methyl group chemical

shifts was developed. These predictions set the stage for a direct NMR-based identification of the methyl configurations of polyisoprenoid natural products such as the side chain of MPM-**1**.

6.0 EXPERIMENTAL

General information: All reactions were performed under argon atmosphere unless otherwise noted. All reaction solvents were freshly dried by passing through a column of activated alumina.[43] All reagents were purchased commercially and used without further purification unless otherwise mentioned. Reaction progresses were monitored by TLC with 0.25 mm E. Merck precoated silica gel plates. All crude mixtures were purified by flash chromatography with silica gel 60 (0.040–0.063 mm) supplied by Sorbent Technology unless otherwise stated. Products and reactions were analyzed by ^{1}H, ^{13}C, and ^{19}F NMR spectrometry, FT-IR, optical rotation, and HRMS.

The NMR spectra were recorded on a Bruker Advance III 400 MHz, a Bruker Advance III 600 MHz, or a Bruker Advance III 700 MHz spectrometer using deuterated chloroform spiked with 1 mole% trimethylsilane (TMS), unless otherwise indicated. The signals are given as in part per million (δ, ppm) and were determined relative to the proton and carbon resonance of TMS at 0 ppm as the internal standard. In the case of ^{19}F NMR spectrometry, no internal standard was used. The spectral data of single molecules were reported in the following order: chemical shift (d), multiplicity, coupling constant (Hz), number of nuclei. The spectral data of mixtures (with the designation M- before number) were not reported, but the spectra are provided in appendix E.

Infrared (IR) spectra were taken on a Mattson Genesis FT-IR spectrometer as thin film on NaCl plate and the peaks are reported in wave numbers (cm^{-1}). Optical rotations were measured on a Perkin-Elmer 241 polarimeter at a Na D-line (λ = 589 nm) using a 1 dm cell. HPLC analyses and separations were performed on a Waters 600E system with a Waters 2487 dual λ absorption detector. Compound names were obtained from ChemDraw Ultra 12.0 (Cambridge Soft Corp.).

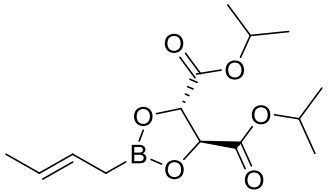

(4S,5S)-Diisopropyl 2-((E)-but-2-en-1-yl)-1,3,2-dioxaborolane-4,5-dicarboxylate (33): To a stirring suspension of KO*t*Bu (23.8 g, 0.21 mol.) in THF (175 mL, freshly distilled) at –78 °C was added *E*-butene (53 mL, 1.06 mol.) via cannula. After addition of *E*-butene, *n*-BuLi (133 mL, 1.6 M) was added while carefully maintaining the internal temperature to be below –65 °C. The resulting orange suspension was warmed to –25 °C and stirred for 30 min before cooling to –78 °C. Triisopropyl borate was then added neat over 45 min (keeping the internal temperature at –70 °C). After addition of the borate, the mixture was stirred for 10 more min then poured into 1N HCl (200 mL, aq). The pH was then adjusted to pH 1 by addition of 1N HCl solution. Diisopropyl-L-tartrate (48.82 g, 0.21 mol.) in ether (50 mL, dry) was then added to the reaction mixture and the aqueous and organic layers were separated. The aqueous layer was washed with ether (4 x 20 mL) and the organic layer was dried over $MgSO_4$ for 2 h. The solution was then filtered under argon atmosphere and concentrated. The crude product was diluted with toluene (150 mL, dry) and used in subsequent reactions without further purification. The concentration of the solution was determined to be 1 M.

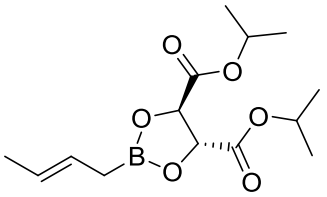

(4*R*,5*R*)-Diisopropyl 2-((E)-but-2-en-1-yl)-1,3,2-dioxaborolane-4,5-dicarboxylate (34): The same procedure used in the synthesis of Roush reagent **33** was used to make **34**, the only difference was the use of diisopropyl-D-tartrate (48.82 g, 0.21 mol) instead of diisopropyl-L-tartrate. The crude product was diluted with toluene (150 mL, dry) and used in subsequent reactions without further purification. The solution was determined to have a concentration of 0.53 M.

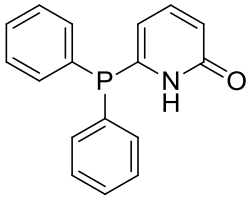

6-(Diphenylphosphino)pyridin-2(1H)-one (41): The ligand for Rh-catalyzed hydroformylation was synthesized in a 3-step procedure from 2,6-dichloropyridine. The synthesis and NMR information were reported by Breit *et al.*[39]

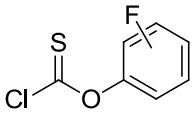

General Procedure 1: the synthesis of fluorinated phenyl chlorothionoformates (54–59)

The corresponding fluorinated phenol in 1N aq. NaOH was added dropwise to a solution of thiophosgene in $CHCl_3$. The resulting mixture was stirred at 0 °C for 1.5 h. The reaction progress was monitored by TLC. After complete consumption of the starting phenol, the reaction was quenched by 1N HCl. The organic layer was dried over $MgSO_4$ and then concentrated. The crude product was used in the next step without further purification.

General Procedure 2: the Roush crotylboration reaction of aldehydes

To a solution of Roush reagent (**33** or **34**, 3 equiv) in toluene was added powdered 4 Å molecular sieves (20 mg/mL), and then cooled to –78 °C. After 10 min, the corresponding aldehyde was added neat to the mixture and the resulting solution was stirred at –78 °C for further 3 h. 2 N NaOH was added to quench the reaction over 20 min at 0 °C then filtered through a pad of celite. The aqueous layer was extracted with ether (10 mL, 3 times). The combined organic layer was dried with K_2CO_3 and concentrated. The crude product was purified by column chromatography (9:1 hexane-diethyl ether).

General Procedure 3: thionocarbonate formation (fluorous tagging)

To the allylic alcohol in CH_2Cl_2 was added pyridine (anhydrous) at 25 °C. After 10 min, the reaction mixture was cooled to 0 °C. *O*-Phenyl chlorothionoformate (2 equiv) was added dropwise into the reaction mixture, which was slowly warmed to room temperature overnight (16 h). Aqueous NH_4Cl was added to quench the reaction at 0 °C followed by aqueous layer extraction with CH_2Cl_2 (10 mL, 3 times). The combined organic layer was dried over $MgSO_4$ and then concentrated. The crude product was purified by column chromatography (99:1 hexanes-diethyl ether).

General procedure 4, Rh-catalyzed hydroformylation:

The pyridone ligand **41** (20 mol%) and Rh $(CO)_2$acac (4 mol%) were added to THF under Ar, and the resulting mixture was stirred at room temp. After 10 min, the corresponding alkene was added neat to the premixed catalysts in THF. The resulting mixture was transported to the pressure vessel and stirred at 60 °C under 150 psi of CO/H_2 for 15 h. After complete

consumption of the starting alkene, the solvent was evaporated under reduced pressure and the crude mixture was purified by column chromatography (3:1 hexanes-diethyl ether).

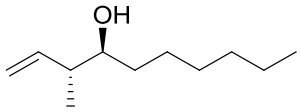

(3*R*,4*S*)-3-Methyldec-1-en-4-ol (30): This crotylation reaction was performed according to General Procedure 2 using heptanal (12 g, 105.1 mmol) and Roush reagent **33** (315 ml, 315 mmol). Allylic alcohol (3*R*,4*S*)-**30** was isolated in 16 g, 89% yield as a colorless oil: $[\alpha]_D^{25} = -0.66$ (c = 1.54, $CHCl_3$); ^{1}H NMR ($CDCl_3$, 300 MHz, ppm) δ = 5.755 (ddd, J = 8.4, 11.3, 16.7 Hz, 1H), 5.106 (d, J = 11.0 Hz, 1H), 5.087 (d, J = 16.8 Hz, 1H), 3.387 (s br, 1H), 2.192 (ddq, J = 6.7, 6.8, 6.9 Hz, 1H), 1.200–1.600 (m, 11H), 1.030 (d, J = 6.9 Hz, 3H), 0.882 (t, J = 6.0 Hz, 3H); ^{13}C NMR ($CDCl_3$, 75 MHz, ppm) δ =140.40, 116.27, 74.70, 44.14, 34.26, 31.87, 29.42, 25.71, 22.66, 16.32, 14.11; FTIR (thin film) ν_{max} 3372, 3075, 2956, 2928, 2857, 1639, 1459, 999, 961, 912 cm^{-1}; HRMS calcd for $C_{11}H_{22}O$: 170.1668, found 170.1670.

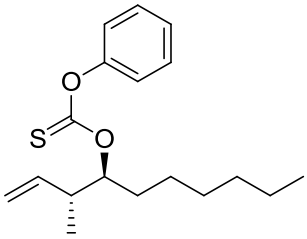

***O*-((3*R*,4*S*)-3-Methyldec-1-en-4-yl) *O*-phenyl carbonothioate 42:** This acylation reaction was performed according to General Procedure 3 using (3*R*,4*S*)-3-methyldec-1-en-4-ol **30** (24 g, 141 mmol) and *O*-phenyl chlorothionoformate (24.3 g, 141 mmol). Alkene (3*R*,4*S*)-**42** was isolated in 34 g, 78% yield as a colorless oil: $[\alpha]_D^{25} = -12.19$ (c = 2.33, $CHCl_3$); ^{1}H NMR ($CDCl_3$, 300 MHz, ppm) δ = 7.415 (t, J = 7.5 Hz, 2H), 7.283 (t, J = 7.5 Hz, 1H), 7.095 (d, J = 7.8 Hz, 2H), 5.871 (ddd, J = 8.4, 11.3, 16.7 Hz, 1H), 5.372 (dt, J = 4.5, 8.4 Hz,1H), 5.113 (d, J = 6.3 Hz, 1H),

5.102 (d, J = 16.8 Hz, 1H), 2.648 (ddq, J = 6.7, 6.8, 6.9 Hz, 1H), 1.500-1.850 (m, 2H), 1.200-1.500 (m, 8H), 1.099 (d, J = 6.9 Hz, 3H), 0.891 (t, J = 6.0 Hz, 3H); ^{13}C NMR ($CDCl_3$, 75 MHz, ppm) δ =195.17, 153.38, 138.86, 129.45, 126.42, 122.03, 116.06, 88.59, 41.10, 31.69, 30.65, 29.17, 25.25, 22.59, 15.70, 14.08; FTIR (thin film) ν_{max} 3076, 2956, 2928, 2857, 1592, 1490, 1276, 1197, 1002, 918, 768 cm^{-1}; HRMS calcd for $C_{18}H_{26}O_2S$: 306.1658, found 306.1653.

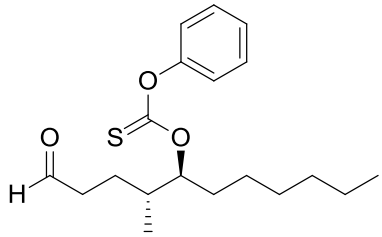

***O*-((4*R*,5*S*)-4-Methyl-1-oxoundecan-5-yl) *O*-phenyl carbonothioate 43:** This Rh-catalyzed hydroformylation reaction was performed according to General Procedure 4 using *O*-((3*R*,4*S*)-3-methyldec-1-en-4-yl) *O*-phenyl carbonothioate **42** (10 g, 330 mmol), pyridone ligand **41** (3.2 g, 100 mmol), and Rh catalyst (0.64 g, 20 mmol). Aldehyde (4*R*,5*S*) **43** was isolated in 9.3 g, 85% yield as a colorless oil: $[\alpha]_D^{25}$ = –2.30 (c = 1.87, $CHCl_3$); ^{1}H NMR ($CDCl_3$, 300 MHz, ppm) δ = 9.799 (t, J = 1.2 Hz, 1H), 7.421 (t, J = 7.5 Hz, 2H), 7.315 (t, J = 7.5 Hz, 1H), 7.099 (d, J = 7.8 Hz, 2H), 5.320 (quint, J = 4.5 Hz,1H), 2.476-2.593 (m, 2H), 2.008 (ddq, J = 6.7, 6.8, 6.9 Hz, 1H), 1.200-1.833 (m, 12H), 0.983 (d, J = 6.9 Hz, 3H), 0.898 (t, J = 6.0 Hz, 3H); ^{13}C NMR ($CDCl_3$, 75 MHz, ppm) δ =201.94, 195.08, 153.34, 129.67, 129.49, 126.49, 122.00, 121.83, 88.98, 41.56, 35.32, 34.68, 31.70, 29.69, 29.22, 25.33, 24.19, 22.67, 22.60, 14.92, 14.15, 14.10; FTIR ν_{max} 2956. 2928, 2857, 2720, 1725, 1592, 1490, 1458, 1358, 1282, 1197, 1003, 770 cm^{-1}; HRMS calcd for $C_{19}H_{28}O_3SNa$: 359.1657, found 359.1672.

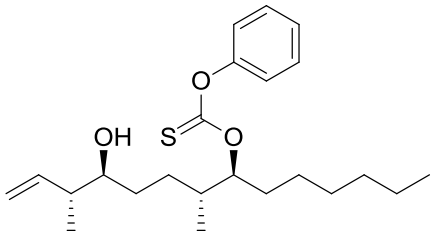

***O*-((7*S*,8*R*,11*S*,12*R*)-11-Hydroxy-8,12-dimethyltetradec-13-en-7-yl) *O*-phenyl carbonothioate 45:** This crotylation reaction was performed according to General Procedure 2 using aldehyde (4*R*,5*S*)-**43** (1.5 g, 4.46 mmol) and Roush reagent **33** (8.9 ml, 8.9 mmol). Allylic alcohol (3*R*,4*S*,7*R*,8*S*)-**45** was isolated in 1.46 g, 83% yield as a colorless oil: $[\alpha]_D^{25}$ = –2.64 (*c* = 1.67, $CHCl_3$); ^{1}H NMR ($CDCl_3$, 300 MHz, ppm) δ = 7.413 (t, *J* = 7.5 Hz, 2H), 7.281 (t, *J* = 7.5 Hz, 1H), 7.102 (d, *J* = 7.8 Hz, 2H), 5.753 (ddd, *J* = 8.4, 11.3, 16.7 Hz, 1H), 5.347 (s br, 1H), 5.133 (d, *J* = 6.9 Hz, 1H), 5.120 (d, *J* = 17.1 Hz, 1H), 3.394 (s br, 1H), 2.217 (ddq, *J* = 6.7, 6.8, 6.9 Hz, 1H), 2.010 (s br, 1H), 1.200-1.800 (m, 14H), 1.043 (d, *J* = 6.9 Hz, 3H), 0.976 (d, *J* = 6.9 Hz, 3H) 0.896 (t, *J* = 6.0 Hz, 3H); ^{13}C NMR ($CDCl_3$, 75 MHz, ppm) δ =195.07, 153.38, 140.25, 140.16, 129.43, 126.39, 122.04, 116.51, 116.47, 89.78, 89.53, 74.83, 74.57, 44.23, 44.16, 35.77, 31.71, 31.65, 29.56, 29.38, 29.23, 25.44, 25.38, 22.60, 16.36, 16.31, 15.06, 14.84, 14.08; FTIR ν_{max} 3443, 3072, 2957, 2928, 2859 1592, 1490, 1458, 1369, 1283, 1197, 1002, 914, 769 cm^{-1}; HRMS calcd for $C_{23}H_{36}O_3SNa$: 415.2283, found 415.2260.

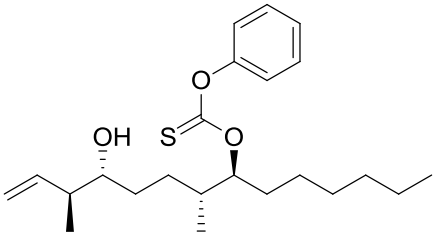

***O*-((7*S*,8*R*,11*R*,12*S*)-11-Hydroxy-8,12-dimethyltetradec-13-en-7-yl) *O*-phenyl carbonothioate 45:** This crotylation reaction was performed according to General Procedure 2 using aldehyde (4*R*,5*S*)-**43** (1.2 g, 3.5 mmol) and Roush reagent **34** (10.1 ml, 5.3 mmol). Allylic

alcohol (3*S*,4*R*,7*R*,8*S*)-**45** was isolated in 1.2 g, 83% yield as a colorless oil: $[\alpha]_D^{25}$ = –0.70 (*c* = 1.62, $CHCl_3$); ^{1}H NMR ($CDCl_3$, 300 MHz, ppm) δ = 7.410 (t, *J* = 7.5 Hz, 2H), 7.279 (t, *J* = 7.5 Hz, 1H), 7.101 (d, *J* = 7.8 Hz, 2H), 5.752 (ddd, *J* = 8.4, 11.3, 16.7 Hz, 1H), 5.340 (s br, 1H), 5.129 (d, *J* = 6.9 Hz, 1H), 5.118 (d, *J* = 17.1 Hz, 1H), 3.389 (s br, 1H), 2.212 (ddq, *J* = 6.7, 6.8, 6.9 Hz, 1H), 1.994 (s br, 1H), 1.200-1.800 (m, 14H), 1.039 (d, *J* = 6.9 Hz, 3H), 0.971 (d, *J* = 6.9 Hz, 3H) 0.896 (t, *J* = 6.0 Hz, 3H); ^{13}C NMR ($CDCl_3$, 75 MHz, ppm) δ = 195.10, 153.35, 140.24, 140.14, 129.44, 126.40, 122.03, 116.53, 116.49, 89.77, 89.52, 74.80, 74.55, 44.23, 44.16, 35.77, 31.93, 31.70, 31.62, 29.70, 29.53, 29.35, 29.23, 28.50, 28.21, 25.43, 25.38, 22.60, 16.36, 16.31, 15.04, 14.82, 14.08; FTIR ν_{max} 3439, 3072, 2956, 2928, 2858, 1592, 1490, 1458, 1368, 1283, 1197, 1002, 914, 768 cm^{-1}; HRMS calcd for $C_{23}H_{36}O_3SNa$: 415.2283, found 415.2267.

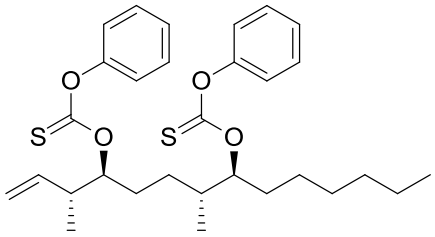

***O*,*O*'-((3*R*,4*S*,7*R*,8*S*)-3,7-Dimethyltetradec-1-ene-4,8-diyl) *O*,*O*'-diphenyl dicarbonothioate 53:** This acylation reaction was performed according to General Procedure 3 using allylic alcohol (3*R*,4*S*,7*R*,8*S*)-**45** (2.2 g, 5.6 mmol) and *O*-phenyl chlorothionoformate (1.06 g, 6.2 mmol). Alkene (3*R*,4*S*,7*R*,8*S*)-**53** was isolated in 2.5 g, 84% yield as a colorless oil: $[\alpha]_D^{25}$ = –1.68 (*c* = 1.79, $CHCl_3$); ^{1}H NMR ($CDCl_3$, 300 MHz, ppm) δ = 7.409 (t, *J* = 7.5 Hz, 4H), 7.269 (t, *J* = 7.5 Hz, 2H), 7.089 (d, *J* = 7.8 Hz, 4H), 5.761 (ddd, *J* = 8.4, 11.3, 16.7 Hz, 1H), 5.282-5.386 (m, 2H), 5.123 (d, *J* = 17.1 Hz, 1H), 5.112 (d, J = 6.9 Hz, 1H), 2.651 (ddq, *J* = 6.7, 6.8, 6.9 Hz, 2H), 1.995 (s br, 1H), 1.200-1.800 (m, 14H), 1.099 (d, *J* = 6.9 Hz, 3H), 0.981 (d, *J* = 6.9 Hz,

3H) 0.894 (t, J = 6.0 Hz, 3H); ^{13}C NMR ($CDCl_3$, 75 MHz, ppm) δ = 195.13, 195.10, 153.33, 138.72, 138.60, 129.45, 126.45, 126.42, 122.04, 122.01, 116.29, 89.35, 89.21, 88.42, 88.07, 77.46, 77.24, 77.04, 76.61, 41.09, 35.81, 35.76, 31.70, 29.90, 29.77, 29.25, 28.26, 28.11, 27.92, 27.51, 25.26, 22.60, 15.78, 15.60, 15.07, 14.99, 14.09; FTIR ν_{max} 3072, 2058, 2929, 2858, 1592, 1489, 1457, 1358, 1280, 1196, 1121, 1002, 919, 829, 769 cm^{-1}; HRMS calcd for $C_{30}H_{40}O_4S_2Na$: 551.2266, found 551.2318.

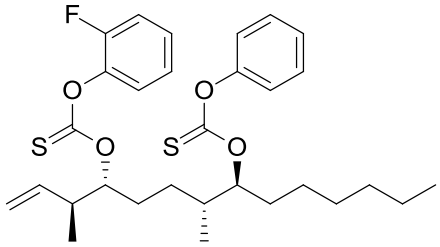

***O*,*O*'-((3*S*,4*R*,7*R*,8*S*)-3,7-Dimethyltetradec-1-ene-4,8-diyl) *O*'-(2-fluorophenyl) *O*-phenyl dicarbonothioate 60:** This acylation reaction was performed according to General Procedure 3 using allylic alcohol (3*S*,4*R*,7*R*,8*S*)-**45** (1.1 g, 2.8 mmol) and the crude mixture of *O*-2-fluorophenyl chlorothionoformate **54** (0.85 g, 4.5 mmol). Alkene (3*S*,4*R*,7*R*,8*S*)-**60** was isolated in 1.3 g, 84% yield as a colorless oil: $[\alpha]_D^{25}$ = –1.22 (c = 1.05, $CHCl_3$); ^{1}H NMR ($CDCl_3$, 400 MHz, ppm) δ = 7.090–7.425 (m, 9H), 5.777 (ddd, J = 8.1, 10.4, 17.1 Hz, 1H), 5.308-5.390 (m, 2H), 5.128 (d, J = 18.1 Hz, 1H), 5.118 (d, J = 9.1 Hz, 1H), 2.665 (ddq, J = 6.7, 6.8, 6.9 Hz, 2H), 1.931-2.002 (m, 1H), 1.800-1.931 (m, 1H), 1.211-1.800 (m, 12H), 1.110 (d, J = 6.9 Hz, 3H), 0.983 (d, J = 6.8 Hz, 3H) 0.894 (t, J = 6.7 Hz, 3H); ^{13}C NMR ($CDCl_3$, 100 MHz, ppm) δ = 195.13, 194.03, 192.43, 155.63, 155.38, 153.39, 152.32, 152.05, 140.99, 140.83, 140.74, 140.58, 138.51, 138.41, 129.47, 128.28, 128.18, 127.78, 127.69, 126.43, 124.75, 124.69, 124.55, 124.50, 124.00, 123.68, 122.07, 117.31, 117.07, 117.01, 116.77, 116.40, 89.41, 89.25, 88.96, 41.14, 35.79, 35.67, 31.72, 29.77, 29.68, 29.25, 28.35, 28.27, 27.81, 27.49, 25.35, 22.63, 15.76, 15.61,

15.06, 14.94, 14.11; FTIR ν_{max} 3072, 2958, 2930, 2859, 1600, 1501, 1459, 1363, 1261, 1196, 1101, 1001, 922, 845, 829, 762 cm^{-1}; HRMS calcd for $C_{30}H_{39}O_4S_2FNa$: 569.2172, found 569.2180.

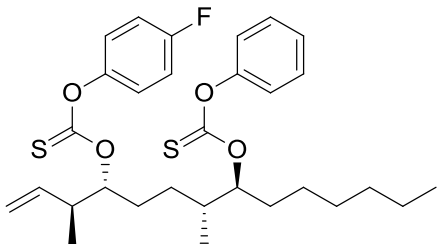

***O*,*O*'-((3*S*,4*R*,7*R*,8*S*)-3,7-Dimethyltetradec-1-ene-4,8-diyl) *O*'-(4-fluorophenyl) *O*-phenyl dicarbonothioate 62:** This acylation reaction was performed according to General Procedure 3 using allylic alcohol (3*S*,4*R*,7*R*,8*S*)-**45** (2.2 g, 6.0 mmol) and *O*-4-fluorophenyl chlorothionoformate **56** (1.3 g, 6.7 mmol). Alkene (3*S*,4*R*,7*R*,8*S*)-**62** was isolated in 2.6 g, 85% yield as a colorless oil: $[\alpha]_D^{25} = -1.35$ (*c* = 1.11, $CHCl_3$); ^{1}H NMR ($CDCl_3$, 400 MHz, ppm) δ = 7.410 (t, *J* = 7.5 Hz, 2H), 7.293 (t, *J* = 7.5 Hz, 1H), 7.099 (d, *J* = 7.8 Hz, 2H), 7.049 (d, *J* = 6.3 Hz, 4H), 5.785 (ddd, *J* = 8.1, 10.4, 17.1 Hz, 1H), 5.308-5.390 (m, 2H), 5.128 (d, *J* = 18.1 Hz, 1H), 5.118 (d, *J* = 9.1 Hz, 1H), 2.665 (ddq, *J* = 6.7, 6.8, 6.9 Hz, 2H), 1.965-2.033 (m, 1H), 1.833-1.936 (m, 1H), 1.220-1.806 (m, 12H), 1.107 (d, *J* = 6.9 Hz, 3H), 0.983 (d, *J* = 6.8 Hz, 3H) 0.896 (t, *J* = 6.7 Hz, 3H); ^{13}C NMR ($CDCl_3$, 100 MHz, ppm) δ = 195.23, 195.16, 161.83, 159.42, 159.39, 153.42, 149.39, 149.36, 149.24, 149.22, 138.70, 138.59, 129.50, 126.47, 123.63, 123.59, 123.55, 123.41, 123.32, 122.09, 116.59, 116.36, 116.31, 116.18, 116.14, 116.07, 115.95, 89.34, 89.21, 88.70, 88.32, 41.16, 36.11, 35.86, 34.71, 34.56, 31.75, 31.63, 30.02, 29.89, 29.30, 29.10, 28.32, 28.13, 27.99, 27.56, 25.32, 25.29, 22.70, 22.65,20.75, 18.81, 15.82, 15.64, 15.13, 15.03, 14.18, 14.14; FTIR ν_{max} 3076, 2958, 2929, 2858, 1502, 1280, 1191, 1003, 922, 839, 738 cm^{-1}; HRMS calcd for $C_{30}H_{39}O_4S_2FNa$: 569.2172, found 569.2173.

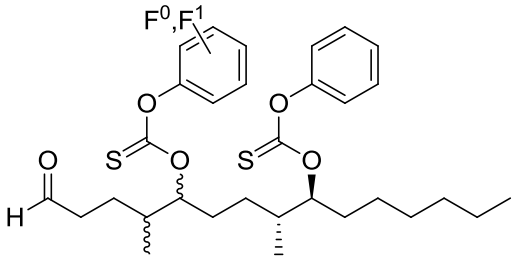

Mixture of *O*,*O*'-((4*R*,5*S*,8*R*,9*S*)-4,8-dimethyl-1-oxopentadecane-5,9-diyl) *O*,*O*'-diphenyl dicarbonothioate and *O*,*O*'-((4*S*,5*R*,8*R*,9*S*)-4,8-dimethyl-1-oxopentadecane-5,9-diyl) *O*'-(2-fluorophenyl) *O*-phenyl dicarbonothioate (M-**65):** This Rh-catalyzed hydroformylation reaction was performed according to General Procedure 4 using 1:1 mixture of (3*R*,4*S*,7*R*,8*S*)-**53** + (3*S*,4*R*,7*R*,8*S*)-**60** (2.0 g, 3.8 mmol), pyridone ligand **41** (0.18 g, 12.2 mmol), and Rh catalyst (0.04 g, 2.5 mmol). Aldehyde M-**65** was isolated in 4.4 g, 82% yield as a colorless oil: HRMS calcd for $C_{31}H_{42}O_5S_2Na_1$: 581.2371, found 581.2336; calcd for $C_{31}H_{41}O_5S_2FNa$: 599.2277, found 599.2228.

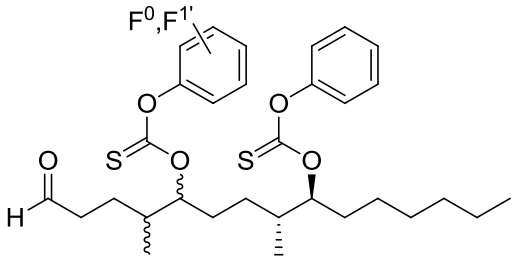

Mixture of *O*,*O*'-((4*R*,5*S*,8*R*,9*S*)-4,8-dimethyl-1-oxopentadecane-5,9-diyl) *O*,*O*'-diphenyl dicarbonothioate and *O*,*O*'-((4*S*,5*R*,8*R*,9*S*)-4,8-dimethyl-1-oxopentadecane-5,9-diyl) *O*'-(4-fluorophenyl) *O*-phenyl dicarbonothioate M-**72:** This Rh-catalyzed hydroformylation reaction was performed according to General Procedure 4 using 1:1 mixture of (3*R*,4*S*,7*R*,8*S*)-**53** + (3*S*,4*R*,7*R*,8*S*)-**62** (5.08 g, 9.4 mmol), pyridone ligand **41** (0.46 g, 1.7 mmol), and Rh catalyst (0.09 g, 0.33 mmol). Aldehyde M-**72** was isolated in 4.4 g, 82% yield as a colorless oil: HRMS

calcd for $C_{31}H_{42}O_5S_2Na$: 581.2371, found 581.2393; calcd for $C_{31}H_{41}O_5S_2FNa$: 599.2277, found 599.2264.

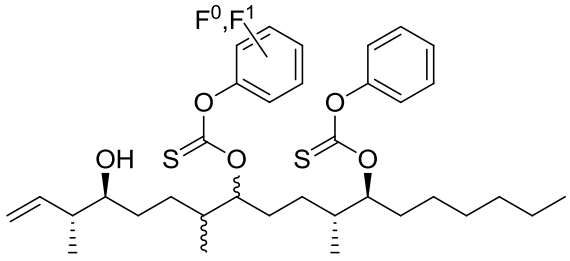

Mixture of *O*,*O*'-((7*S*,8*R*,11*S*,12*R*,15*S*,16*R*)-15-hydroxy-8,12,16-trimethyloctadec-17-ene-7,11-diyl) *O*,*O*'-diphenyl dicarbonothioate and *O*'-(2-fluorophenyl) *O*,*O*'-((7*S*,8*R*,11*R*,12*S*, 15*S*,16*R*)-15-hydroxy-8,12,16-trimethyloctadec-17-ene-7,11-diyl) *O*-phenyl dicarbonothioate M-**66:** This Roush crotylation reaction was performed according to General Procedure 2 using mixture aldehyde M-**65** (0.6 g, 0.52 mmol) and Roush reagent **33** (1.0 ml, 1.0 mmol). Allylic alcohol M-**66** was isolated in 0.52 g, 80% yield as a colorless oil: HRMS calcd for $C_{31}H_{50}O_5S_2Na_1$: 637.2997, found 637.3007; HRMS calcd for $C_{23}H_{36}O_3S_1F_1Na_1$: 655.2903, found 655.2900.

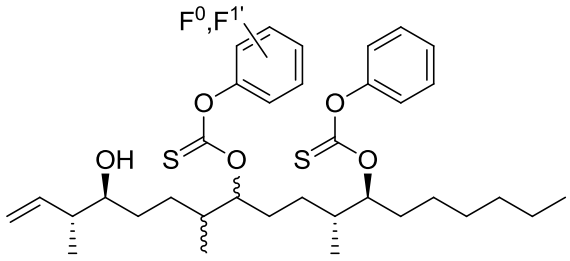

Mixture of *O*,*O*'-((7*S*,8*R*,11*S*,12*R*,15*S*,16*R*)-15-hydroxy-8,12,16-trimethyloctadec-17-ene-7,11-diyl) *O*,*O*'-diphenyl dicarbonothioate and *O*'-(4-fluorophenyl) *O*,*O*'-((7*S*,8*R*,11*R*,12*S*, 15*S*,16*R*)-15-hydroxy-8,12,16-trimethyloctadec-17-ene-7,11-diyl) *O*-phenyl dicarbonothioate M-**73:** This Roush crotylation reaction was performed according to General Procedure 2 using mixture aldehyde M-**72** (2.16 g, 3.8 mmol) and Roush reagent **33** (8.0 ml, 8.0 mmol).

Allylic alcohol M-**73** was isolated in 2.0 g, 84% yield as a colorless oil: HRMS calcd for $C_{31}H_{50}O_5S_2Na$: 637.2997, found 637.3015; HRMS calcd for $C_{23}H_{36}O_3SFNa$: 655.2903, found 655.2964.

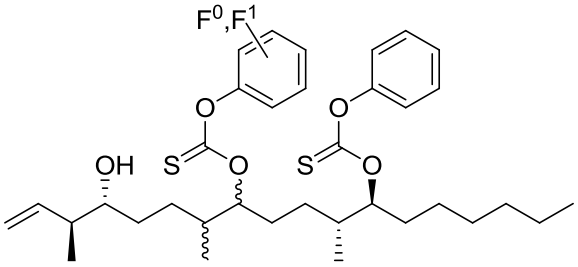

Mixture of *O*,*O*'-((7*S*,8*R*,11*S*,12*R*,15*R*,16*S*)-15-hydroxy-8,12,16-trimethyloctadec-17-ene-7,11-diyl) *O*,*O*'-diphenyl dicarbonothioate and *O*'-(2-fluorophenyl) *O*,*O*'-((7*S*,8*R*,11*R*,12*S*,15*R*,16*S*)-15-hydroxy-8,12,16-trimethyloctadec-17-ene-7,11-diyl) *O*-phenyl dicarbonothioate M-**67:** This Roush crotylation reaction was performed according to General Procedure 2 using mixture aldehyde M-**65** (0.6 g, 0.52 mmol) and Roush reagent **34** (1.0 ml, 1 mmol). Allylic alcohol M-**67** was isolated in 0.52 g, 79% yield as a colorless oil: HRMS calcd for $C_{31}H_{50}O_5S_2Na$: 637.2997, found 637.3005; HRMS calcd for $C_{23}H_{36}O_3SFNa$: 655.2903, found 655.2878.

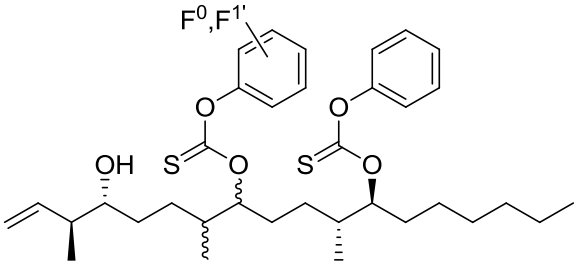

Mixture of *O*,*O*'-((7*S*,8*R*,11*S*,12*R*,15*R*,16*S*)-15-hydroxy-8,12,16-trimethyloctadec-17-ene-7,11-diyl) *O*,*O*'-diphenyl dicarbonothioate and *O*'-(4-fluorophenyl) *O*,*O*'-((7*S*,8*R*,11*R*,12*S*,15*R*,16*S*)-15-hydroxy-8,12,16-trimethyloctadec-17-ene-7,11-diyl) *O*-phenyl dicarbonothioate M-**74:** This Roush crotylation reaction was performed according to General Procedure 2

using mixture aldehyde M-**72** (2.36 g, 4.16 mmol) and Roush reagent **34** (15 ml, 8.3 mmol). Allylic alcohol M-**74** was isolated in 2.18 g, 83% yield as a colorless oil: HRMS calcd for $C_{31}H_{50}O_5S_2Na$: 637.2997, found 637.3016; HRMS calcd for $C_{23}H_{36}O_3SFNa$: 655.2903, found 655.2924.

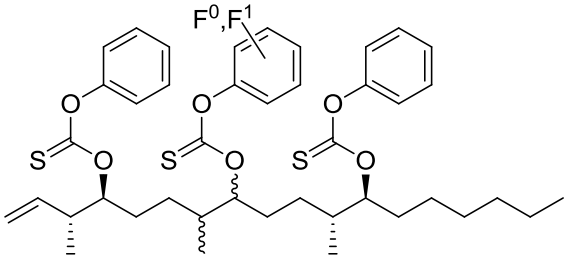

Mixture of *O*,*O*',*O*''-triphenyl *O*,*O*',*O*''((3*R*,4*S*,7*R*,8*S*, 11*R*,12*S*)-3,7,11-trimethyloctadec-1-ene-4,8, 12-triyl) tri-carbonothioate and *O*'-(2-fluorophenyl) *O*,*O*''-diphenyl *O*,*O*',*O*''-((3*R*,4*S*,7*S*,8*R*,11*R*,12*S*)-3,7,11-tri-methyloctadec-1-ene-4,8,12-triyl) tricarbonothioate M-**68:** This acylation reaction was performed according to General Procedure 3 using mixture allylic alcohol M-**66** (0.3 g, 0.24 mmol) and *O*-phenyl chlorothionoformate (0.09 g, 0.54 mmol). Alkene M-**68** was isolated in 0.32 g, 88% yield as a colorless oil: HRMS calcd for $C_{42}H_{54}O_6S_3Na$: 773.2980, found 773.2962; HRMS calcd for $C_{42}H_{53}O_6S_3FNa$: 791.2886, found 791.2934.

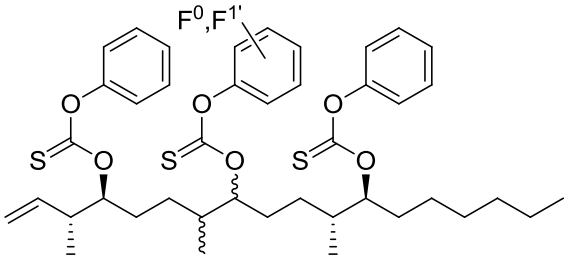

Mixture of *O*,*O*',*O*''-triphenyl *O*,*O*',*O*''((3*R*,4*S*,7*R*,8*S*, 11*R*,12*S*)-3,7,11-trimethyloctadec-1-ene-4,8, 12-triyl) tricarbonothioate and *O*'-(4-fluorophenyl) *O*,*O*''-diphenyl *O*,*O*',*O*''-((3*R*,4*S*,7*S*,8*R*,11*R*,12*S*)-3,7,11-tri-methyloctadec-1-ene-4,8,12-triyl) tricarbonothioate M-

75: This acylation reaction was performed according to General Procedure 3 using mixture allylic alcohol M-**73** (2.0 g, 3.1 mmol) and *O*-phenyl chlorothionoformate (0.61 g, 3.6 mmol). Alkene M-**75** was isolated in 2.6 g, 86% yield as a colorless oil: HRMS calcd for $C_{42}H_{54}O_6S_3Na$: 773.2980, found 773.2962; HRMS calcd for $C_{42}H_{53}O_6S_3FNa$: 791.2886, found 791.2870.

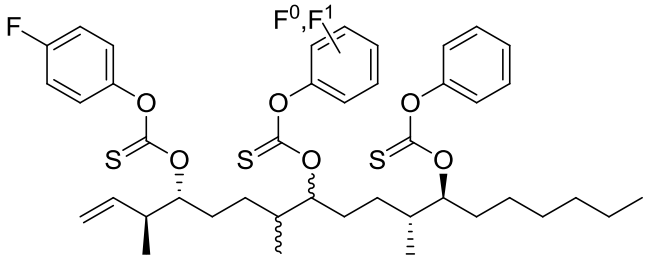

Mixture of *O*''-(4-fluorophenyl) *O*,*O*'-diphenyl *O*,*O*',*O*''-((3*S*,4*R*,7*R*,8*S*,11*R*,12*S*)-3,7,11-trimethyloctadec-1-ene-4,8, 12-triyl) tricarbonothioate and *O*''-(4-fluoro-phenyl) *O*'-(2-fluorophenyl) *O*-phenyl *O*,*O*',*O*''-((3*S*,4*R*,7*S*,8*R*,11*R*,12*S*)-3,7,11-trimethyloctadec-1-ene-4,8, 12-triyl) tricarbonothioate M-**69:** This acylation reaction was performed according to General Procedure 3 using allylic alcohol M-**67** (0.3 g, 0.24 mmol) and *O*-4-fluorophenyl chlorothiono-formate (0.1 g, 0.54 mmol). Alkene M-**69** was isolated in 0.32 g, 88% yield as colorless oil: HRMS calcd for $C_{42}H_{52}O_6S_3F_2Na$: 809.2792, found 809.2755; HRMS calcd for $C_{42}H_{53}O_6S_3FNa$: 791.2886, found 791.2934.

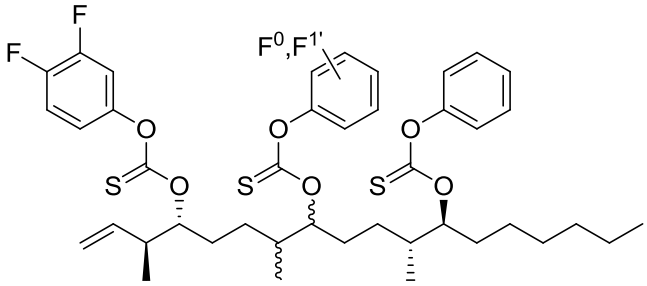

Mixture of *O*''-(3,4-difluorophenyl) *O*,*O*'-diphenyl *O*,*O*',*O*''-((3*S*,4*R*,7*R*,8*S*,11*R*,12*S*)-3,7,11-trimethyloctadec-1-ene-4,8, 12-triyl) tricarbonothioate and *O*''-(3,4-difluoro-phenyl) *O*'-(4-fluorophenyl) *O*-phenyl *O*,*O*',*O*''-((3*S*,4*R*,7*S*,8*R*,11*R*,12*S*)-3,7,11-trimethyloctadec-1-ene-4,8,

12-triyl) tricarbonothioate M-**76:** This acylation reaction was performed according to General Procedure 3 using allylic alcohol M-**74** (2.0 g, 3.16 mmol) and the crude product of *O*-3,4-difluorophenyl chlorothiono-formate **57** (~0.70 g, 3.30 mmol). Alkene M-**76** was isolated in 2.2 g, 88% yield as a colorless oil: HRMS calcd for $C_{42}H_{52}O_6S_3F_2Na$: 809.2792, found 809.2757; HRMS calcd for $C_{42}H_{51}O_6S_3F_3Na$: 827.2698, found 827.2710.

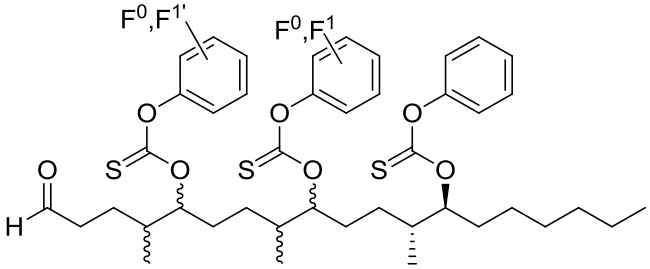

Mixture of *O*,*O*',*O*''-triphenyl *O*,*O*',*O*''-((4*R*, 5*S*, 8*R*, 9*S*, 12*R*,13*S*)-4,8,12-trimethyl-1-oxononadecane-5,9, 13-triyl) tricarbonothioate, *O*'-(2-fluorophenyl) *O*, *O*''-diphenyl *O*,*O*', *O*''-((4*R*,5*S*,8*S*,9*R*,12*R*,13*S*)-4,8,12-trimethyl-1-oxononadecane-5,9,13-triyl) tricarbonothioate, *O*''-(4-fluorophenyl) *O*,*O*'-diphenyl *O*,*O*',*O*''-((4*S*,5*R*,8*R*,9*S*,12*R*,13*S*)-4,8,12-trimethyl-1-oxononadecane-5,9,13-triyl) tricarbonothioate, and *O*''-(4-fluorophenyl) *O*'-(2-fluorophenyl) *O*-phenyl *O*,*O*',*O*''-((4*S*,5*R*,8*S*,9*R*,12*R*,13*S*)-4,8,12-trimethyl-1-oxononadecane-5,9,13-triyl) tricarbonothioate M-**70:** This Rh-catalyzed hydroformylation reaction was performed according to General Procedure 4 using 1:1 mixture of M-**68** plus M-**69** (0.3 g, 0.39 mmol), pyridone ligand **41** (0.07 g, 0.14 mmol), and Rh catalyst (0.007 g, 0.027 mmol). Aldehyde M-**70** was isolated in 0.26 g, 83% yield as a colorless oil: HRMS calcd for $C_{43}H_{56}O_7S_3Na_1$: 803.3086, found 803.3066; HRMS calcd for $C_{43}H_{55}O_7S_3FNa$: 821.2992, found 821.3021; HRMS calcd for $C_{43}H_{54}O_7S_3F_2Na$: 839.2897, found 839.2896.

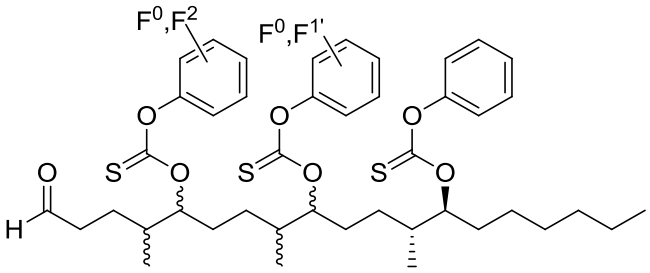

Mixture of *O*,*O*',*O*''-triphenyl *O*,*O*',*O*''-((4*R*, 5*S*, 8*R*, 9*S*, 12*R*,13*S*)-4,8,12-trimethyl-1-oxononadecane-5,9, 13-triyl) tricarbonothioate, *O*'-(4-fluorophenyl) *O*, *O*''-diphenyl *O*,*O*', *O*''-((4*R*,5*S*,8*S*,9*R*,12*R*,13*S*)-4,8,12-trimethyl-1-oxononadecane-5,9,13-triyl) tricarbonothioate, *O*''-(3,4-difluorophenyl) *O*,*O*'-diphenyl *O*,*O*', *O*''-((4*S*,5*R*,8*R*,9*S*,12*R*,13*S*)-4,8,12-trimethyl-1-oxononadecane-5,9,13-triyl) tricarbonothioate, and *O*''-(3,4-difluorophenyl) *O*'-(4-fluorophenyl) *O*-phenyl *O*,*O*',*O*''-((4*S*,5*R*,8*S*,9*R*,12*R*,13*S*)-4,8,12-trimethyl-1-oxononadecane-5,9,13-triyl) tricarbonothioate M-**77:** This Rh-catalyzed hydroformylation reaction was performed according to General Procedure 4 using 1:1 mixture of M-**75** plus M-**76** (3.6 g, 4.6 mmol), pyridone ligand **41** (0.81 g, 1.6 mmol), and Rh catalyst (0.09 g, 0.32 mmol). Aldehyde M-**77** was isolated in 3.0 g, 80% yield as a colorless oil: HRMS calcd for $C_{43}H_{56}O_7S_3Na$: 803.3086, found 803.3066; HRMS calcd for $C_{43}H_{55}O_7S_3FNa$: 821.2992, found 821.2988; HRMS calcd for $C_{43}H_{54}O_7S_3F_2Na$: 839.2897, found 839.2916; HRMS calcd for $C_{43}H_{53}O_7S_3F_3Na$: 857.2803, found 857.2819.

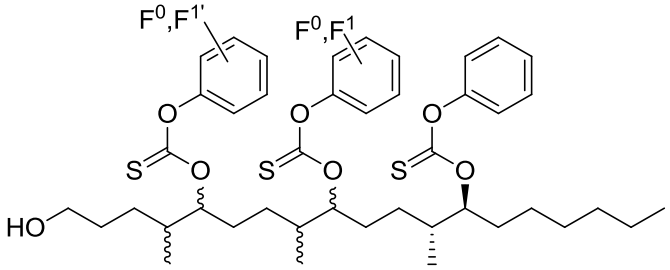

Mixture of *O*,*O*',*O*''-((4*R*,5*S*,8*R*,9*S*,12*R*,13*S*)-1-hydroxy-4,8,12-trimethylnonadecane-5,9,13-triyl) *O*,*O*',*O*''-triphenyl tricarbonothioate, O'-(2-fluorophenyl) *O*,*O*',*O*''-((4*R*,5*S*,8*S*,9*R*,

12*R*,13*S*)-1-hydroxy-4,8,12-tri-methylnonadecane-5,9,13-triyl) *O*,*O*''-diphenyl tri-carbonothioate, *O*''-(4-fluorophenyl) *O*,*O*',*O*''-((4*S*,5*R*,8*R*,9*S*,12*R*,13*S*)-1-hydroxy-4,8,12-trimethylnonadecane-5,9,13-triyl) *O*,*O*'-diphenyl tricarbonothioate, and *O*''-(4-fluorophenyl) *O*'-(2-fluorophenyl) *O*,*O*',*O*''-((4*S*,5*R*,8*S*,9*R*,12*R*,13*S*)-1-hydroxy-4,8,12-trimethylnonadecane-5,9,13-triyl) *O*-phenyl tricarbonothioate M-**71:** To a solution of M-**70** in THF (4 mL) at 0 °C was added DIBAL-*H* (0.30 mL, 0.29 mmol). The reaction was stirred for 3 h at 0 °C. The reaction was quenched by addition of saturated aq NH_4Cl (1 mL) followed by extraction of the aqueous layer with Et_2O (5 mL, 3 times). The combined organic layers was dried over $MgSO_4$ and concentrated. The crude product was purified by column chromatography (9:1 hexanes-diethylether). Mixture alcohol M-**71** was isolated in 0.14 g, 71.5% yield as a colorless viscous oil: HRMS calcd for $C_{43}H_{58}O_7S_3Na$: 805.3242, found 805.3220; HRMS calcd for $C_{43}H_{57}O_7S_3F_1Na$: 823.3148, found 823.3088; HRMS calcd for $C_{43}H_{56}O_7S_3F_2Na$: 841.3054, found 841.3113.

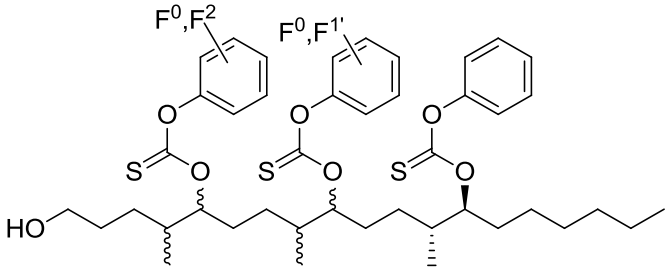

Mixture of *O*,*O*',*O*''-((4*R*,5*S*,8*R*,9*S*,12*R*,13*S*)-1-hydroxy-4,8,12-trimethylnonadecane-5,9,13-triyl) *O*,*O*',*O*''-triphenyl tricarbonothioate, O'-(4-fluorophenyl) *O*,*O*',*O*''-((4*R*,5*S*,8*S*,9*R*,12*R*,13*S*)-1-hydroxy-4,8,12-trimethylnonadecane-5,9,13-triyl) *O*,*O*''-diphenyl tri-carbonothioate, *O*''-(3,4-difluorophenyl) *O*,*O*',*O*''-((4*S*,5*R*,8*R*,9*S*,12*R*,13*S*)-1-hydroxy-4,8, 12-trimethylnonadecane-5,9,13-triyl) *O*,*O*'-diphenyl tricarbonothioate, and *O*''-(3,4-difluorophenyl) *O*'-(4-fluorophenyl) *O*,*O*',*O*''-((4*S*,5*R*,8*S*,9*R*,12*R*,13*S*)-1-hydroxy-4,8,12-trimethyl-

nonadecane-5,9,13-triyl) *O*-phenyl tricarbonothioate M-**78:** To a solution of M-**77** in THF (10 mL) at 0 °C was added DIBAL-*H* (1.95 mL, 1.95 mmol.). The reaction was stirred for 3 h at 0 °C. The reaction was quenched with addition of saturated aq NH_4Cl (3 mL) followed by extraction of the aqueous layer with Et_2O (5 mL, 3 times). The combined organic layers was dried over $MgSO_4$ and concentrated. The crude product was purified by column chromatography (9:1 hexanes-diethylether). Mixture alcohol M-**78** was isolated in 0.88 g, 88% yield as a colorless viscous oil: HRMS calcd for $C_{43}H_{58}O_7S_3Na$: 805.3242, found 805.3287; HRMS calcd for $C_{43}H_{57}O_7S_3FNa$: 823.3148, found 823.3119; HRMS calcd for $C_{43}H_{56}O_7S_3F_2Na$: 841.3054, found 841.3100; HRMS calcd for $C_{43}H_{55}O_7S_3F_3Na$: 859.2960, found 859.3012.

Fluorous HPLC demixing

The F-HPLC demixing procedures and conditions were described in details in Section 3.2.4. The purity of each demixed product contain ~70% of the title product and ~10% of each of the other quasiisomers as fully explained in section 3.3.3.

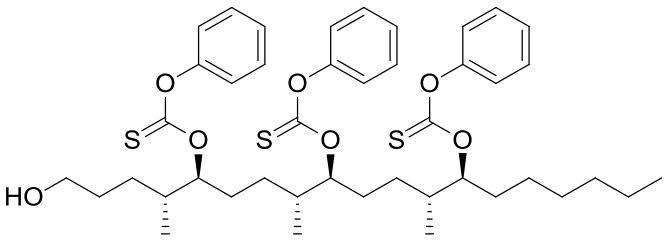

***O*,*O*',*O*''-((4*R*,5*S*,8*R*,9*S*,12*R*,13*S*)-1-Hydroxy-4,8,12-trimethylnonadecane-5,9,13-triyl) *O*,*O*',*O*''-triphenyl tricarbonothioate [(4*R*,5*S*,8*R*,9*S*,12*R*,13*S*)-78]:** (4*R*,5*S*,8*R*,9*S*,12*R*,13*S*)-**78** was obtained in 32 mg, 74% recovery: $[\alpha]_D^{25}$ = +9.32 (*c* = 0.21, $CHCl_3$); ^{1}H NMR ($CDCl_3$, 400 MHz, ppm) δ = 7.395 (t, *J* = 7.8 Hz, 4H), 7.347 (t, *J* = 7.8 Hz, 2H), 7.266 (t, *J* = 7.8Hz 3H), 7.098 (d, *J* = 7.7 Hz, 6H), 5.323-5.344 (m, 3H), 3.638 (t, *J* =6.1, 2H), 1.969-2.036 (m, 3H),

1.251-1.952 (m, 22H), 1.007 (d, J = 6.8 Hz, 3H), 1.001 (d, J = 6.3 Hz, 3H), 0.985 (d, J = 6.7 Hz, 3H), 0.891 (t, J = 6.7 Hz, 3H); ^{13}C NMR ($CDCl_3$, 100 MHz, ppm) δ = 195.11, 195.08, 153.36, 153.33, 153.30, 129.46, 126.44, 122.04, 122.02, 89.46, 89.14, 89.11, 89.06, 62.96, 35.99, 35.91, 35.88, 35.62, 31.70, 30.23, 30.20, 30.04, 29.77, 29.26, 29.25, 28.47, 28.33, 28.27, 28.06, 28.00, 27.86, 27.66, 27.58, 27.53, 27.41, 27.03, 25.28, 22.60, 15.15, 15.10, 15.04, 14.97, 14.93, 14.87, 14.09; FTIR ν_{max} 3354, 3044, 2959, 2927, 2857, 1592, 1489, 1457, 1359, 1281, 1197, 1003, 769 cm^{-1}; HRMS calcd for $C_{43}H_{58}O_7S_3Na$: 805.3242, found 805.3222.

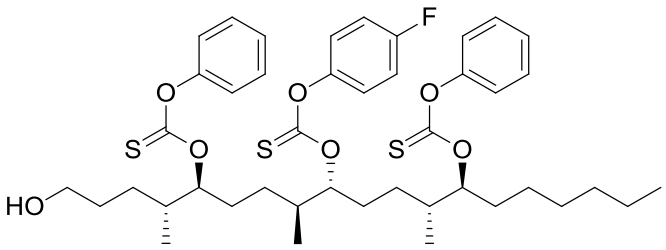

***O*'-(4-Fluorophenyl) *O*,*O*',*O*''-((4*R*,5*S*,8*S*,9*R*,12*R*,13*S*)-1-hydroxy-4,8,12-trimethylnonadecane-5,9,13-triyl) *O*,*O*''-diphenyl tricarbonothioate [(4*R*,5*S*,8*S*,9*R*,12*R*,13*S*)-78]:** (4*R*,5*S*,8*S*,9*R*,12*R*,13*S*)-**78** was obtained in 28 mg, 72% recovery: $[\alpha]_D^{25}$ = +2.33 (c = 0.32, $CHCl_3$); ^{1}H NMR ($CDCl_3$, 400 MHz, ppm) δ = 7.390 (t, J = 7.8 Hz, 4H), 7.383 (t, J = 7.8 Hz, 2H), 7.274 (t, J = 7.8Hz 3H), 7.098 (d, J = 8.2 Hz, 2H), 7.091 (d, J = 8.3 Hz, 2H), 7.001-7.068 (m, 4H), 5.313-5.356 (m, 3H), 3.654 (t, J =6.0, 2H), 1.968-2.075 (m, 3H), 1.252-1.939 (m, 22H), 1.002 (d, J = 6.5 Hz, 3H), 0.994 (d, J = 6.7 Hz, 6H), 0.891 (t, J = 6.6 Hz, 3H).); ^{13}C NMR ($CDCl_3$, 100 MHz, ppm) δ = 195.29, 195.25, 195.17, 161.81, 159.38, 153.39, 153.34, 153.32, 149.23, 149.20, 129.50, 126.50, 126.47, 123.68, 123.60, 122.08, 122.05, 116.30, 116.07, 89.44, 89.15, 89.06, 62.96, 36.02, 35.89, 35.67, 31.73, 30.25, 30.22, 30.11, 29.87, 29.30, 28.52, 28.39, 28.32, 28.12, 28.04, 27.88, 27.74, 27.57, 27.44, 27.06, 25.27, 22.63, 15.19, 15.14, 15.10, 15.04, 14.96, 14.92,

14.90, 14.12; FTIR ν_{max} 3352, 2959, 2928, 2859, 1592, 1502, 1457, 1359, 1281, 1198, 1004, 738 cm^{-1}; HRMS calcd for $C_{43}H_{57}O_7S_3FNa$: 823.3148, found 823.3115.

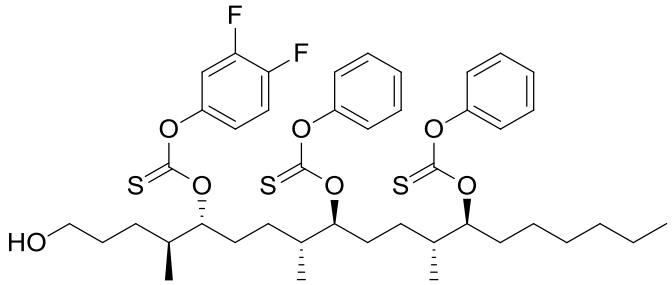

***O*''-(3,4-Difluorophenyl) *O*,*O*',*O*''-((4*S*,5*R*,8*R*,9*S*,12*R*,13*S*)-1-hydroxy-4,8,12-trimethylnona decane-5,9,13-triyl) *O*,*O*'-diphenyl tricarbonothioate [(4*S*,5*R*,8*R*,9*S*,12*R*,13*S*)-78]:** (4*S*,5*R*, 8*R*,9*S*,12*R*,13*S*)-**78** was obtained in 30 mg, 71% recovery: $[\alpha]_D^{25}$ = –1.34 (*c* = 0.25, $CHCl_3$); ^{1}H NMR ($CDCl_3$, 400 MHz, ppm) δ = 7.347-7.411 (m, 4H), 7.287-7.289 (m, 2H), 7.086-7.176 (m, 5H), 6.952-7.001 (m, 1H), 6.823-6.865 (m, 1H), 5.323-5.344 (m, 3H), 3.638 (t, *J* =6.1, 2H), 1.969-2.036 (m, 3H), 1.251-1.952 (m, 22H), 1.007 (d, *J* = 6.8 Hz, 3H), 1.001 (d, *J* = 6.3 Hz, 3H), 0.985 (d, *J* = 6.7 Hz, 3H), 0.891 (t, *J* = 6.7 Hz, 3H); ^{13}C NMR ($CDCl_3$, 100 MHz, ppm) δ = 195.22, 195.16, 194.64, 153.39, 153.35, 151.44, 149.91, 148.94, 148.80, 148.74, 148.70, 148.65, 148.62, 148.57, 148.45, 129.50, 129.49, 126.52, 122.06, 118.45, 118.39, 118.35, 117.44, 117.25, 112.51, 112.31, 90.10, 89.64, 89.42, 89.33, 89.11, 62.91, 53.46, 35.98, 35.88, 35.84, 35.61, 31.72, 30.20, 30.02, 29.77, 29.28, 28.51, 28.39, 28.29, 28.12, 28.03, 27.89, 27.67, 27.47, 26.97, 25.30, 22.62, 15.18, 15.11, 15.03, 14.97, 14.94, 14.87, 14.10; FTIR ν_{max} 3385, 2959, 2928, 2858, 1513, 1490, 1458, 1284, 1195, 1004, 771 cm^{-1}; HRMS calcd for $C_{43}H_{56}O_7S_3F_2Na$: 841.3054, found 841.3025.

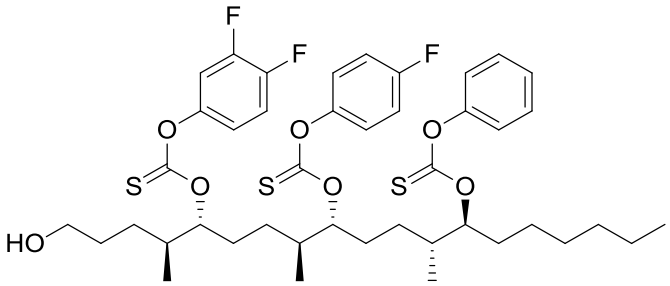

***O*''-(3,4-Difluorophenyl) *O*'-(4-fluorophenyl) *O*,*O*',*O*''-((4*S*,5*R*,8*S*,9*R*,12*R*,13*S*)-1-hydroxy-4,8,12-trimethyl-nonadecane-5,9,13-triyl) *O*-phenyl tricarbonothioate [(4*S*,5*R*,8*S*,9*R*,12*R*, 13*S*)-78]:** (4*S*,5*R*,8*S*,9*R*,12*R*,13*S*)-**78** was obtained in 29 mg, 71% recovery: $[\alpha]_D^{25}$ = –5.81 (*c* = 0.22, $CHCl_3$); ^{1}H NMR ($CDCl_3$, 400 MHz, ppm) δ = 7.347-7.412 (m, 2H), 7.287-7.297 (m, 1H), 7.086-7.185 (m, 7H), 6.945-7.001 (m, 1H), 6.818-6.861 (m, 1H), 5.289-5.352 (m, 3H), 3.654 (t, *J* =6.1, 2H), 1.955-2.080 (m, 3H), 1.195-1.942 (m, 22H), 1.007 (d, *J* = 6.7 Hz, 3H), 0.994 (d, *J* = 6.5 Hz, 3H), 0.986 (d, *J* = 6.7 Hz, 3H), 0.891 (t, *J* = 6.7 Hz, 3H); ^{13}C NMR ($CDCl_3$, 100 MHz, ppm) δ = 195.24, 195.15, 194.65, 161.82, 159.38, 153.36, 153.32, 151.43, 151.29, 150.03, 149.91, 149.14, 149.12, 148.80, 148.68, 148.65, 148.60, 148.57, 147.57, 147.45, 129.47, 126.46, 123.61, 123.52, 122.05, 118.38, 118.34, 118.29, 117.43, 117.24, 116.30, 116.06, 112.49, 112.30, 90.06, 89.60, 89.36, 89.11, 89.07, 88.86, 62.90, 35.95, 35.89, 35.66, 31.71, 30.20, 30.10, 29.85, 29.28, 28.50, 28.37, 28.28, 28.11, 28.02, 27.86, 27.62, 27.58, 27.43, 27.01, 26.95, 25.24, 22.61, 15.11, 14.96, 14.89, 14.86, 14.09; FTIR ν_{max} 3377, 2959, 2929, 2859, 1504, 1290, 1198, 1005, 839, 796, 772, 738 cm^{-1}; HRMS calcd for $C_{43}H_{55}O_7S_3F_3Na$: 859.2960, found 859.2902.

General Procedure 5: radical deoxygenation

To a solution of triphenylthionocarbonate tagged trimethylnonadecanol and 5 equiv of dimethyl-imidazolium carbene-borane (diMe-Imd-BH_3) in benzene-*d* were added AIBN. The reaction mixture was heated at 80 °C. After 2 h, the solvent was evaporated and the residue was first

extracted with hexanes (3 x 5 mL) then concentrated. The crude product was isolated by column chromatography (9:1) hexane-diethyl ether.

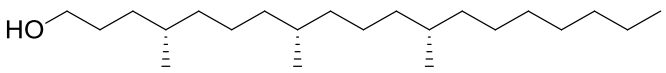

(4*S*,8*S*,12*S*)-4,8,12-Trimethylnonadecan-1-ol [(4*S*,8*S*, 12*S*)-79]: This deoxygenation reaction was performed according to General Procedure 5 using triphenylthionocarbonate (4*R*,5*S*,8*R*,9*S*,12*R*,13*S*)-**78** (0.020 g, 0.024 mmol), diMe-Imd-BH_3 (0.037 g, 0.12 mmol), and AIBN (0.020 g, 0.12 mmol). Alcohol (4*S*,8*S*,12*S*)-**79** was obtained in 0.006 g, 69% yield: $[\alpha]_D^{25} =$ –7.2 (c = 0.28, $CHCl_3$); ^{1}H NMR ($CDCl_3$, 700 MHz, ppm) δ = 3.635 (t, J = 6.6 Hz, 2H), 1.664–1.504 (m, 2H), 1.443–1.003 (m, 30H), 0.882 (t, J = 7.0 Hz, 3H), 0.874 (d, J = 6.6 Hz, 3H), 0.840 (d, J = 6.6 Hz, 6H); ^{13}C NMR ($CDCl_3$, 100 MHz, ppm) δ = 63.51, 37.43, 37.37, 37.33, 37.16, 37.06, 33.00, 32.90, 32.80, 32.78, 32.65, 31.94, 30.36, 30.00, 29.42, 27.10, 25.33, 25.18, 24.47, 24.44, 22.71, 19.79, 19.77, 19.67, 14.15; FTIR ν_{max} 3333, 2959, 2924, 2854 cm^{-1}; HRMS calcd for $C_{22}H_{45}O$: 325.3470, found 325.3443.

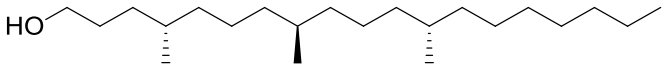

(4*S*,8*R*,12*S*)-4,8,12-Trimethylnonadecan-1-ol [(4*S*,8*R*, 12*S*)-79]: This deoxygenation reaction was performed according to General Procedure 5 using triphenylthionocarbonate (4*R*,5*S*,8*S*,9*R*,12*R*,13*S*)-**78** (0.020 g, 0.025 mmol), diMe-Imd-BH_3 (0.014 g, 0.125 mmol), and AIBN (0.020 g, 0.125 mmol). Alcohol (4*S*,8*R*,12*S*)-**79** was obtained in 0.0052 g, 64% yield: $[\alpha]_D^{25} =$ 1.5 (c = 0.38, $CHCl_3$); ^{1}H NMR ($CDCl_3$, 700 MHz, ppm) δ = 3.635 (t, J = 6.6 Hz, 2H), 1.664–1.504 (m, 2H), 1.443–1.003 (m, 30H), 0.882 (t, J = 7.0 Hz, 3H), 0.872 (d, J = 6.6 Hz, 3H), 0.842 (d, J = 6.6 Hz, 3H), 0.839 (d, J = 6.6 Hz, 3H); ^{13}C NMR ($CDCl_3$, 100 MHz, ppm) δ =

63.51, 37.40, 37.35, 37.28, 37.15, 32.99, 32.91, 32.76, 32.63, 32.44, 31.94, 30.36, 30.00, 29.71, 29.41, 27.11, 25.32, 25.17, 24.47, 24.43, 22.71, 19.70, 19.66, 19.61, 14.14; FTIR ν_{max} 3349, 2959, 2925, 2855 cm^{-1}; HRMS calcd for $C_{22}H_{45}O_1$: 325.3470, found 325.3442.

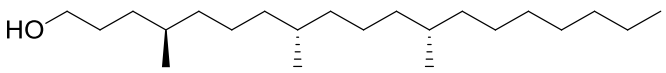

(4*R*,8*S*,12*S*)-4,8,12-Trimethylnonadecan-1-ol [(4*R*,8*S*, 12*S*)-79]: This deoxygenation reaction was performed according to General Procedure 5 using triphenylthionocarbonate (4*S*,5*R*,8*R*,9*S*,12*R*,13*S*)-**78** (0.018 g, 0.022 mmol), diMe-Imd-BH_3 (0.012 g, 0.110 mmol), and AIBN (0.018 g, 0.110 mmol). Alcohol (4*R*,8*S*,12*S*)-**79** was obtained in 0.0047 mg, 65.5% yield: $[\alpha]_D^{25}$ = 2.0 (*c* = 0.29, $CHCl_3$); ^{1}H NMR ($CDCl_3$, 700 MHz, ppm) δ = 3.635 (t, *J* = 6.6 Hz, 2H), 1.664–1.504 (m, 2H), 1.443–1.003 (m, 30H), 0.882 (t, *J* = 7.0 Hz, 3H), 0.872 (d, *J* = 6.6 Hz, 3H), 0.842 (d, *J* = 6.6 Hz, 3H), 0.840 (d, *J* = 6.6 Hz, 3H); ^{13}C NMR ($CDCl_3$, 100 MHz, ppm) δ = 63.51, 37.49, 37.43, 37.38, 37.33, 37.16, 37.06, 32.99, 32.90, 32.78, 32.63, 31.94, 30.37, 30.36, 30.00, 29.71, 29.42, 27.10, 25.18, 24.48, 24.43, 22.71, 19.77, 19.73, 19.61, 14.15; FTIR ν_{max} 3333, 2958, 2925, 2854 cm^{-1}; HRMS calcd for $C_{22}H_{45}O$: 325.3470, found 325.3444.

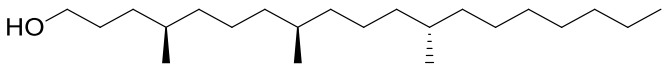

(4*R*,8*R*,12*S*)-4,8,12-Trimethylnonadecan-1-ol [(4*R*,8*R*, 12*S*)-79]: This deoxygenation reaction was performed according to General Procedure 5 using triphenylthionocarbonate (4*S*,5*R*,8*S*,9*R*,12*R*,13*S*)-**78** (0.017 g, 0.020 mmol), dime-Imd-BH_3 (0.011 g, 0.100 mmol), and AIBN (0.017 g, 0.100 mmol). Alcohol (4*R*,8*R*,12*S*)-**79** was obtained in 0.0042 mg, 63.3% yield: $[\alpha]_D^{25}$ = –2.4 (*c* = 0.2, $CHCl_3$); ^{1}H NMR ($CDCl_3$, 700 MHz, ppm) δ = 3.634 (t, *J* = 6.6 Hz, 2H), 1.664–1.504 (m, 2H), 1.443–1.003 (m, 30H), 0.882 (t, *J* = 7.0 Hz, 3H), 0.874 (d, *J* = 6.6 Hz,

3H), 0.842 (d, J = 6.6 Hz, 3H), 0.839 (d, J = 6.6 Hz, 3H); ^{13}C NMR ($CDCl_3$, 100 MHz, ppm) δ = 63.50, 37.47, 37.43, 37.38, 37.33, 37.16, 33.00, 32.91, 32.78, 32.76, 32.66, 31.93, 30.37, 30.00, 29.41, 27.11, 25.18, 24.46, 24.45, 23.46, 22.70, 19.73, 19.70, 19.67, 14.13; FTIR ν_{max} 3334, 2958, 2925, 2855 cm^{-1}; HRMS calcd for $C_{22}H_{45}O$: 325.3470, found 325.3449.

APPENDIX A

HYDROFORMYLATION APPARATUS

Figure A.1. The initial hydroformylation setup

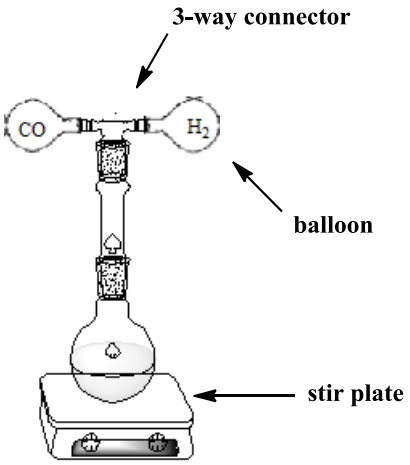

Figure A.2. Parr EA3911 Hydrogenator

Figure A.3. Parr© general purpose pressure reactor

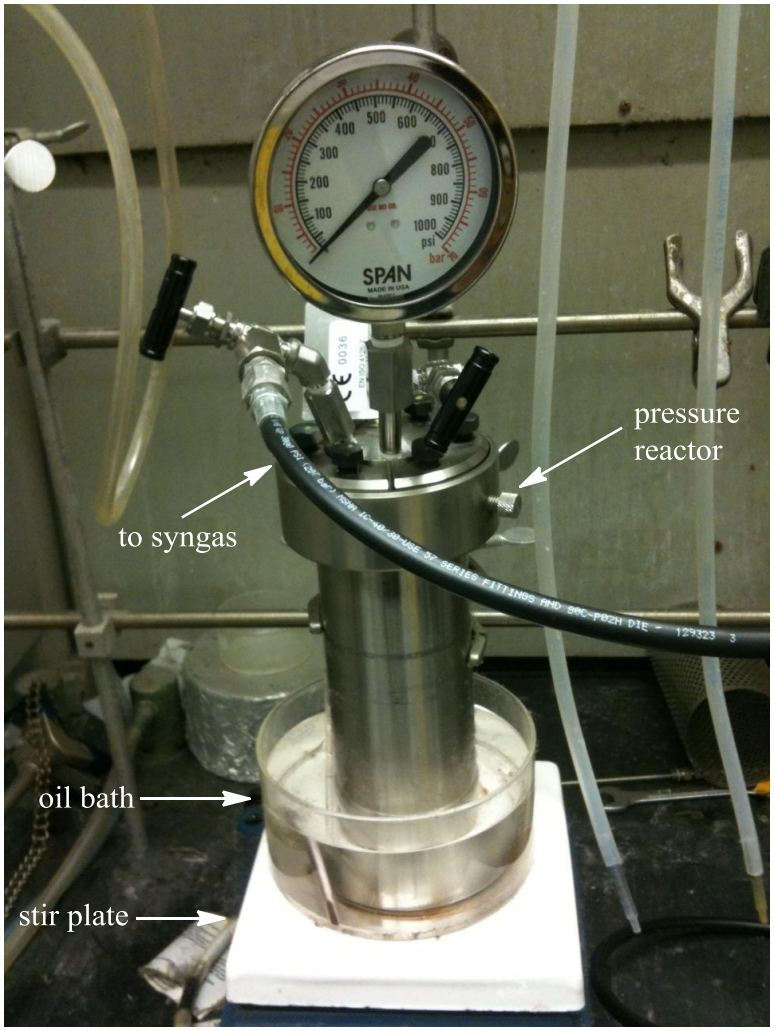

APPENDIX B

FLUOROUS HPLC TRACE

Figure B.1. F-HPLC trace of substrates **53**, **60**, **61**, **62**, **63**, and **64** on a PFP column[a,b]

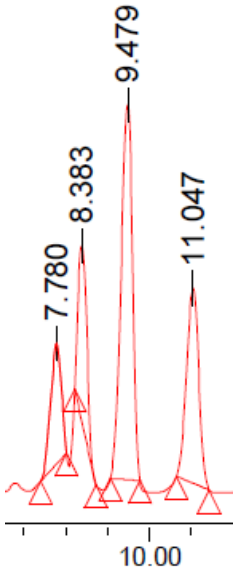

a. conditions: isocratic 75:25 acetonitrile/H_2O, 1 mL/min

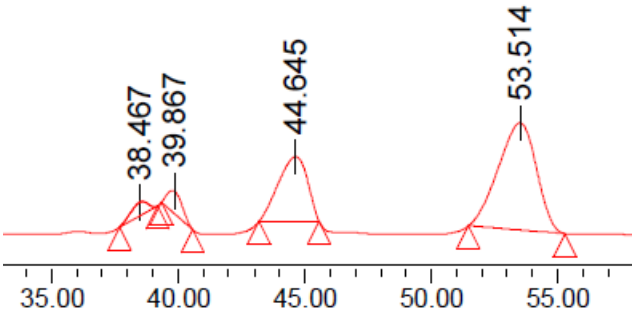

b. conditions: isocratic 65:35 acetonitrile/H_2O, 1 mL/min

Figure B.2. F-HPLC trace of M-**71** on a PFP column

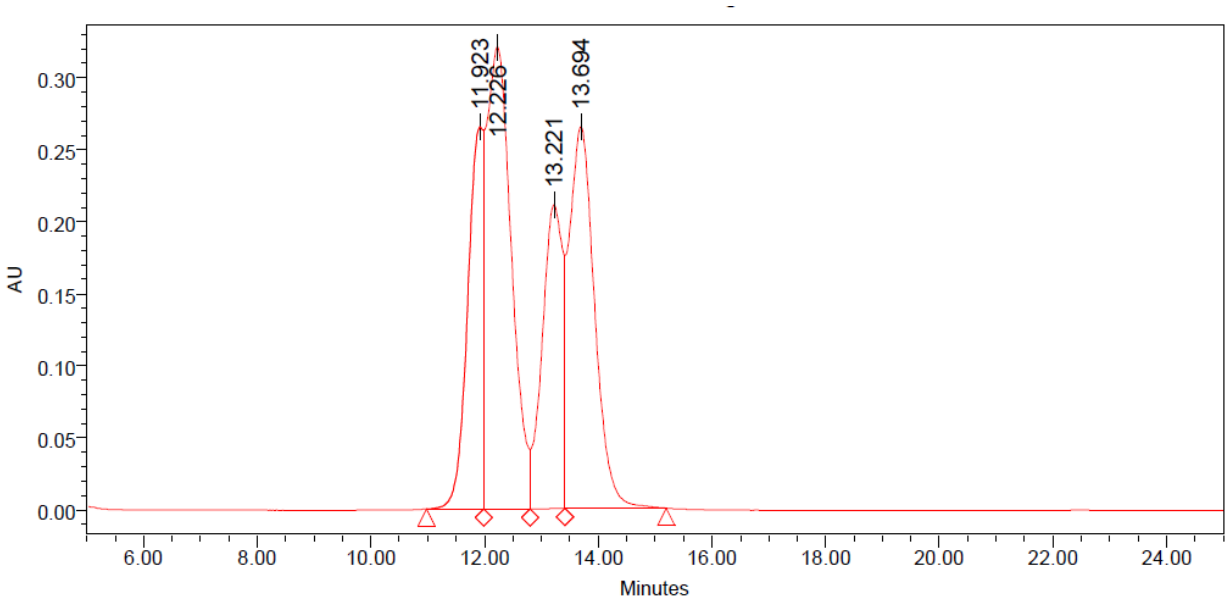

conditions: isocratic 65:35 acetonitrile/H_2O, 1 mL/min

Figure B.3. F-HPLC trace of M-**78** on a reverse phase RP-C18 column

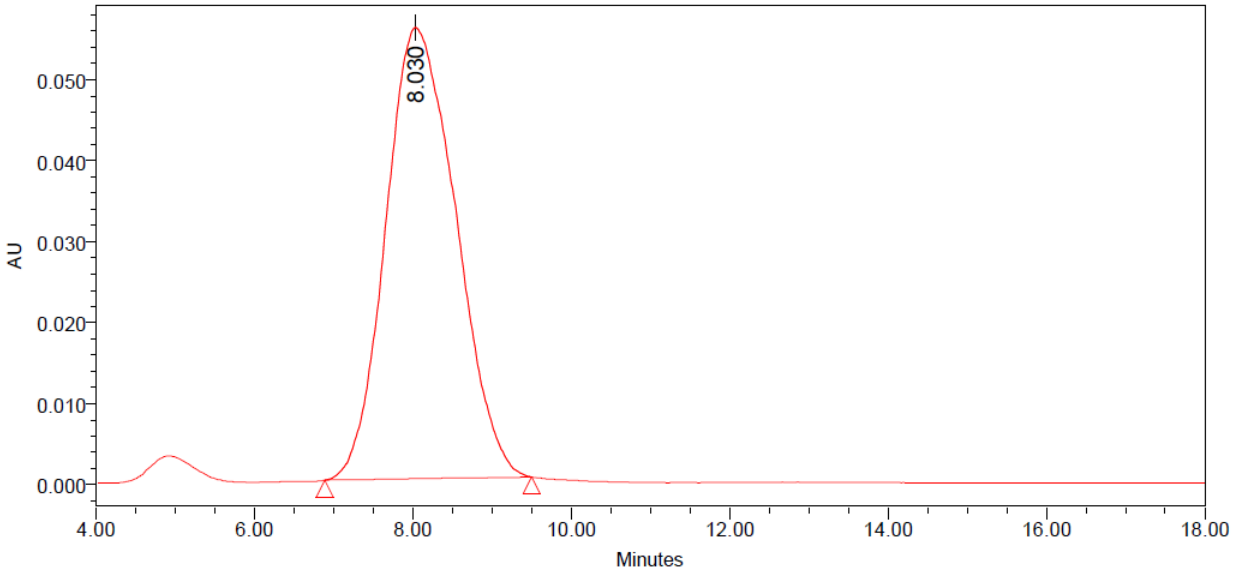

conditions: isocratic 80:20 acetonitrile/H_2O, 1 mL/min

APPENDIX C

1D TOCSY OF FOUR ISOMERS OF 4,8,12-TRIMETHYLNONADECANOL

Figure C.1. 1D TOCSY of (4*S*,8*R*,12*S*)-**79**

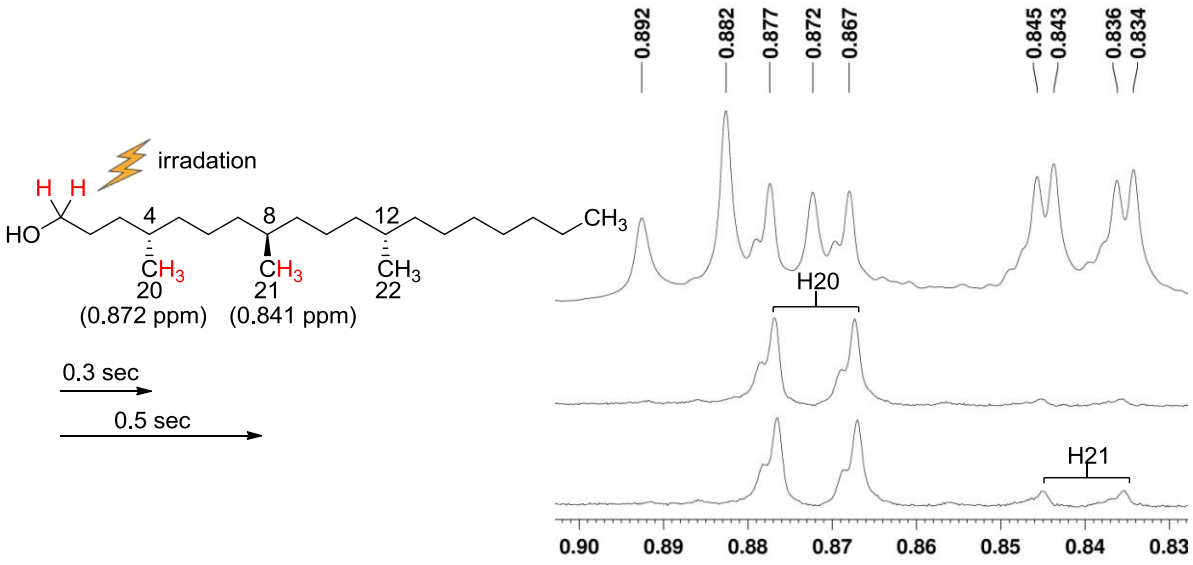

Figure C.2. 1D TOCSY of (4*R*,8*S*,12*S*)-**79**

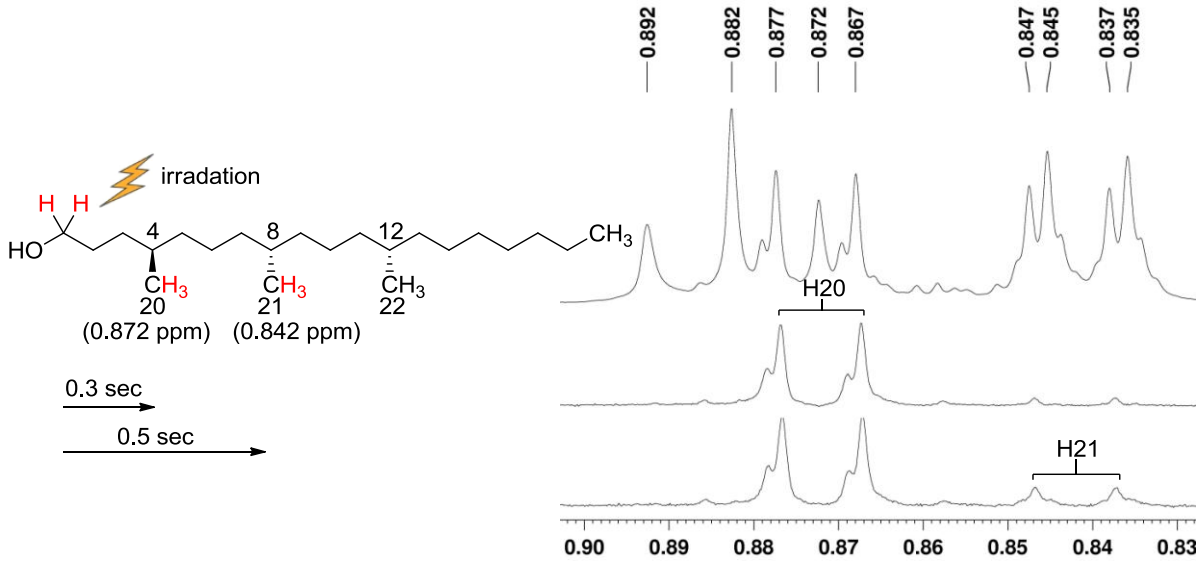

Figure C.3. 1D TOCSY of (4*R*,8*R*,12*S*)-**79**

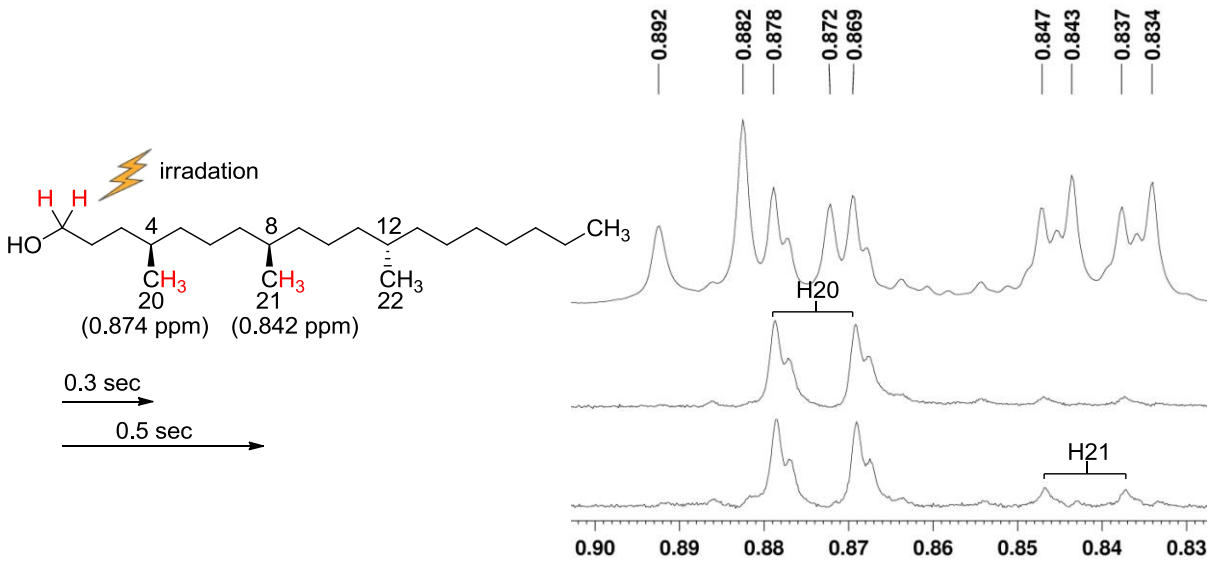

APPENDIX D

2D INVERSE HMQC OF FOUR ISOMERS OF 4,8,12-TRIMETHYLNONADECANOL

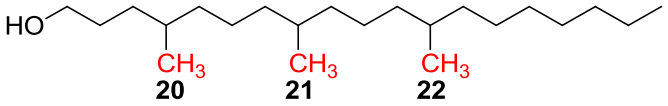

Figure D.1. Inverse 2D HMQC experiment of (4*S*,8*R*,12*S*)-**79**

(4*S*,8*R*,12*S*)-**79**

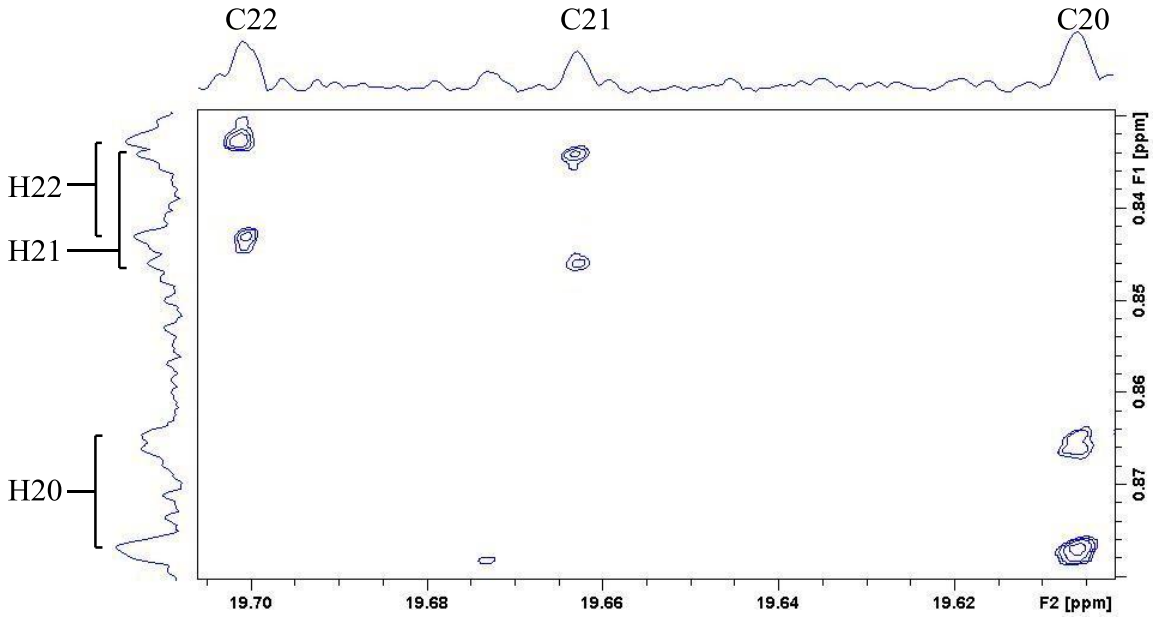

Figure D.2. Inverse 2D HMQC experiment of (4*R*,8*S*,12*S*)-**79**

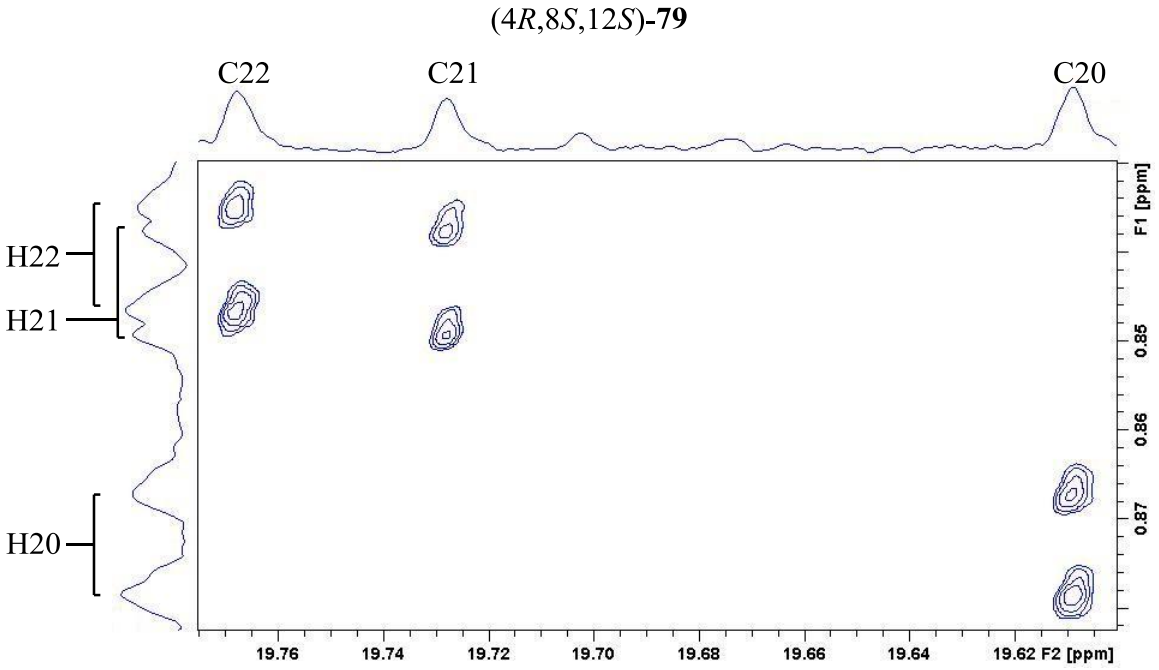

Figure D.3. Inverse 2D HMQC experiment of (4*R*,8*R*,12*S*)-**79**

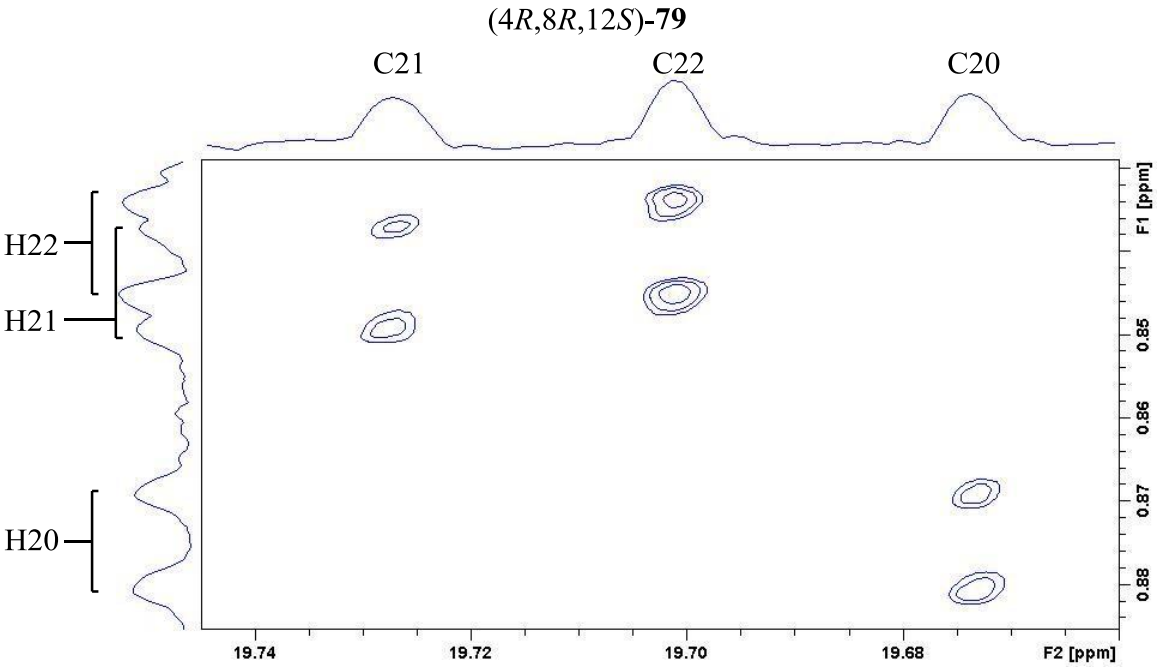

APPENDIX E

^{1}H, ^{13}C, AND ^{19}F NMR SPECTRA

The ^{1}H NMR spectra were recorded on a Bruker Advance III 700 MHz; the ^{13}C NMR spectra were recorded on a Bruker Advance III 600 MHz; and the ^{19}F NMR spectra were recorded on a Bruker Advance III 400 MHz.

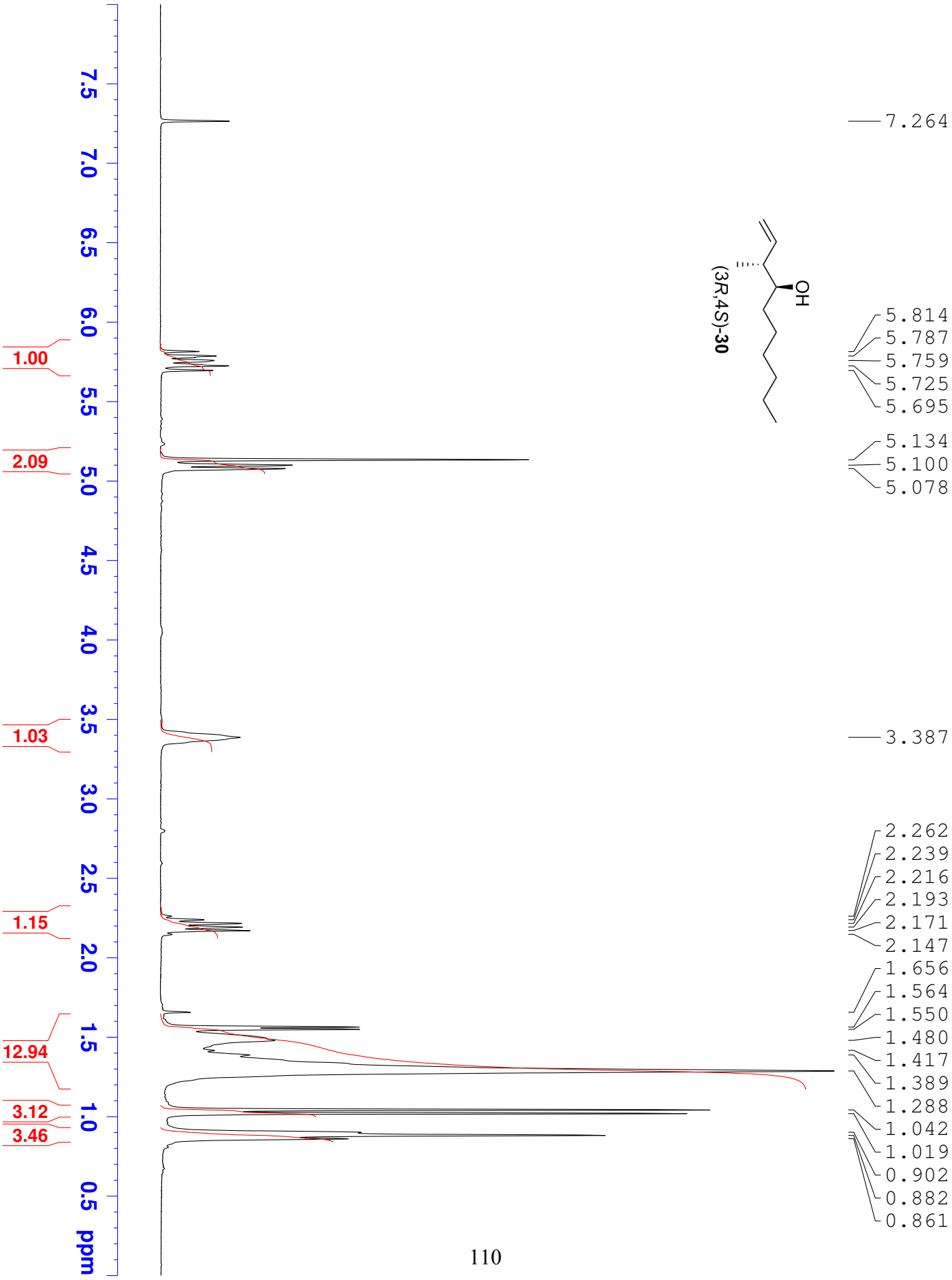
7.264
5.814
5.787
5.759
5.725
5.695
5.134
5.100
5.078
3.387
2.262
2.239
2.216
2.193
2.171
2.147
1.656
1.564
1.550
1.480
1.417
1.389
1.288
1.042
1.019
0.902
0.882
0.861
1.00
2.09
1.03
1.15
12.94
3.12
3.46
7.5
7.0
6.5
6.0
5.5
5.0
4.5
4.0
3.5
3.0
2.5
2.0
1.5
1.0
0.5
ppm
OH
(3R,4S)-30

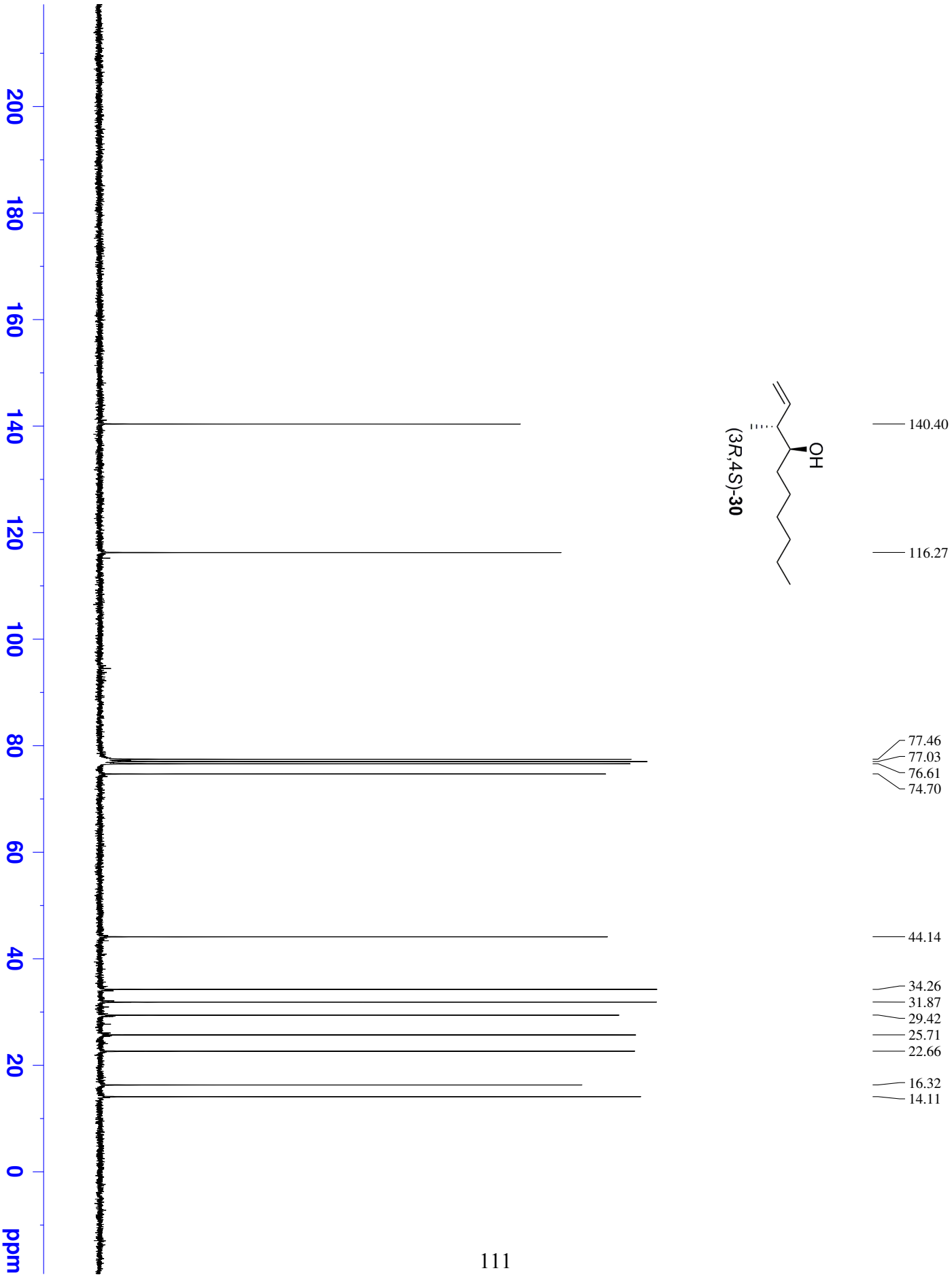
200
180
160
140
120
100
80
60
40
20
0
ppm
OH
(3R,4S)-30
140.40
116.27
77.46
77.03
76.61
74.70
44.14
34.26
31.87
29.42
25.71
22.66
16.32
14.11

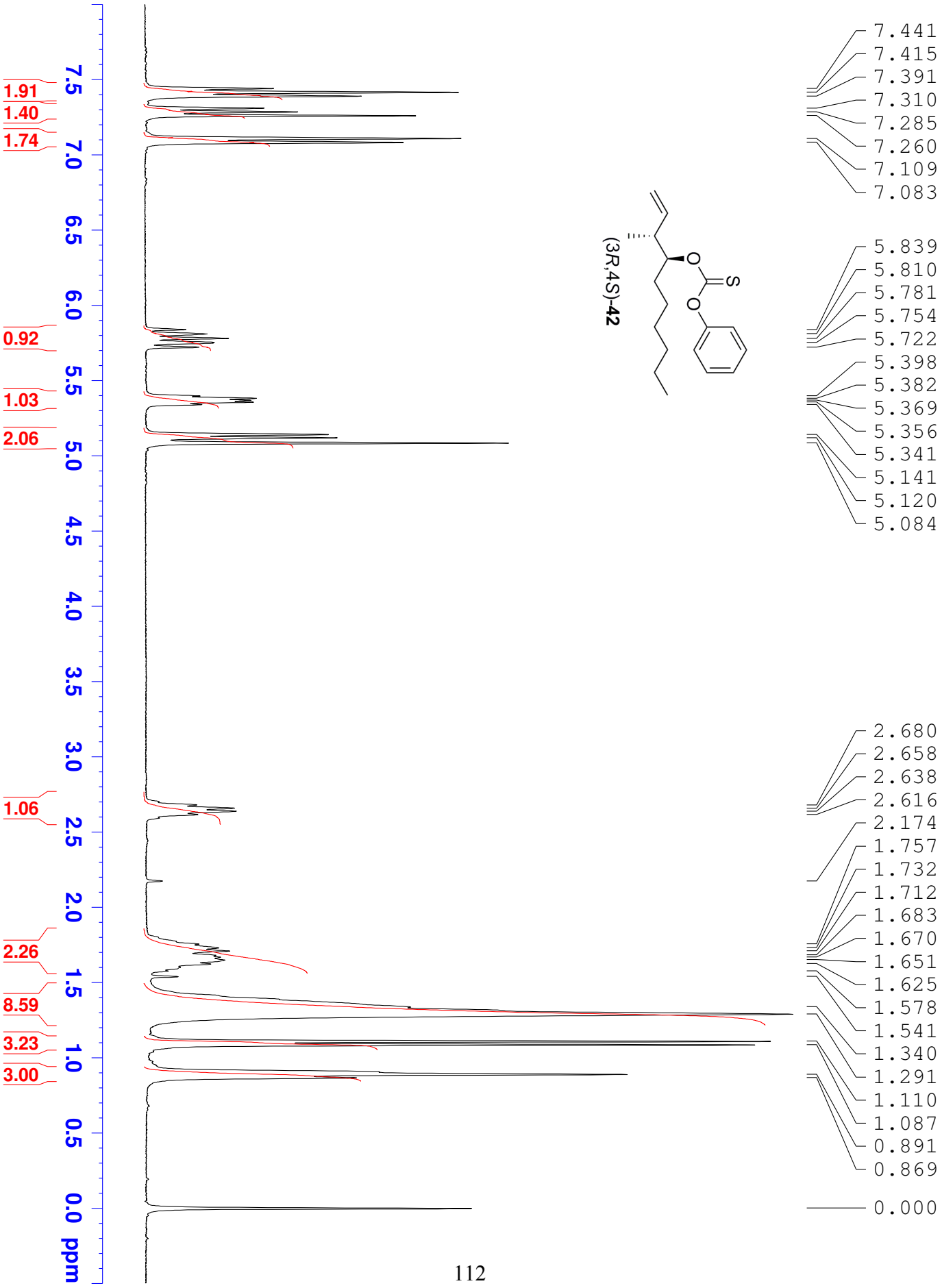
7.441
7.415
7.391
7.310
7.285
7.260
7.109
7.083
5.839
5.810
5.781
5.754
5.722
5.398
5.382
5.369
5.356
5.341
5.141
5.120
5.084
2.680
2.658
2.638
2.616
2.174
1.757
1.732
1.712
1.683
1.670
1.651
1.625
1.578
1.541
1.340
1.291
1.110
1.087
0.891
0.869
0.000
1.91
1.40
1.74
0.92
1.03
2.06
1.06
2.26
8.59
3.23
3.00
7.5
7.0
6.5
6.0
5.5
5.0
4.5
4.0
3.5
3.0
2.5
2.0
1.5
1.0
0.5
0.0
ppm
(3R,4S)-42

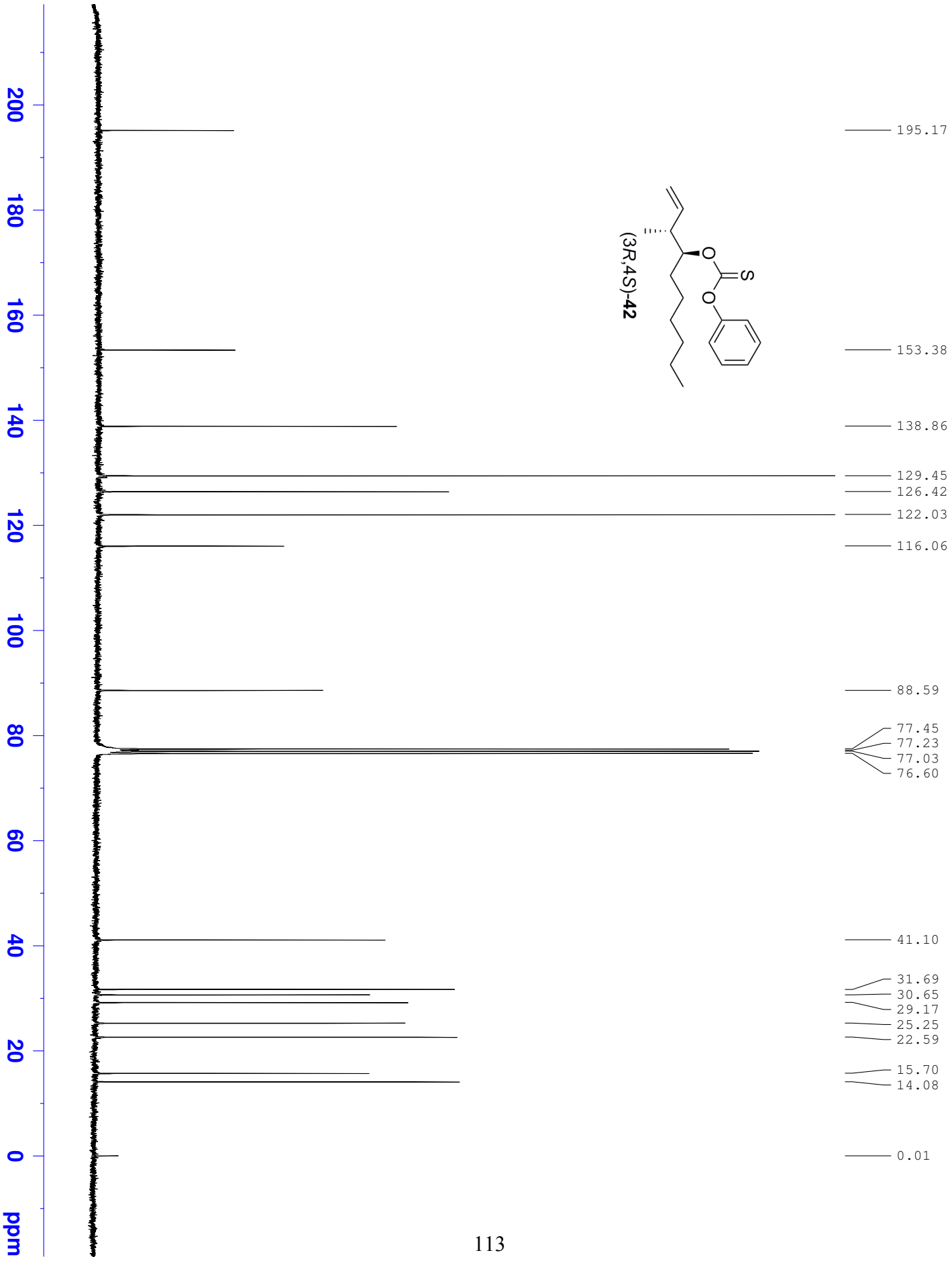
200
180
160
140
120
100
80
60
40
20
0
ppm
195.17
153.38
138.86
129.45
126.42
122.03
116.06
88.59
77.45
77.23
77.03
76.60
41.10
31.69
30.65
29.17
25.25
22.59
15.70
14.08
0.01
(3R,4S)-42
O
S
O

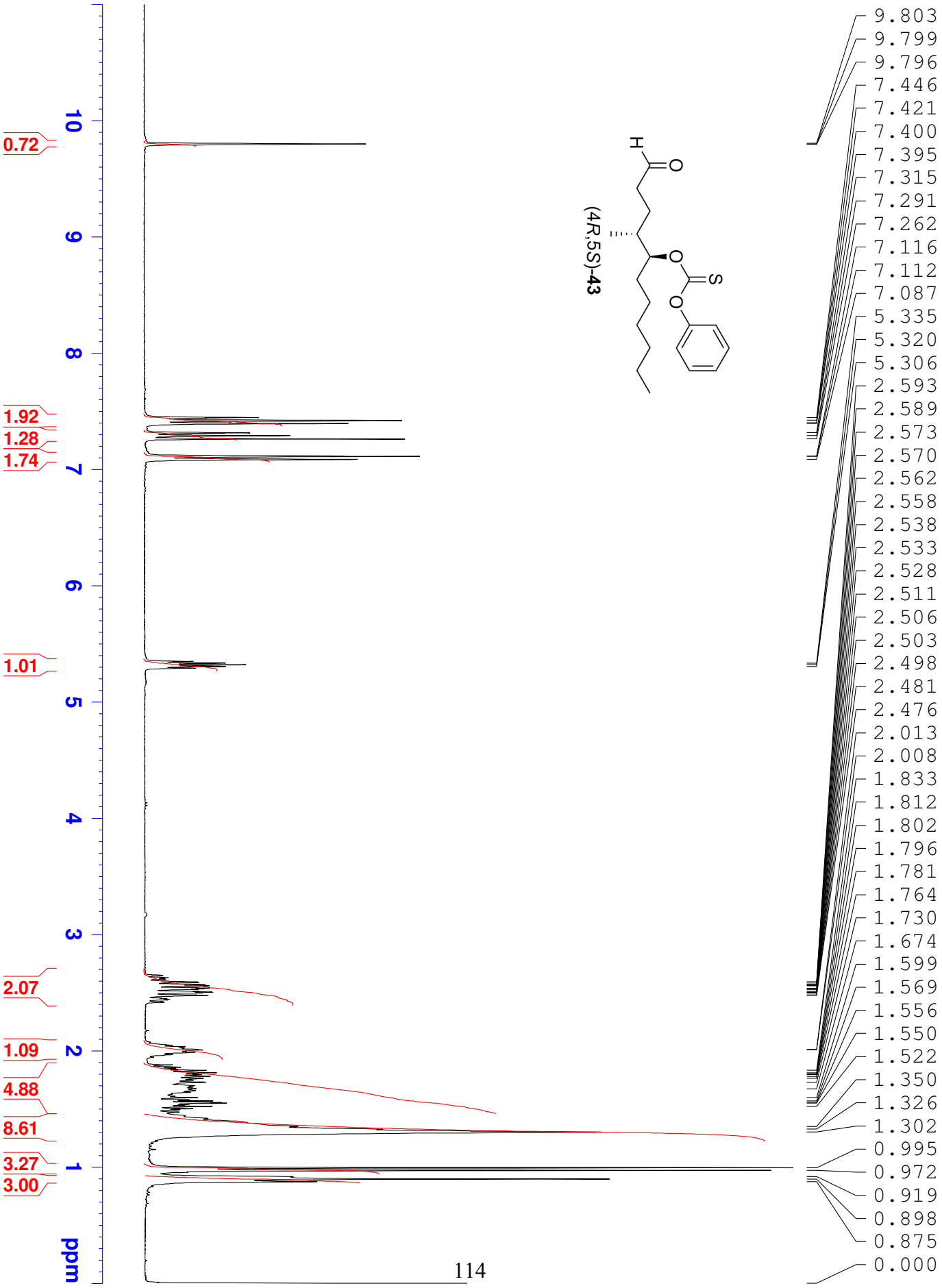
(4R,5S)-43
10
9
8
7
6
5
4
3
2
1
ppm
0.72
1.92
1.28
1.74
1.01
2.07
1.09
4.88
8.61
3.27
3.00
9.803
9.799
9.796
7.446
7.421
7.400
7.395
7.315
7.291
7.262
7.116
7.112
7.087
5.335
5.320
5.306
2.593
2.589
2.573
2.570
2.562
2.558
2.538
2.533
2.528
2.511
2.506
2.503
2.498
2.481
2.476
2.013
2.008
1.833
1.812
1.802
1.796
1.781
1.764
1.730
1.674
1.599
1.569
1.556
1.550
1.522
1.350
1.326
1.302
0.995
0.972
0.919
0.898
0.875
0.000

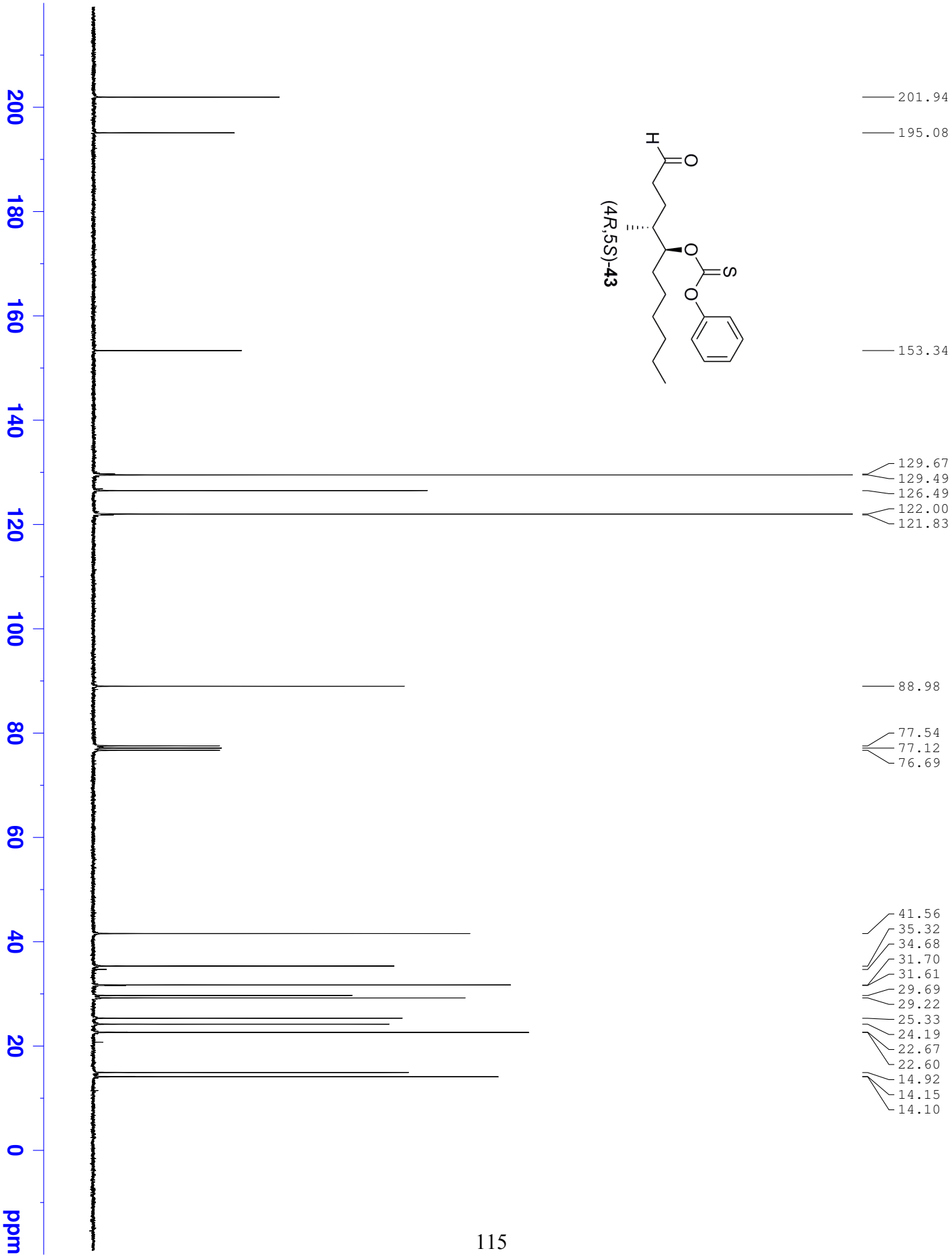
200
180
160
140
120
100
80
60
40
20
0
ppm
201.94
195.08
153.34
129.67
129.49
126.49
122.00
121.83
88.98
77.54
77.12
76.69
41.56
35.32
34.68
31.70
31.61
29.69
29.22
25.33
24.19
22.67
22.60
14.92
14.15
14.10
(4R,5S)-43

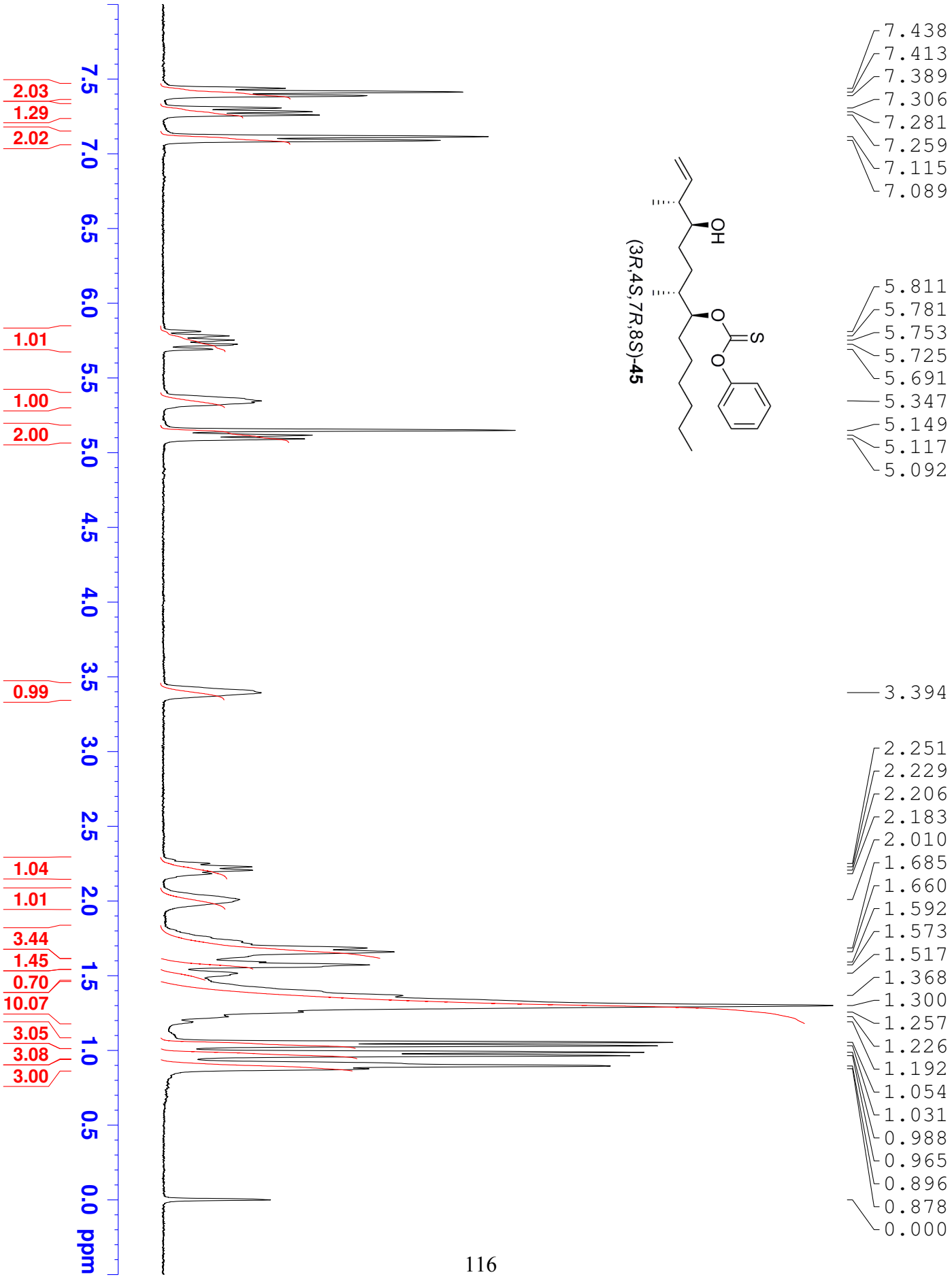
7.438
7.413
7.389
7.306
7.281
7.259
7.115
7.089
5.811
5.781
5.753
5.725
5.691
5.347
5.149
5.117
5.092
3.394
2.251
2.229
2.206
2.183
2.010
1.685
1.660
1.592
1.573
1.517
1.368
1.300
1.257
1.226
1.192
1.054
1.031
0.988
0.965
0.896
0.878
0.000
2.03
1.29
2.02
1.01
1.00
2.00
0.99
1.04
1.01
3.44
1.45
0.70
10.07
3.05
3.08
3.00
7.5
7.0
6.5
6.0
5.5
5.0
4.5
4.0
3.5
3.0
2.5
2.0
1.5
1.0
0.5
0.0
ppm
OH
O
O
S
(3R,4S,7R,8S)-45

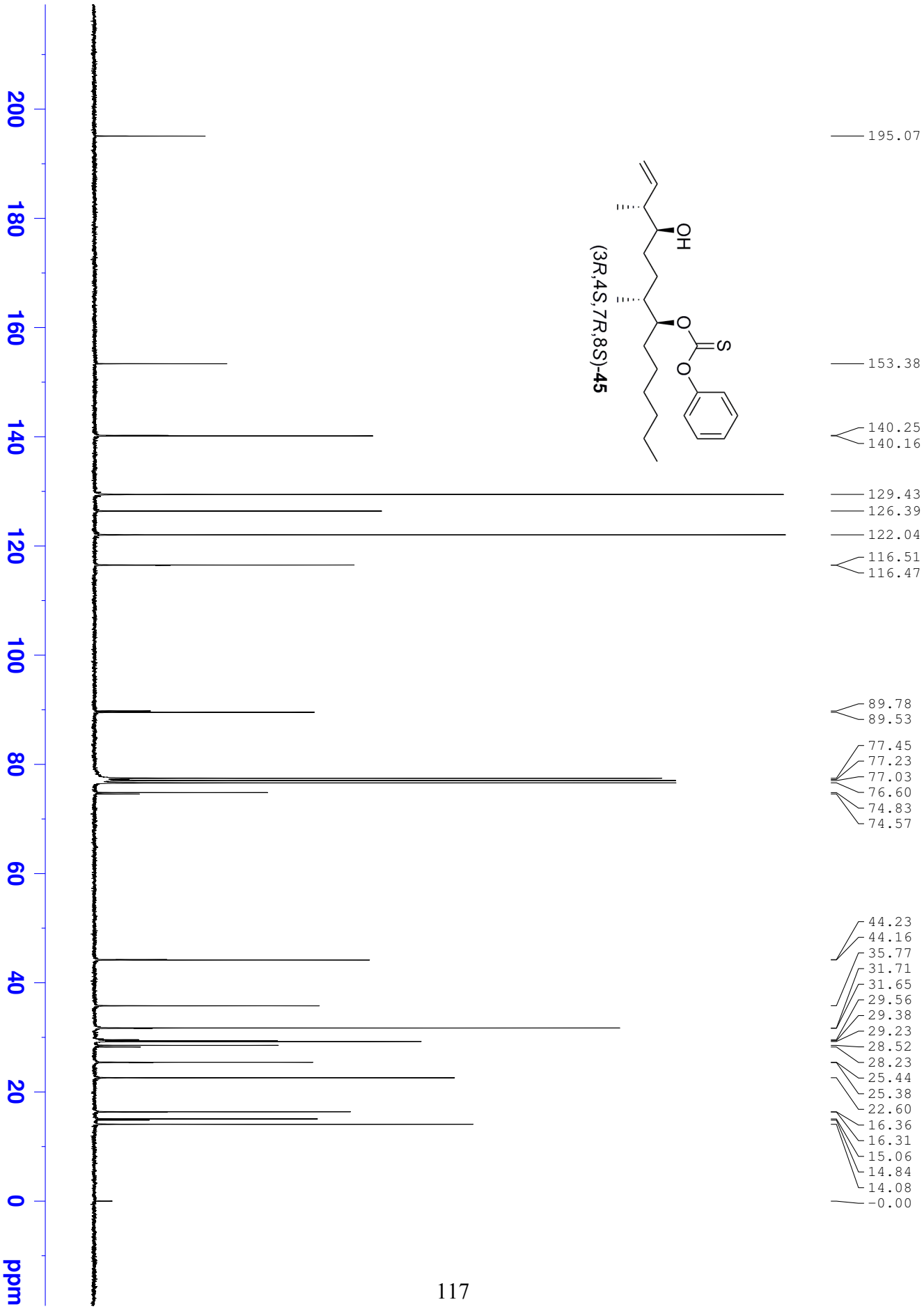
200
180
160
140
120
100
80
60
40
20
0
ppm
OH
O
S
O
(3R,4S,7R,8S)-45
195.07
153.38
140.25
140.16
129.43
126.39
122.04
116.51
116.47
89.78
89.53
77.45
77.23
77.03
76.60
74.83
74.57
44.23
44.16
35.77
31.71
31.65
29.56
29.38
29.23
28.52
28.23
25.44
25.38
22.60
16.36
16.31
15.06
14.84
14.08
-0.00

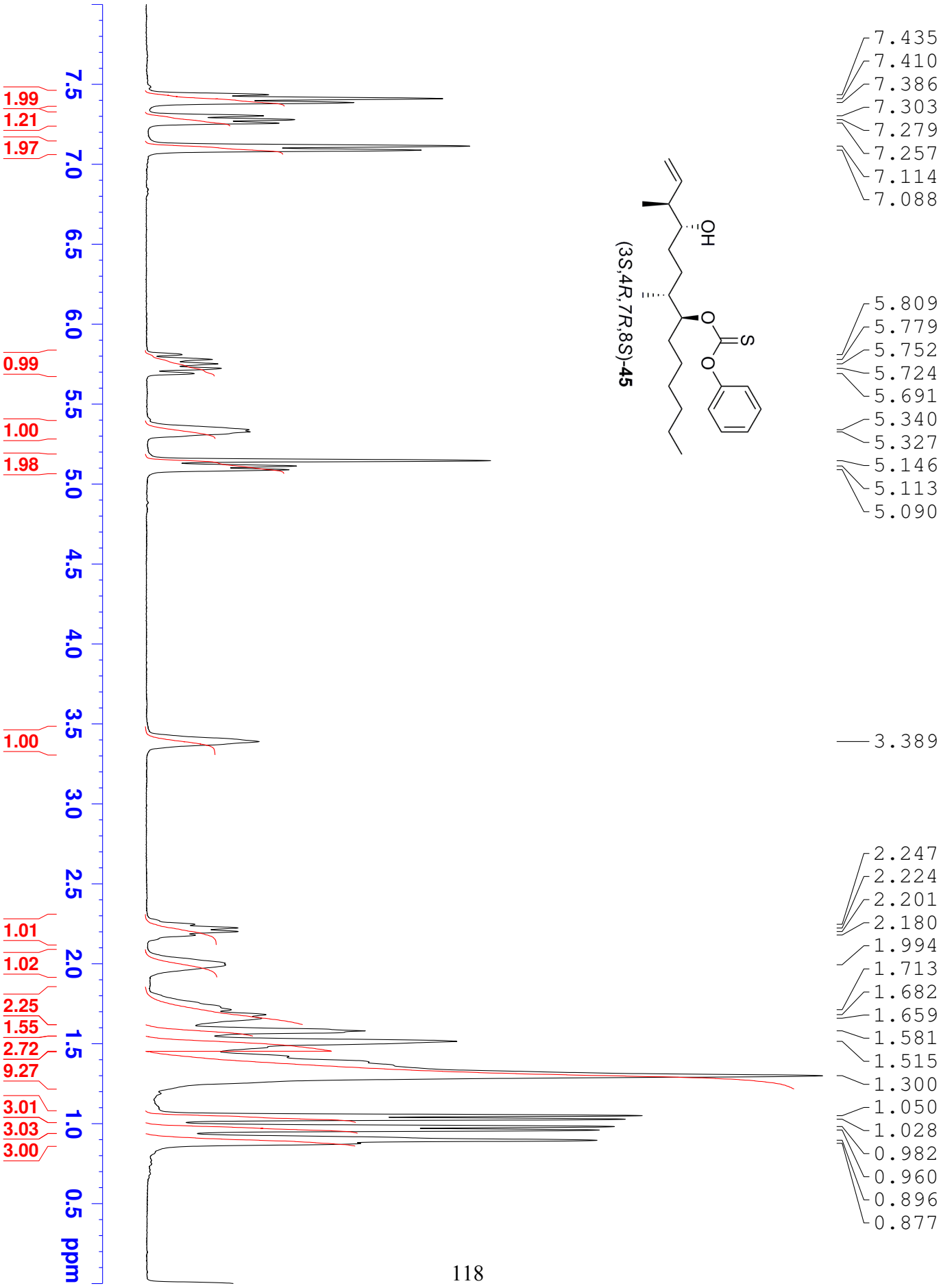
7.435
7.410
7.386
7.303
7.279
7.257
7.114
7.088
5.809
5.779
5.752
5.724
5.691
5.340
5.327
5.146
5.113
5.090
3.389
2.247
2.224
2.201
2.180
1.994
1.713
1.682
1.659
1.581
1.515
1.300
1.050
1.028
0.982
0.960
0.896
0.877
1.99
1.21
1.97
0.99
1.00
1.98
1.00
1.01
1.02
2.25
1.55
2.72
9.27
3.01
3.03
3.00
7.5
7.0
6.5
6.0
5.5
5.0
4.5
4.0
3.5
3.0
2.5
2.0
1.5
1.0
0.5
ppm
OH
O
O
S
O
(3S,4R,7R,8S)-45

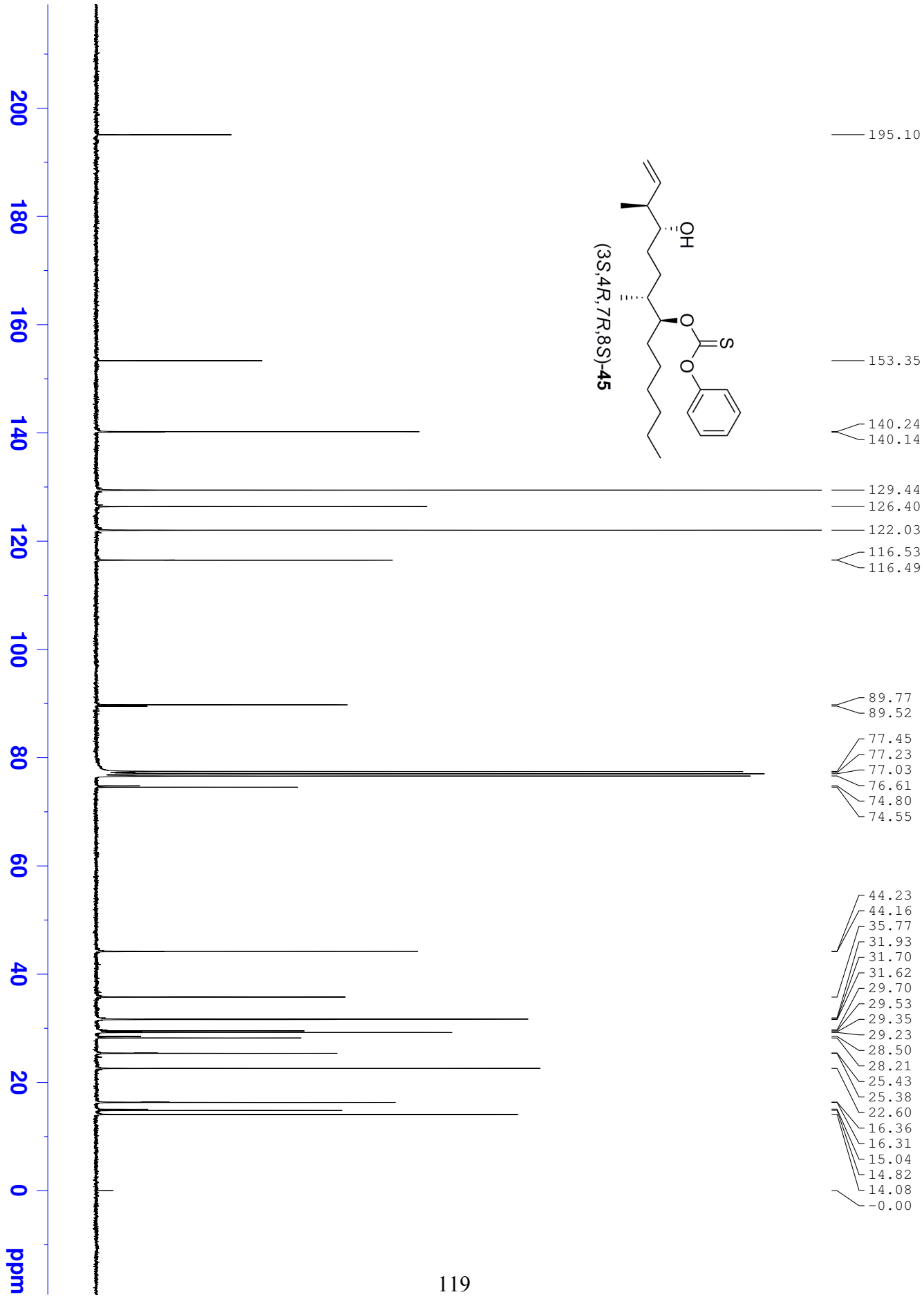
200
180
160
140
120
100
80
60
40
20
0
ppm
195.10
153.35
140.24
140.14
129.44
126.40
122.03
116.53
116.49
89.77
89.52
77.45
77.23
77.03
76.61
74.80
74.55
44.23
44.16
35.77
31.93
31.70
31.62
29.70
29.53
29.35
29.23
28.50
28.21
25.43
25.38
22.60
16.36
16.31
15.04
14.82
14.08
-0.00
OH
O
S
O
(3S,4R,7R,8S)-45

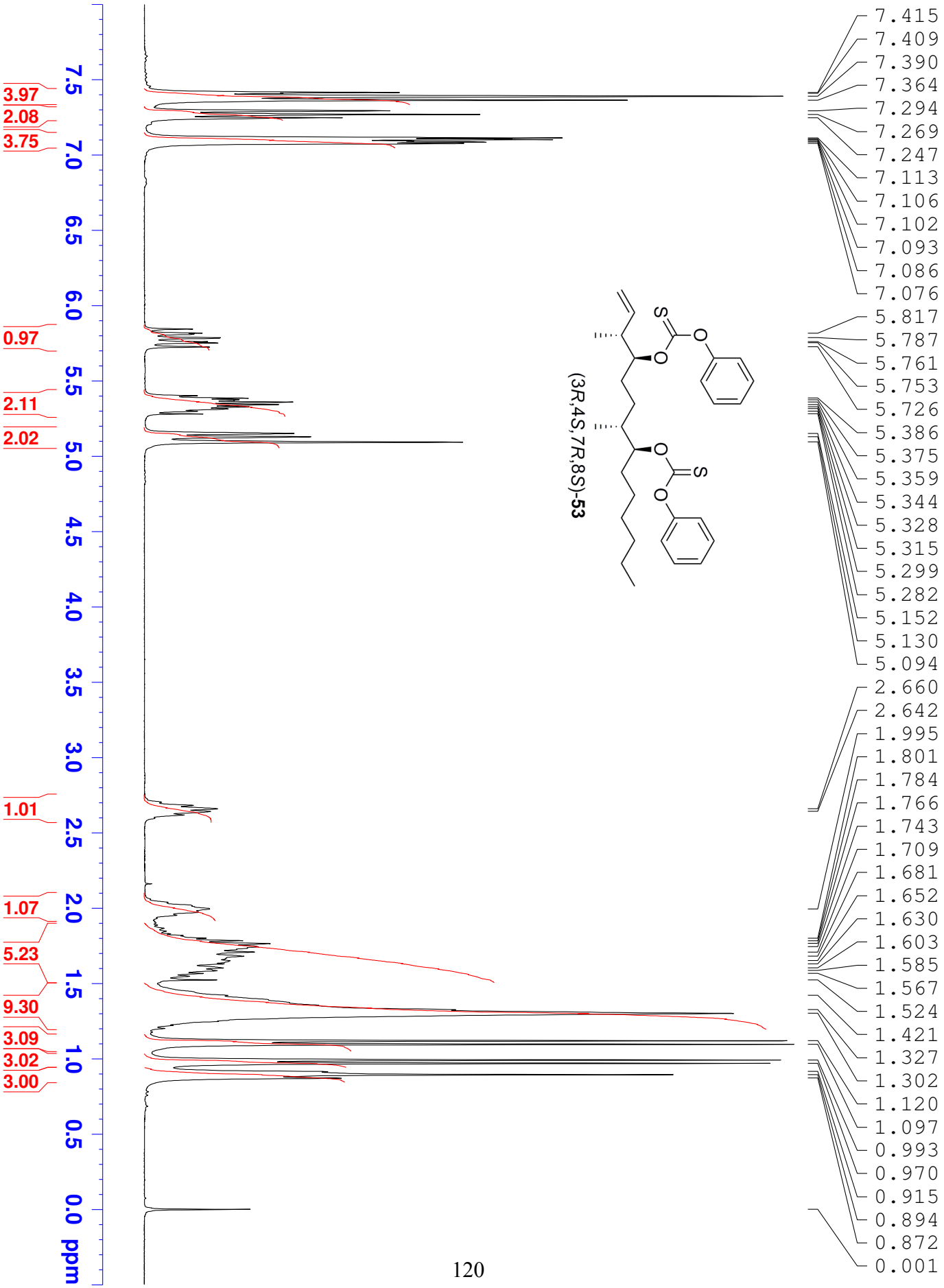
7.415
7.409
7.390
7.364
7.294
7.269
7.247
7.113
7.106
7.102
7.093
7.086
7.076
5.817
5.787
5.761
5.753
5.726
5.386
5.375
5.359
5.344
5.328
5.315
5.299
5.282
5.152
5.130
5.094
2.660
2.642
1.995
1.801
1.784
1.766
1.743
1.709
1.681
1.652
1.630
1.603
1.585
1.567
1.524
1.421
1.327
1.302
1.120
1.097
0.993
0.970
0.915
0.894
0.872
0.001
3.97
2.08
3.75
0.97
2.11
2.02
1.01
1.07
5.23
9.30
3.09
3.02
3.00
7.5
7.0
6.5
6.0
5.5
5.0
4.5
4.0
3.5
3.0
2.5
2.0
1.5
1.0
0.5
0.0
ppm
(3R,4S,7R,8S)-53

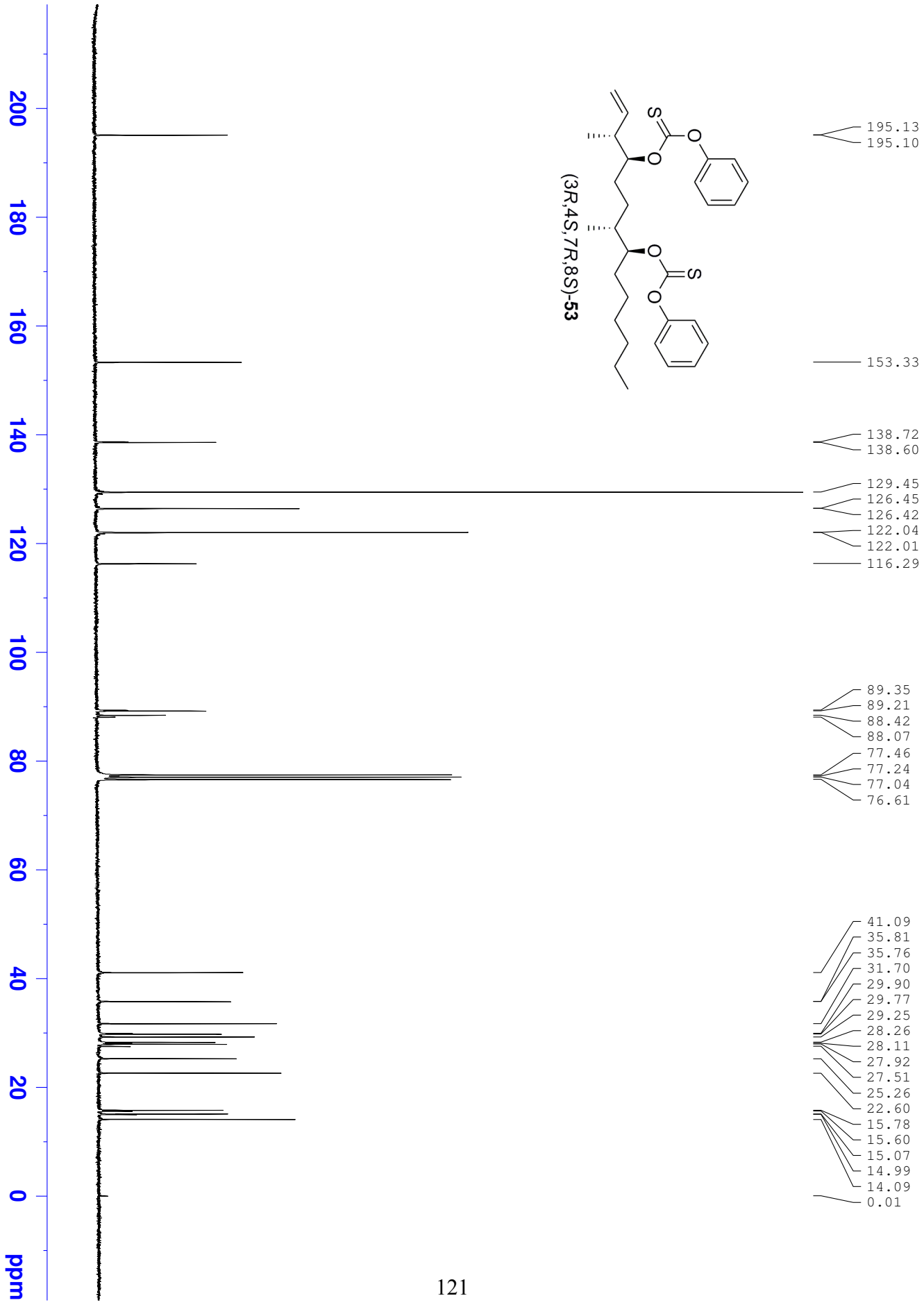
(3R,4S,7R,8S)-53
195.13
195.10
153.33
138.72
138.60
129.45
126.45
126.42
122.04
122.01
116.29
89.35
89.21
88.42
88.07
77.46
77.24
77.04
76.61
41.09
35.81
35.76
31.70
29.90
29.77
29.25
28.26
28.11
27.92
27.51
25.26
22.60
15.78
15.60
15.07
14.99
14.09
0.01
200
180
160
140
120
100
80
60
40
20
0
ppm

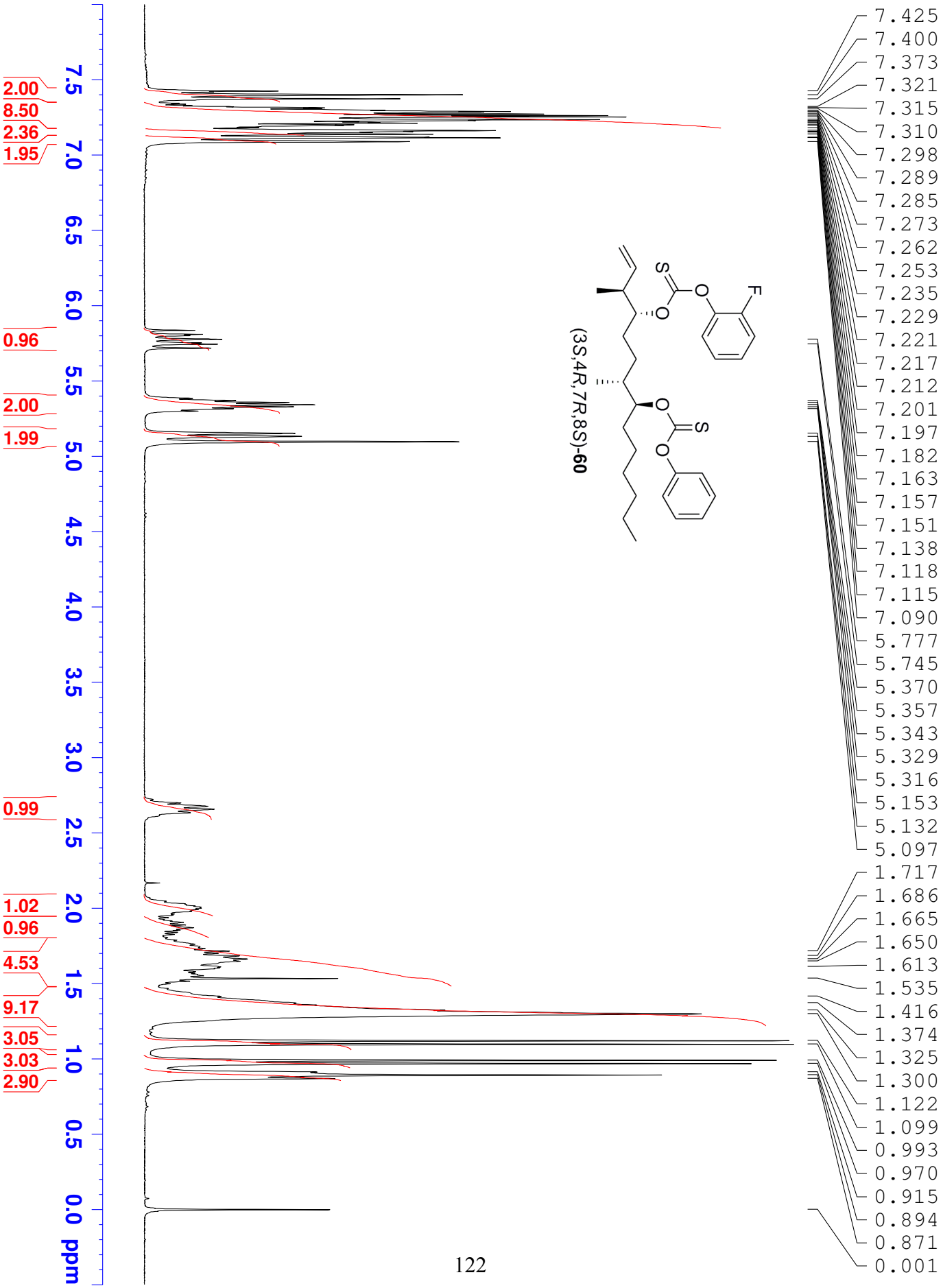
(3S,4R,7R,8S)-60
7.425
7.400
7.373
7.321
7.315
7.310
7.298
7.289
7.285
7.273
7.262
7.253
7.235
7.229
7.221
7.217
7.212
7.201
7.197
7.182
7.163
7.157
7.151
7.138
7.118
7.115
7.090
5.777
5.745
5.370
5.357
5.343
5.329
5.316
5.153
5.132
5.097
1.717
1.686
1.665
1.650
1.613
1.535
1.416
1.374
1.325
1.300
1.122
1.099
0.993
0.970
0.915
0.894
0.871
0.001
2.00
8.50
2.36
1.95
0.96
2.00
1.99
0.99
1.02
0.96
4.53
9.17
3.05
3.03
2.90
ppm

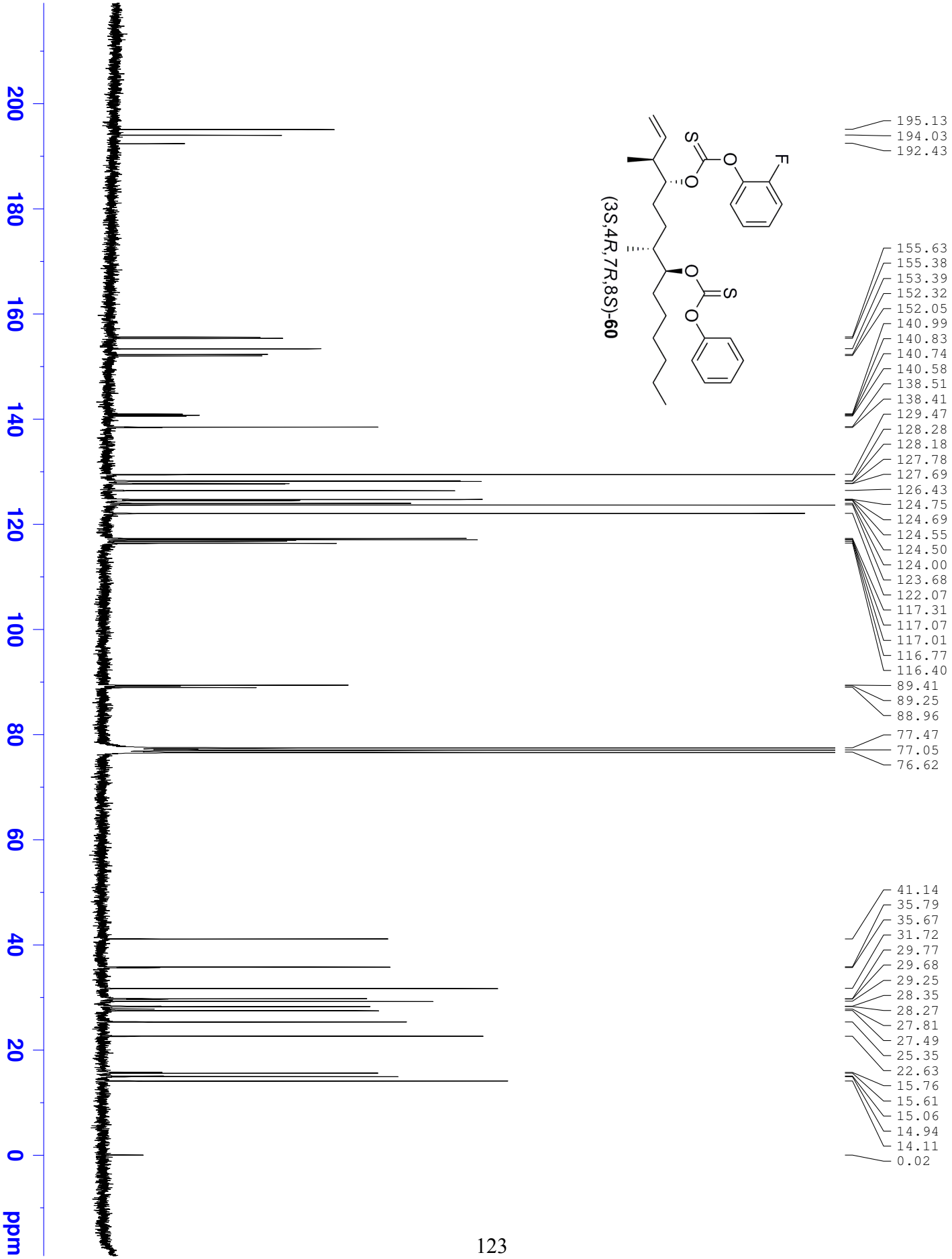
200
180
160
140
120
100
80
60
40
20
0
ppm
(3S,4R,7R,8S)-60
195.13
194.03
192.43
155.63
155.38
153.39
152.32
152.05
140.99
140.83
140.74
140.58
138.51
138.41
129.47
128.28
128.18
127.78
127.69
126.43
124.75
124.69
124.55
124.50
124.00
123.68
122.07
117.31
117.07
117.01
116.77
116.40
89.41
89.25
88.96
77.47
77.05
76.62
41.14
35.79
35.67
31.72
29.77
29.68
29.25
28.35
28.27
27.81
27.49
25.35
22.63
15.76
15.61
15.06
14.94
14.11
0.02

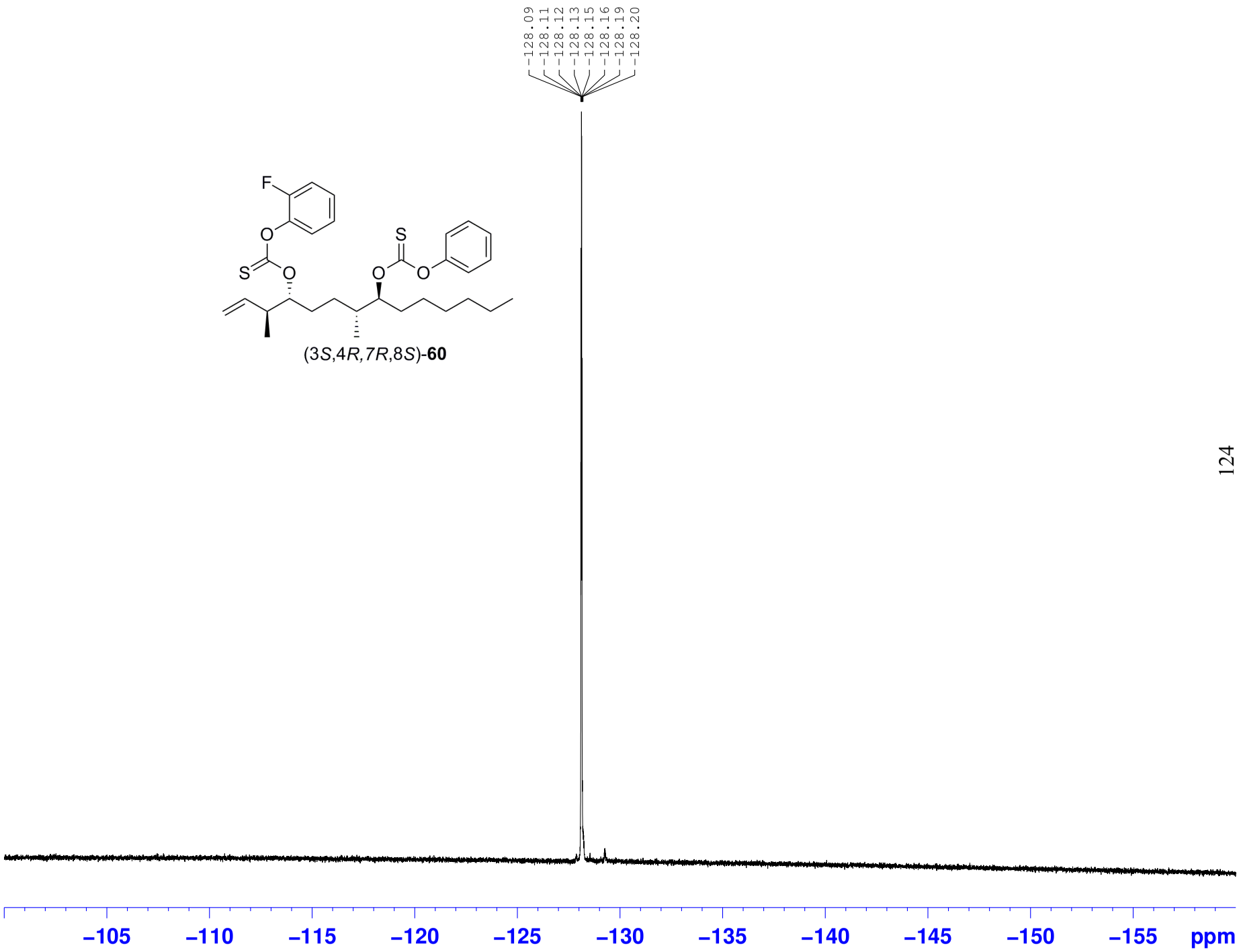
-128.09
-128.11
-128.12
-128.13
-128.15
-128.16
-128.19
-128.20
F
O
S
O
O
S
O
(3S,4R,7R,8S)-60
−105
−110
−115
−120
−125
−130
−135
−140
−145
−150
−155
ppm

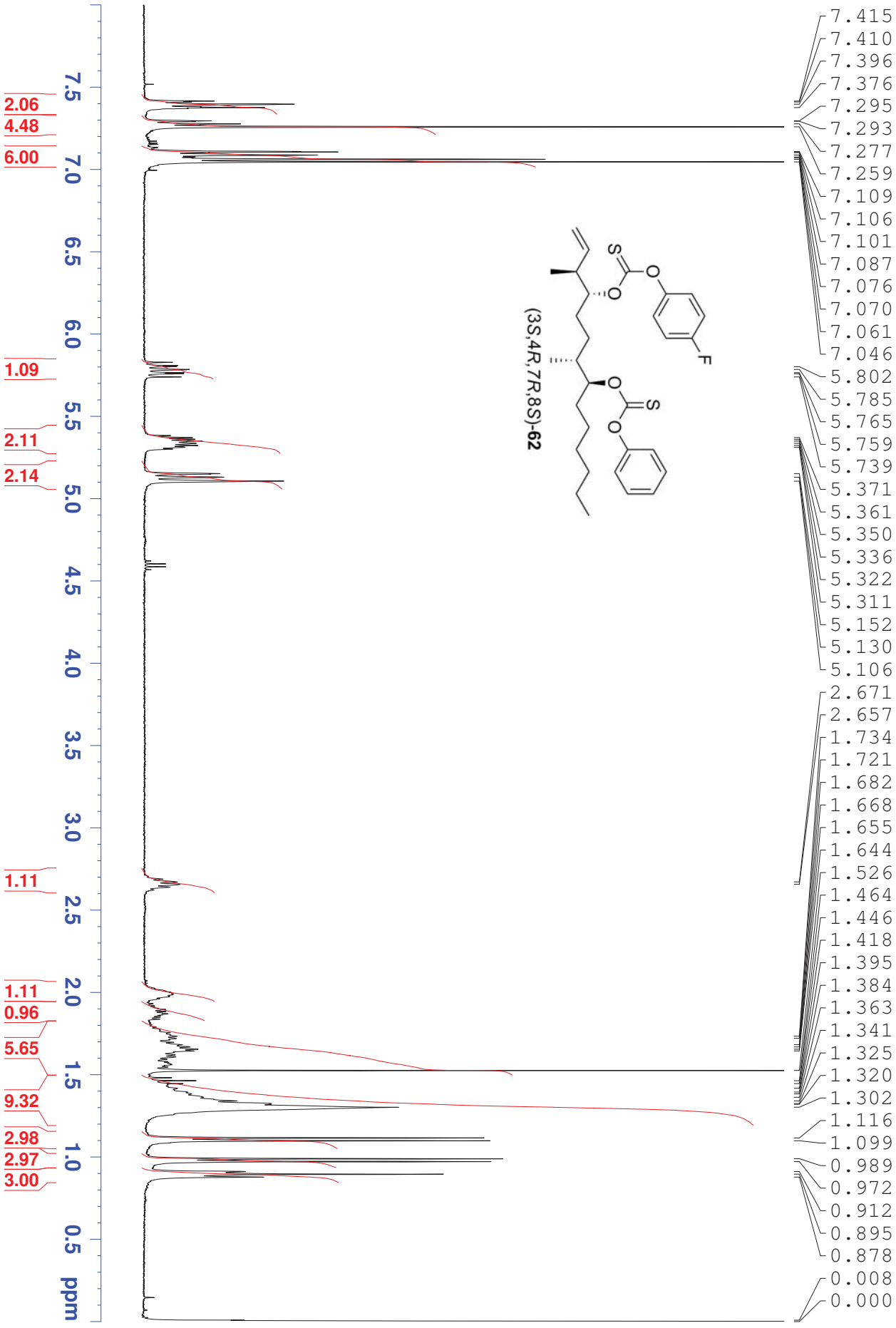
7.415
7.410
7.396
7.376
7.295
7.293
7.277
7.259
7.109
7.106
7.101
7.087
7.076
7.070
7.061
7.046
5.802
5.785
5.765
5.759
5.739
5.371
5.361
5.350
5.336
5.322
5.311
5.152
5.130
5.106
2.671
2.657
1.734
1.721
1.682
1.668
1.655
1.644
1.526
1.464
1.446
1.418
1.395
1.384
1.363
1.341
1.325
1.320
1.302
1.116
1.099
0.989
0.972
0.912
0.895
0.878
0.008
0.000
2.06
4.48
6.00
1.09
2.11
2.14
1.11
1.11
0.96
5.65
9.32
2.98
2.97
3.00
7.5
7.0
6.5
6.0
5.5
5.0
4.5
4.0
3.5
3.0
2.5
2.0
1.5
1.0
0.5
ppm
(3S,4R,7R,8S)-62

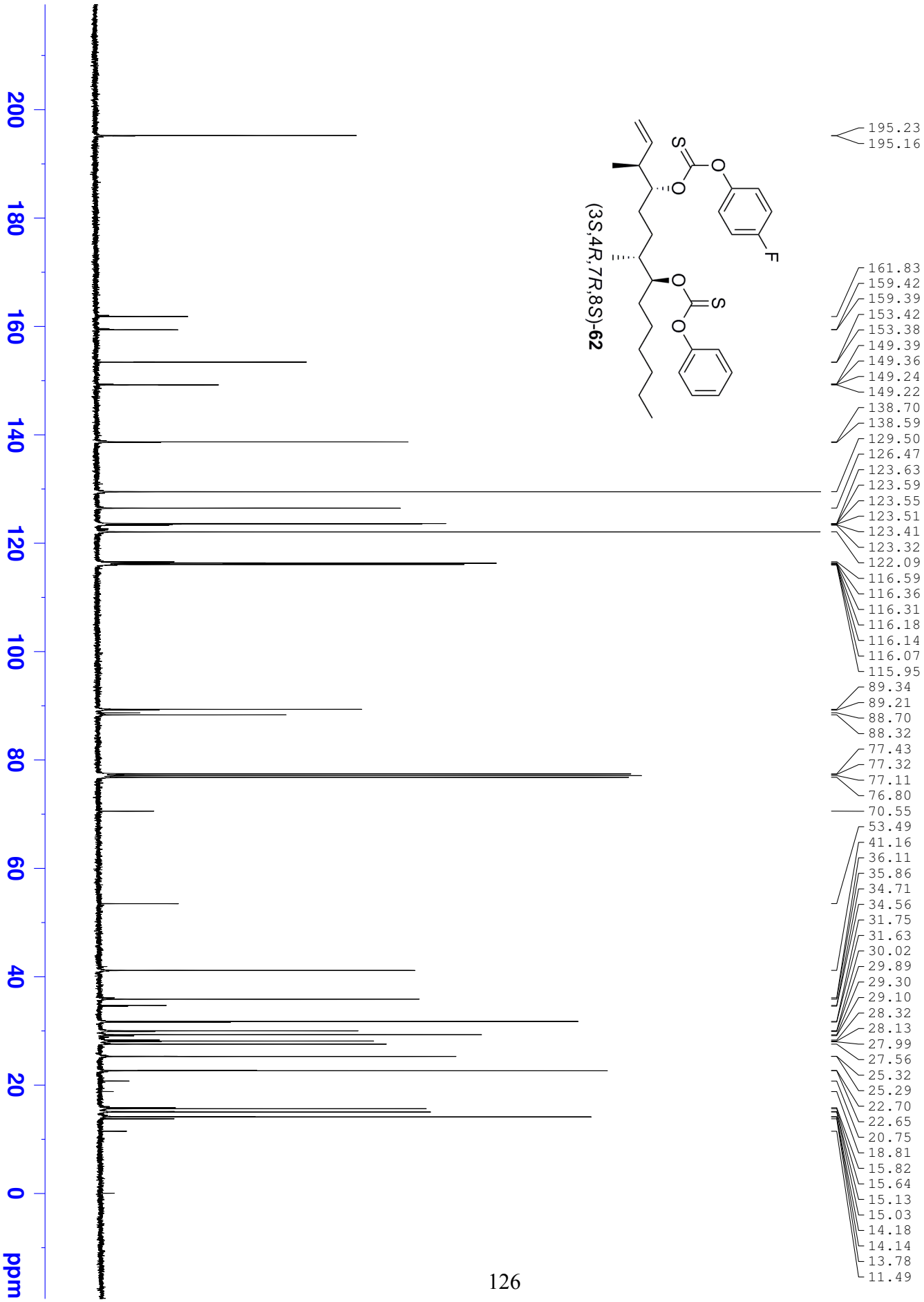
(3S,4R,7R,8S)-62
195.23
195.16
161.83
159.42
159.39
153.42
153.38
149.39
149.36
149.24
149.22
138.70
138.59
129.50
126.47
123.63
123.59
123.55
123.51
123.41
123.32
122.09
116.59
116.36
116.31
116.18
116.14
116.07
115.95
89.34
89.21
88.70
88.32
77.43
77.32
77.11
76.80
70.55
53.49
41.16
36.11
35.86
34.71
34.56
31.75
31.63
30.02
29.89
29.30
29.10
28.32
28.13
27.99
27.56
25.32
25.29
22.70
22.65
20.75
18.81
15.82
15.64
15.13
15.03
14.18
14.14
13.78
11.49
200
180
160
140
120
100
80
60
40
20
0
ppm

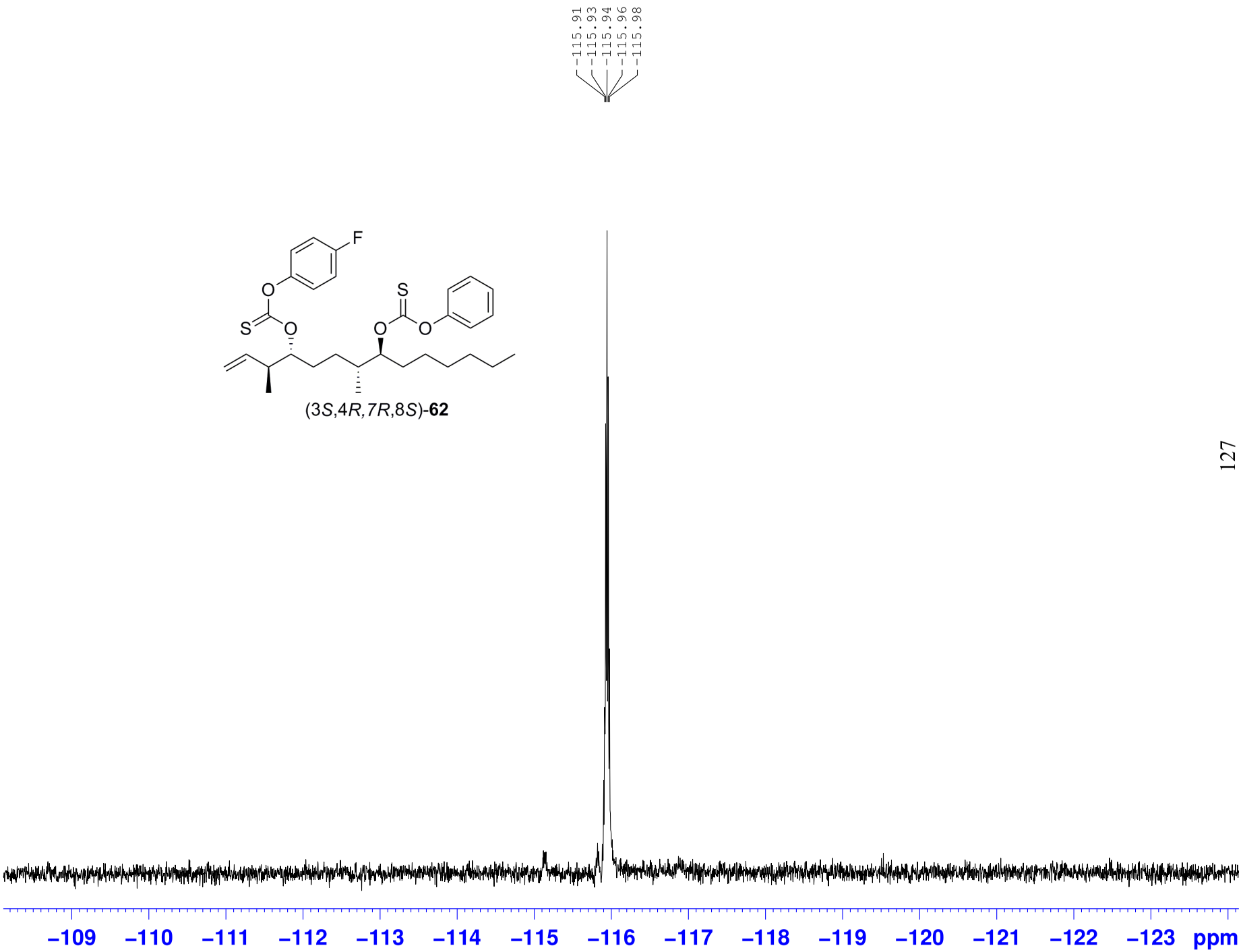
-115.91
-115.93
-115.94
-115.96
-115.98
F
O
S
O
S
O
O
(3S,4R,7R,8S)-62
127
−109
−110
−111
−112
−113
−114
−115
−116
−117
−118
−119
−120
−121
−122
−123
ppm

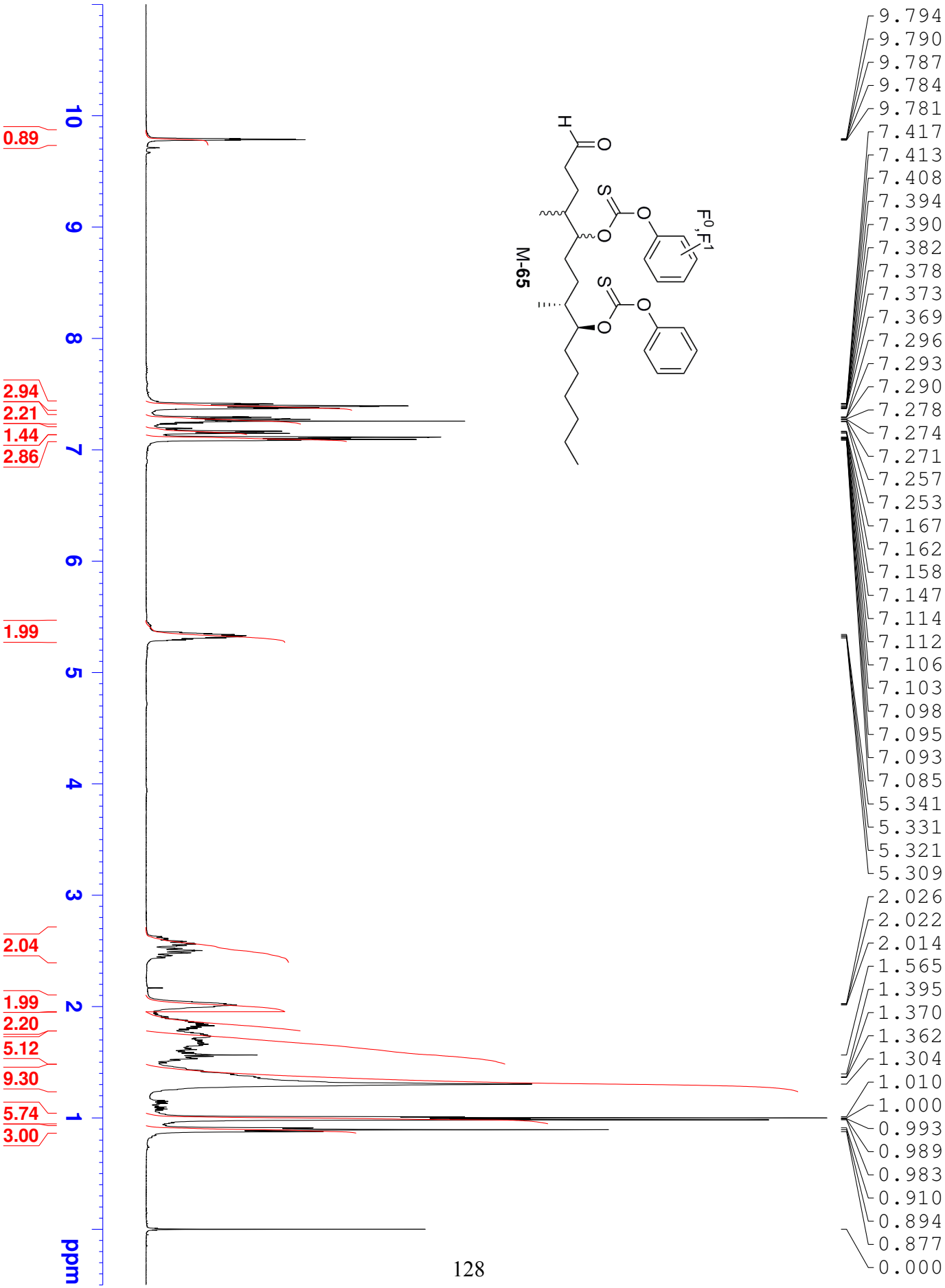
M-65
F0,F1
0.89
2.94
2.21
1.44
2.86
1.99
2.04
1.99
2.20
5.12
9.30
5.74
3.00
ppm
9.794
9.790
9.787
9.784
9.781
7.417
7.413
7.408
7.394
7.390
7.382
7.378
7.373
7.369
7.296
7.293
7.290
7.278
7.274
7.271
7.257
7.253
7.167
7.162
7.158
7.147
7.114
7.112
7.106
7.103
7.098
7.095
7.093
7.085
5.341
5.331
5.321
5.309
2.026
2.022
2.014
1.565
1.395
1.370
1.362
1.304
1.010
1.000
0.993
0.989
0.983
0.910
0.894
0.877
0.000

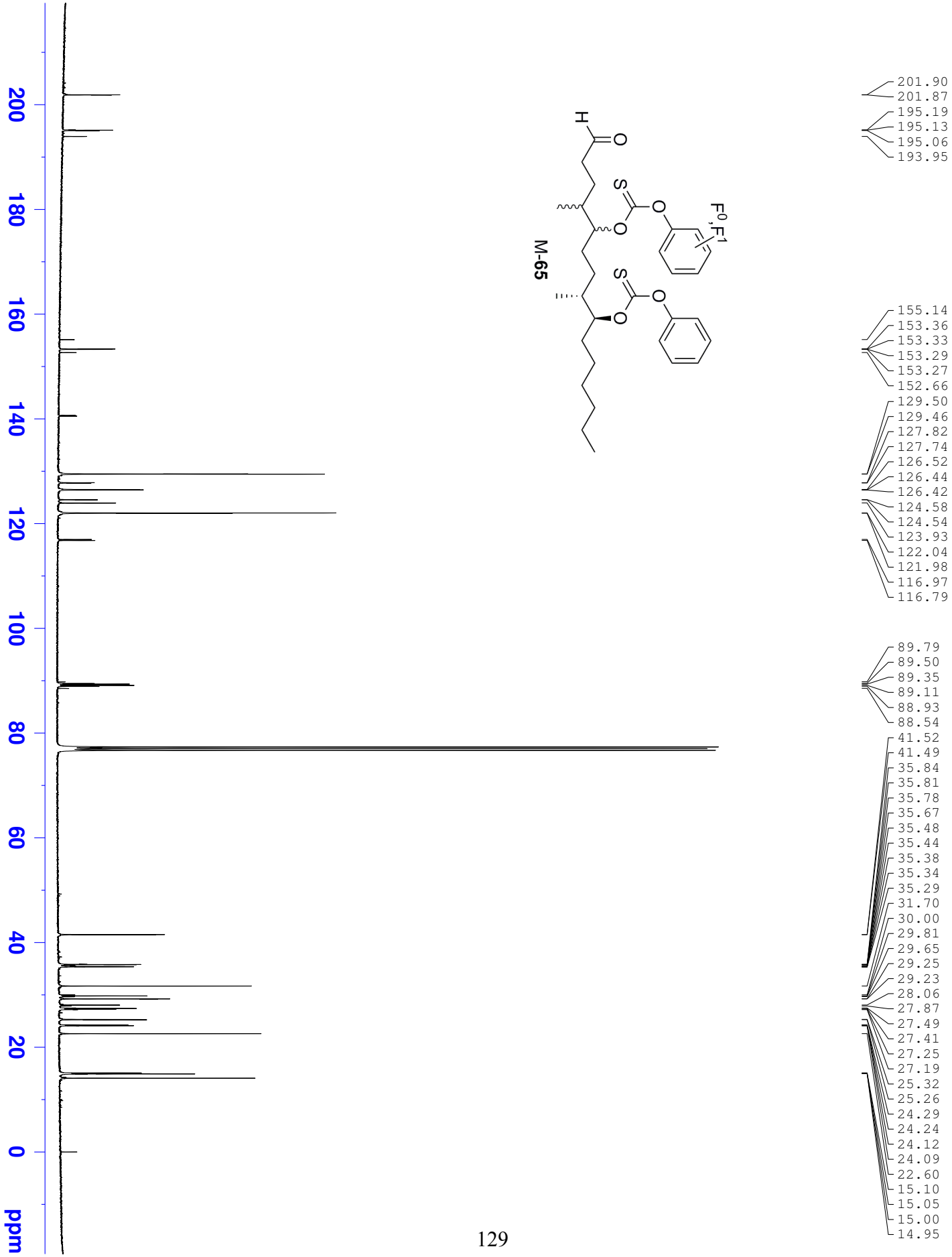
200
180
160
140
120
100
80
60
40
20
0
ppm
M-65
F0,F1
201.90
201.87
195.19
195.13
195.06
193.95
155.14
153.36
153.33
153.29
153.27
152.66
129.50
129.46
127.82
127.74
126.52
126.44
126.42
124.58
124.54
123.93
122.04
121.98
116.97
116.79
89.79
89.50
89.35
89.11
88.93
88.54
41.52
41.49
35.84
35.81
35.78
35.67
35.48
35.44
35.38
35.34
35.29
31.70
30.00
29.81
29.65
29.25
29.23
28.06
27.87
27.49
27.41
27.25
27.19
25.32
25.26
24.29
24.24
24.12
24.09
22.60
15.10
15.05
15.00
14.95

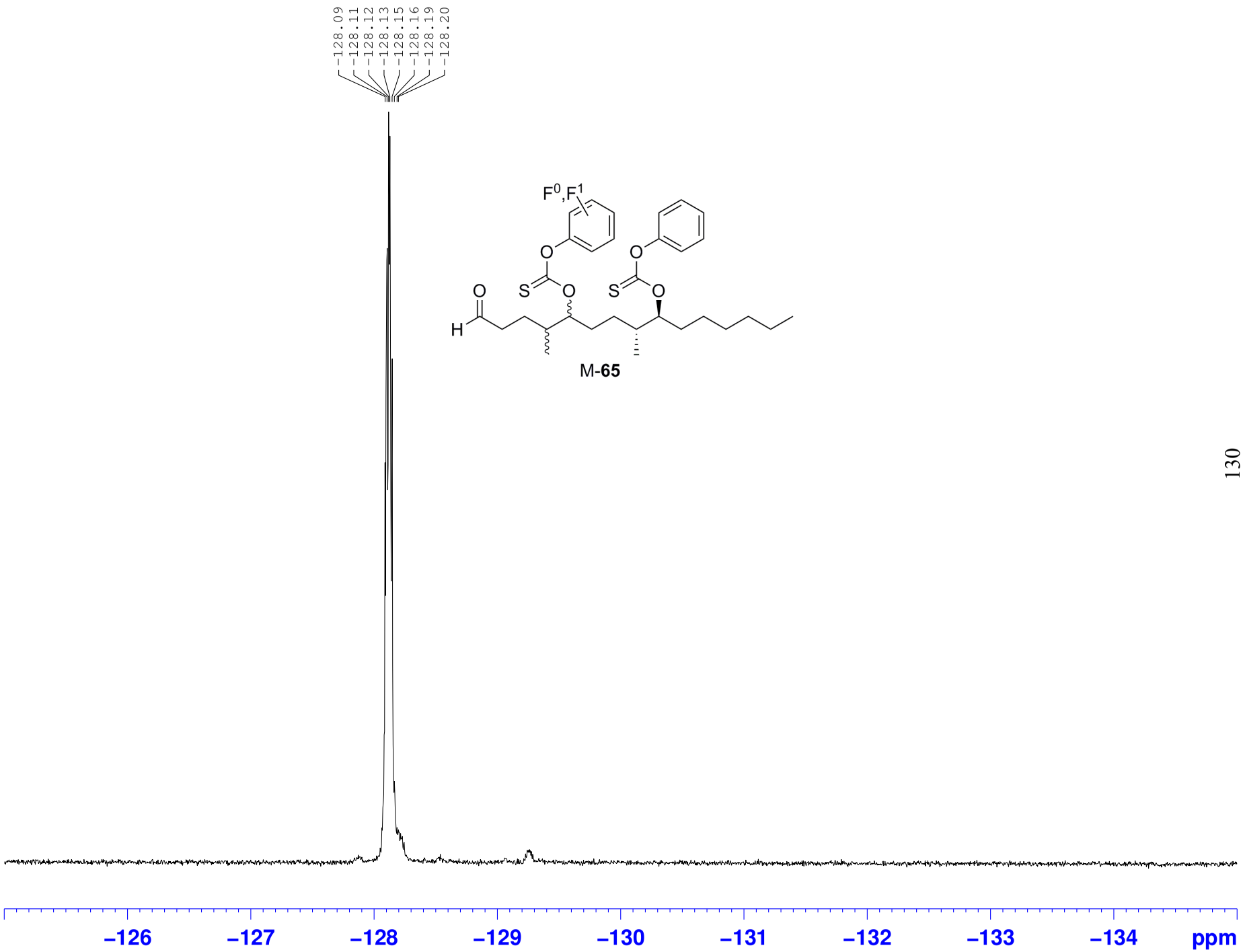
-128.09
-128.11
-128.12
-128.13
-128.15
-128.16
-128.19
-128.20
F0,F1
O
S
O
O
S
O
O
H
M-65
130
−126
−127
−128
−129
−130
−131
−132
−133
−134
ppm

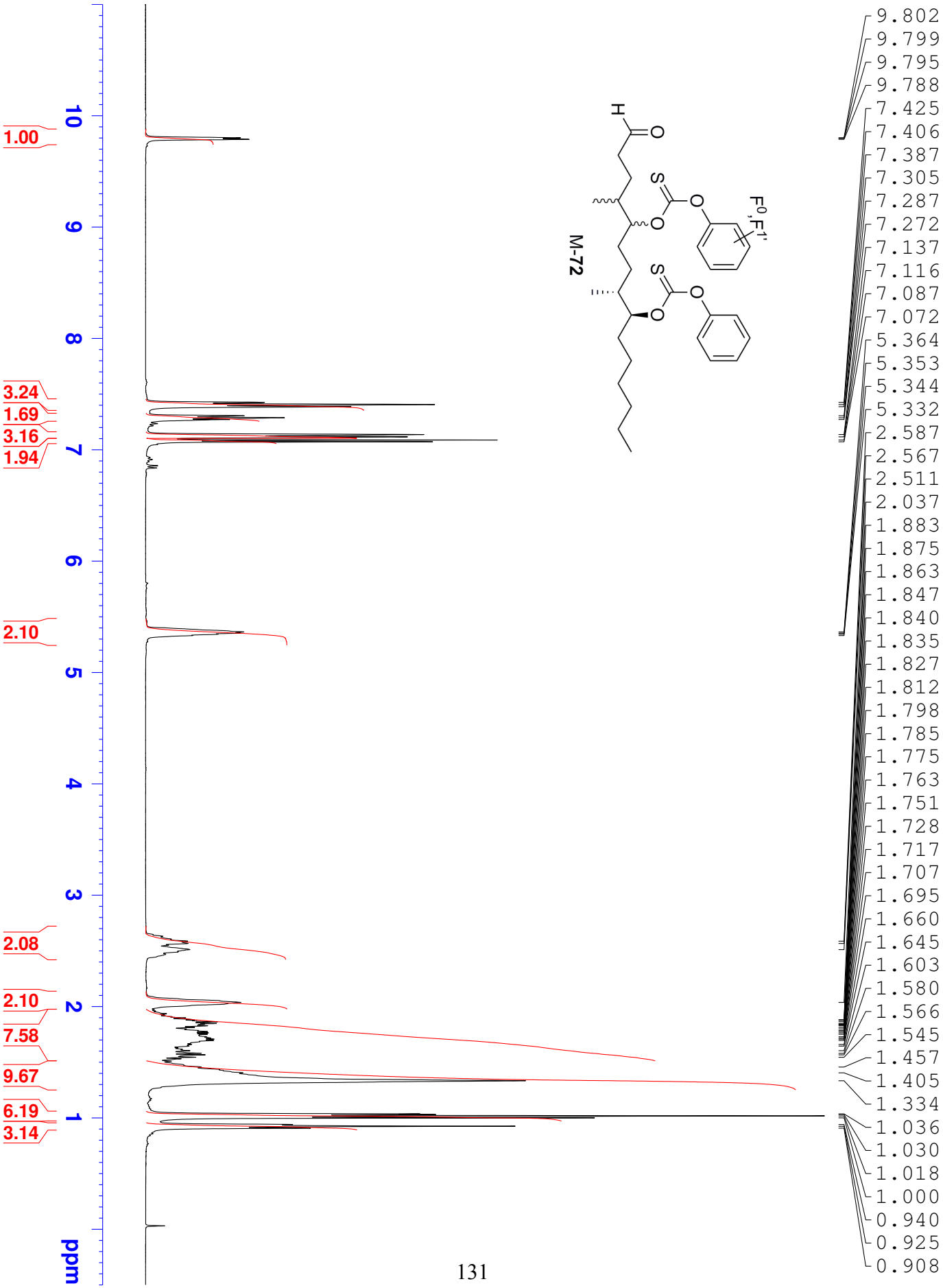
M-72
F0',F1'
1.00
3.24
1.69
3.16
1.94
2.10
2.08
2.10
7.58
9.67
6.19
3.14
ppm
9.802
9.799
9.795
9.788
7.425
7.406
7.387
7.305
7.287
7.272
7.137
7.116
7.087
7.072
5.364
5.353
5.344
5.332
2.587
2.567
2.511
2.037
1.883
1.875
1.863
1.847
1.840
1.835
1.827
1.812
1.798
1.785
1.775
1.763
1.751
1.728
1.717
1.707
1.695
1.660
1.645
1.603
1.580
1.566
1.545
1.457
1.405
1.334
1.036
1.030
1.018
1.000
0.940
0.925
0.908

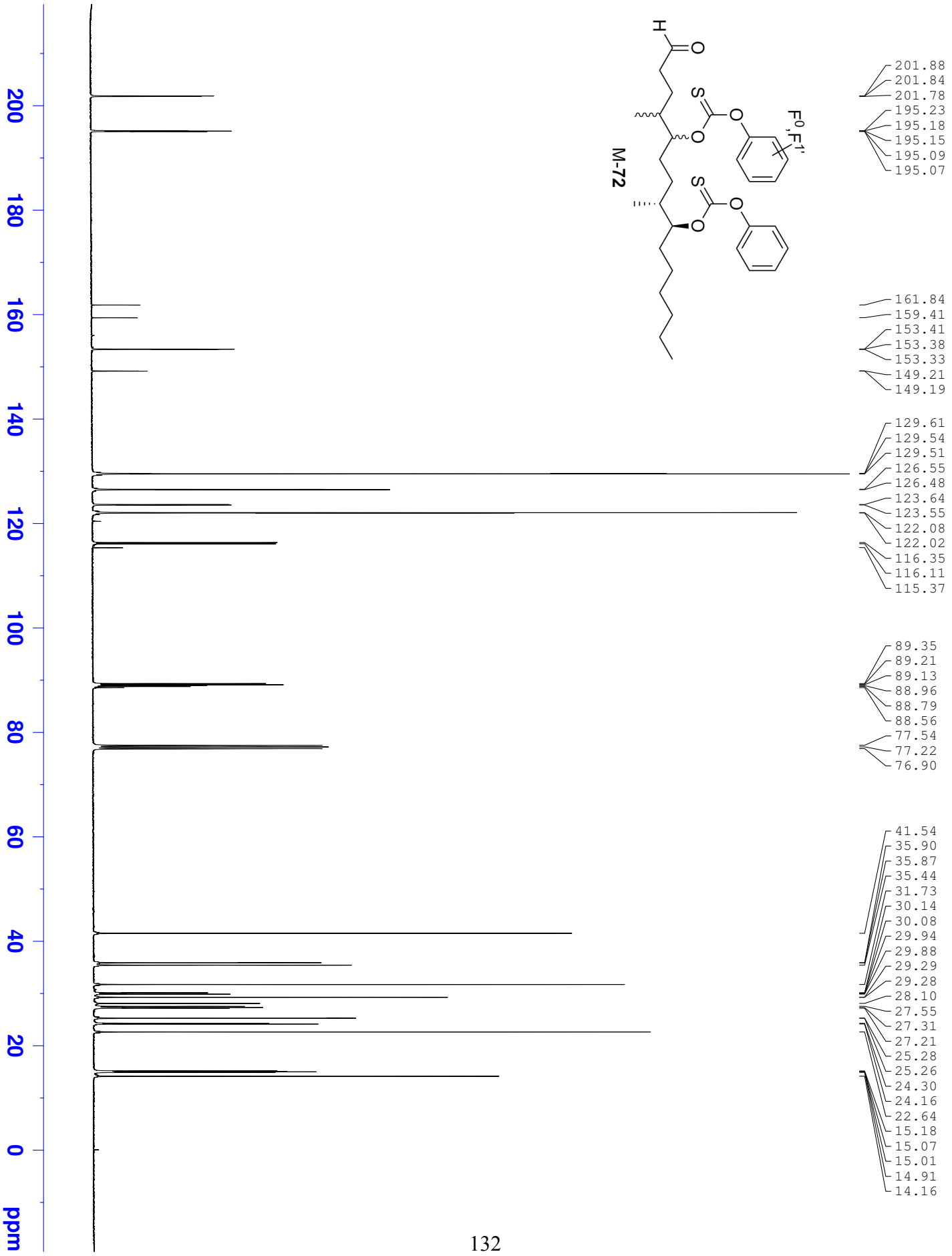
M-72
F0,F1'
201.88
201.84
201.78
195.23
195.18
195.15
195.09
195.07
161.84
159.41
153.41
153.38
153.33
149.21
149.19
129.61
129.54
129.51
126.55
126.48
123.64
123.55
122.08
122.02
116.35
116.11
115.37
89.35
89.21
89.13
88.96
88.79
88.56
77.54
77.22
76.90
41.54
35.90
35.87
35.44
31.73
30.14
30.08
29.94
29.88
29.29
29.28
28.10
27.55
27.31
27.21
25.28
25.26
24.30
24.16
22.64
15.18
15.07
15.01
14.91
14.16
200
180
160
140
120
100
80
60
40
20
0
ppm

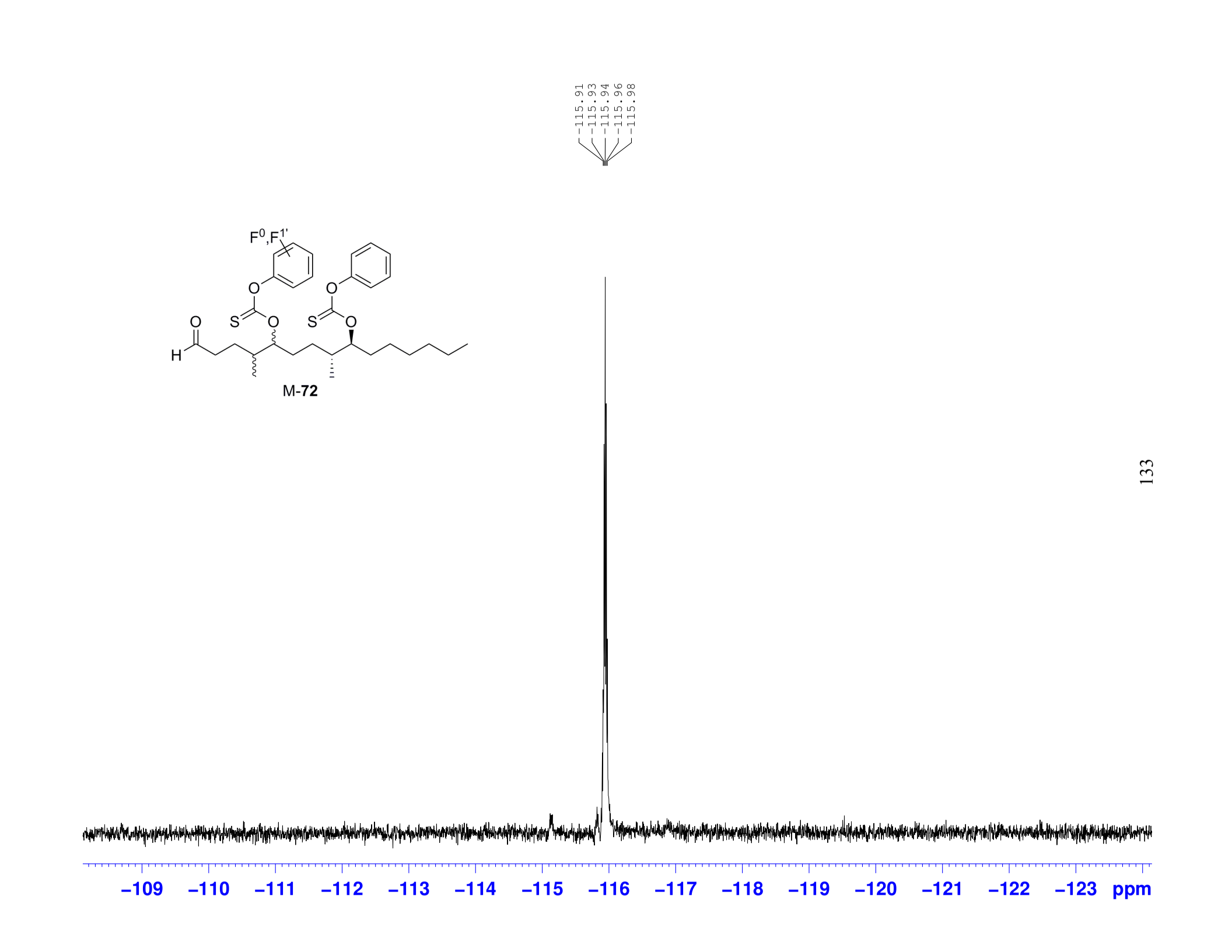
-115.91
-115.93
-115.94
-115.96
-115.98
F0,F1'
O
S
O
S
O
O
H
M-72
133
−109
−110
−111
−112
−113
−114
−115
−116
−117
−118
−119
−120
−121
−122
−123
ppm

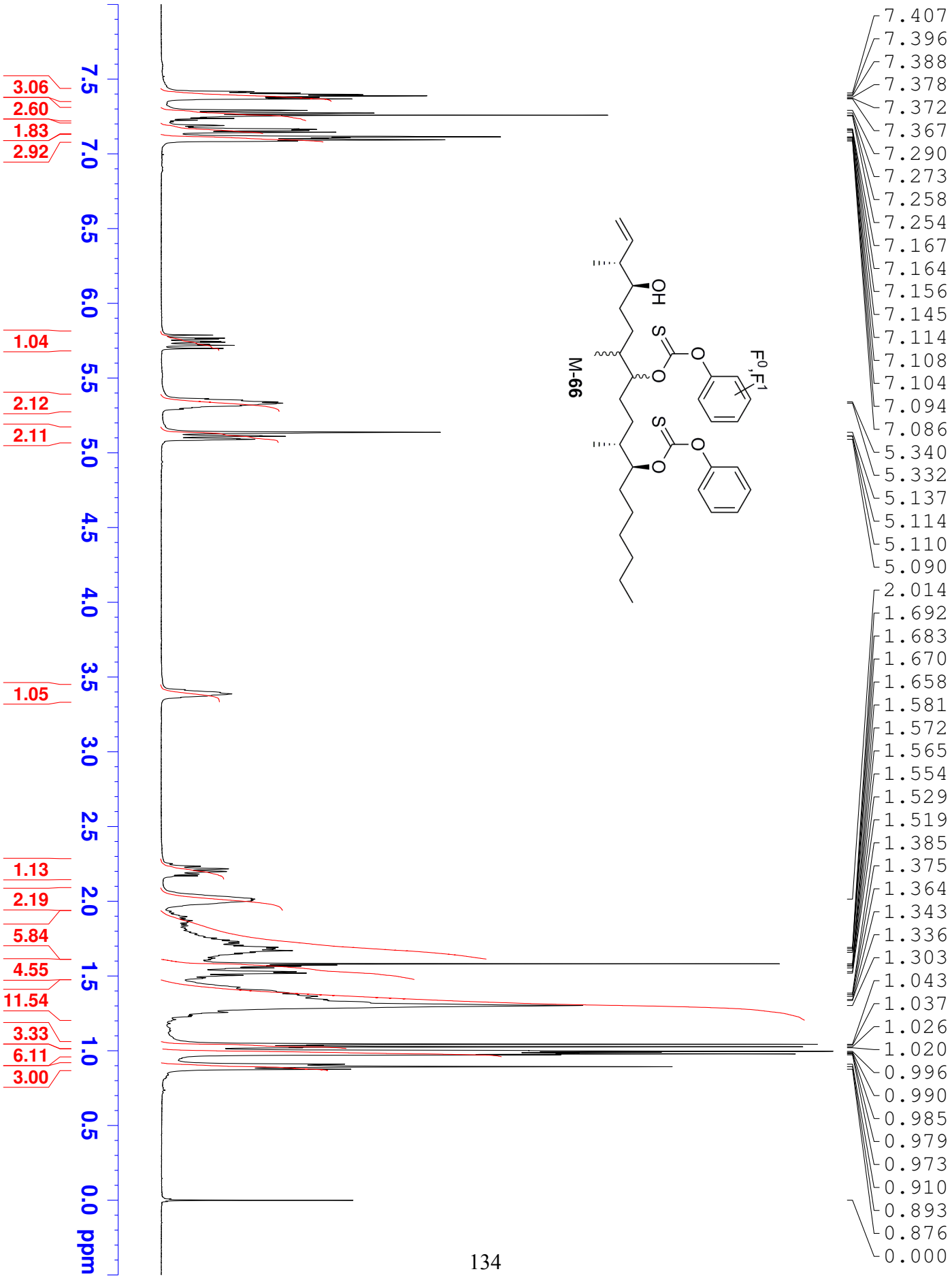
3.06
2.60
1.83
2.92
1.04
2.12
2.11
1.05
1.13
2.19
5.84
4.55
11.54
3.33
6.11
3.00
7.5
7.0
6.5
6.0
5.5
5.0
4.5
4.0
3.5
3.0
2.5
2.0
1.5
1.0
0.5
0.0
ppm
OH
S
O
O
S
O
O
F0,F1
M-66
7.407
7.396
7.388
7.378
7.372
7.367
7.290
7.273
7.258
7.254
7.167
7.164
7.156
7.145
7.114
7.108
7.104
7.094
7.086
5.340
5.332
5.137
5.114
5.110
5.090
2.014
1.692
1.683
1.670
1.658
1.581
1.572
1.565
1.554
1.529
1.519
1.385
1.375
1.364
1.343
1.336
1.303
1.043
1.037
1.026
1.020
0.996
0.990
0.985
0.979
0.973
0.910
0.893
0.876
0.000

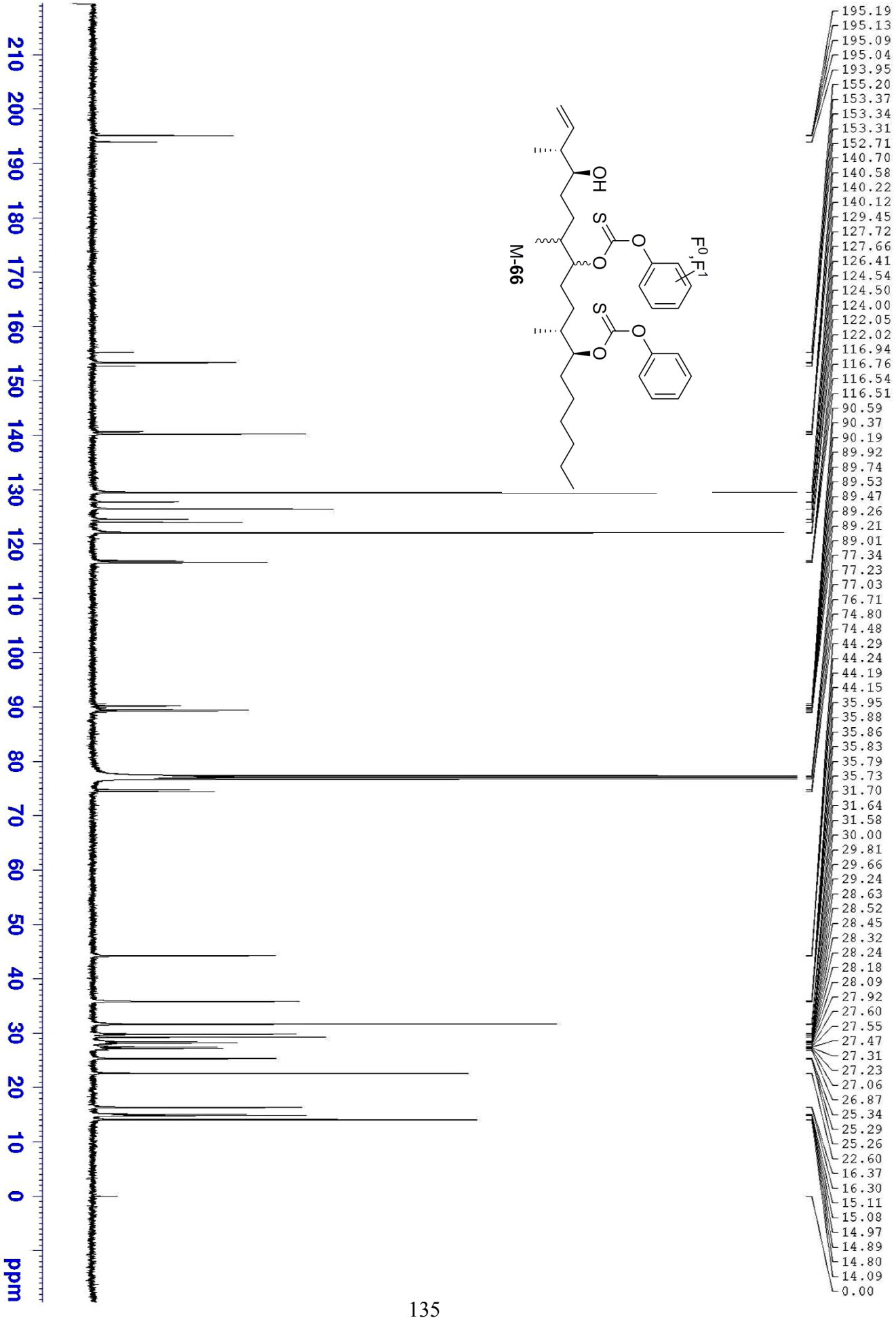
M-66
OH
S
O
O
S
O
O
F0,F1
210
200
190
180
170
160
150
140
130
120
110
100
90
80
70
60
50
40
30
20
10
0
ppm
195.19
195.13
195.09
195.04
193.95
155.20
153.37
153.34
153.31
152.71
140.70
140.58
140.22
140.12
129.45
127.72
127.66
126.41
124.54
124.50
124.00
122.05
122.02
116.94
116.76
116.54
116.51
90.59
90.37
90.19
89.92
89.74
89.53
89.47
89.26
89.21
89.01
77.34
77.23
77.03
76.71
74.80
74.48
44.29
44.24
44.19
44.15
35.95
35.88
35.86
35.83
35.79
35.73
31.70
31.64
31.58
30.00
29.81
29.66
29.24
28.63
28.52
28.45
28.32
28.24
28.18
28.09
27.92
27.60
27.55
27.47
27.31
27.23
27.06
26.87
25.34
25.29
25.26
22.60
16.37
16.30
15.11
15.08
14.97
14.89
14.80
14.09
0.00

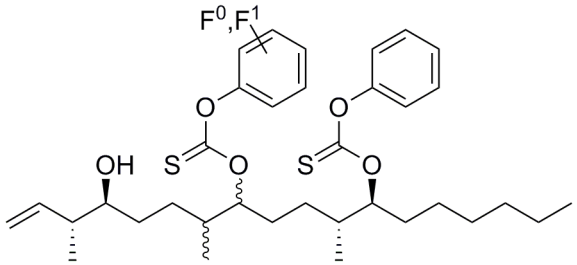
F0,F1
O
O
OH
S
O
S
O

M-**66**

-128.01
-128.01
-128.02
-128.03
-128.05
-128.06
-128.08
-128.09
−127.2
−127.4
−127.6
−127.8
−128.0
−128.2
−128.4
−128.6
−128.8
ppm

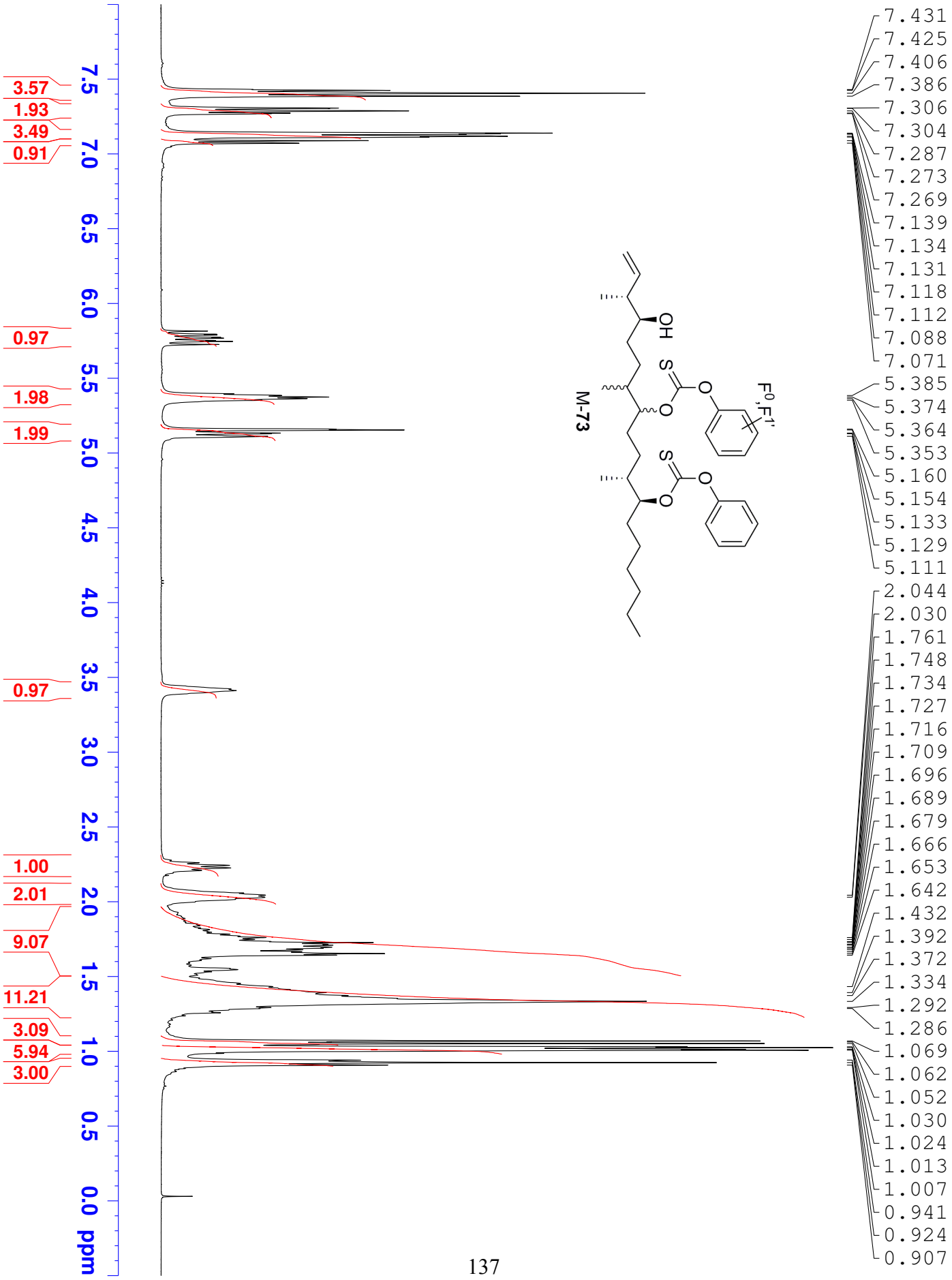
3.57
1.93
3.49
0.91
0.97
1.98
1.99
0.97
1.00
2.01
9.07
11.21
3.09
5.94
3.00
7.5
7.0
6.5
6.0
5.5
5.0
4.5
4.0
3.5
3.0
2.5
2.0
1.5
1.0
0.5
0.0
ppm
OH
S
O
O
S
O
O
F0,F1'
M-73
7.431
7.425
7.406
7.386
7.306
7.304
7.287
7.273
7.269
7.139
7.134
7.131
7.118
7.112
7.088
7.071
5.385
5.374
5.364
5.353
5.160
5.154
5.133
5.129
5.111
2.044
2.030
1.761
1.748
1.734
1.727
1.716
1.709
1.696
1.689
1.679
1.666
1.653
1.642
1.432
1.392
1.372
1.334
1.292
1.286
1.069
1.062
1.052
1.030
1.024
1.013
1.007
0.941
0.924
0.907

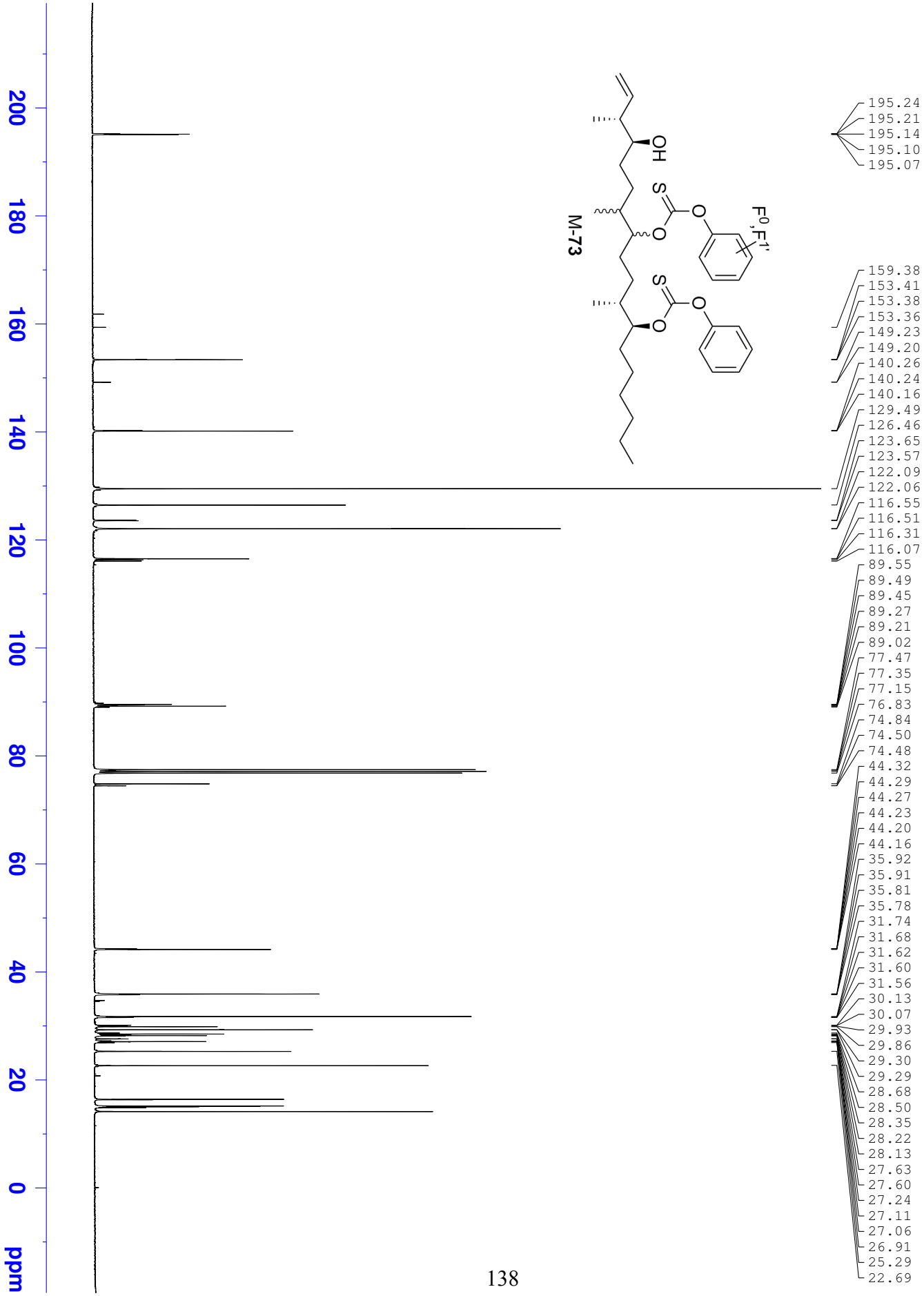
200
180
160
140
120
100
80
60
40
20
0
ppm
OH
S
O
O
S
O
O
F0,F1'
M-73
195.24
195.21
195.14
195.10
195.07
159.38
153.41
153.38
153.36
149.23
149.20
140.26
140.24
140.16
129.49
126.46
123.65
123.57
122.09
122.06
116.55
116.51
116.31
116.07
89.55
89.49
89.45
89.27
89.21
89.02
77.47
77.35
77.15
76.83
74.84
74.50
74.48
44.32
44.29
44.27
44.23
44.20
44.16
35.92
35.91
35.81
35.78
31.74
31.68
31.62
31.60
31.56
30.13
30.07
29.93
29.86
29.30
29.29
28.68
28.50
28.35
28.22
28.13
27.63
27.60
27.24
27.11
27.06
26.91
25.29
22.69

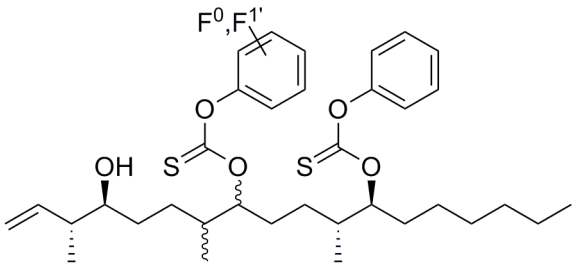

M-**73**

-115.78
-115.79
-115.80
-115.82
-115.83
-115.85
-115.86

–115.4 –115.6 –115.8 –116.0 –116.2 ppm

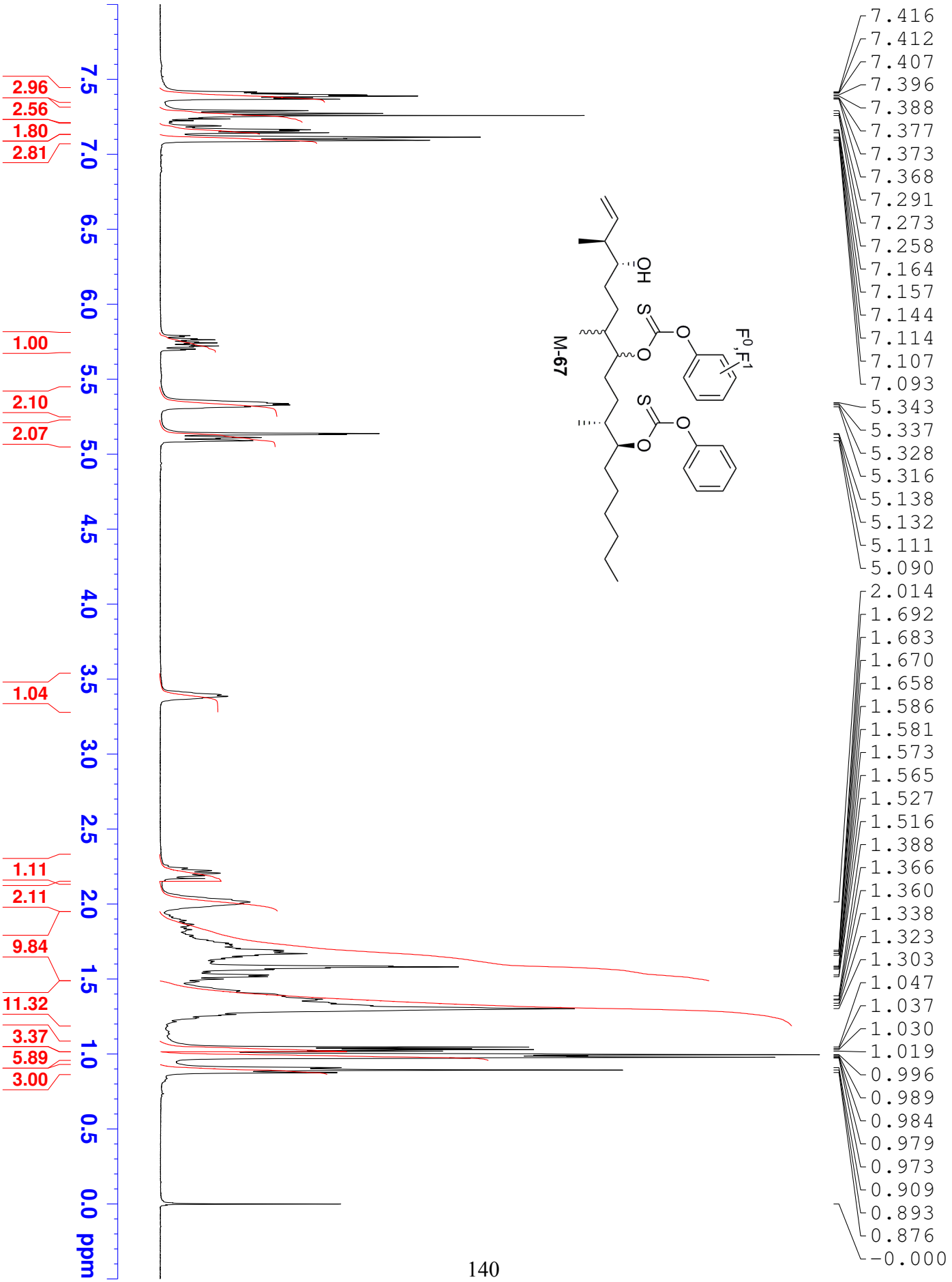
2.96
2.56
1.80
2.81
1.00
2.10
2.07
1.04
1.11
2.11
9.84
11.32
3.37
5.89
3.00
7.5
7.0
6.5
6.0
5.5
5.0
4.5
4.0
3.5
3.0
2.5
2.0
1.5
1.0
0.5
0.0
ppm
M-67
OH
S
O
O
S
O
O
F0,F1
7.416
7.412
7.407
7.396
7.388
7.377
7.373
7.368
7.291
7.273
7.258
7.164
7.157
7.144
7.114
7.107
7.093
5.343
5.337
5.328
5.316
5.138
5.132
5.111
5.090
2.014
1.692
1.683
1.670
1.658
1.586
1.581
1.573
1.565
1.527
1.516
1.388
1.366
1.360
1.338
1.323
1.303
1.047
1.037
1.030
1.019
0.996
0.989
0.984
0.979
0.973
0.909
0.893
0.876
-0.000

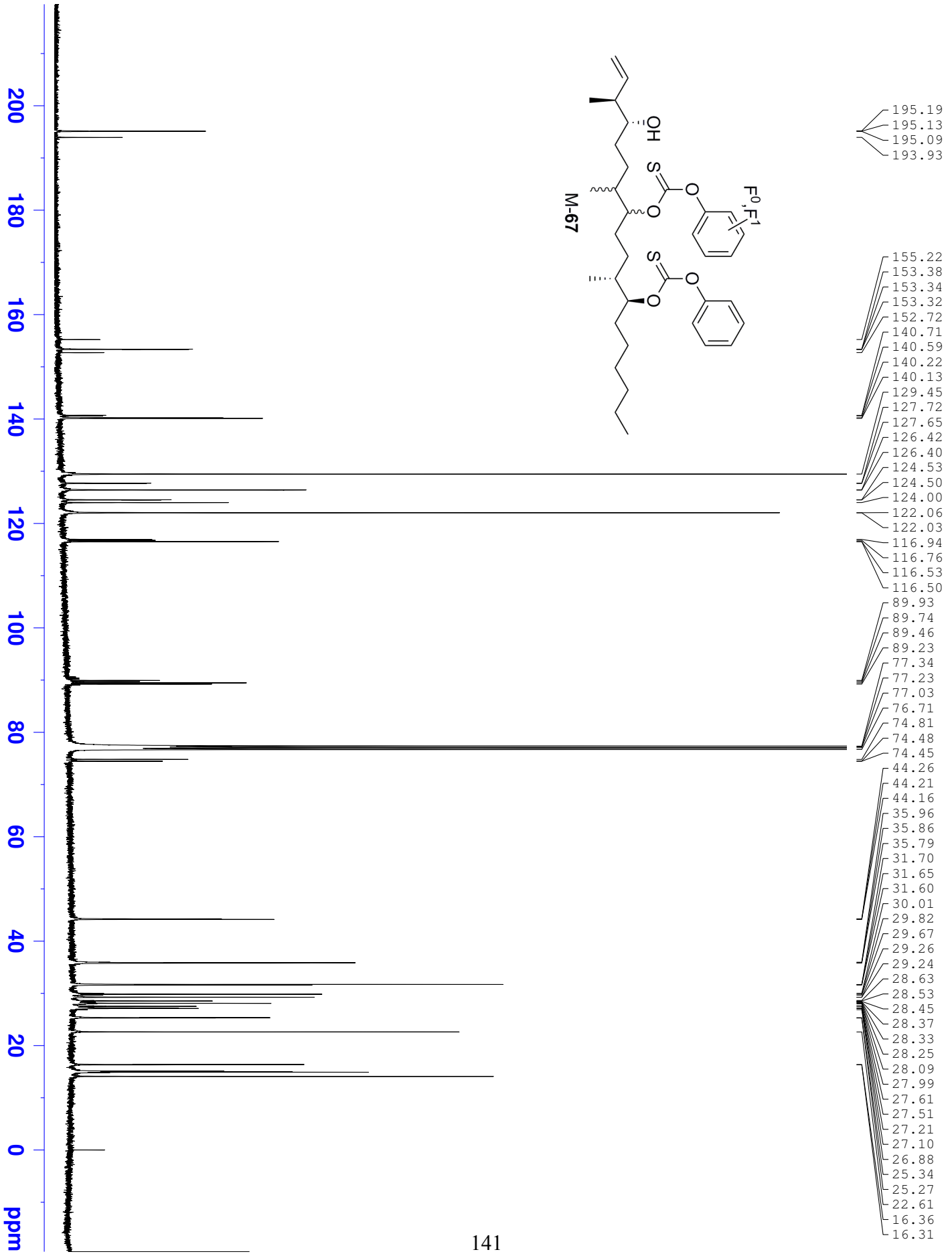
M-67
OH
S
O
O
S
O
O
F0,F1
195.19
195.13
195.09
193.93
155.22
153.38
153.34
153.32
152.72
140.71
140.59
140.22
140.13
129.45
127.72
127.65
126.42
126.40
124.53
124.50
124.00
122.06
122.03
116.94
116.76
116.53
116.50
89.93
89.74
89.46
89.23
77.34
77.23
77.03
76.71
74.81
74.48
74.45
44.26
44.21
44.16
35.96
35.86
35.79
31.70
31.65
31.60
30.01
29.82
29.67
29.26
29.24
28.63
28.53
28.45
28.37
28.33
28.25
28.09
27.99
27.61
27.51
27.21
27.10
26.88
25.34
25.27
22.61
16.36
16.31
200
180
160
140
120
100
80
60
40
20
0
ppm

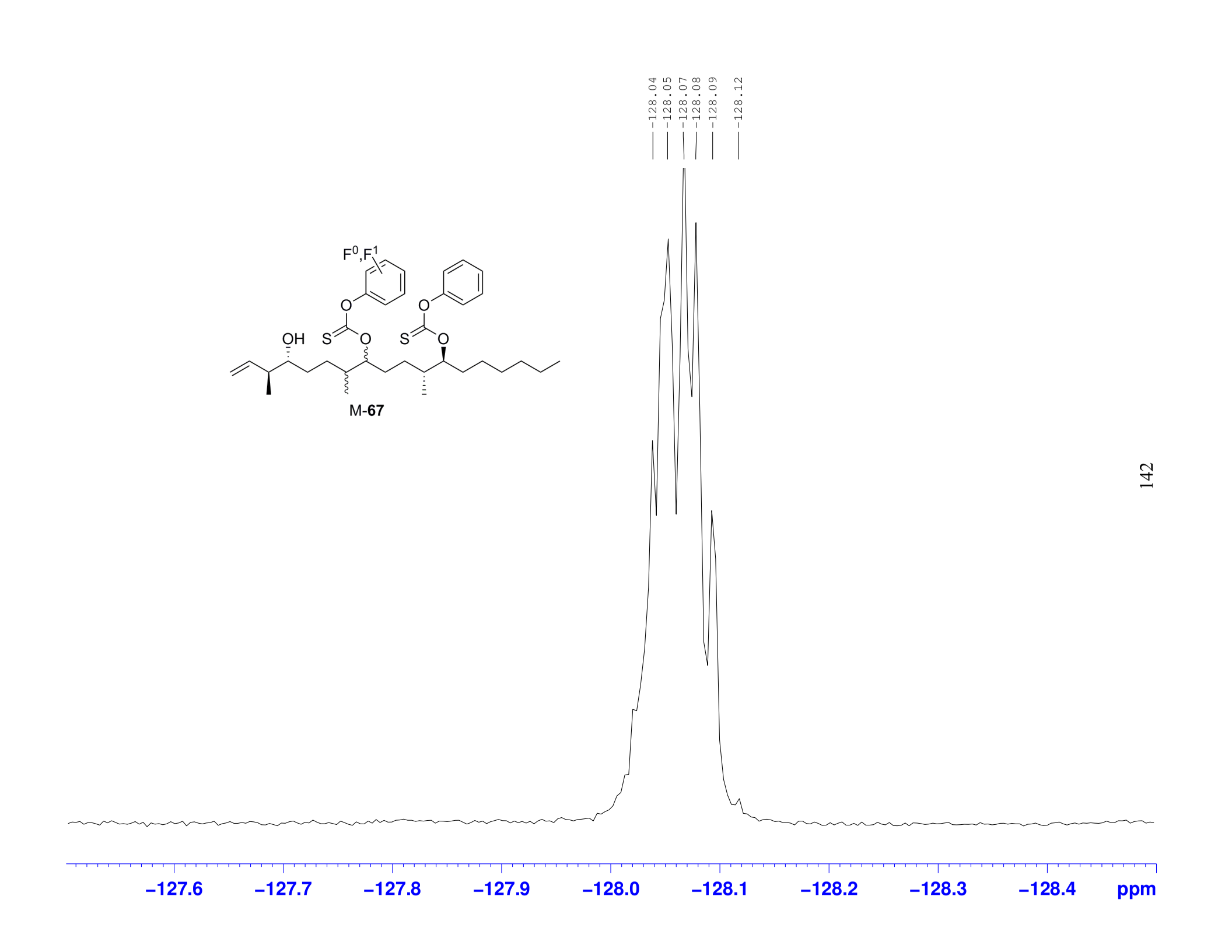
-128.04
-128.05
-128.07
-128.08
-128.09
-128.12
F0,F1
OH
S
O
S
O
O
O
M-67
142
−127.6
−127.7
−127.8
−127.9
−128.0
−128.1
−128.2
−128.3
−128.4
ppm

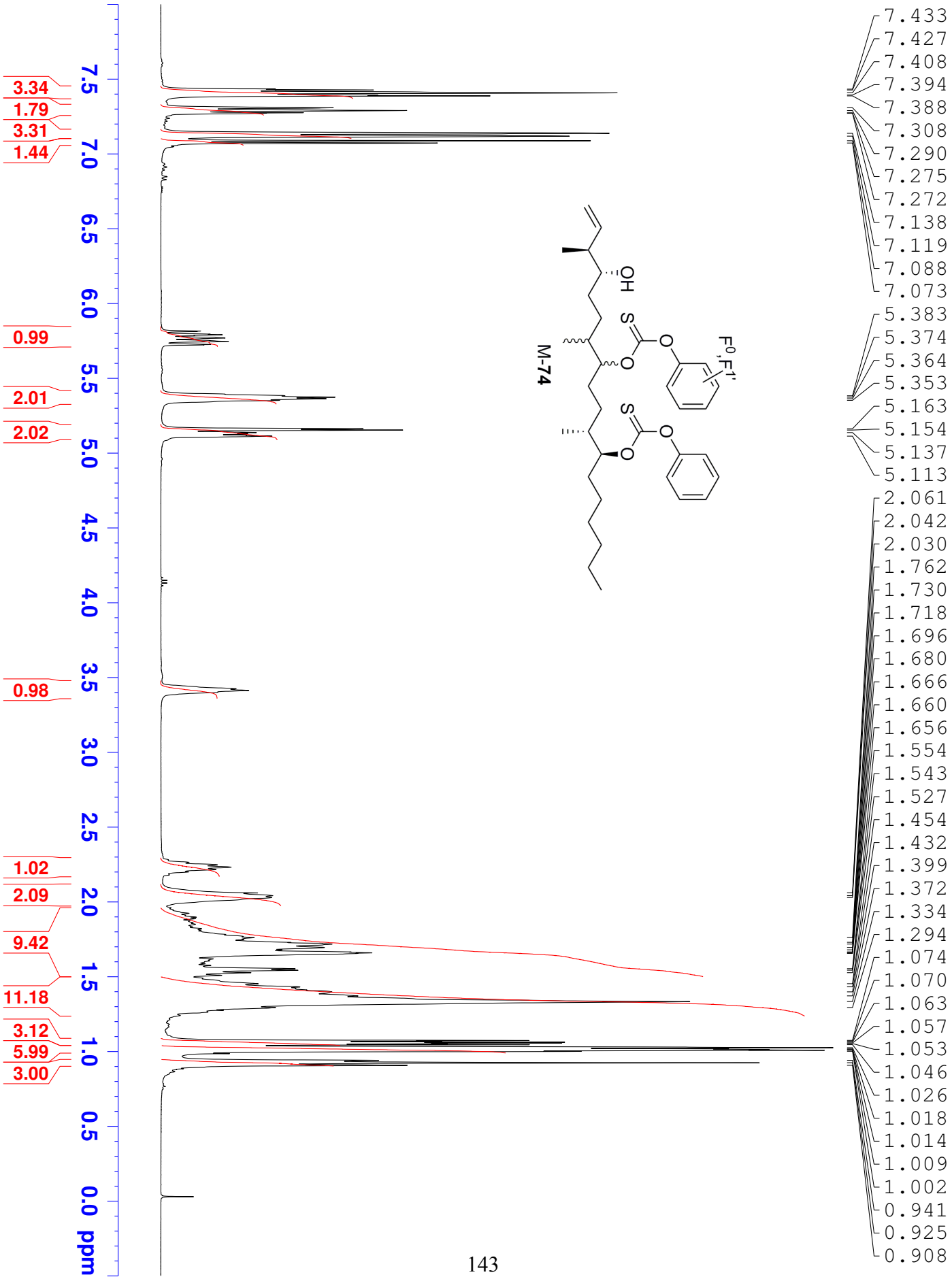
3.34
1.79
3.31
1.44
0.99
2.01
2.02
0.98
1.02
2.09
9.42
11.18
3.12
5.99
3.00
7.5
7.0
6.5
6.0
5.5
5.0
4.5
4.0
3.5
3.0
2.5
2.0
1.5
1.0
0.5
0.0
ppm
OH
S
O
O
S
O
O
F0,F1'
M-74
7.433
7.427
7.408
7.394
7.388
7.308
7.290
7.275
7.272
7.138
7.119
7.088
7.073
5.383
5.374
5.364
5.353
5.163
5.154
5.137
5.113
2.061
2.042
2.030
1.762
1.730
1.718
1.696
1.680
1.666
1.660
1.656
1.554
1.543
1.527
1.454
1.432
1.399
1.372
1.334
1.294
1.074
1.070
1.063
1.057
1.053
1.046
1.026
1.018
1.014
1.009
1.002
0.941
0.925
0.908

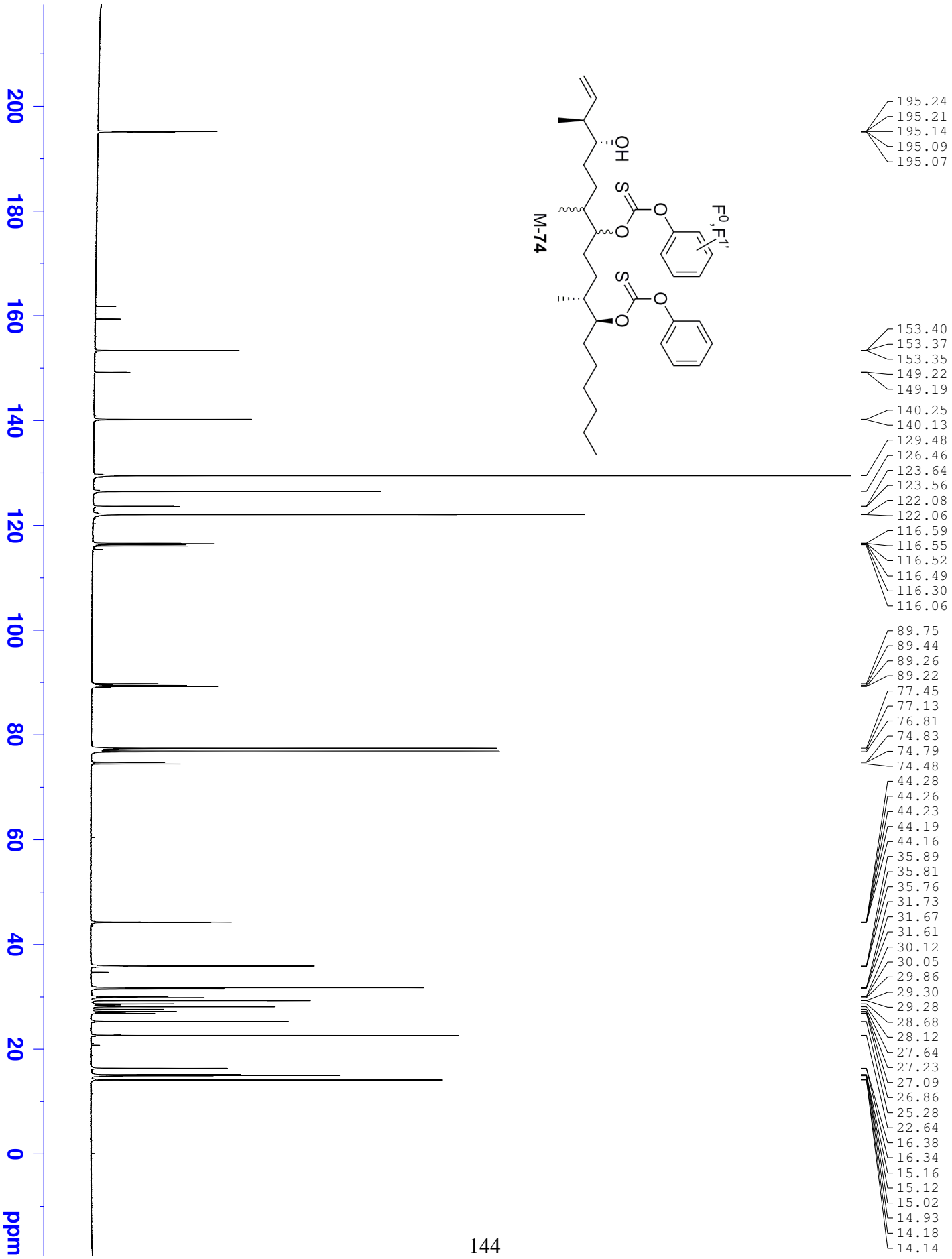
200
180
160
140
120
100
80
60
40
20
0
ppm
M-74
OH
S
O
O
F0,F1'
195.24
195.21
195.14
195.09
195.07
153.40
153.37
153.35
149.22
149.19
140.25
140.13
129.48
126.46
123.64
123.56
122.08
122.06
116.59
116.55
116.52
116.49
116.30
116.06
89.75
89.44
89.26
89.22
77.45
77.13
76.81
74.83
74.79
74.48
44.28
44.26
44.23
44.19
44.16
35.89
35.81
35.76
31.73
31.67
31.61
30.12
30.05
29.86
29.30
29.28
28.68
28.12
27.64
27.23
27.09
26.86
25.28
22.64
16.38
16.34
15.16
15.12
15.02
14.93
14.18
14.14

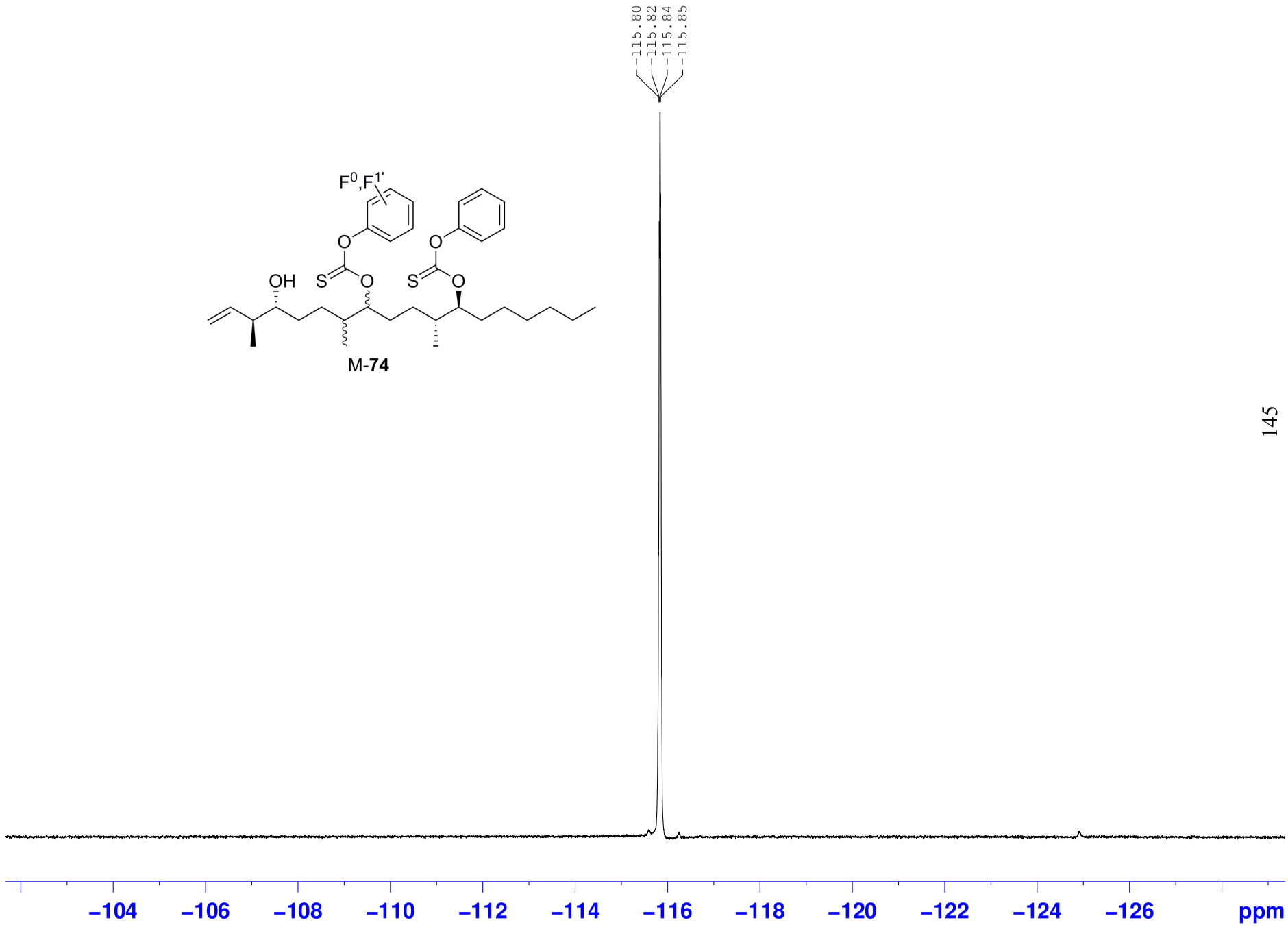
-115.80
-115.82
-115.84
-115.85
F0,F1'
O
O
OH
S
O
S
O
M-74
145
−104
−106
−108
−110
−112
−114
−116
−118
−120
−122
−124
−126
ppm

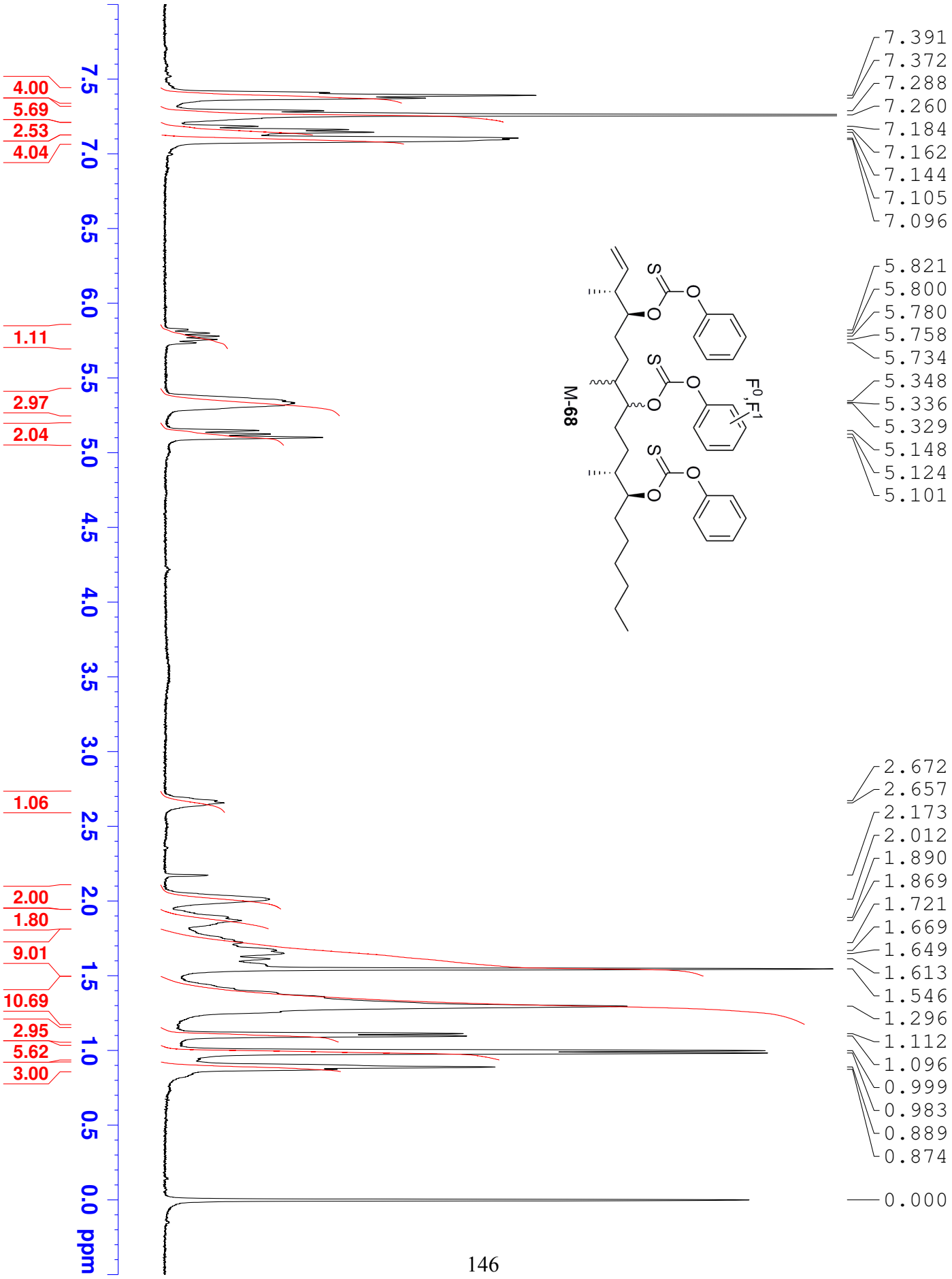
7.391
7.372
7.288
7.260
7.184
7.162
7.144
7.105
7.096
5.821
5.800
5.780
5.758
5.734
5.348
5.336
5.329
5.148
5.124
5.101
2.672
2.657
2.173
2.012
1.890
1.869
1.721
1.669
1.649
1.613
1.546
1.296
1.112
1.096
0.999
0.983
0.889
0.874
0.000
4.00
5.69
2.53
4.04
1.11
2.97
2.04
1.06
2.00
1.80
9.01
10.69
2.95
5.62
3.00
7.5
7.0
6.5
6.0
5.5
5.0
4.5
4.0
3.5
3.0
2.5
2.0
1.5
1.0
0.5
0.0
ppm
M-68
F0,F1

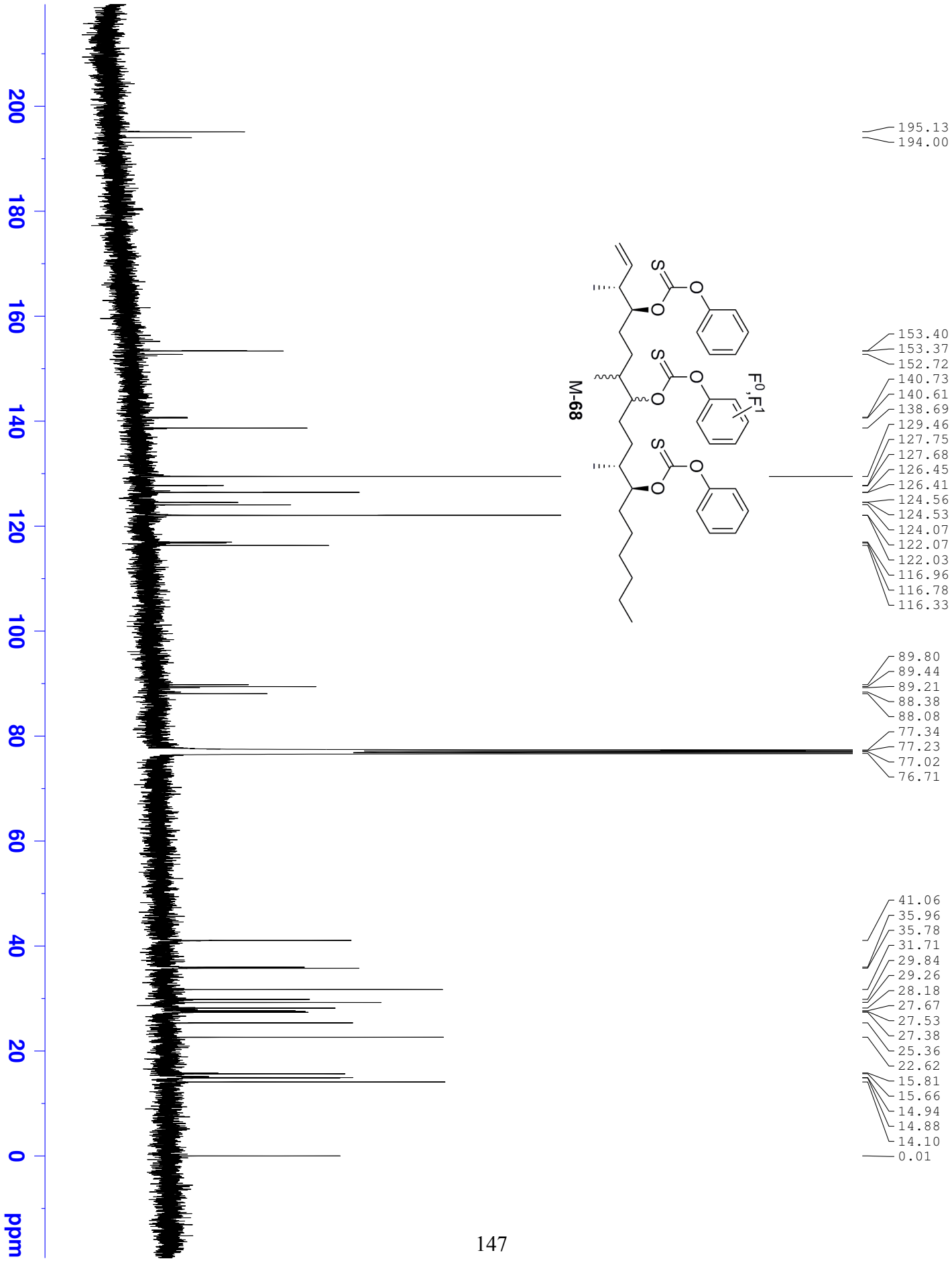
200
180
160
140
120
100
80
60
40
20
0
ppm
195.13
194.00
153.40
153.37
152.72
140.73
140.61
138.69
129.46
127.75
127.68
126.45
126.41
124.56
124.53
124.07
122.07
122.03
116.96
116.78
116.33
89.80
89.44
89.21
88.38
88.08
77.34
77.23
77.02
76.71
41.06
35.96
35.78
31.71
29.84
29.26
28.18
27.67
27.53
27.38
25.36
22.62
15.81
15.66
14.94
14.88
14.10
0.01
M-68
F0,F1

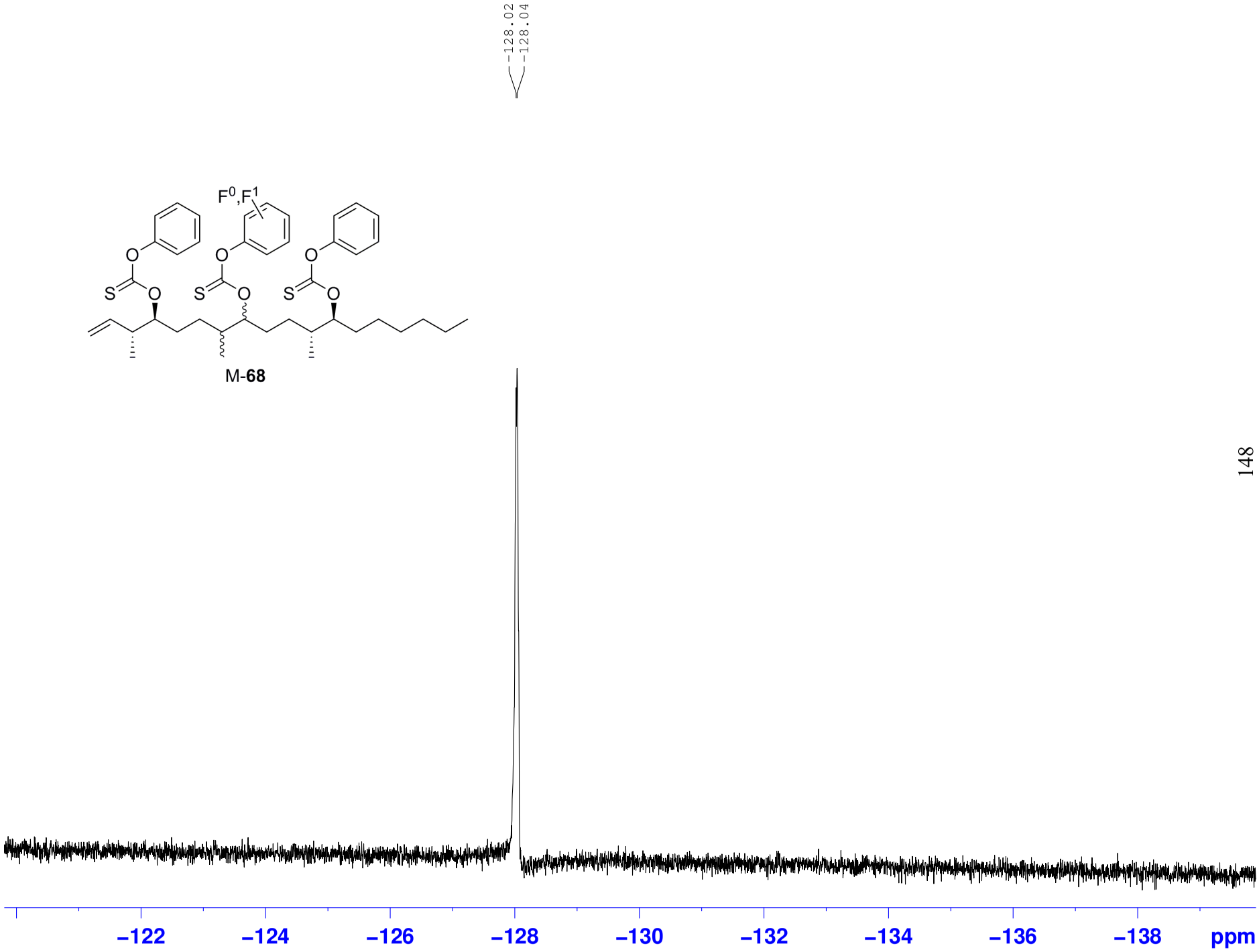
-128.02
-128.04
F0,F1
O
S
O
M-68
148
−122
−124
−126
−128
−130
−132
−134
−136
−138
ppm

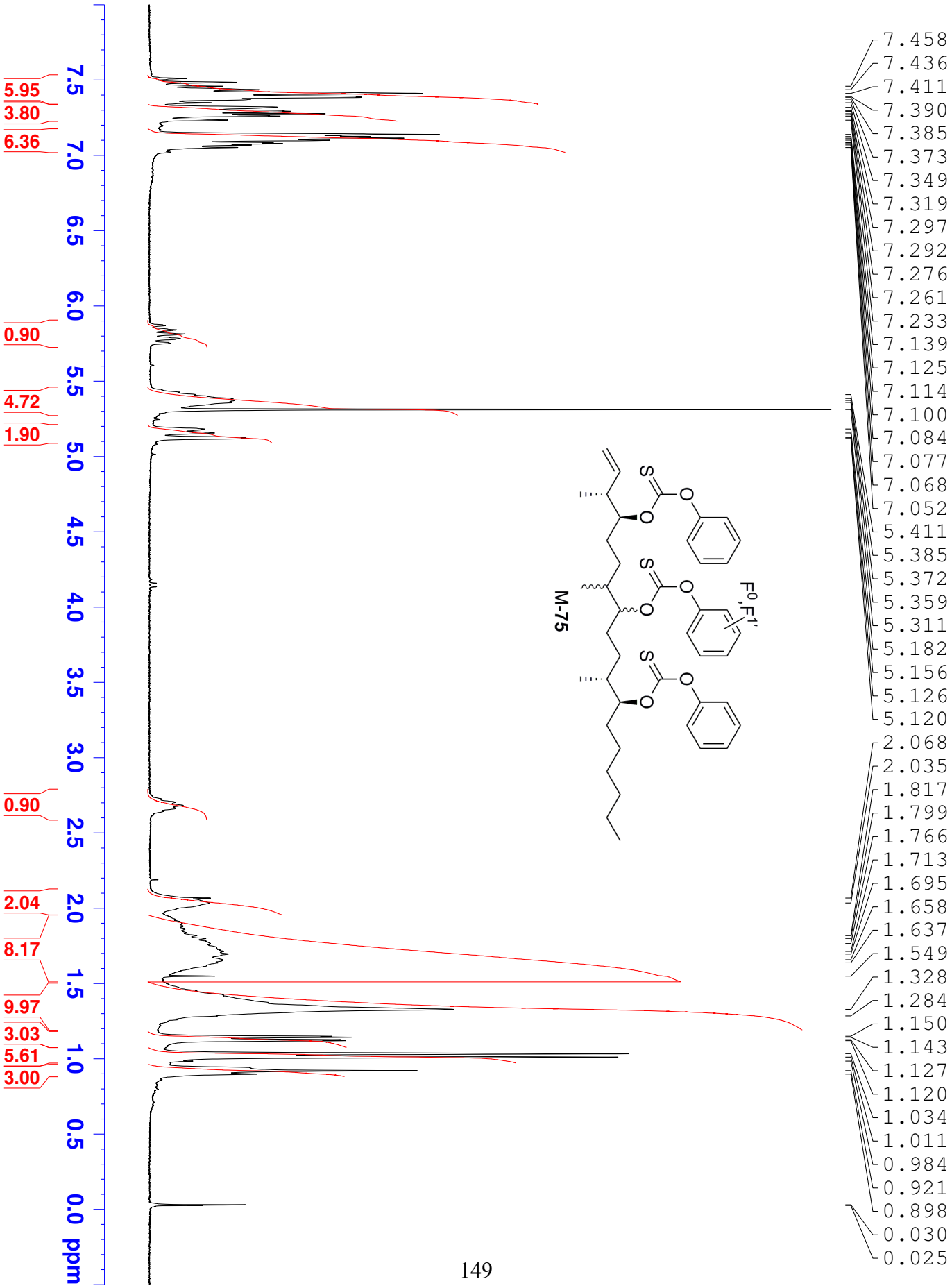
7.458
7.436
7.411
7.390
7.385
7.373
7.349
7.319
7.297
7.292
7.276
7.261
7.233
7.139
7.125
7.114
7.100
7.084
7.077
7.068
7.052
5.411
5.385
5.372
5.359
5.311
5.182
5.156
5.126
5.120
2.068
2.035
1.817
1.799
1.766
1.713
1.695
1.658
1.637
1.549
1.328
1.284
1.150
1.143
1.127
1.120
1.034
1.011
0.984
0.921
0.898
0.030
0.025
5.95
3.80
6.36
0.90
4.72
1.90
0.90
2.04
8.17
9.97
3.03
5.61
3.00
7.5
7.0
6.5
6.0
5.5
5.0
4.5
4.0
3.5
3.0
2.5
2.0
1.5
1.0
0.5
0.0
ppm
M-75
F0,F1'

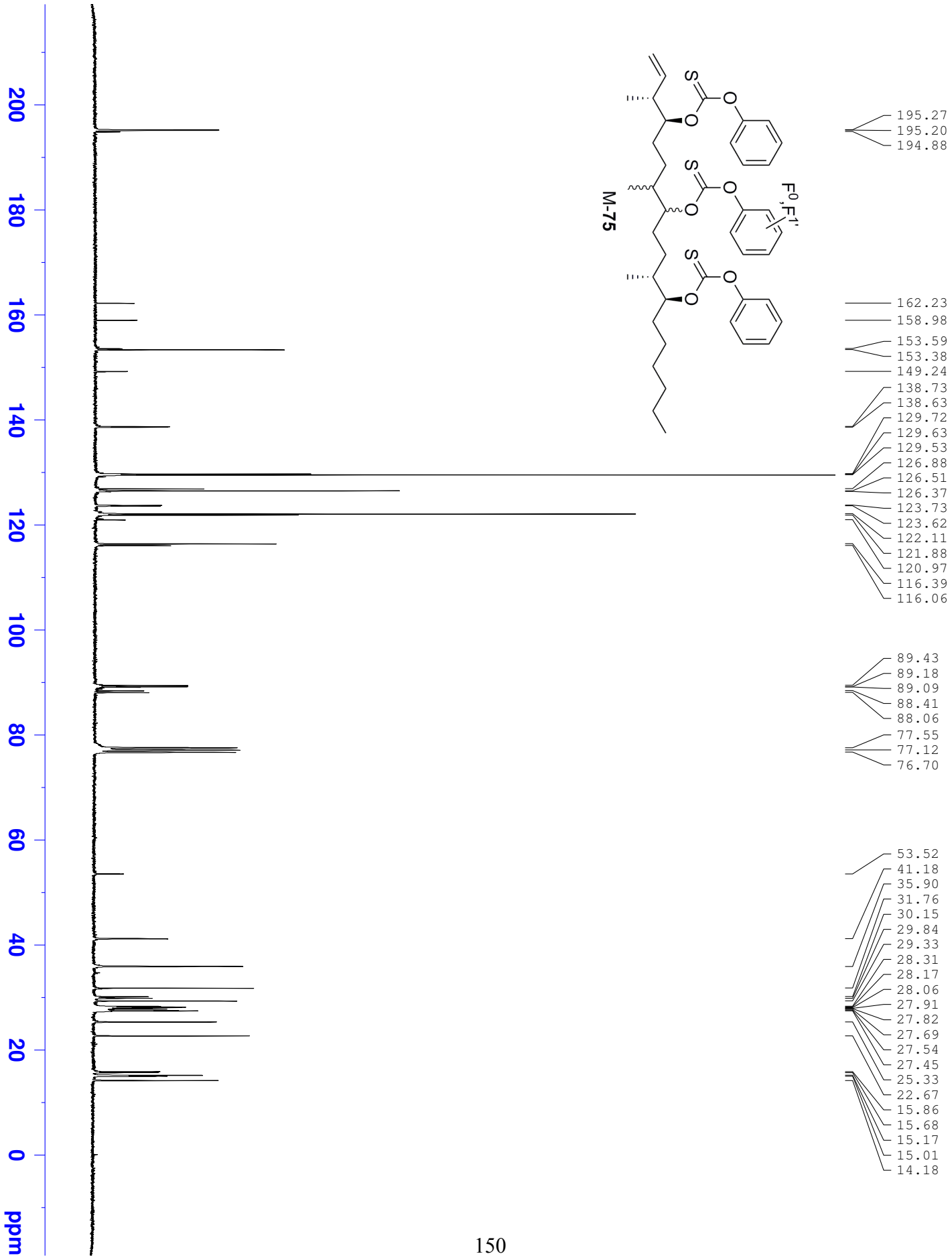
M-75
F0,F1'
195.27
195.20
194.88
162.23
158.98
153.59
153.38
149.24
138.73
138.63
129.72
129.63
129.53
126.88
126.51
126.37
123.73
123.62
122.11
121.88
120.97
116.39
116.06
89.43
89.18
89.09
88.41
88.06
77.55
77.12
76.70
53.52
41.18
35.90
31.76
30.15
29.84
29.33
28.31
28.17
28.06
27.91
27.82
27.69
27.54
27.45
25.33
22.67
15.86
15.68
15.17
15.01
14.18
200
180
160
140
120
100
80
60
40
20
0
ppm

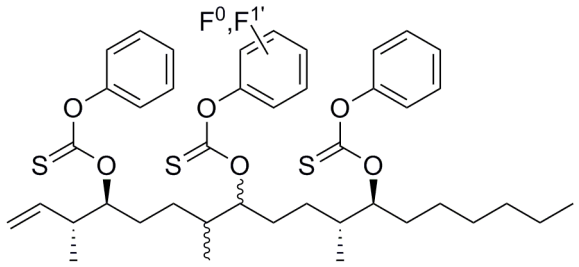

M-**75**

-115.75

151

–113.5 –114.0 –114.5 –115.0 –115.5 –116.0 –116.5 –117.0 –117.5 –118.0 ppm

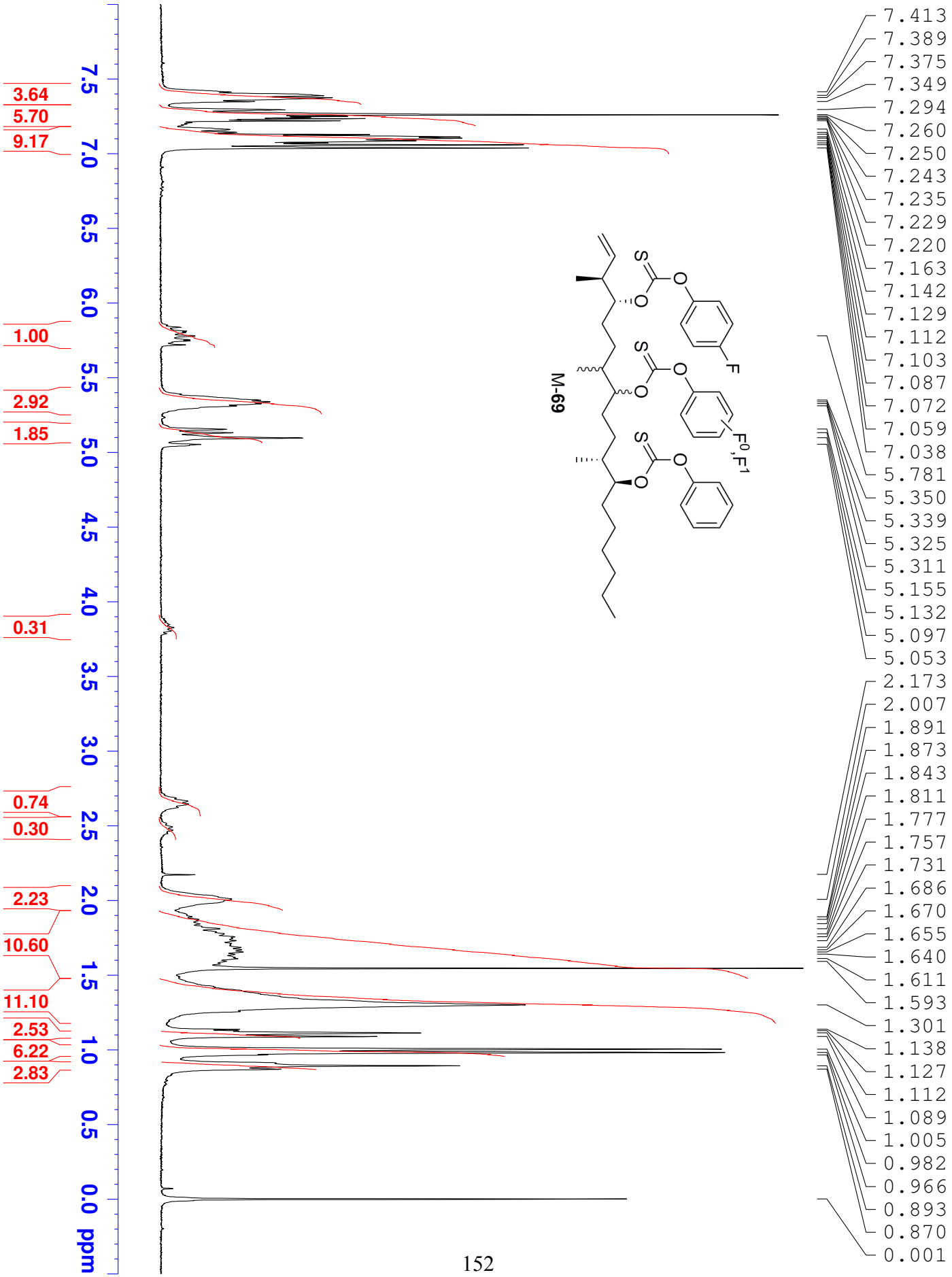
M-69
F
F0,F1
3.64
5.70
9.17
1.00
2.92
1.85
0.31
0.74
0.30
2.23
10.60
11.10
2.53
6.22
2.83
7.5
7.0
6.5
6.0
5.5
5.0
4.5
4.0
3.5
3.0
2.5
2.0
1.5
1.0
0.5
0.0
ppm
7.413
7.389
7.375
7.349
7.294
7.260
7.250
7.243
7.235
7.229
7.220
7.163
7.142
7.129
7.112
7.103
7.087
7.072
7.059
7.038
5.781
5.350
5.339
5.325
5.311
5.155
5.132
5.097
5.053
2.173
2.007
1.891
1.873
1.843
1.811
1.777
1.757
1.731
1.686
1.670
1.655
1.640
1.611
1.593
1.301
1.138
1.127
1.112
1.089
1.005
0.982
0.966
0.893
0.870
0.001

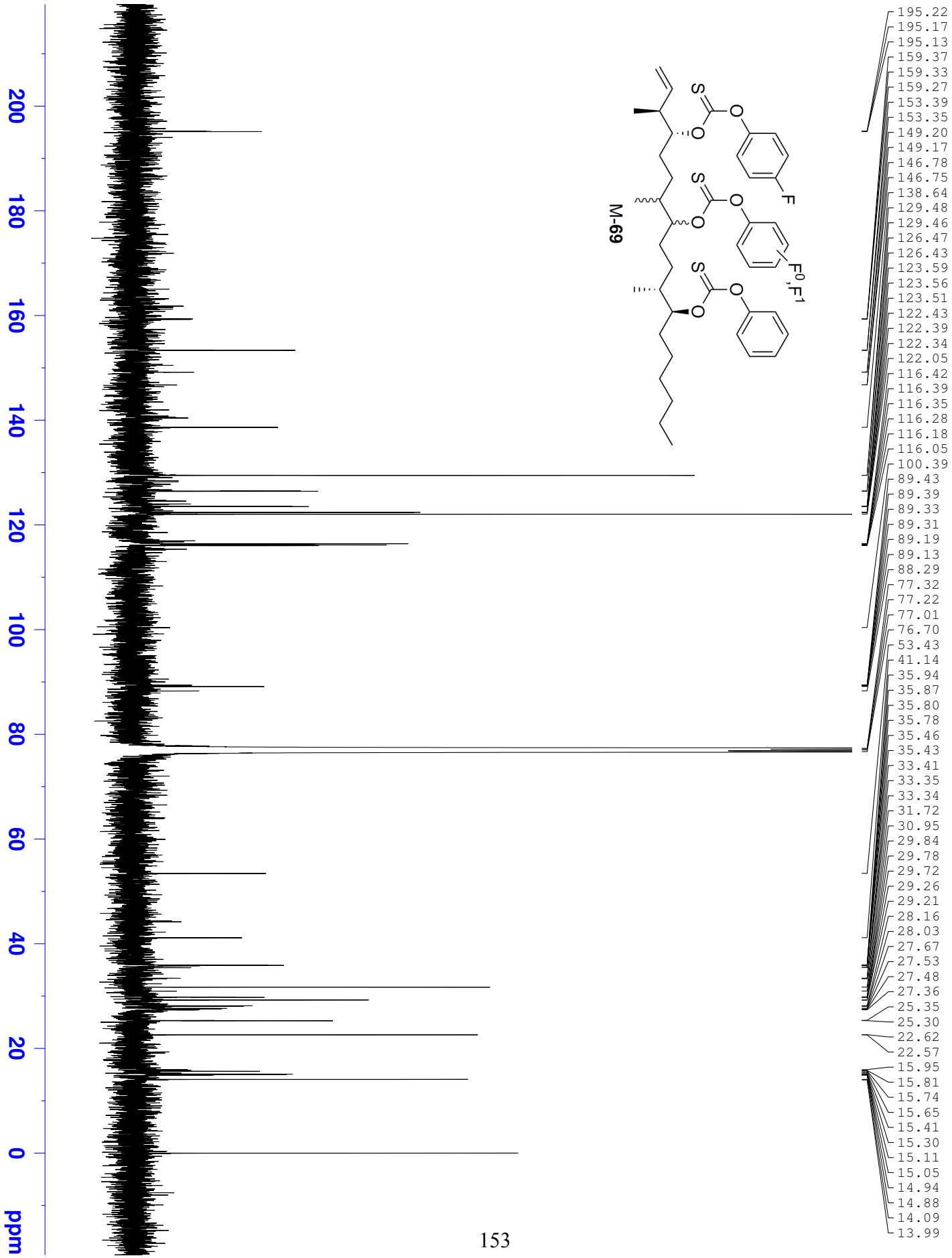
M-69
F
F0,F1
195.22
195.17
195.13
159.37
159.33
159.27
153.39
153.35
149.20
149.17
146.78
146.75
138.64
129.48
129.46
126.47
126.43
123.59
123.56
123.51
122.43
122.39
122.34
122.05
116.42
116.39
116.35
116.28
116.18
116.05
100.39
89.43
89.39
89.33
89.31
89.19
89.13
88.29
77.32
77.22
77.01
76.70
53.43
41.14
35.94
35.87
35.80
35.78
35.46
35.43
33.41
33.35
33.34
31.72
30.95
29.84
29.78
29.72
29.26
29.21
28.16
28.03
27.67
27.53
27.48
27.36
25.35
25.30
22.62
22.57
15.95
15.81
15.74
15.65
15.41
15.30
15.11
15.05
14.94
14.88
14.09
13.99
200
180
160
140
120
100
80
60
40
20
0
ppm

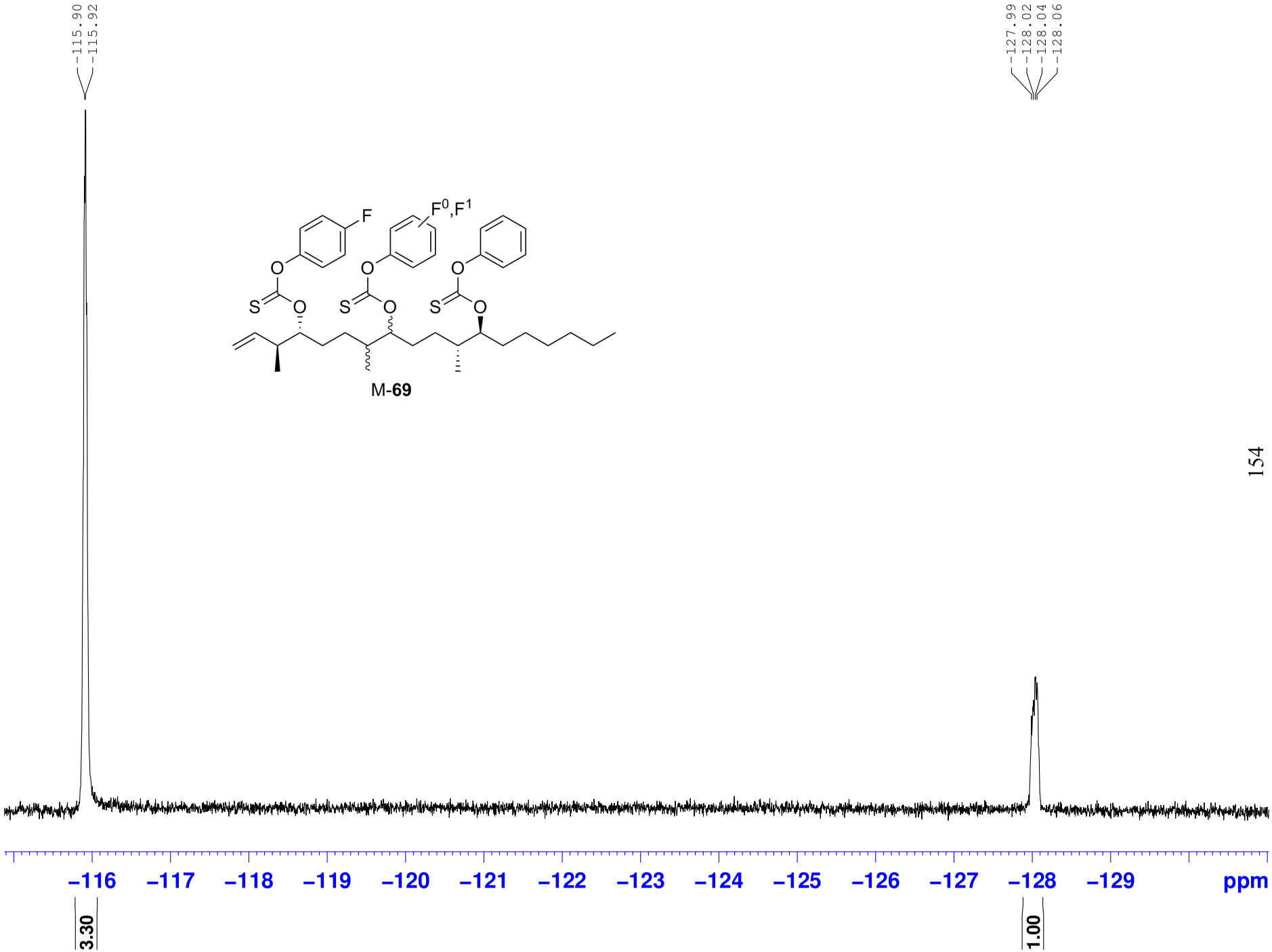
-115.90
-115.92
-127.99
-128.02
-128.04
-128.06
F
F0,F1
O
S
O
M-69
154
−116
−117
−118
−119
−120
−121
−122
−123
−124
−125
−126
−127
−128
−129
ppm
3.30
1.00

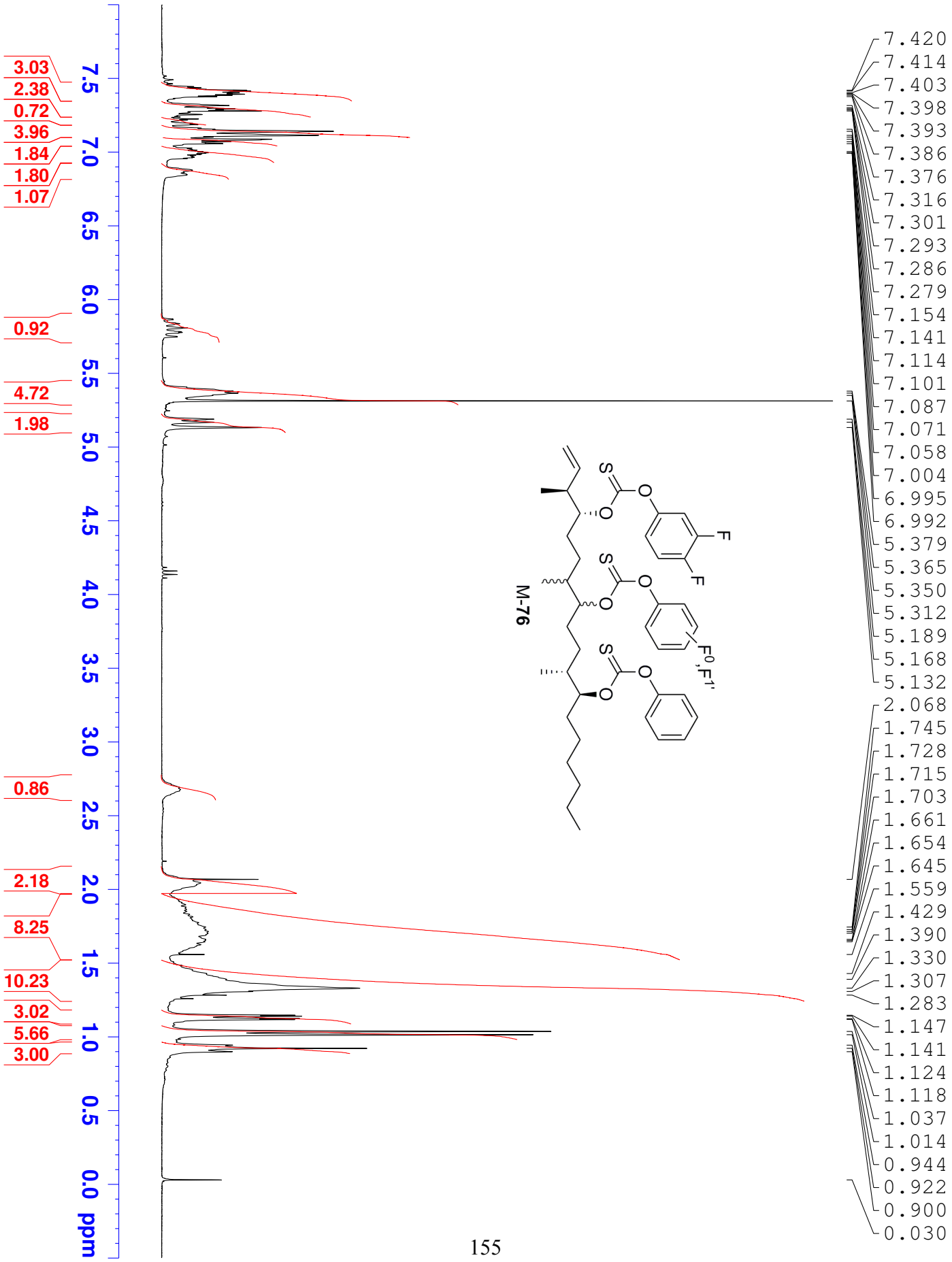
3.03
2.38
0.72
3.96
1.84
1.80
1.07
0.92
4.72
1.98
0.86
2.18
8.25
10.23
3.02
5.66
3.00
7.5
7.0
6.5
6.0
5.5
5.0
4.5
4.0
3.5
3.0
2.5
2.0
1.5
1.0
0.5
0.0
ppm
M-76
F
F
F0,F1'
7.420
7.414
7.403
7.398
7.393
7.386
7.376
7.316
7.301
7.293
7.286
7.279
7.154
7.141
7.114
7.101
7.087
7.071
7.058
7.004
6.995
6.992
5.379
5.365
5.350
5.312
5.189
5.168
5.132
2.068
1.745
1.728
1.715
1.703
1.661
1.654
1.645
1.559
1.429
1.390
1.330
1.307
1.283
1.147
1.141
1.124
1.118
1.037
1.014
0.944
0.922
0.900
0.030

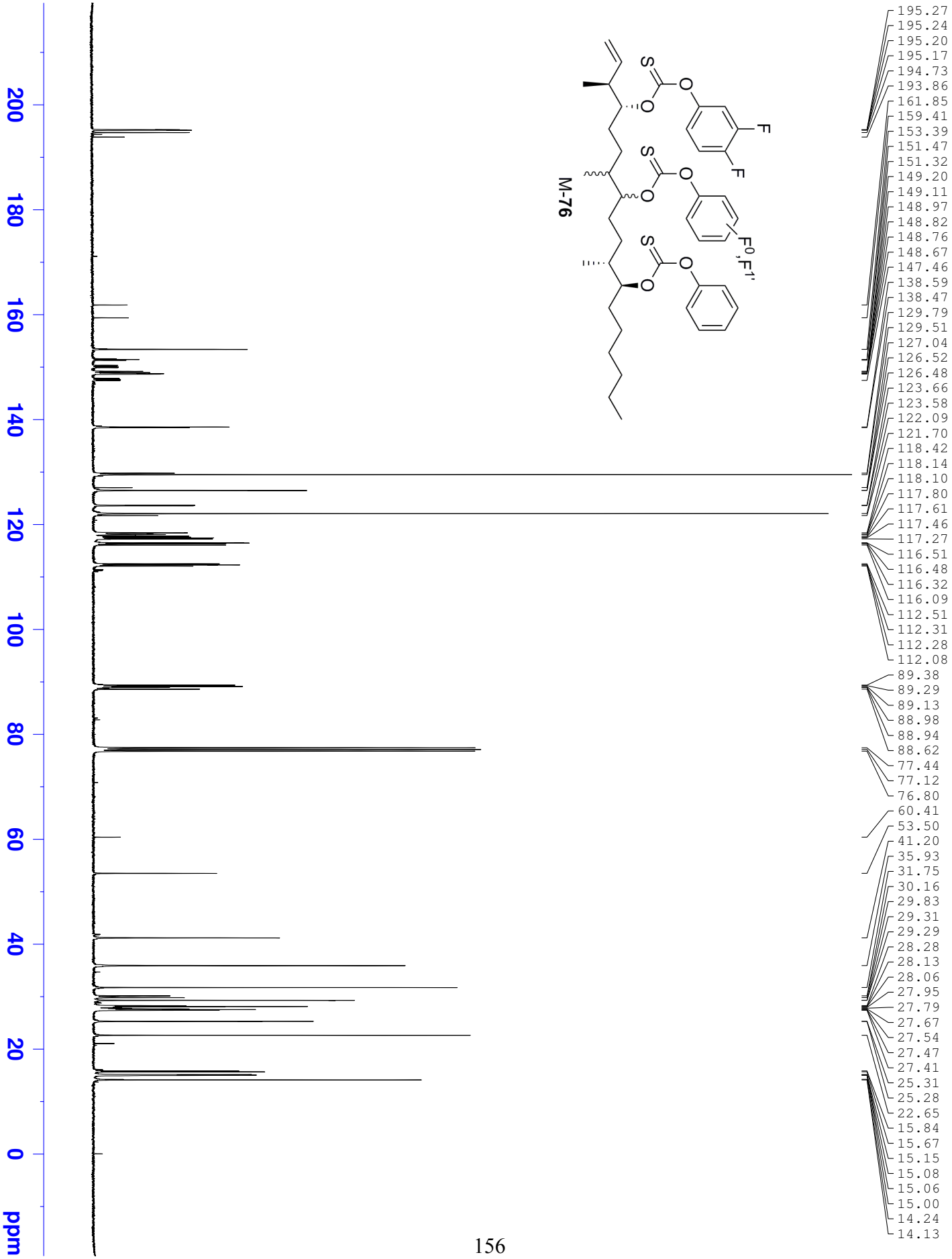
M-76
F
F
F0,F1'
195.27
195.24
195.20
195.17
194.73
193.86
161.85
159.41
153.39
151.47
151.32
149.20
149.11
148.97
148.82
148.76
148.67
147.46
138.59
138.47
129.79
129.51
127.04
126.52
126.48
123.66
123.58
122.09
121.70
118.42
118.14
118.10
117.80
117.61
117.46
117.27
116.51
116.48
116.32
116.09
112.51
112.31
112.28
112.08
89.38
89.29
89.13
88.98
88.94
88.62
77.44
77.12
76.80
60.41
53.50
41.20
35.93
31.75
30.16
29.83
29.31
29.29
28.28
28.13
28.06
27.95
27.79
27.67
27.54
27.47
27.41
25.31
25.28
22.65
15.84
15.67
15.15
15.08
15.06
15.00
14.24
14.13
200
180
160
140
120
100
80
60
40
20
0
ppm

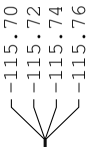
-115.70
-115.72
-115.74
-115.76

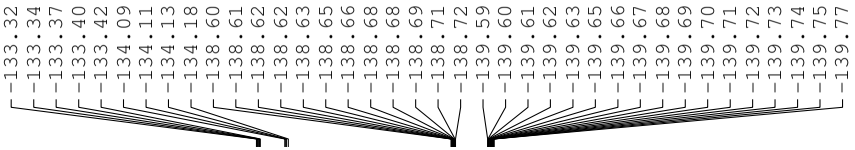
-133.32
-133.34
-133.37
-133.40
-133.42
-134.09
-134.11
-134.13
-134.18
-138.60
-138.61
-138.62
-138.62
-138.63
-138.65
-138.66
-138.68
-138.68
-138.69
-138.71
-138.72
-139.59
-139.60
-139.61
-139.62
-139.63
-139.65
-139.66
-139.67
-139.68
-139.69
-139.70
-139.71
-139.72
-139.73
-139.74
-139.75
-139.77

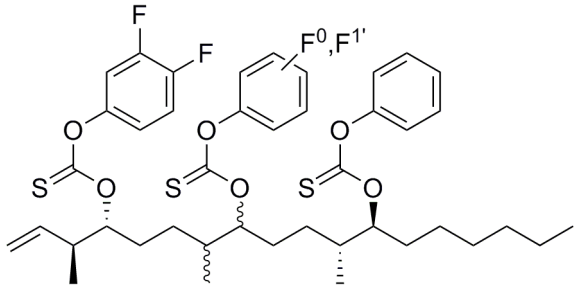
F
F
F0,F1'
O
S
O

M-**76**

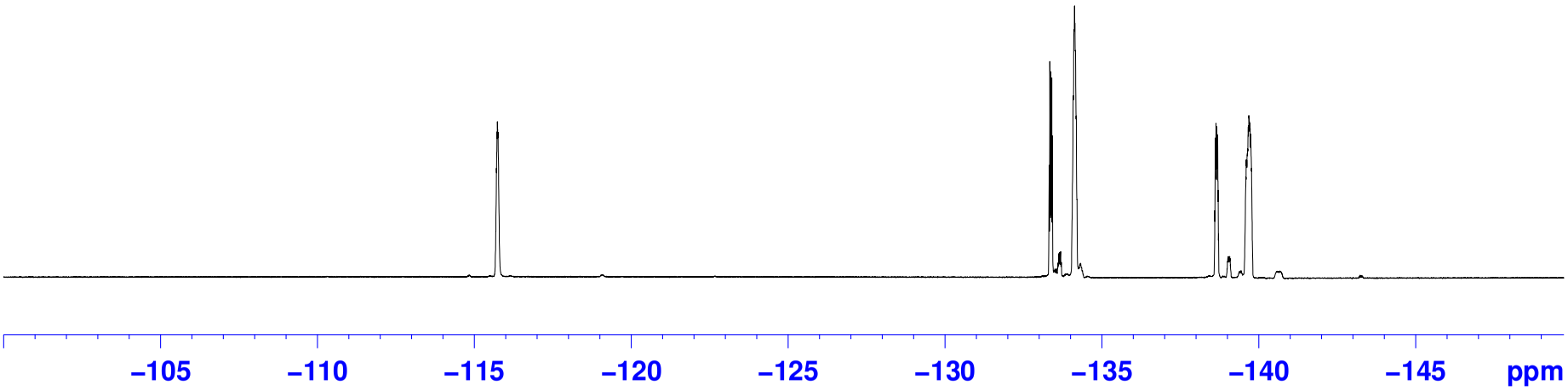
−105
−110
−115
−120
−125
−130
−135
−140
−145
ppm

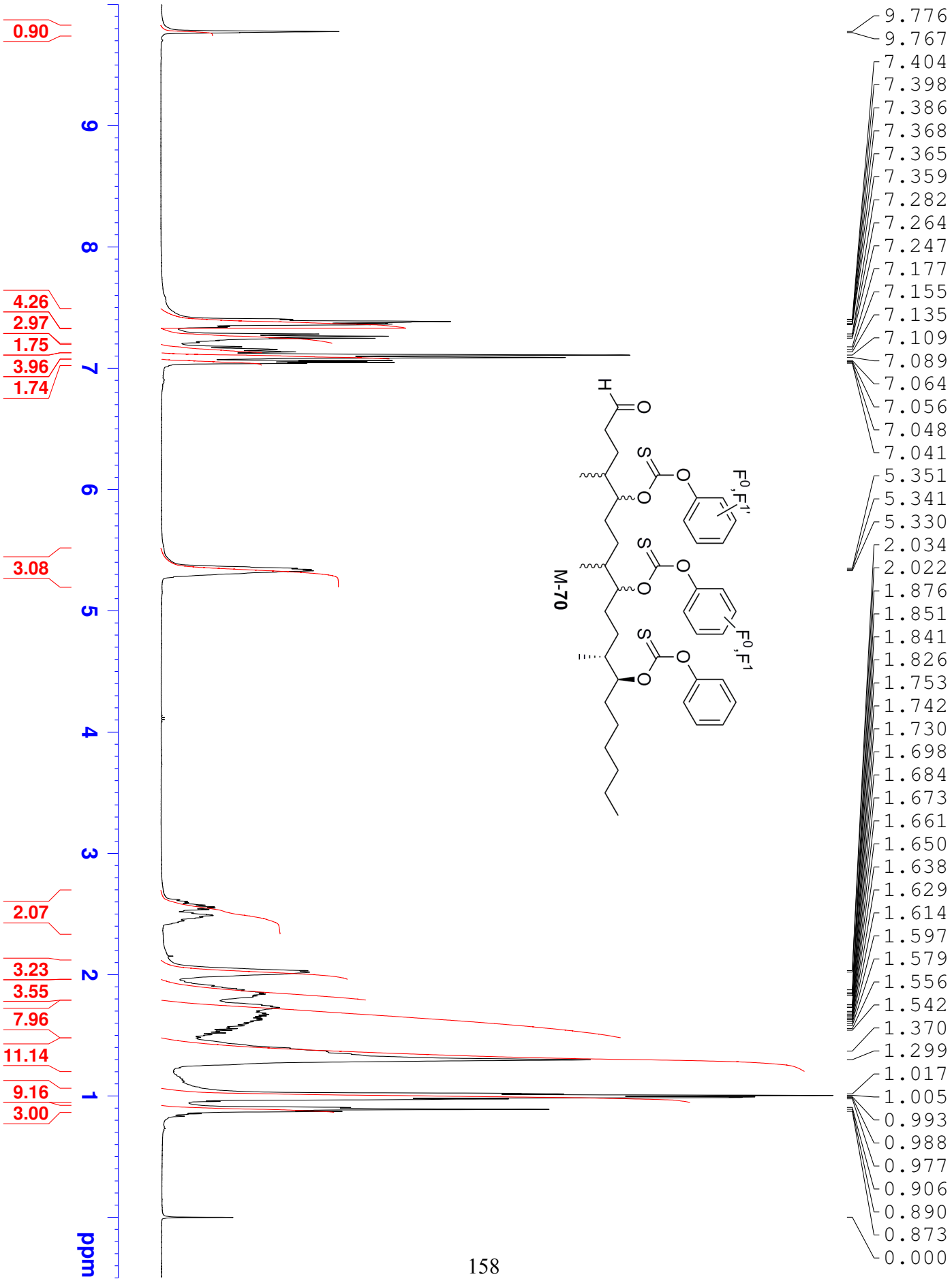
0.90
4.26
2.97
1.75
3.96
1.74
3.08
2.07
3.23
3.55
7.96
11.14
9.16
3.00
ppm
9
8
7
6
5
4
3
2
1
M-70
F0,F1'
F0,F1
9.776
9.767
7.404
7.398
7.386
7.368
7.365
7.359
7.282
7.264
7.247
7.177
7.155
7.135
7.109
7.089
7.064
7.056
7.048
7.041
5.351
5.341
5.330
2.034
2.022
1.876
1.851
1.841
1.826
1.753
1.742
1.730
1.698
1.684
1.673
1.661
1.650
1.638
1.629
1.614
1.597
1.579
1.556
1.542
1.370
1.299
1.017
1.005
0.993
0.988
0.977
0.906
0.890
0.873
0.000

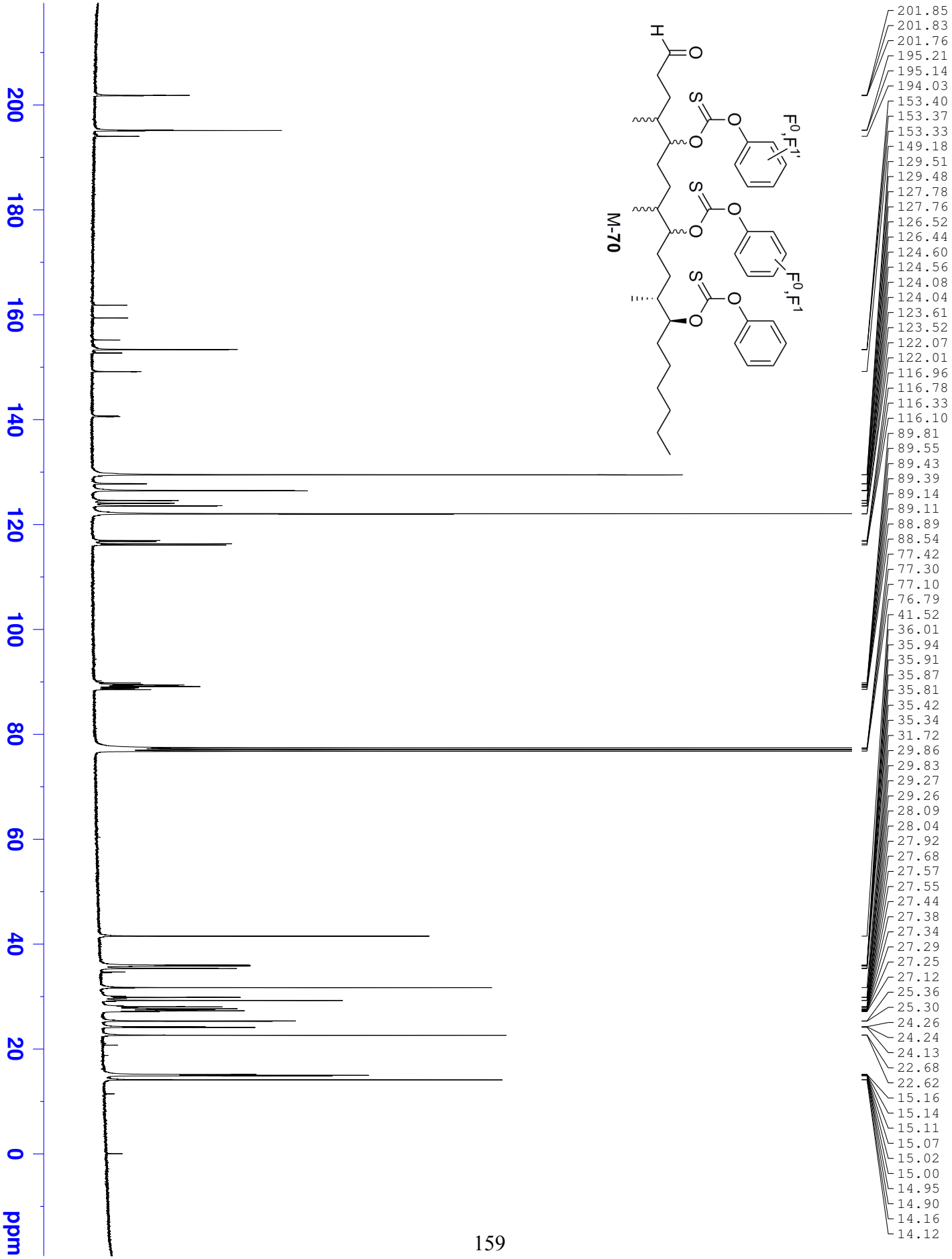
M-70
F0,F1'
F0,F1
ppm
200
180
160
140
120
100
80
60
40
20
0
201.85
201.83
201.76
195.21
195.14
194.03
153.40
153.37
153.33
149.18
129.51
129.48
127.78
127.76
126.52
126.44
124.60
124.56
124.08
124.04
123.61
123.52
122.07
122.01
116.96
116.78
116.33
116.10
89.81
89.55
89.43
89.39
89.14
89.11
88.89
88.54
77.42
77.30
77.10
76.79
41.52
36.01
35.94
35.91
35.87
35.81
35.42
35.34
31.72
29.86
29.83
29.27
29.26
28.09
28.04
27.92
27.68
27.57
27.55
27.44
27.38
27.34
27.29
27.25
27.12
25.36
25.30
24.26
24.24
24.13
22.68
22.62
15.16
15.14
15.11
15.07
15.02
15.00
14.95
14.90
14.16
14.12

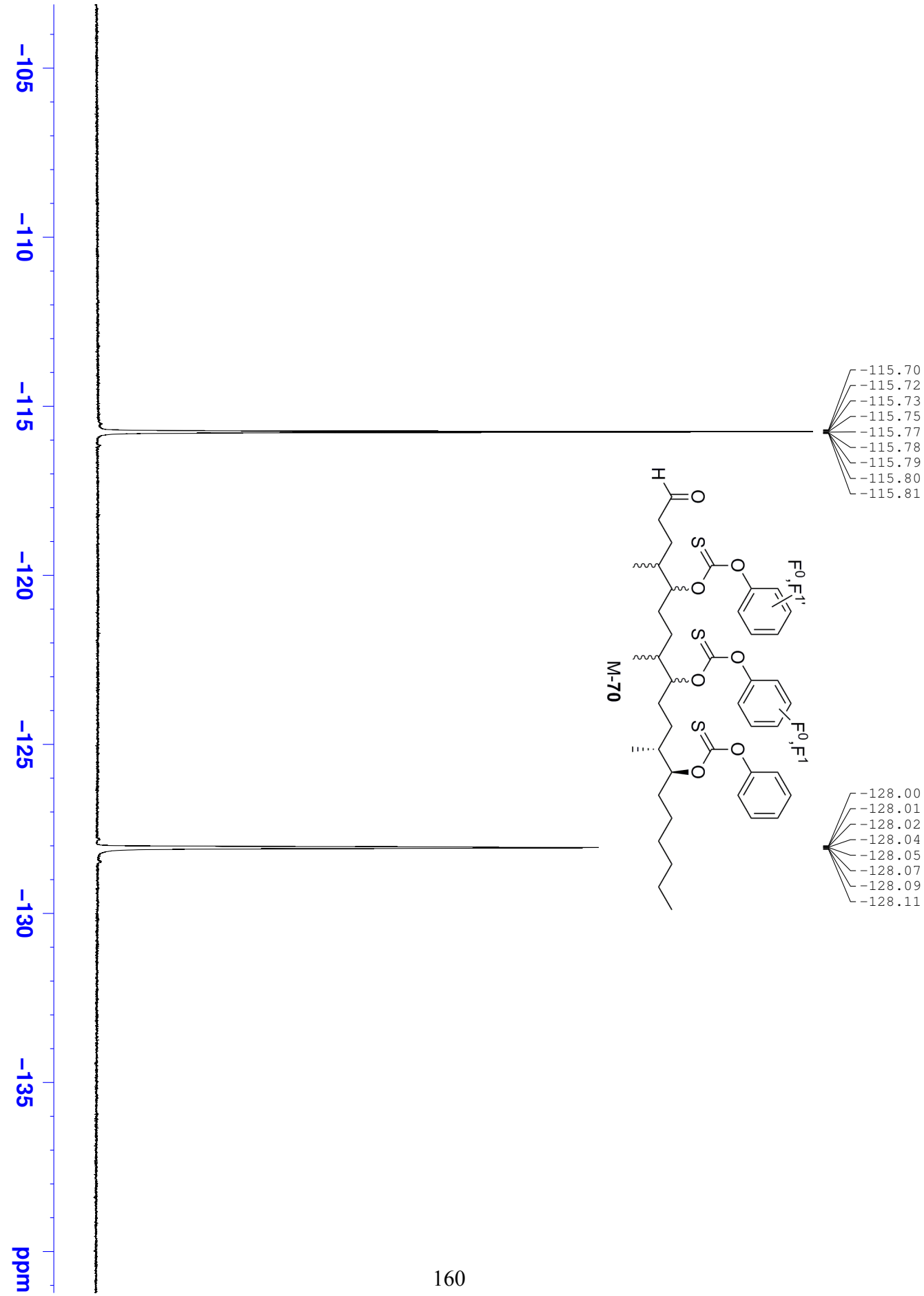
-105
-110
-115
-120
-125
-130
-135
ppm
-115.70
-115.72
-115.73
-115.75
-115.77
-115.78
-115.79
-115.80
-115.81
-128.00
-128.01
-128.02
-128.04
-128.05
-128.07
-128.09
-128.11
M-70
F0,F1'
F0,F1

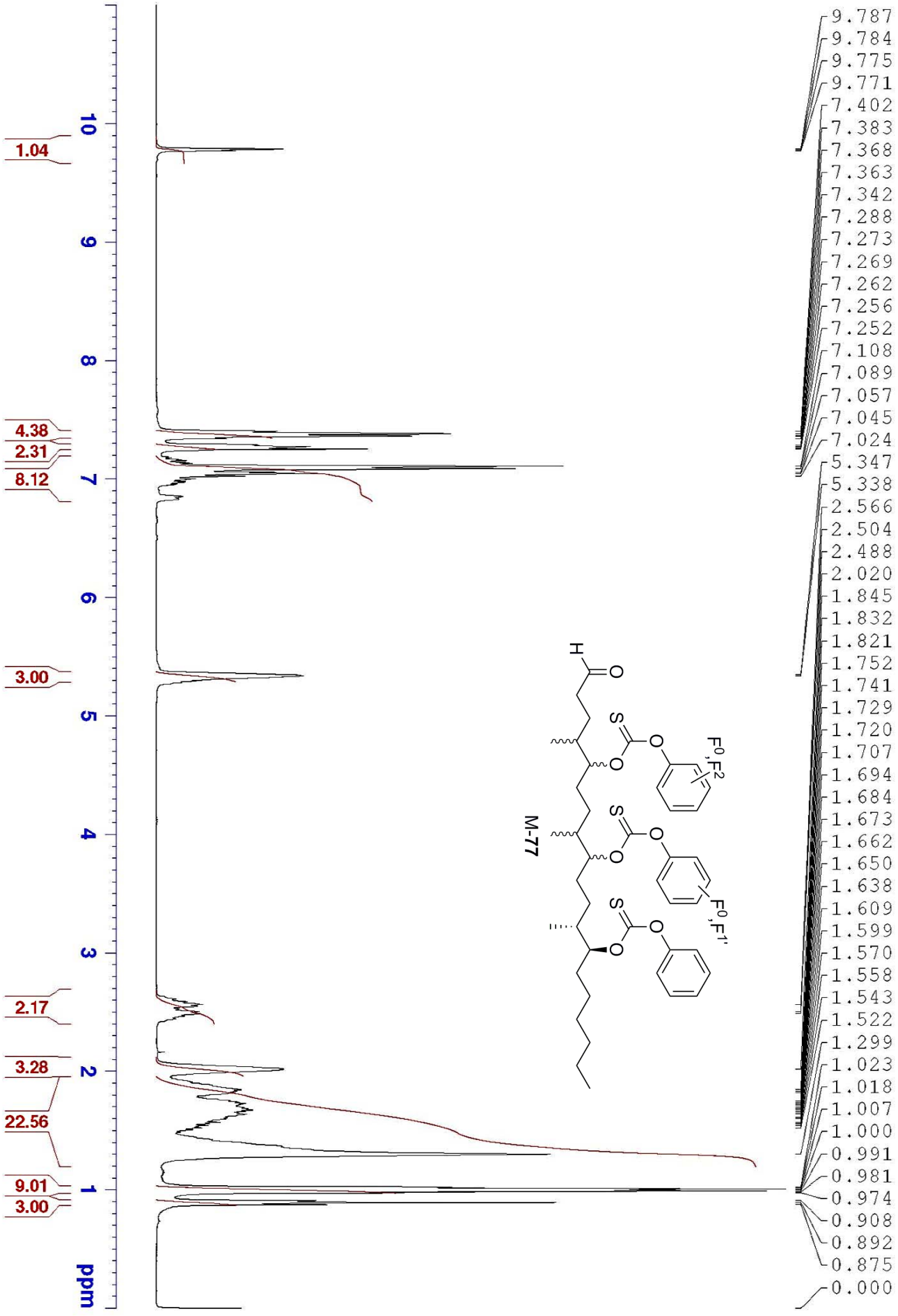
9.787
9.784
9.775
9.771
7.402
7.383
7.368
7.363
7.342
7.288
7.273
7.269
7.262
7.256
7.252
7.108
7.089
7.057
7.045
7.024
5.347
5.338
2.566
2.504
2.488
2.020
1.845
1.832
1.821
1.752
1.741
1.729
1.720
1.707
1.694
1.684
1.673
1.662
1.650
1.638
1.609
1.599
1.570
1.558
1.543
1.522
1.299
1.023
1.018
1.007
1.000
0.991
0.981
0.974
0.908
0.892
0.875
0.000
1.04
4.38
2.31
8.12
3.00
2.17
3.28
22.56
9.01
3.00
ppm
M-77
F0,F2
F0,F1'

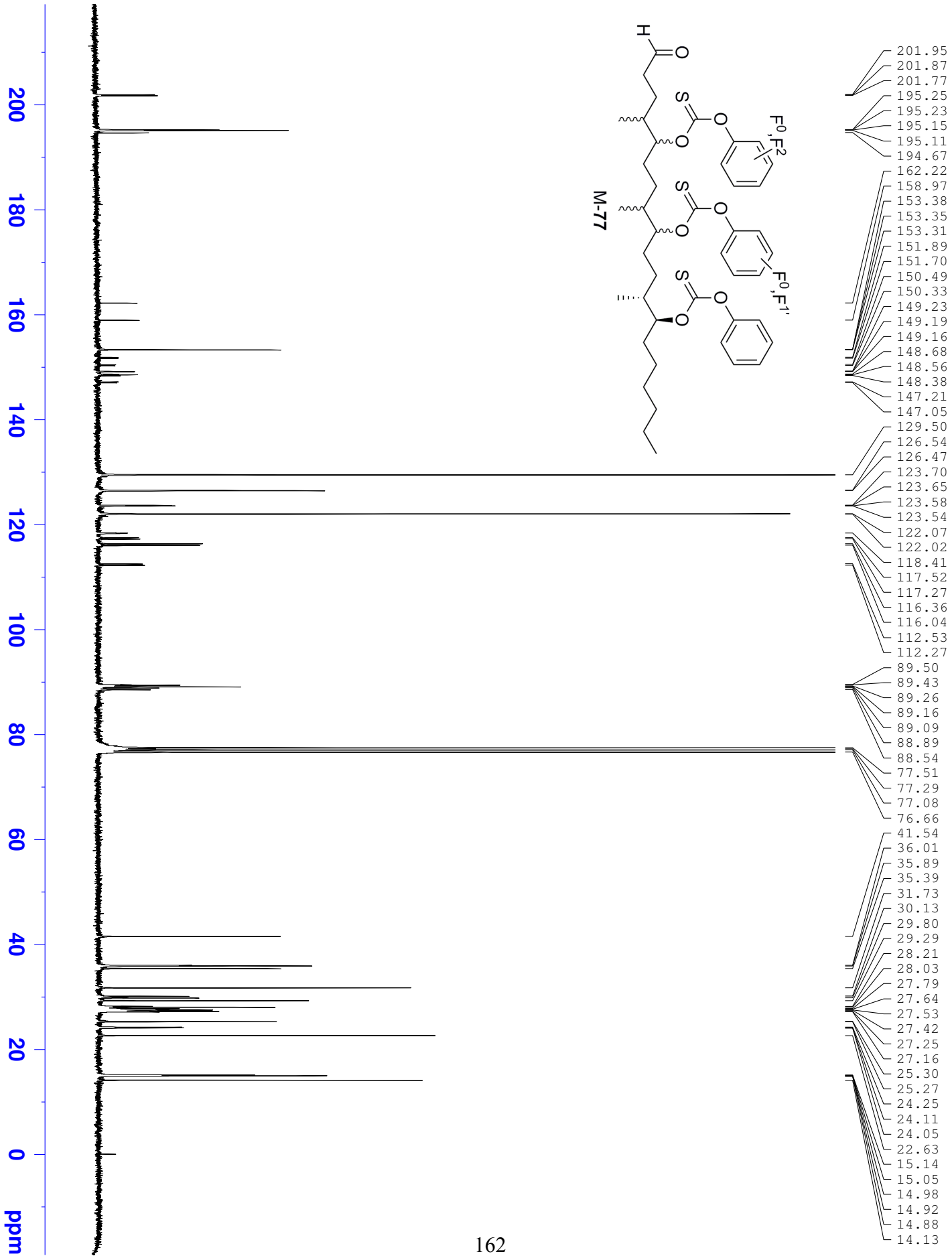
M-77
F0,F2
F0,F1'
201.95
201.87
201.77
195.25
195.23
195.15
195.11
194.67
162.22
158.97
153.38
153.35
153.31
151.89
151.70
150.49
150.33
149.23
149.19
149.16
148.68
148.56
148.38
147.21
147.05
129.50
126.54
126.47
123.70
123.65
123.58
123.54
122.07
122.02
118.41
117.52
117.27
116.36
116.04
112.53
112.27
89.50
89.43
89.26
89.16
89.09
88.89
88.54
77.51
77.29
77.08
76.66
41.54
36.01
35.89
35.39
31.73
30.13
29.80
29.29
28.21
28.03
27.79
27.64
27.53
27.42
27.25
27.16
25.30
25.27
24.25
24.11
24.05
22.63
15.14
15.05
14.98
14.92
14.88
14.13
200
180
160
140
120
100
80
60
40
20
0
ppm

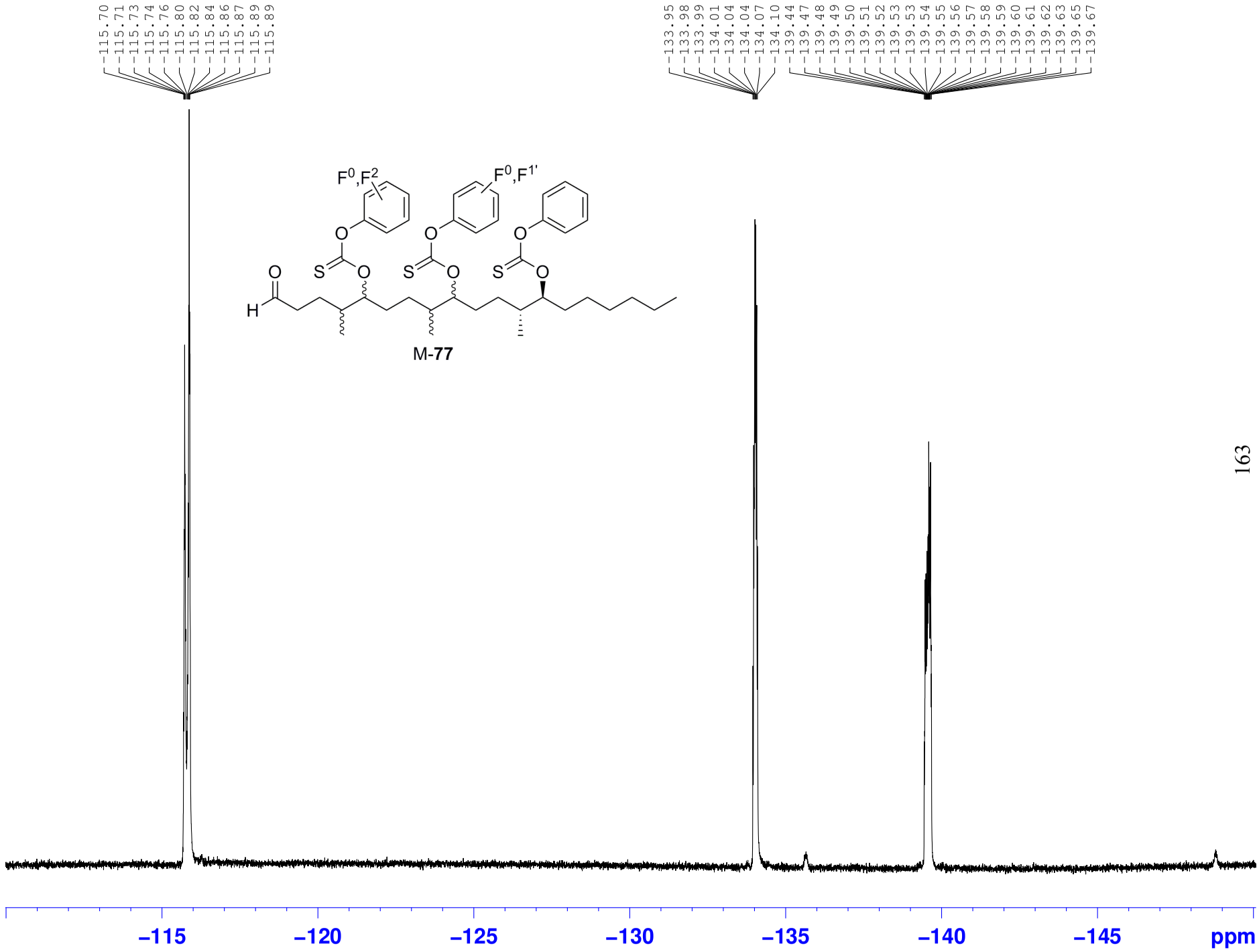
-115.70
-115.71
-115.73
-115.74
-115.76
-115.80
-115.82
-115.84
-115.86
-115.87
-115.89
-115.89
-133.95
-133.98
-133.99
-134.01
-134.04
-134.04
-134.07
-134.10
-139.44
-139.47
-139.48
-139.49
-139.50
-139.51
-139.52
-139.53
-139.53
-139.54
-139.55
-139.56
-139.57
-139.58
-139.59
-139.60
-139.61
-139.62
-139.63
-139.65
-139.67
F0,F2
F0,F1'
O
S
H
M-77
163
−115
−120
−125
−130
−135
−140
−145
ppm

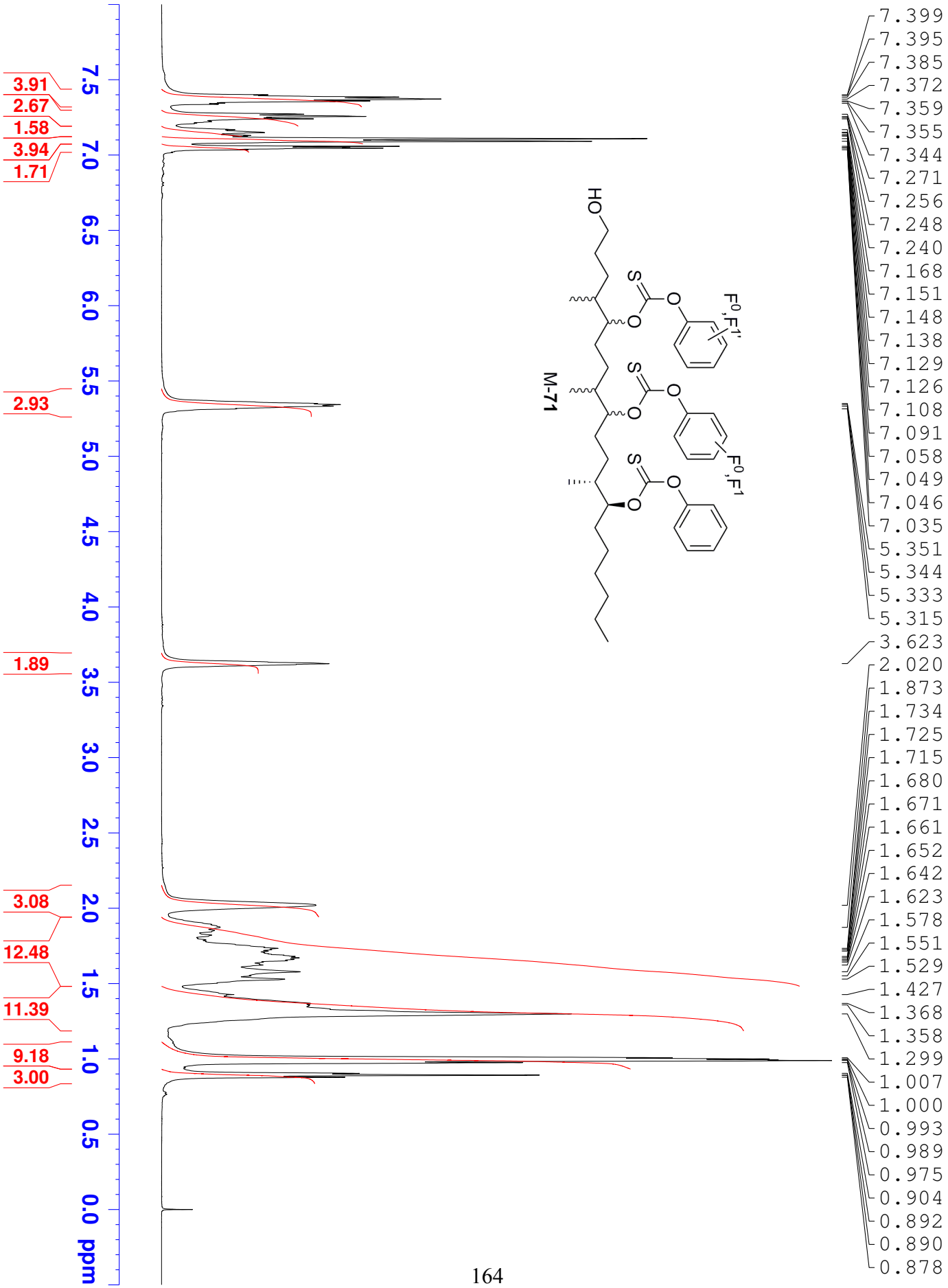
3.91
2.67
1.58
3.94
1.71
2.93
1.89
3.08
12.48
11.39
9.18
3.00
7.5
7.0
6.5
6.0
5.5
5.0
4.5
4.0
3.5
3.0
2.5
2.0
1.5
1.0
0.5
0.0
ppm
HO
S
O
F0,F1'
F0,F1
M-71
7.399
7.395
7.385
7.372
7.359
7.355
7.344
7.271
7.256
7.248
7.240
7.168
7.151
7.148
7.138
7.129
7.126
7.108
7.091
7.058
7.049
7.046
7.035
5.351
5.344
5.333
5.315
3.623
2.020
1.873
1.734
1.725
1.715
1.680
1.671
1.661
1.652
1.642
1.623
1.578
1.551
1.529
1.427
1.368
1.358
1.299
1.007
1.000
0.993
0.989
0.975
0.904
0.892
0.890
0.878

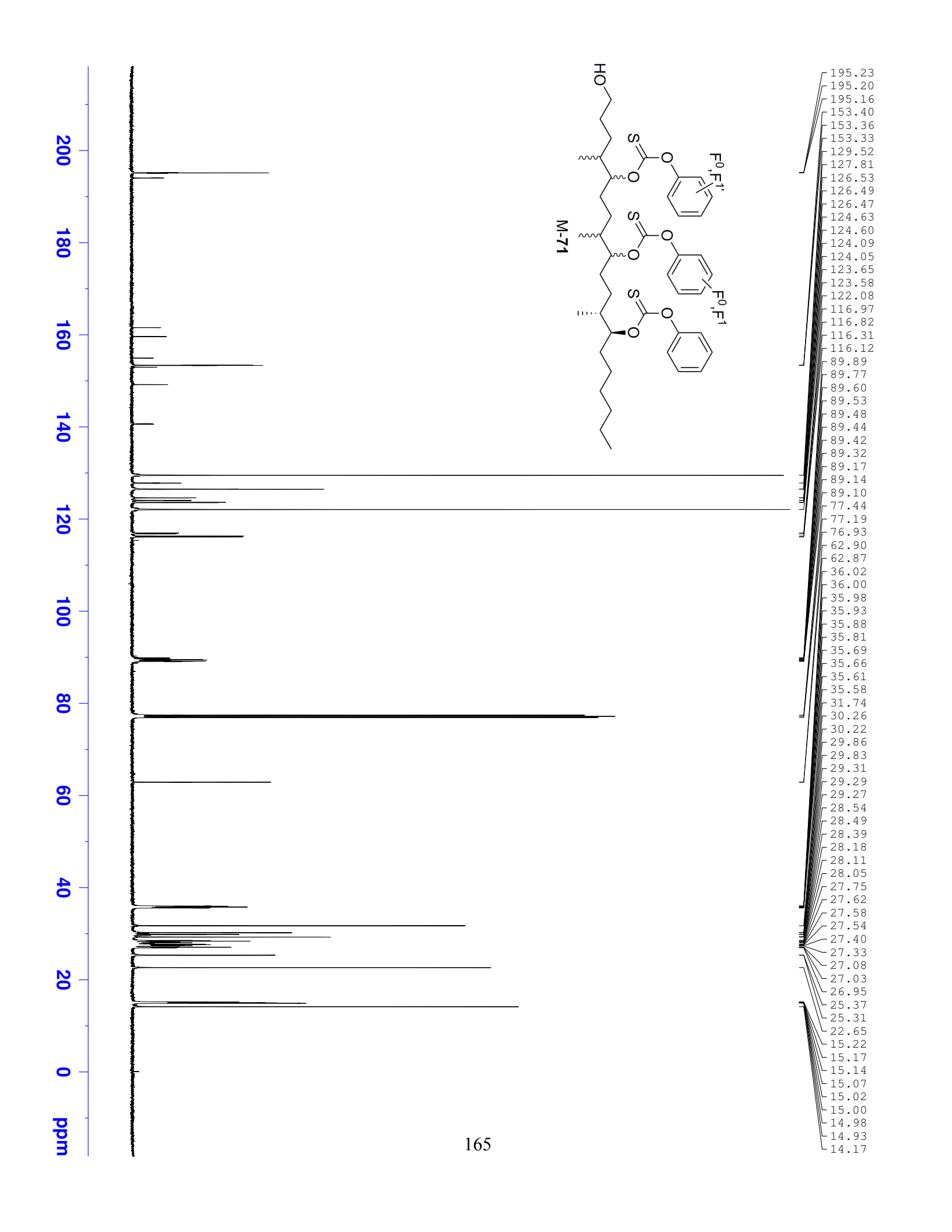
200
180
160
140
120
100
80
60
40
20
0
ppm
HO
S
O
F0,F1'
F0,F1
M-71
195.23
195.20
195.16
153.40
153.36
153.33
129.52
127.81
126.53
126.49
126.47
124.63
124.60
124.09
124.05
123.65
123.58
122.08
116.97
116.82
116.31
116.12
89.89
89.77
89.60
89.53
89.48
89.44
89.42
89.32
89.17
89.14
89.10
77.44
77.19
76.93
62.90
62.87
36.02
36.00
35.98
35.93
35.88
35.81
35.69
35.66
35.61
35.58
31.74
30.26
30.22
29.86
29.83
29.31
29.29
29.27
28.54
28.49
28.39
28.18
28.11
28.05
27.75
27.62
27.58
27.54
27.40
27.33
27.08
27.03
26.95
25.37
25.31
22.65
15.22
15.17
15.14
15.07
15.02
15.00
14.98
14.93
14.17

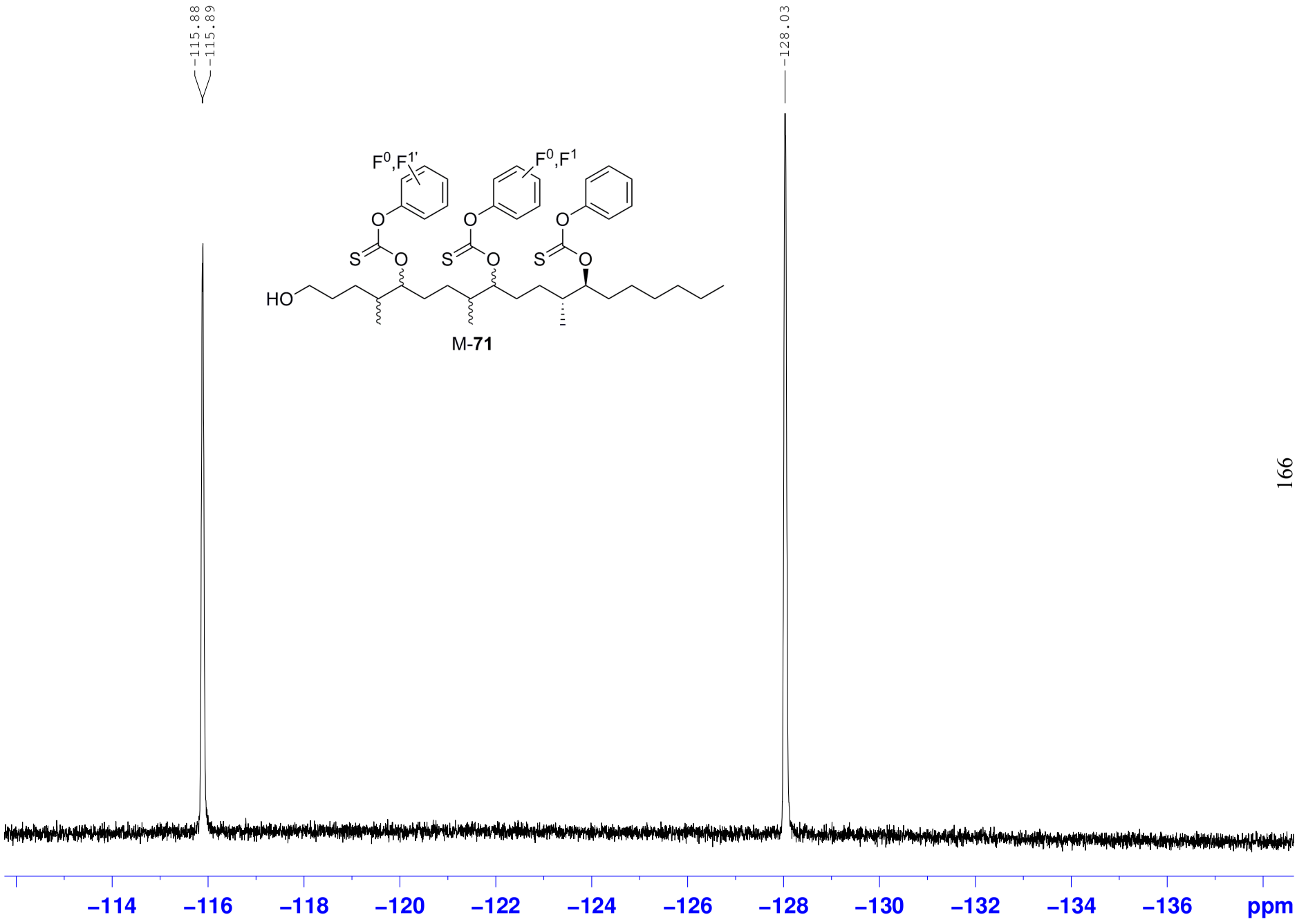
-115.88
-115.89
-128.03
F0,F1'
F0,F1
O
S
HO
M-71
−114
−116
−118
−120
−122
−124
−126
−128
−130
−132
−134
−136
ppm

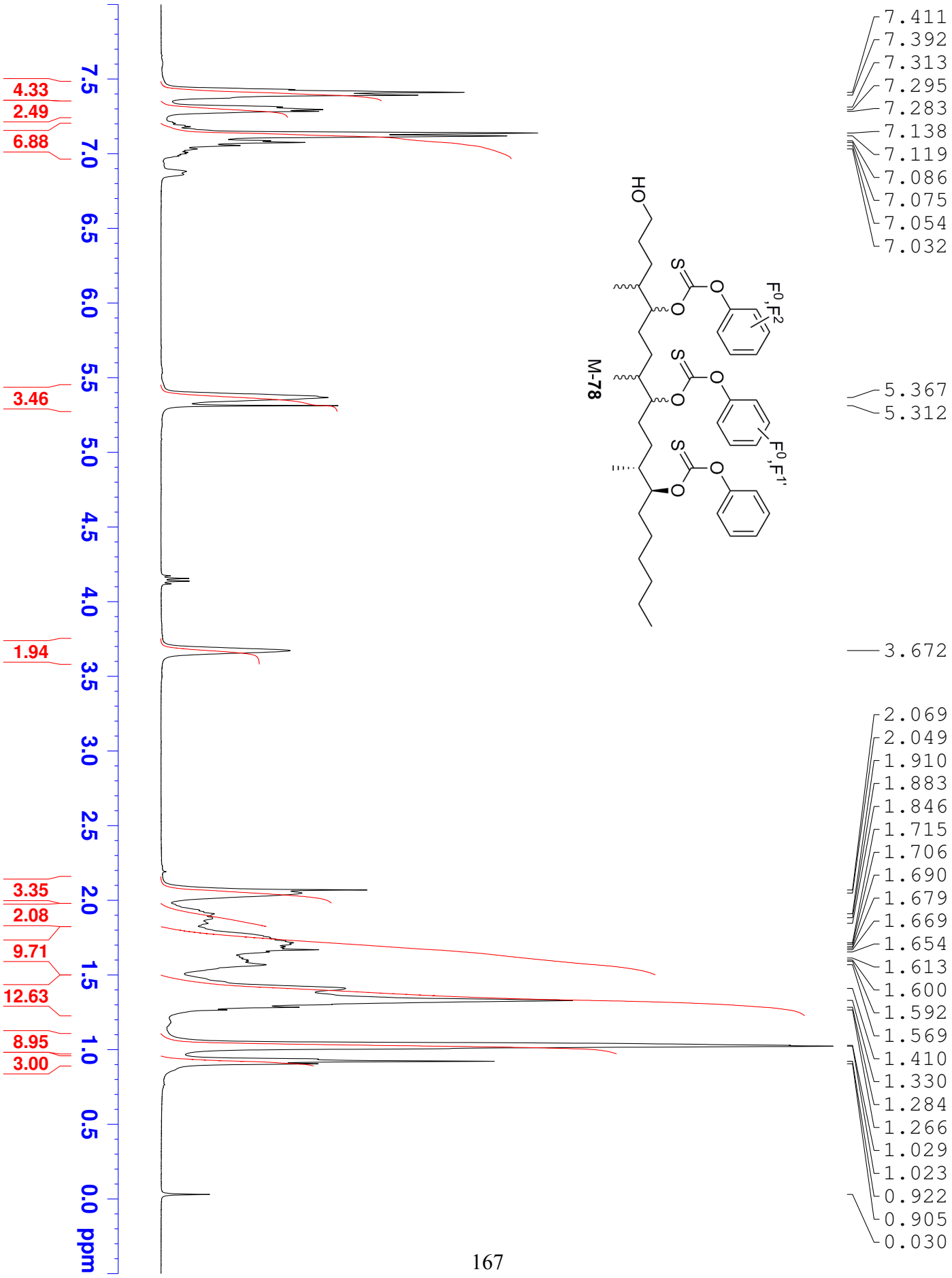
4.33
2.49
6.88
3.46
1.94
3.35
2.08
9.71
12.63
8.95
3.00
7.5
7.0
6.5
6.0
5.5
5.0
4.5
4.0
3.5
3.0
2.5
2.0
1.5
1.0
0.5
0.0
ppm
HO
S
O
F0,F2
F0,F1'
M-78
7.411
7.392
7.313
7.295
7.283
7.138
7.119
7.086
7.075
7.054
7.032
5.367
5.312
3.672
2.069
2.049
1.910
1.883
1.846
1.715
1.706
1.690
1.679
1.669
1.654
1.613
1.600
1.592
1.569
1.410
1.330
1.284
1.266
1.029
1.023
0.922
0.905
0.030

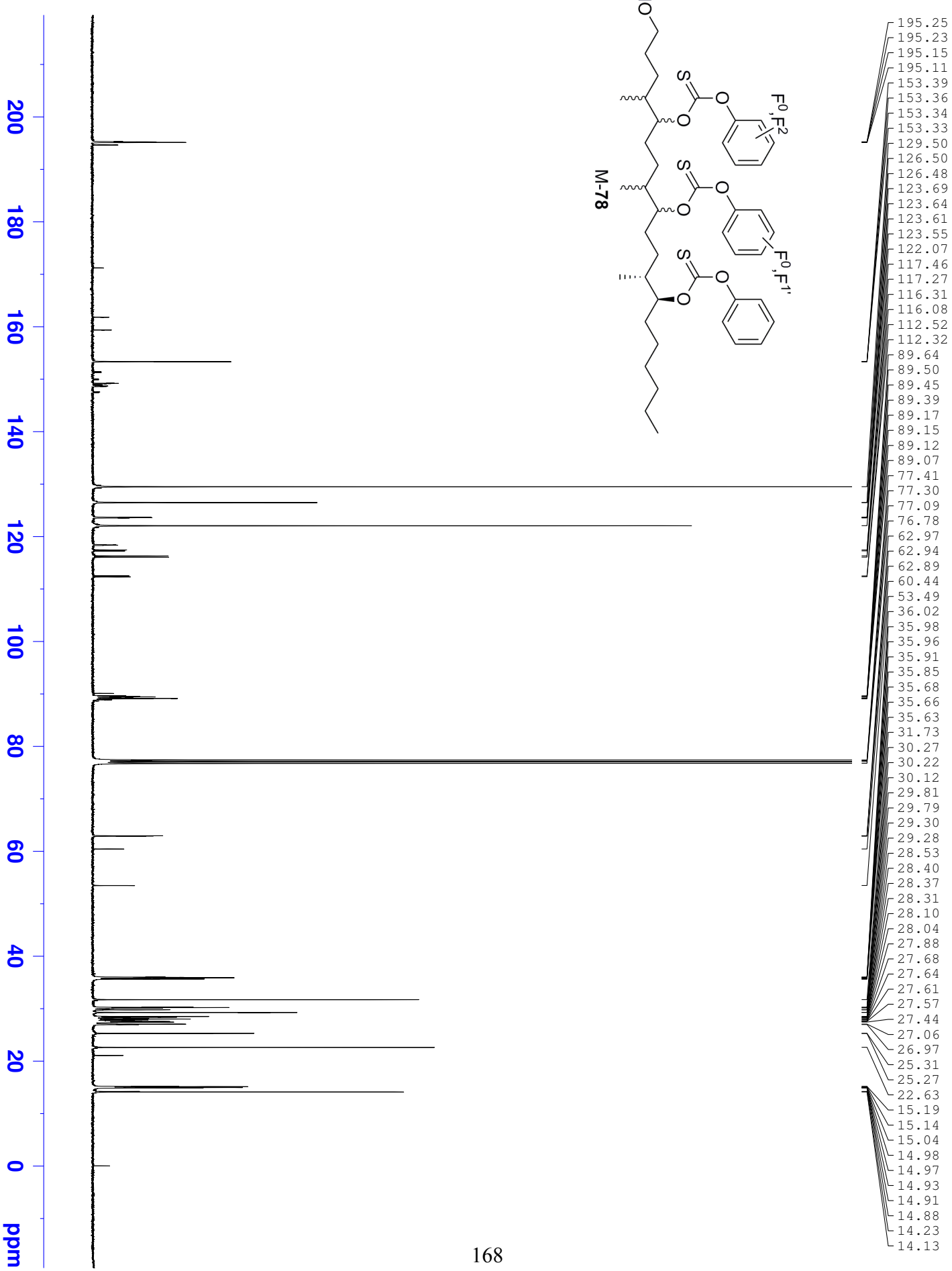
HO
S
O
O
F0,F2
F0,F1'
M-78
195.25
195.23
195.15
195.11
153.39
153.36
153.34
153.33
129.50
126.50
126.48
123.69
123.64
123.61
123.55
122.07
117.46
117.27
116.31
116.08
112.52
112.32
89.64
89.50
89.45
89.39
89.17
89.15
89.12
89.07
77.41
77.30
77.09
76.78
62.97
62.94
62.89
60.44
53.49
36.02
35.98
35.96
35.91
35.85
35.68
35.66
35.63
31.73
30.27
30.22
30.12
29.81
29.79
29.30
29.28
28.53
28.40
28.37
28.31
28.10
28.04
27.88
27.68
27.64
27.61
27.57
27.44
27.06
26.97
25.31
25.27
22.63
15.19
15.14
15.04
14.98
14.97
14.93
14.91
14.88
14.23
14.13
200
180
160
140
120
100
80
60
40
20
0
ppm

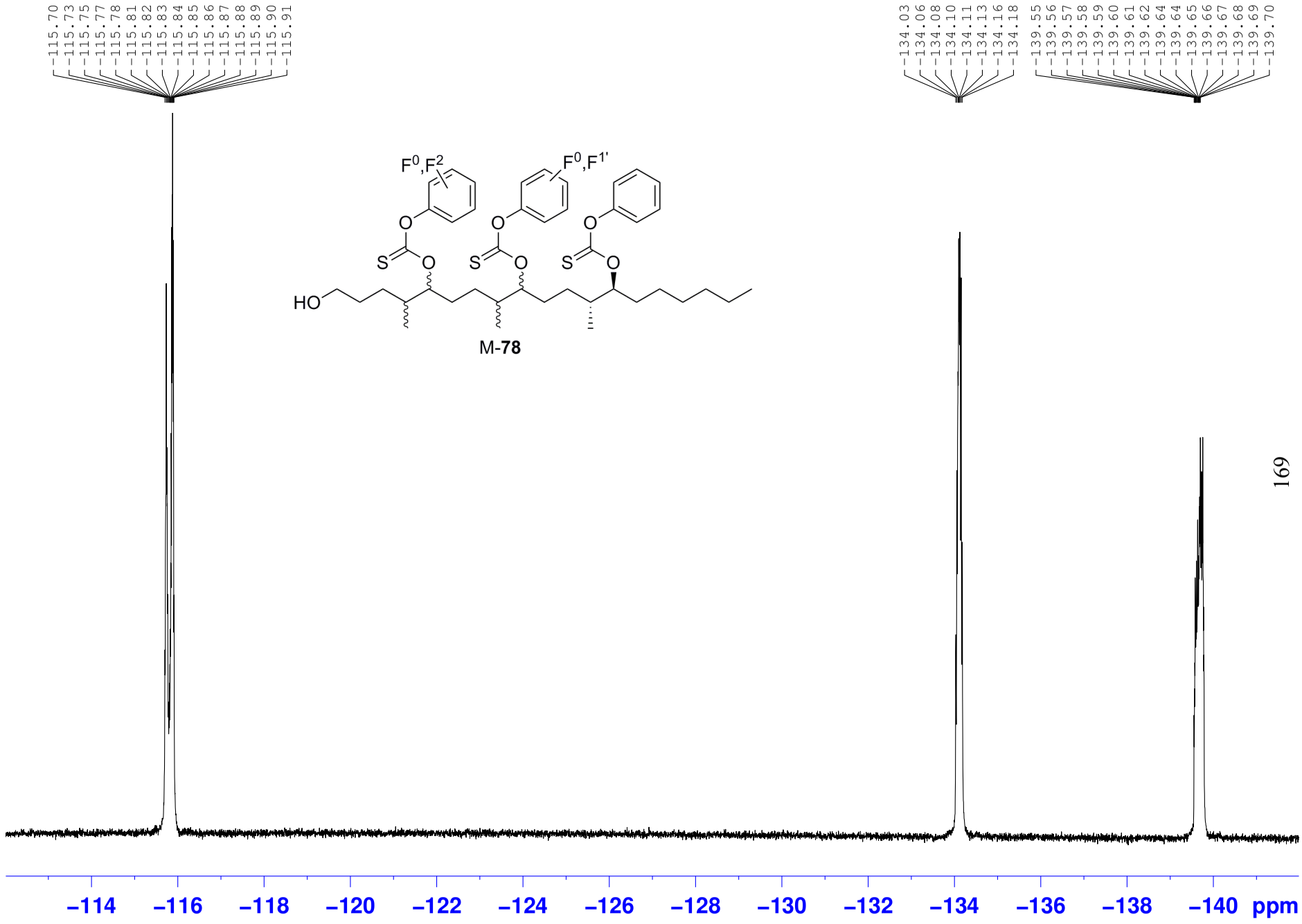
-115.70
-115.73
-115.75
-115.77
-115.78
-115.81
-115.82
-115.83
-115.84
-115.85
-115.86
-115.87
-115.88
-115.89
-115.90
-115.91
-134.03
-134.06
-134.08
-134.10
-134.11
-134.13
-134.16
-134.18
-139.55
-139.56
-139.57
-139.58
-139.59
-139.60
-139.61
-139.62
-139.64
-139.64
-139.65
-139.66
-139.67
-139.68
-139.69
-139.70
F0,F2
F0,F1'
O
S
HO
M-78
169
−114
−116
−118
−120
−122
−124
−126
−128
−130
−132
−134
−136
−138
−140
ppm

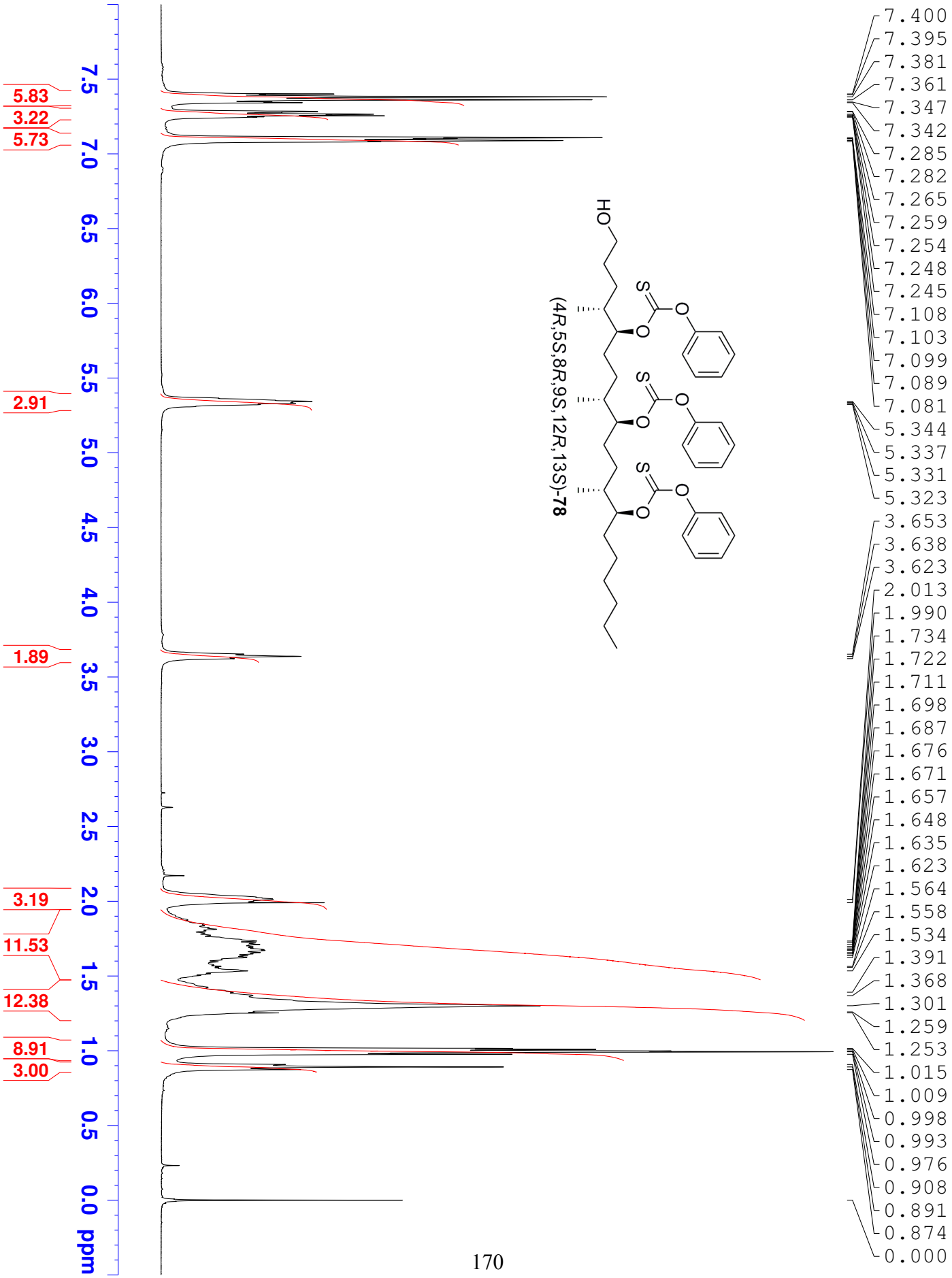
5.83
3.22
5.73
2.91
1.89
3.19
11.53
12.38
8.91
3.00
7.5
7.0
6.5
6.0
5.5
5.0
4.5
4.0
3.5
3.0
2.5
2.0
1.5
1.0
0.5
0.0
ppm
HO
S
O
(4R,5S,8R,9S,12R,13S)-78
7.400
7.395
7.381
7.361
7.347
7.342
7.285
7.282
7.265
7.259
7.254
7.248
7.245
7.108
7.103
7.099
7.089
7.081
5.344
5.337
5.331
5.323
3.653
3.638
3.623
2.013
1.990
1.734
1.722
1.711
1.698
1.687
1.676
1.671
1.657
1.648
1.635
1.623
1.564
1.558
1.534
1.391
1.368
1.301
1.259
1.253
1.015
1.009
0.998
0.993
0.976
0.908
0.891
0.874
0.000

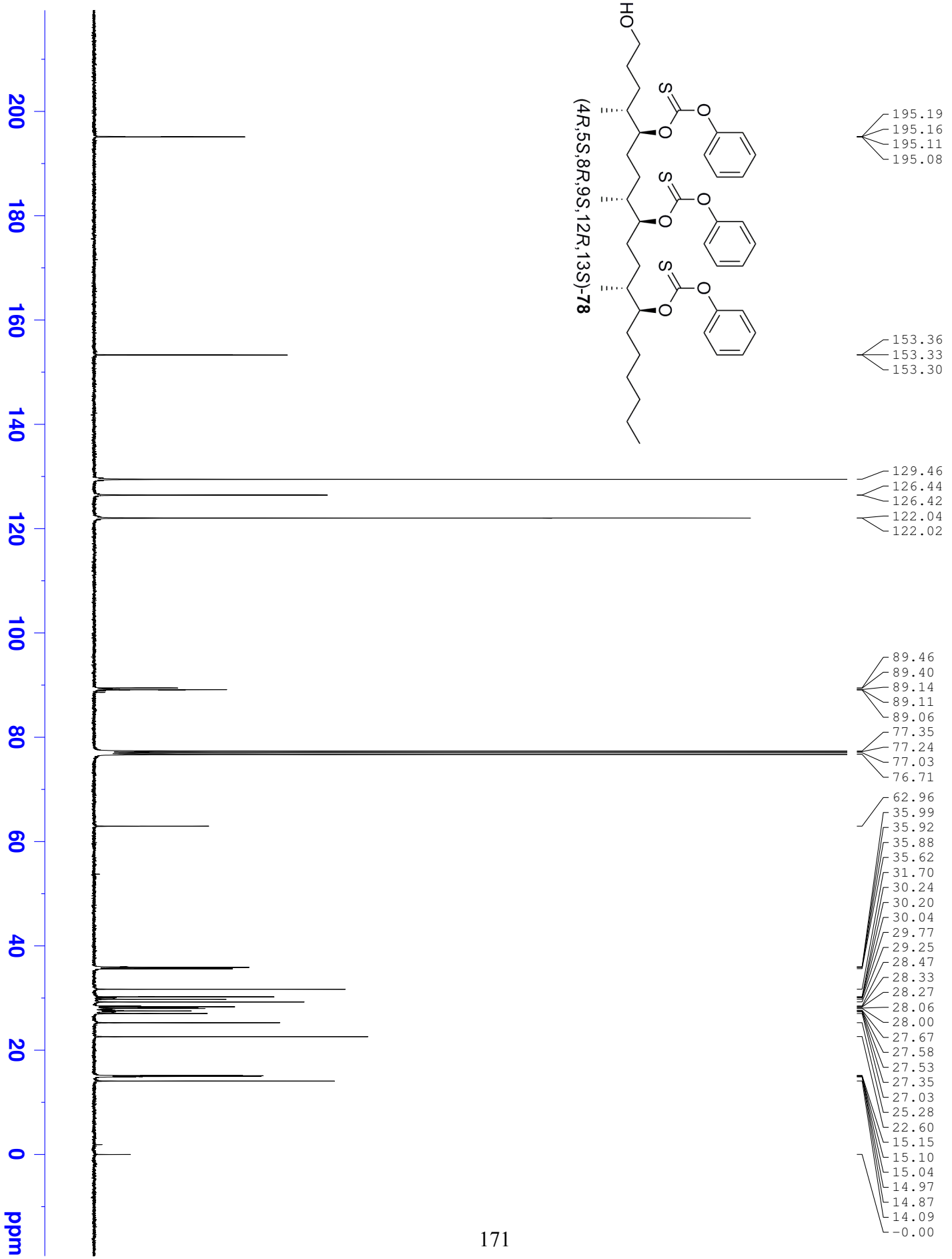
(4R,5S,8R,9S,12R,13S)-78
HO
S
O
195.19
195.16
195.11
195.08
153.36
153.33
153.30
129.46
126.44
126.42
122.04
122.02
89.46
89.40
89.14
89.11
89.06
77.35
77.24
77.03
76.71
62.96
35.99
35.92
35.88
35.62
31.70
30.24
30.20
30.04
29.77
29.25
28.47
28.33
28.27
28.06
28.00
27.67
27.58
27.53
27.35
27.03
25.28
22.60
15.15
15.10
15.04
14.97
14.87
14.09
-0.00
200
180
160
140
120
100
80
60
40
20
0
ppm

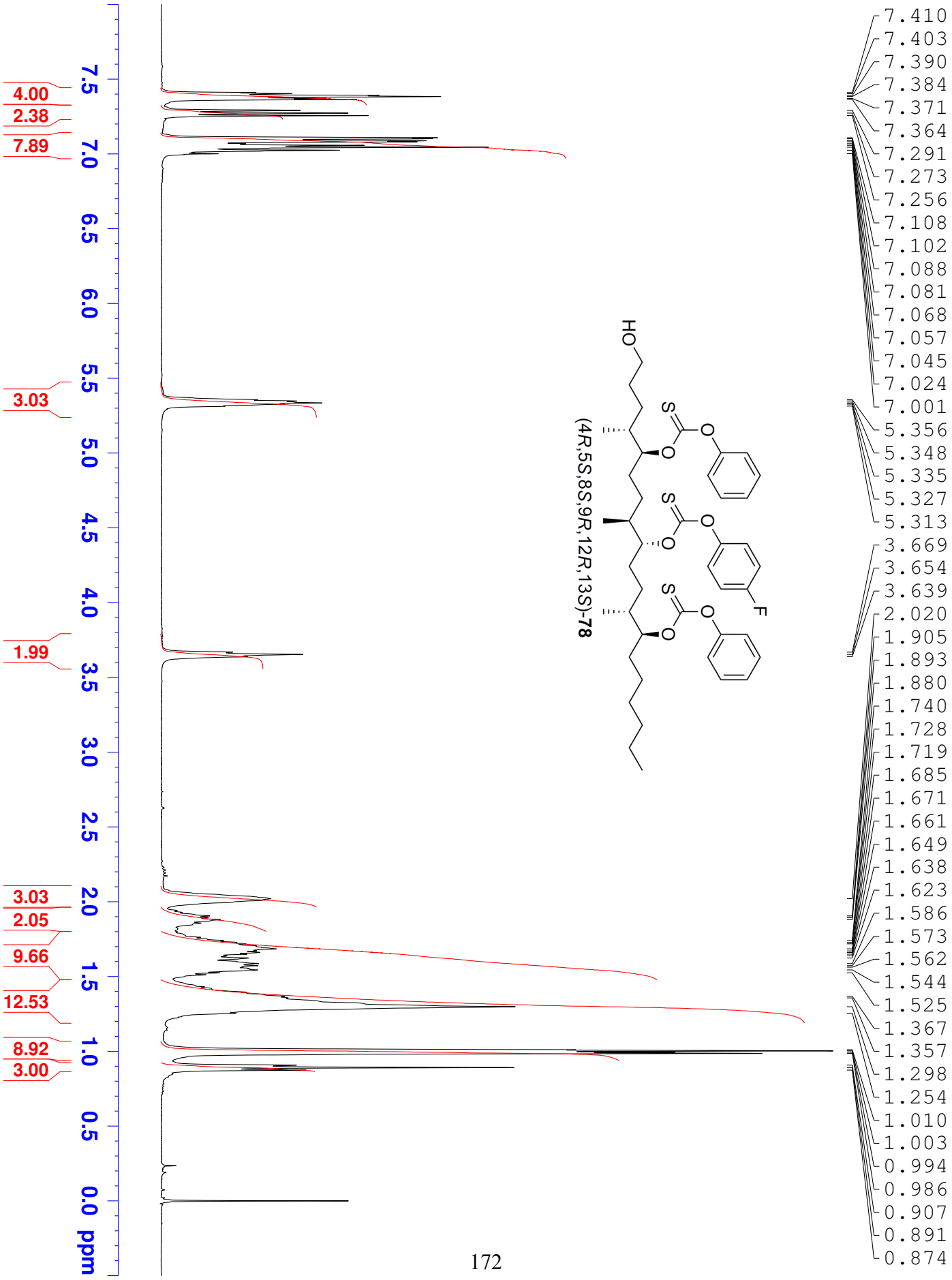
7.410
7.403
7.390
7.384
7.371
7.364
7.291
7.273
7.256
7.108
7.102
7.088
7.081
7.068
7.057
7.045
7.024
7.001
5.356
5.348
5.335
5.327
5.313
3.669
3.654
3.639
2.020
1.905
1.893
1.880
1.740
1.728
1.719
1.685
1.671
1.661
1.649
1.638
1.623
1.586
1.573
1.562
1.544
1.525
1.367
1.357
1.298
1.254
1.010
1.003
0.994
0.986
0.907
0.891
0.874
4.00
2.38
7.89
3.03
1.99
3.03
2.05
9.66
12.53
8.92
3.00
7.5
7.0
6.5
6.0
5.5
5.0
4.5
4.0
3.5
3.0
2.5
2.0
1.5
1.0
0.5
0.0
ppm
HO
S
O
O
S
O
O
S
O
O
F
(4R,5S,8S,9R,12R,13S)-78

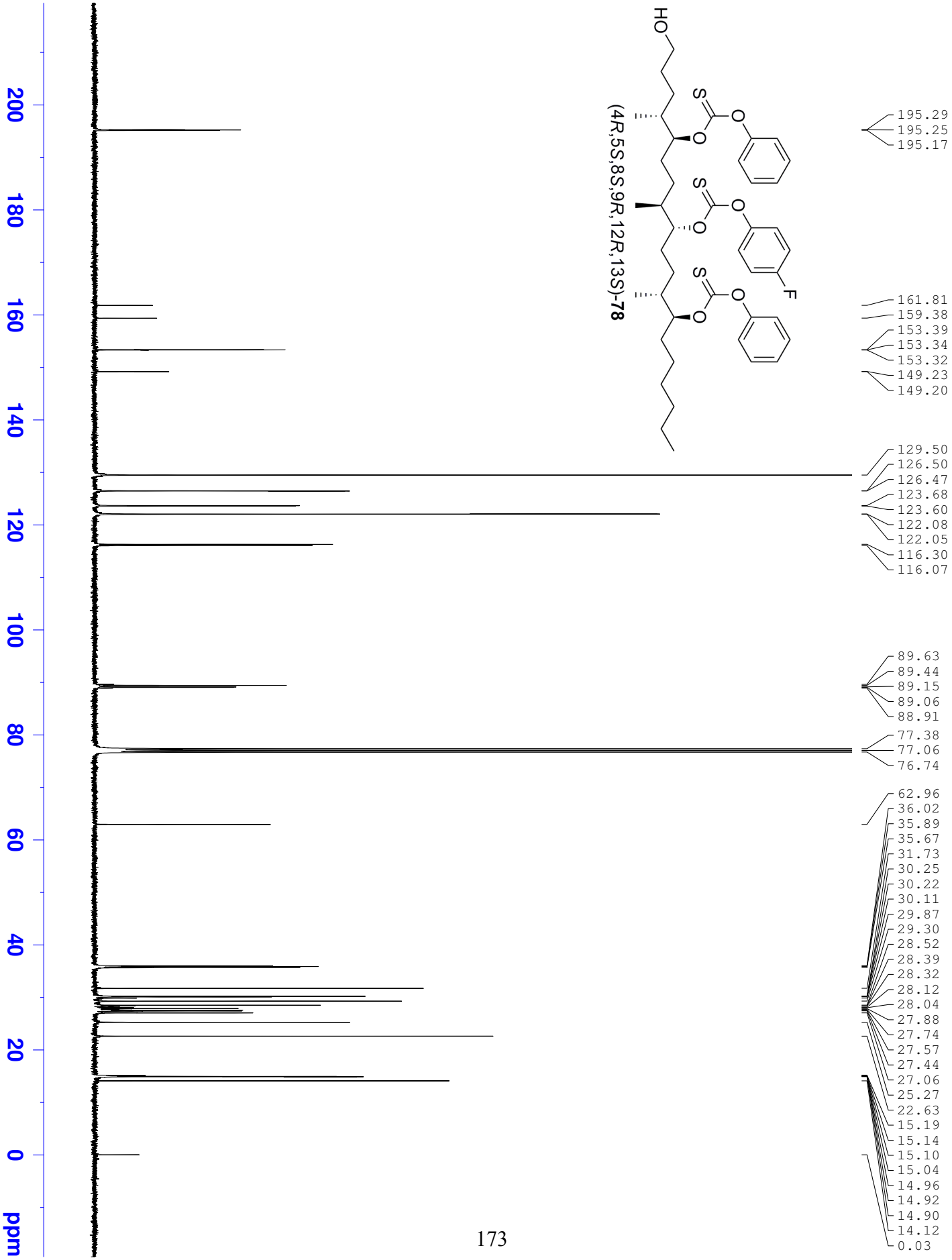
HO
S
O
O
S
O
O
S
O
O
F
(4R,5S,8S,9R,12R,13S)-78
195.29
195.25
195.17
161.81
159.38
153.39
153.34
153.32
149.23
149.20
129.50
126.50
126.47
123.68
123.60
122.08
122.05
116.30
116.07
89.63
89.44
89.15
89.06
88.91
77.38
77.06
76.74
62.96
36.02
35.89
35.67
31.73
30.25
30.22
30.11
29.87
29.30
28.52
28.39
28.32
28.12
28.04
27.88
27.74
27.57
27.44
27.06
25.27
22.63
15.19
15.14
15.10
15.04
14.96
14.92
14.90
14.12
0.03
200
180
160
140
120
100
80
60
40
20
0
ppm

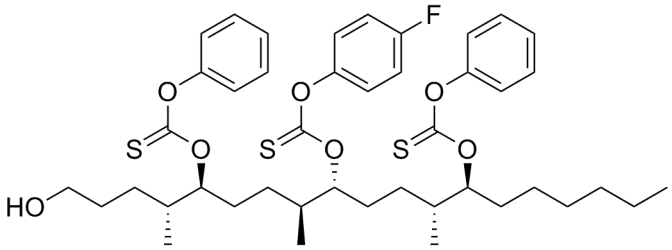

(4*R*,5*S*,8*S*,9*R*,12*R*,13*S*)-**78**

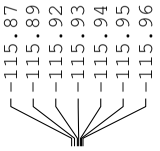

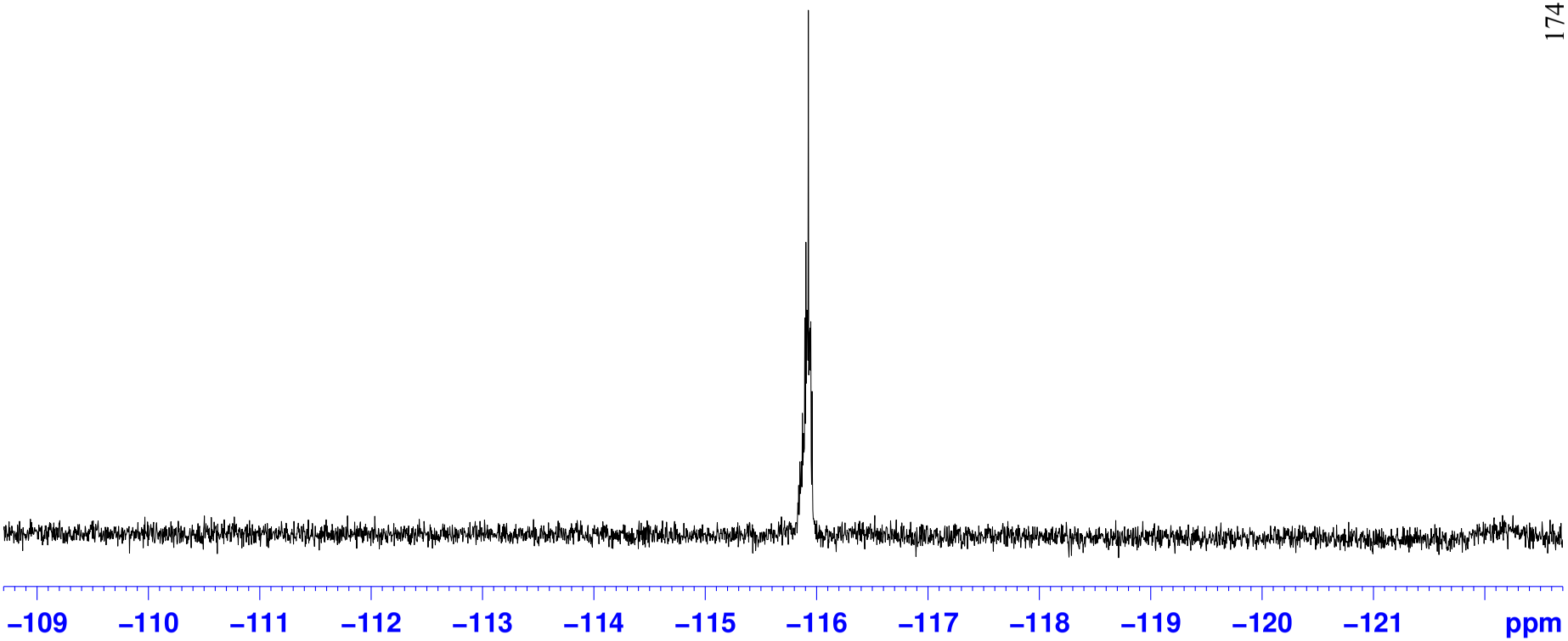

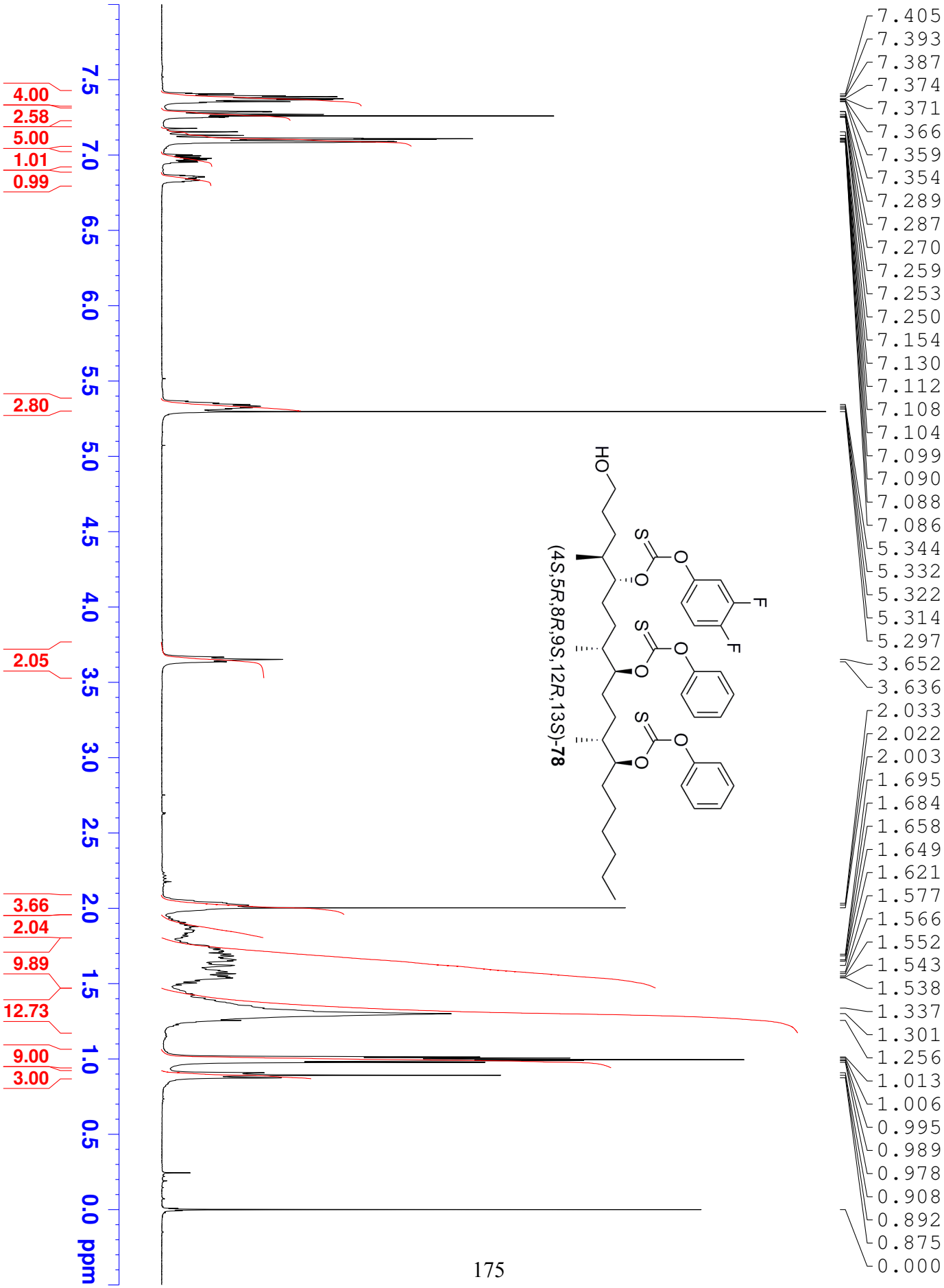
4.00
2.58
5.00
1.01
0.99
2.80
2.05
3.66
2.04
9.89
12.73
9.00
3.00
7.5
7.0
6.5
6.0
5.5
5.0
4.5
4.0
3.5
3.0
2.5
2.0
1.5
1.0
0.5
0.0
ppm
HO
S
O
F
(4S,5R,8R,9S,12R,13S)-78
7.405
7.393
7.387
7.374
7.371
7.366
7.359
7.354
7.289
7.287
7.270
7.259
7.253
7.250
7.154
7.130
7.112
7.108
7.104
7.099
7.090
7.088
7.086
5.344
5.332
5.322
5.314
5.297
3.652
3.636
2.033
2.022
2.003
1.695
1.684
1.658
1.649
1.621
1.577
1.566
1.552
1.543
1.538
1.337
1.301
1.256
1.013
1.006
0.995
0.989
0.978
0.908
0.892
0.875
0.000

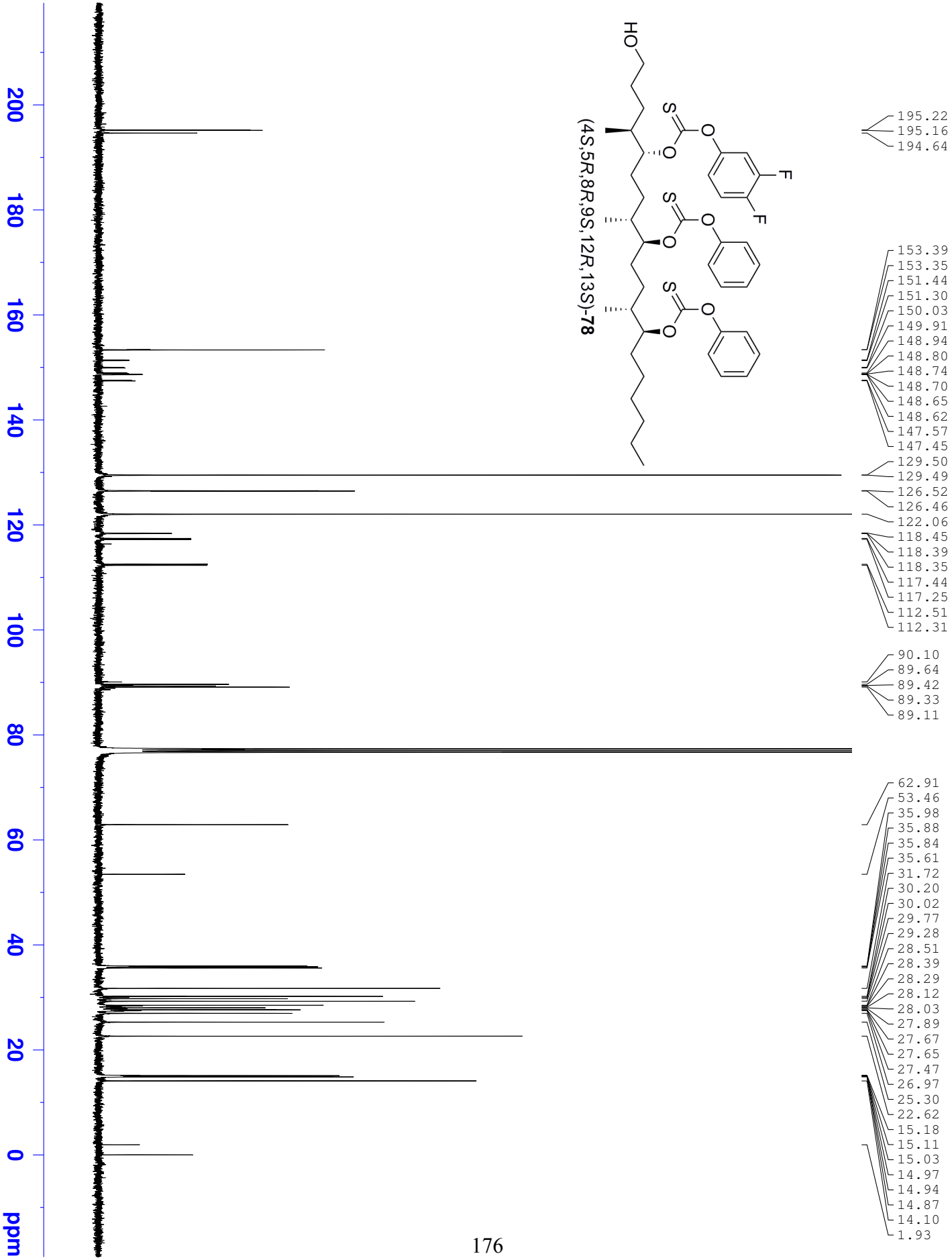
200
180
160
140
120
100
80
60
40
20
0
ppm
HO
S
O
O
F
F
(4S,5R,8R,9S,12R,13S)-78
195.22
195.16
194.64
153.39
153.35
151.44
151.30
150.03
149.91
148.94
148.80
148.74
148.70
148.65
148.62
147.57
147.45
129.50
129.49
126.52
126.46
122.06
118.45
118.39
118.35
117.44
117.25
112.51
112.31
90.10
89.64
89.42
89.33
89.11
62.91
53.46
35.98
35.88
35.84
35.61
31.72
30.20
30.02
29.77
29.28
28.51
28.39
28.29
28.12
28.03
27.89
27.67
27.65
27.47
26.97
25.30
22.62
15.18
15.11
15.03
14.97
14.94
14.87
14.10
1.93

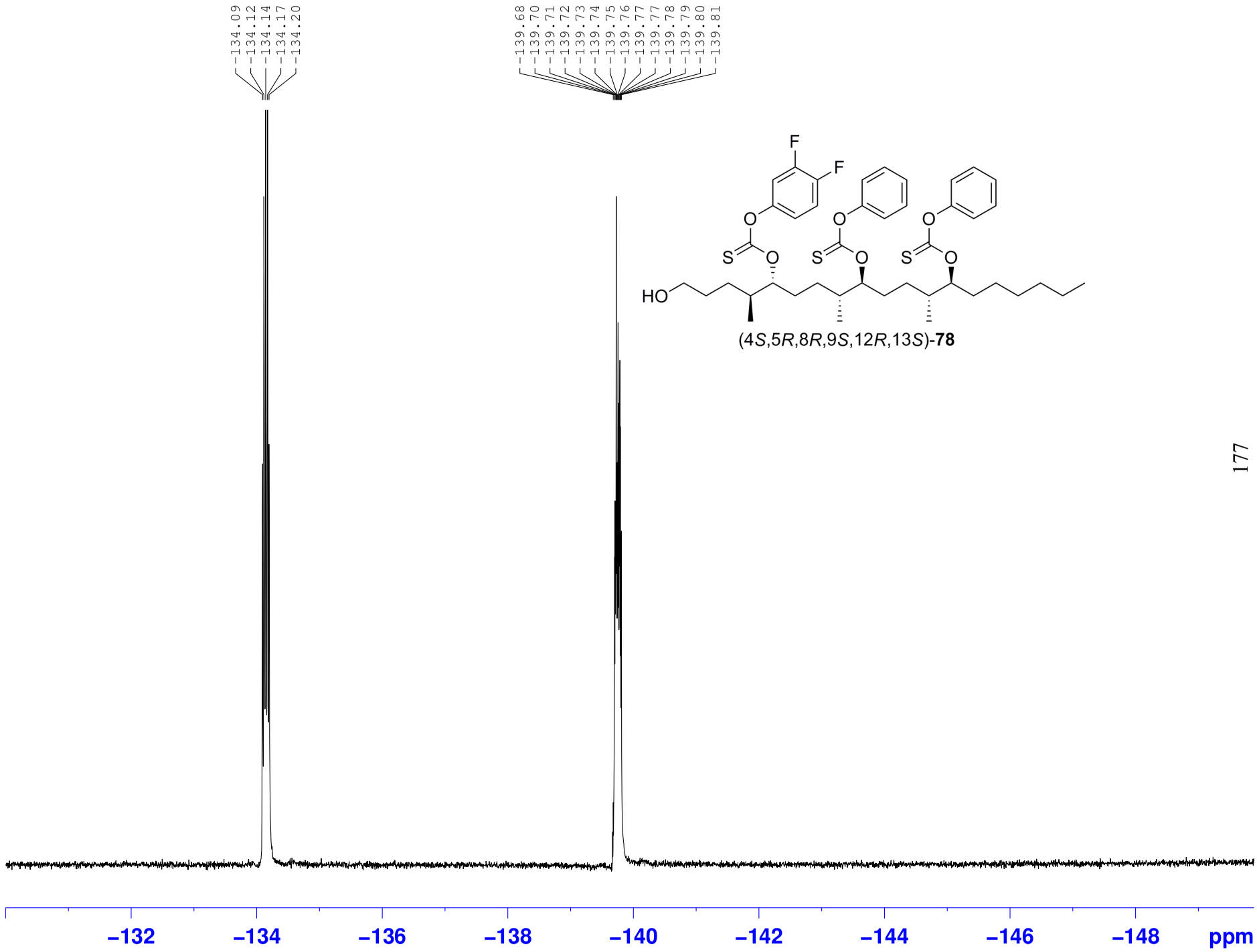
-134.09
-134.12
-134.14
-134.17
-134.20
-139.68
-139.70
-139.71
-139.72
-139.73
-139.74
-139.75
-139.76
-139.77
-139.77
-139.78
-139.79
-139.80
-139.81
F
F
O
S
O
HO
(4S,5R,8R,9S,12R,13S)-78
177
−132
−134
−136
−138
−140
−142
−144
−146
−148
ppm

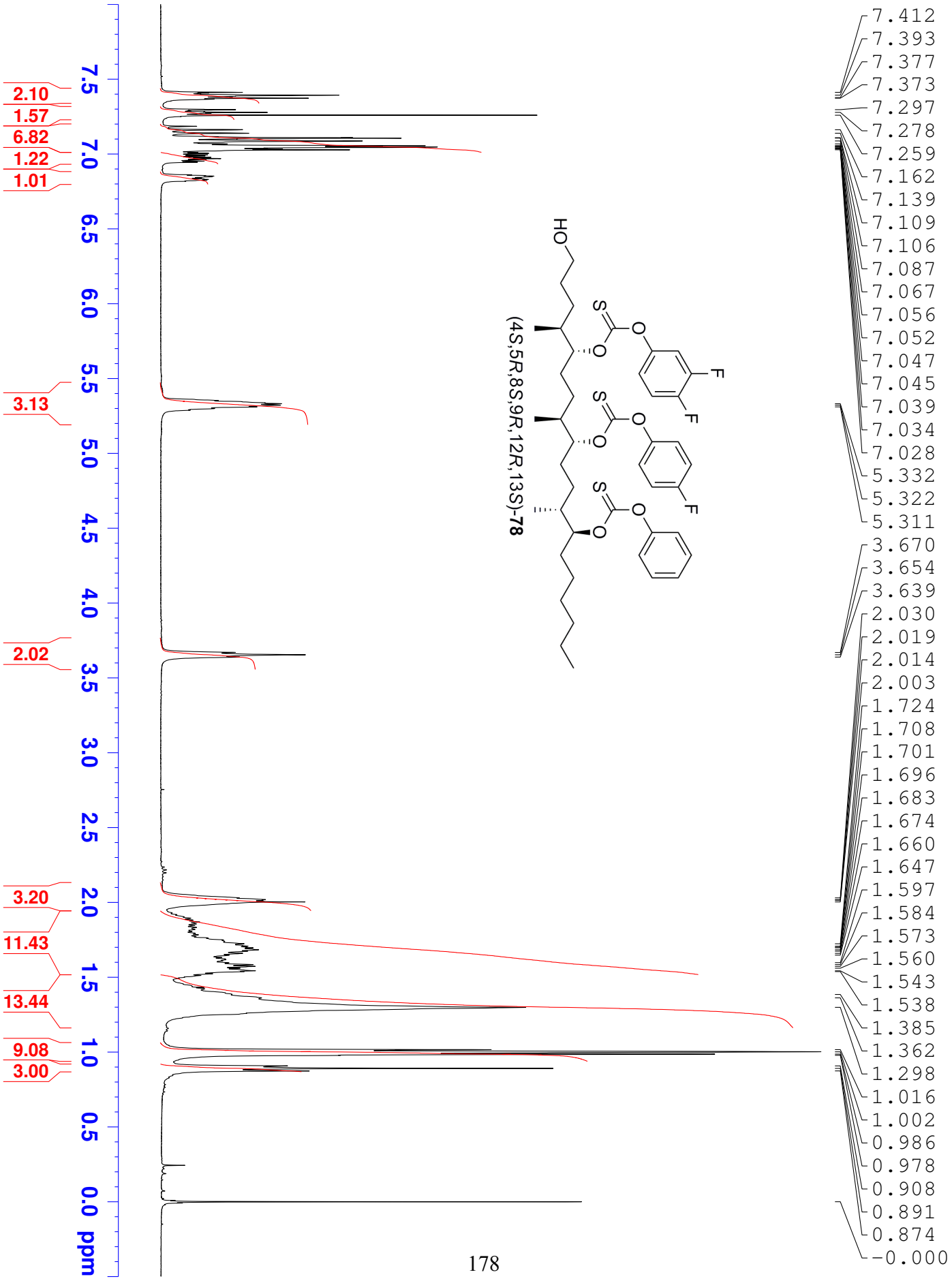
2.10
1.57
6.82
1.22
1.01
3.13
2.02
3.20
11.43
13.44
9.08
3.00
7.5
7.0
6.5
6.0
5.5
5.0
4.5
4.0
3.5
3.0
2.5
2.0
1.5
1.0
0.5
0.0
ppm
HO
O
S
O
O
F
F
F
(4S,5R,8S,9R,12R,13S)-78
7.412
7.393
7.377
7.373
7.297
7.278
7.259
7.162
7.139
7.109
7.106
7.087
7.067
7.056
7.052
7.047
7.045
7.039
7.034
7.028
5.332
5.322
5.311
3.670
3.654
3.639
2.030
2.019
2.014
2.003
1.724
1.708
1.701
1.696
1.683
1.674
1.660
1.647
1.597
1.584
1.573
1.560
1.543
1.538
1.385
1.362
1.298
1.016
1.002
0.986
0.978
0.908
0.891
0.874
-0.000

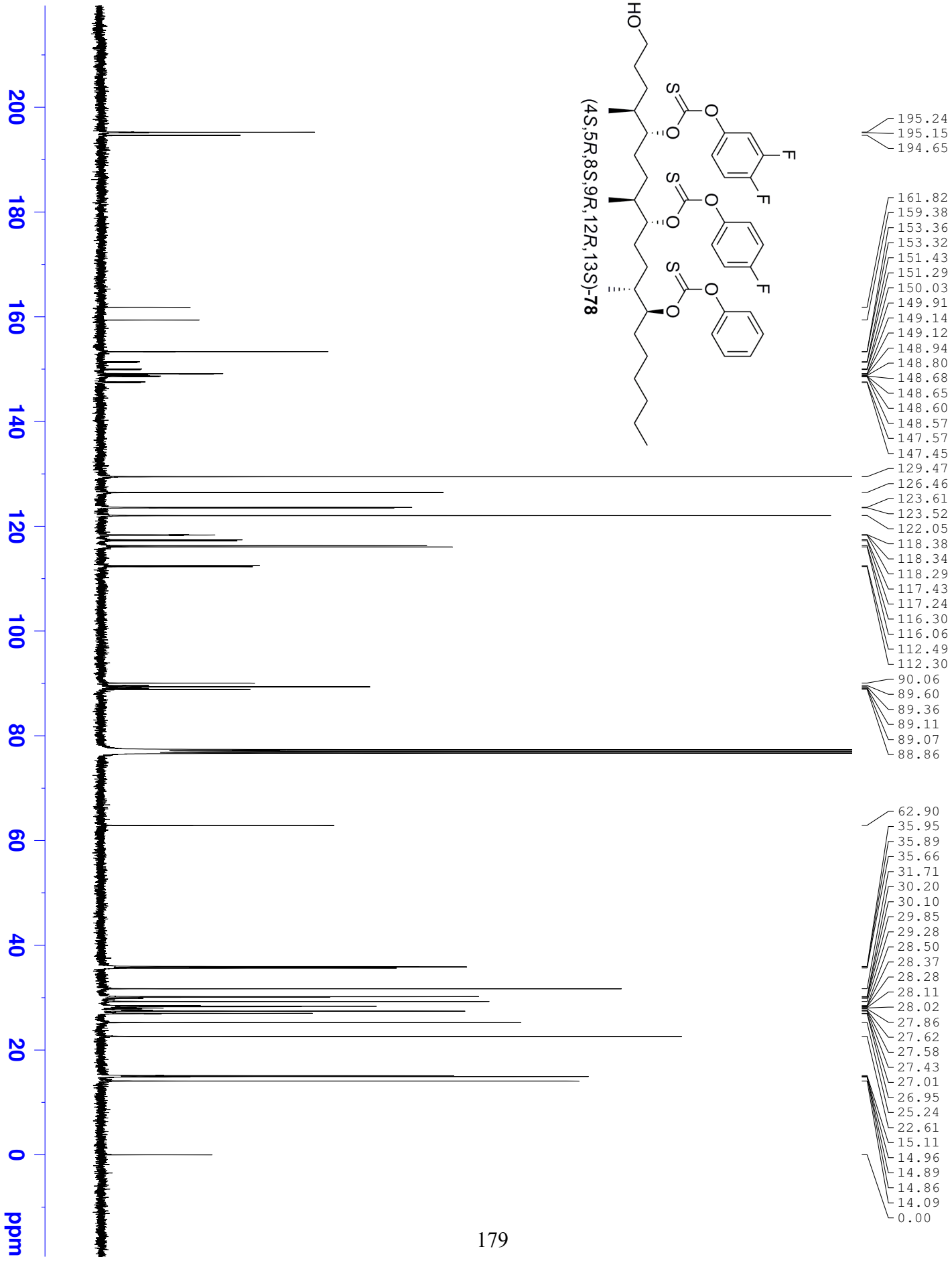
200
180
160
140
120
100
80
60
40
20
0
ppm
HO
S
O
F
(4S,5R,8S,9R,12R,13S)-78
195.24
195.15
194.65
161.82
159.38
153.36
153.32
151.43
151.29
150.03
149.91
149.14
149.12
148.94
148.80
148.68
148.65
148.60
148.57
147.57
147.45
129.47
126.46
123.61
123.52
122.05
118.38
118.34
118.29
117.43
117.24
116.30
116.06
112.49
112.30
90.06
89.60
89.36
89.11
89.07
88.86
62.90
35.95
35.89
35.66
31.71
30.20
30.10
29.85
29.28
28.50
28.37
28.28
28.11
28.02
27.86
27.62
27.58
27.43
27.01
26.95
25.24
22.61
15.11
14.96
14.89
14.86
14.09
0.00

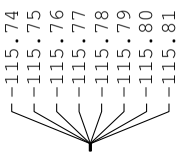

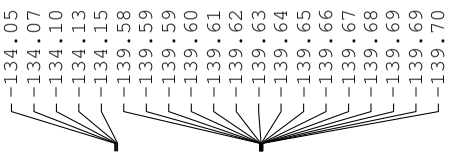

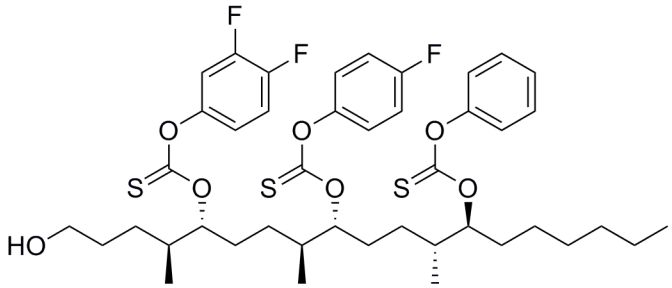

(4*S*,5*R*,8*S*,9*R*,12*R*,13*S*)-**78**

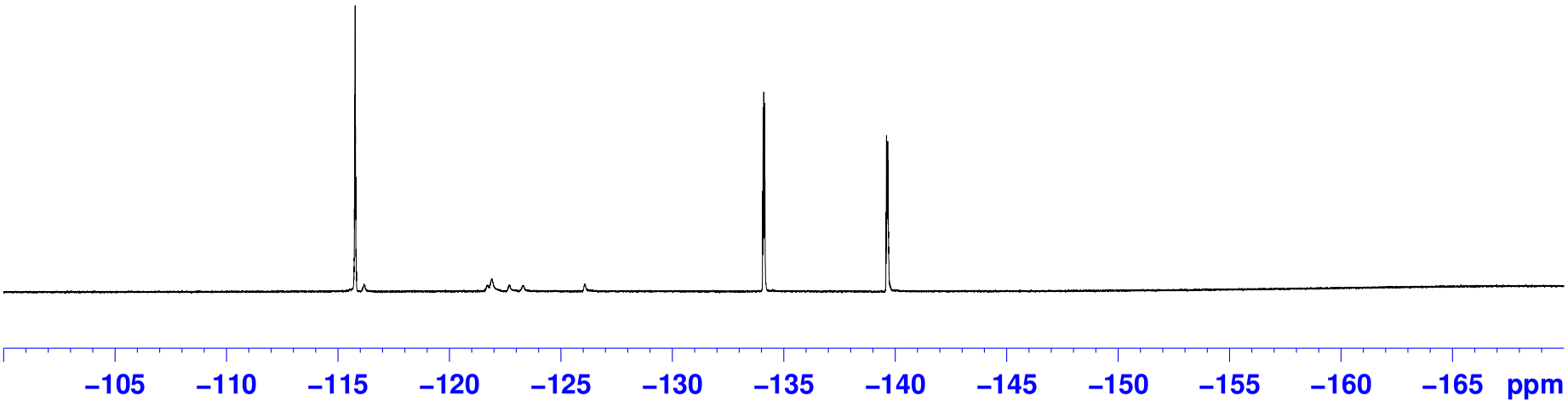

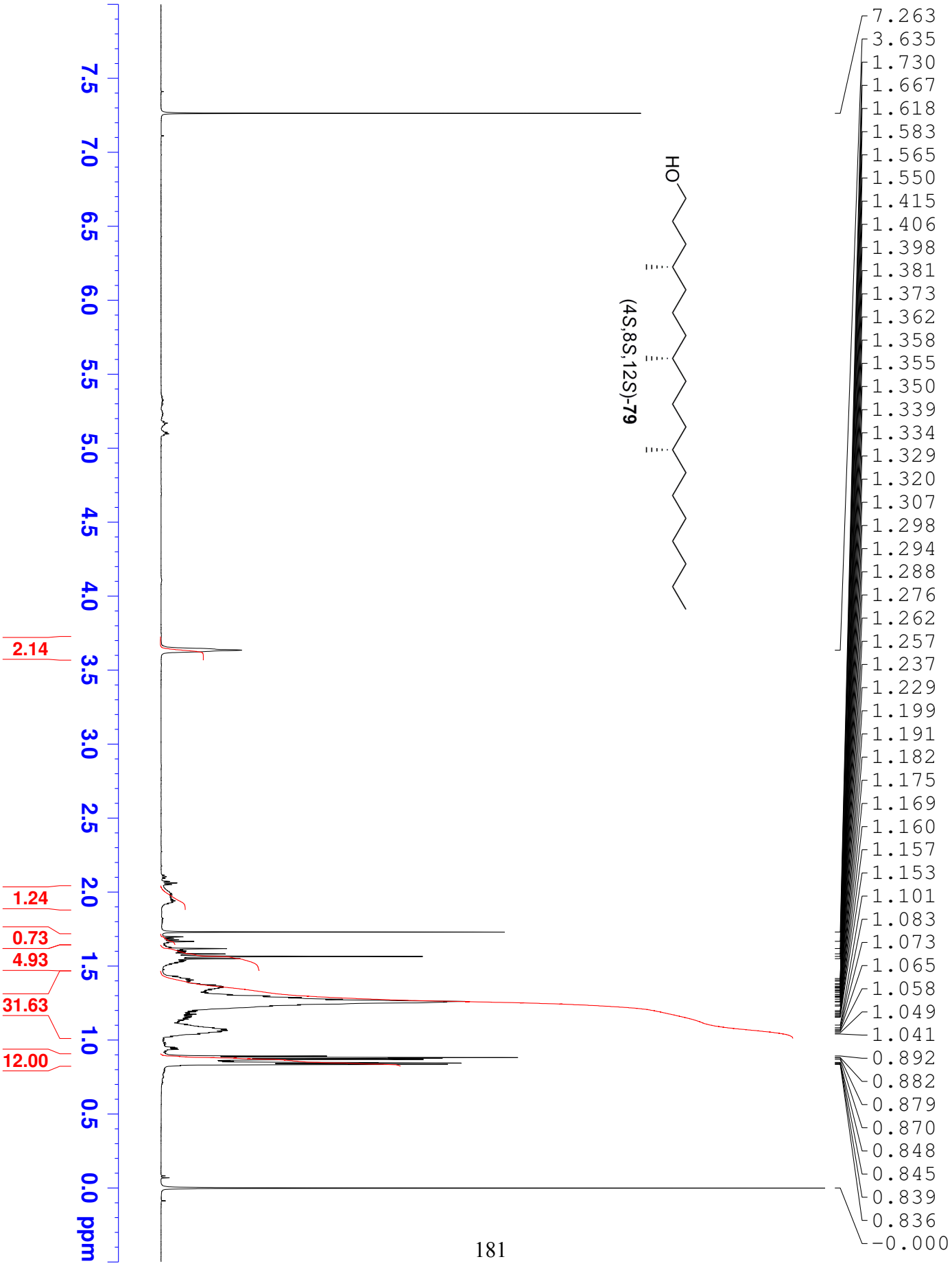
HO
(4S,8S,12S)-79
7.263
3.635
1.730
1.667
1.618
1.583
1.565
1.550
1.415
1.406
1.398
1.381
1.373
1.362
1.358
1.355
1.350
1.339
1.334
1.329
1.320
1.307
1.298
1.294
1.288
1.276
1.262
1.257
1.237
1.229
1.199
1.191
1.182
1.175
1.169
1.160
1.157
1.153
1.101
1.083
1.073
1.065
1.058
1.049
1.041
0.892
0.882
0.879
0.870
0.848
0.845
0.839
0.836
-0.000
2.14
1.24
0.73
4.93
31.63
12.00
7.5
7.0
6.5
6.0
5.5
5.0
4.5
4.0
3.5
3.0
2.5
2.0
1.5
1.0
0.5
0.0
ppm

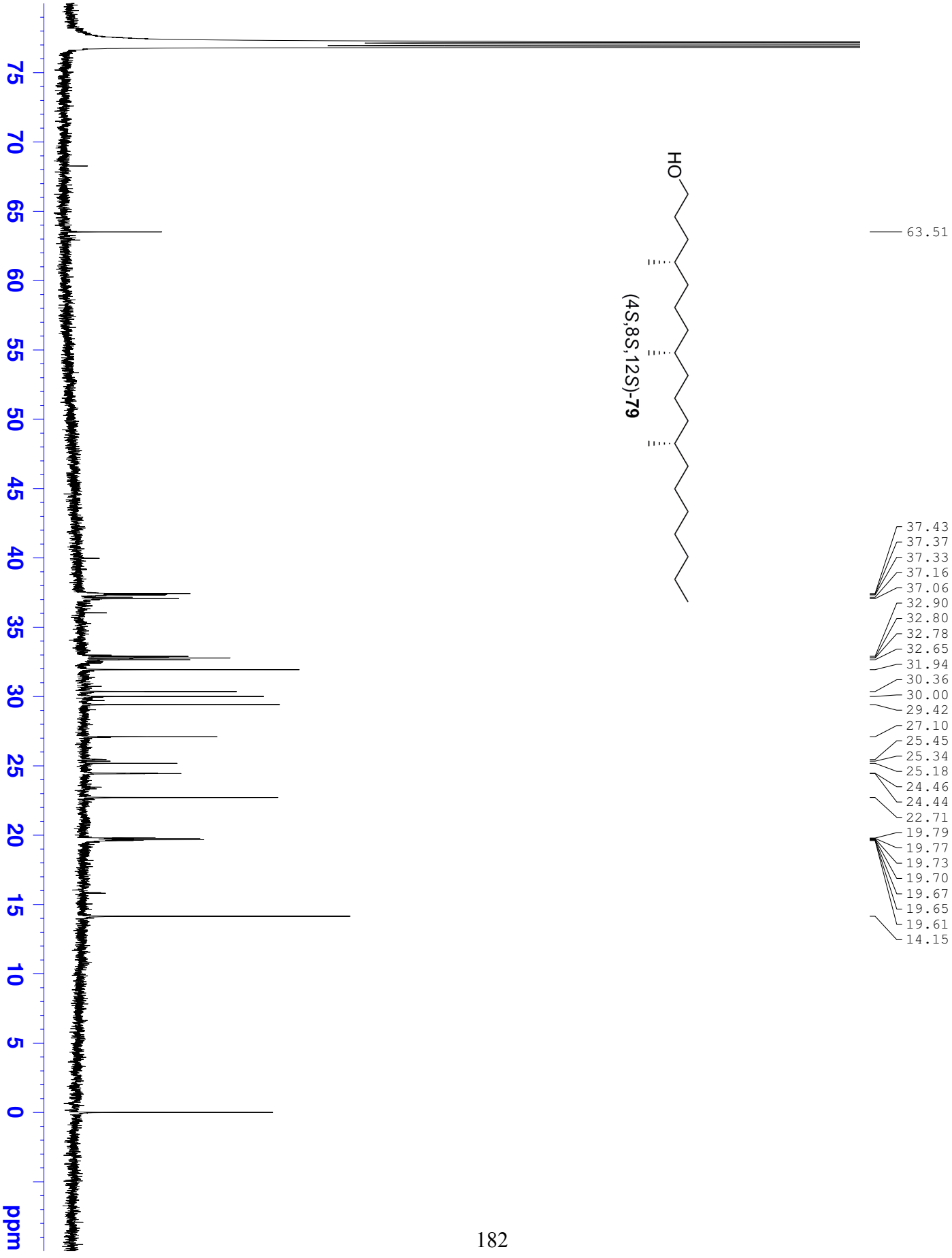
HO
(4S,8S,12S)-79
63.51
37.43
37.37
37.33
37.16
37.06
32.90
32.80
32.78
32.65
31.94
30.36
30.00
29.42
27.10
25.45
25.34
25.18
24.46
24.44
22.71
19.79
19.77
19.73
19.70
19.67
19.65
19.61
14.15
75
70
65
60
55
50
45
40
35
30
25
20
15
10
5
0
ppm

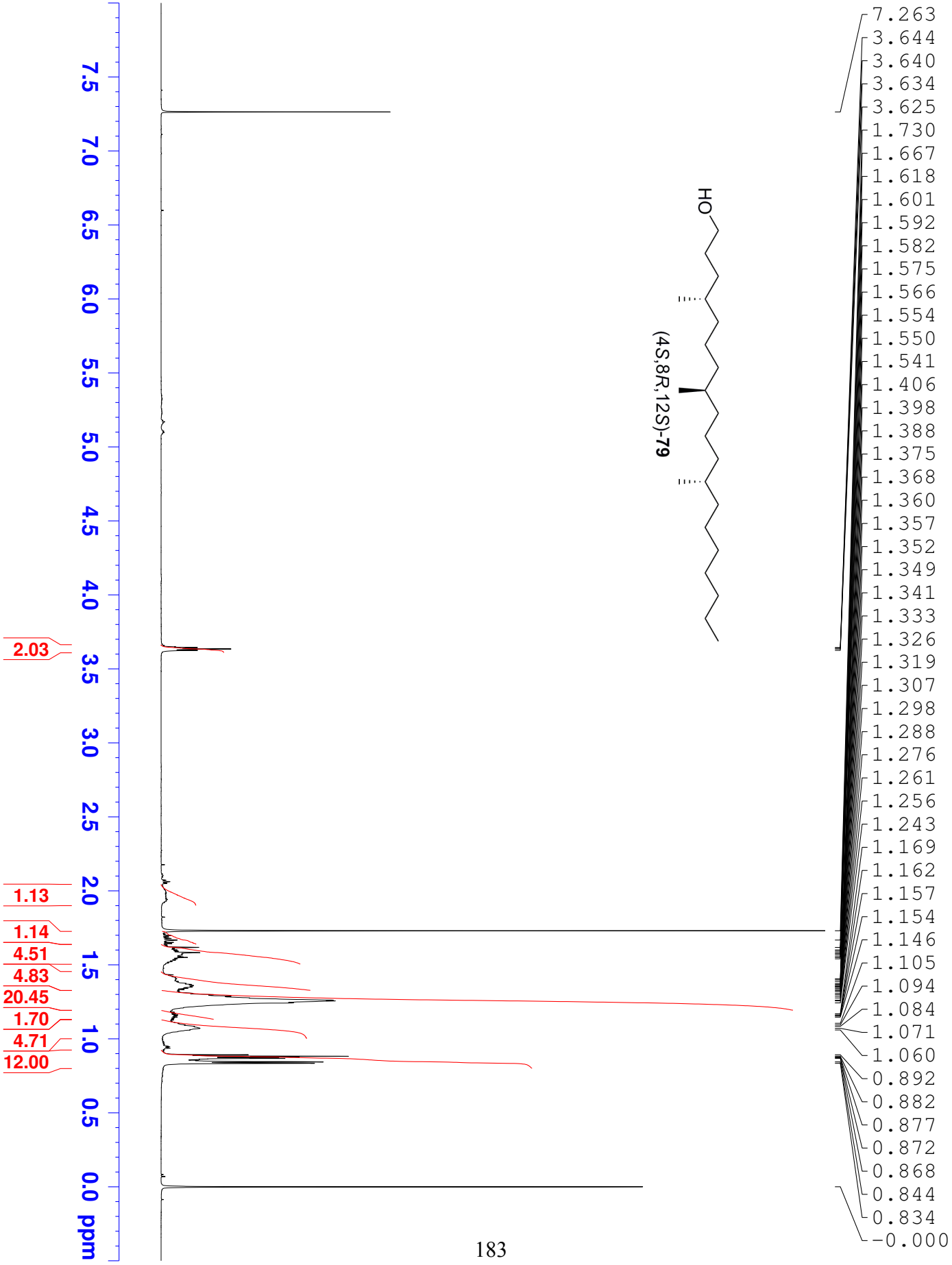
HO
(4S,8R,12S)-79
7.263
3.644
3.640
3.634
3.625
1.730
1.667
1.618
1.601
1.592
1.582
1.575
1.566
1.554
1.550
1.541
1.406
1.398
1.388
1.375
1.368
1.360
1.357
1.352
1.349
1.341
1.333
1.326
1.319
1.307
1.298
1.288
1.276
1.261
1.256
1.243
1.169
1.162
1.157
1.154
1.146
1.105
1.094
1.084
1.071
1.060
0.892
0.882
0.877
0.872
0.868
0.844
0.834
-0.000
2.03
1.13
1.14
4.51
4.83
20.45
1.70
4.71
12.00
7.5
7.0
6.5
6.0
5.5
5.0
4.5
4.0
3.5
3.0
2.5
2.0
1.5
1.0
0.5
0.0
ppm

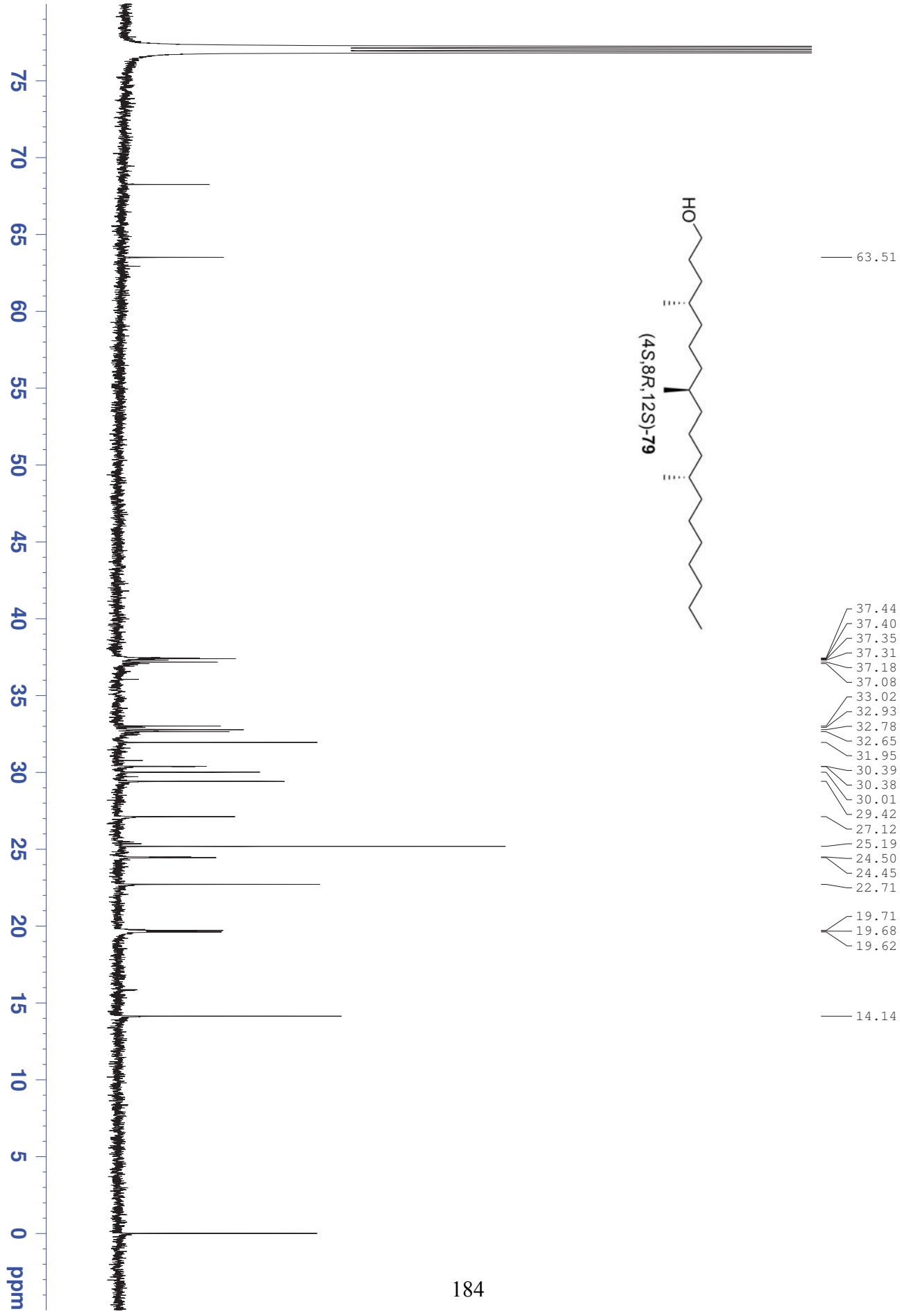
75
70
65
60
55
50
45
40
35
30
25
20
15
10
5
0
ppm
HO
(4S,8R,12S)-79
63.51
37.44
37.40
37.35
37.31
37.18
37.08
33.02
32.93
32.78
32.65
31.95
30.39
30.38
30.01
29.42
27.12
25.19
24.50
24.45
22.71
19.71
19.68
19.62
14.14

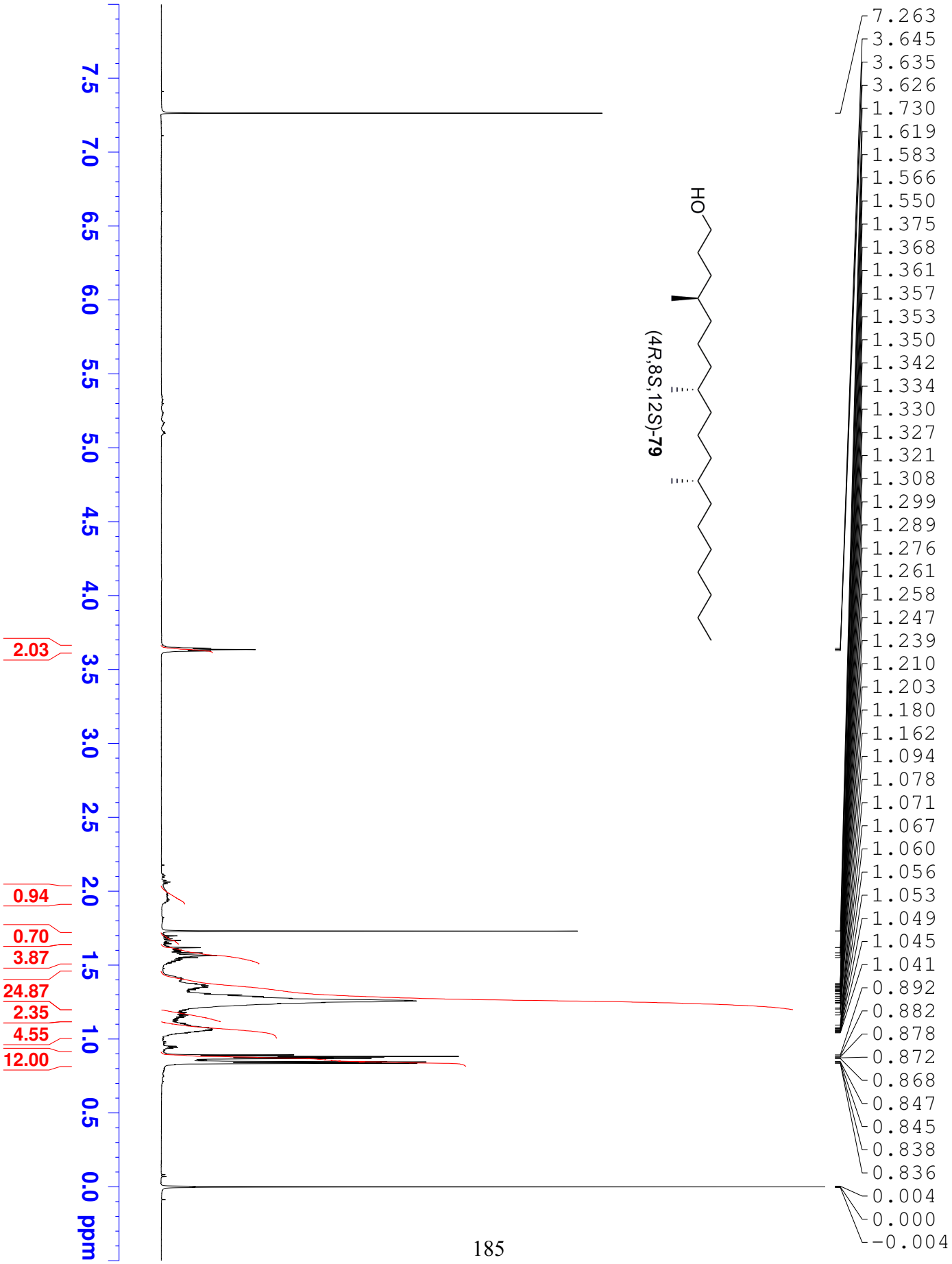
7.263
3.645
3.635
3.626
1.730
1.619
1.583
1.566
1.550
1.375
1.368
1.361
1.357
1.353
1.350
1.342
1.334
1.330
1.327
1.321
1.308
1.299
1.289
1.276
1.261
1.258
1.247
1.239
1.210
1.203
1.180
1.162
1.094
1.078
1.071
1.067
1.060
1.056
1.053
1.049
1.045
1.041
0.892
0.882
0.878
0.872
0.868
0.847
0.845
0.838
0.836
0.004
0.000
-0.004
HO
(4R,8S,12S)-79
2.03
0.94
0.70
3.87
24.87
2.35
4.55
12.00
7.5
7.0
6.5
6.0
5.5
5.0
4.5
4.0
3.5
3.0
2.5
2.0
1.5
1.0
0.5
0.0
ppm

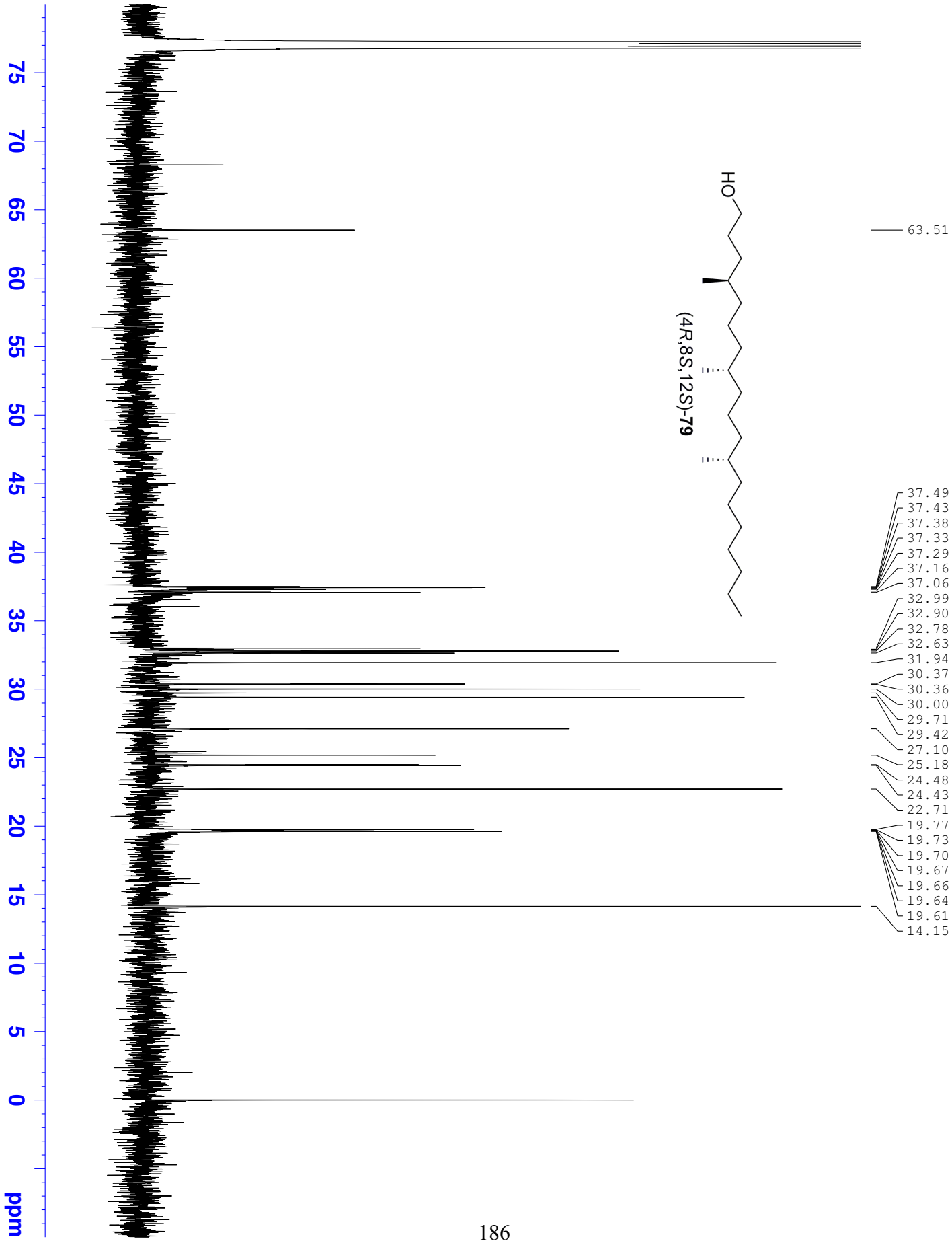
HO
(4R,8S,12S)-79
63.51
37.49
37.43
37.38
37.33
37.29
37.16
37.06
32.99
32.90
32.78
32.63
31.94
30.37
30.36
30.00
29.71
29.42
27.10
25.18
24.48
24.43
22.71
19.77
19.73
19.70
19.67
19.66
19.64
19.61
14.15
75
70
65
60
55
50
45
40
35
30
25
20
15
10
5
0
ppm

HO
(4R,8R,12S)-79
7.262
3.634
1.728
1.667
1.618
1.602
1.593
1.583
1.556
1.549
1.539
1.531
1.416
1.407
1.398
1.381
1.374
1.363
1.358
1.350
1.342
1.335
1.327
1.320
1.308
1.299
1.289
1.277
1.262
1.257
1.219
1.195
1.178
1.170
1.166
1.159
1.155
1.151
1.147
1.143
1.109
1.078
1.071
1.061
1.050
0.892
0.882
0.879
0.871
0.865
0.854
0.845
0.836
0.000
2.07
1.23
0.68
6.05
25.32
1.80
4.57
12.00
7.5
7.0
6.5
6.0
5.5
5.0
4.5
4.0
3.5
3.0
2.5
2.0
1.5
1.0
0.5
0.0
ppm

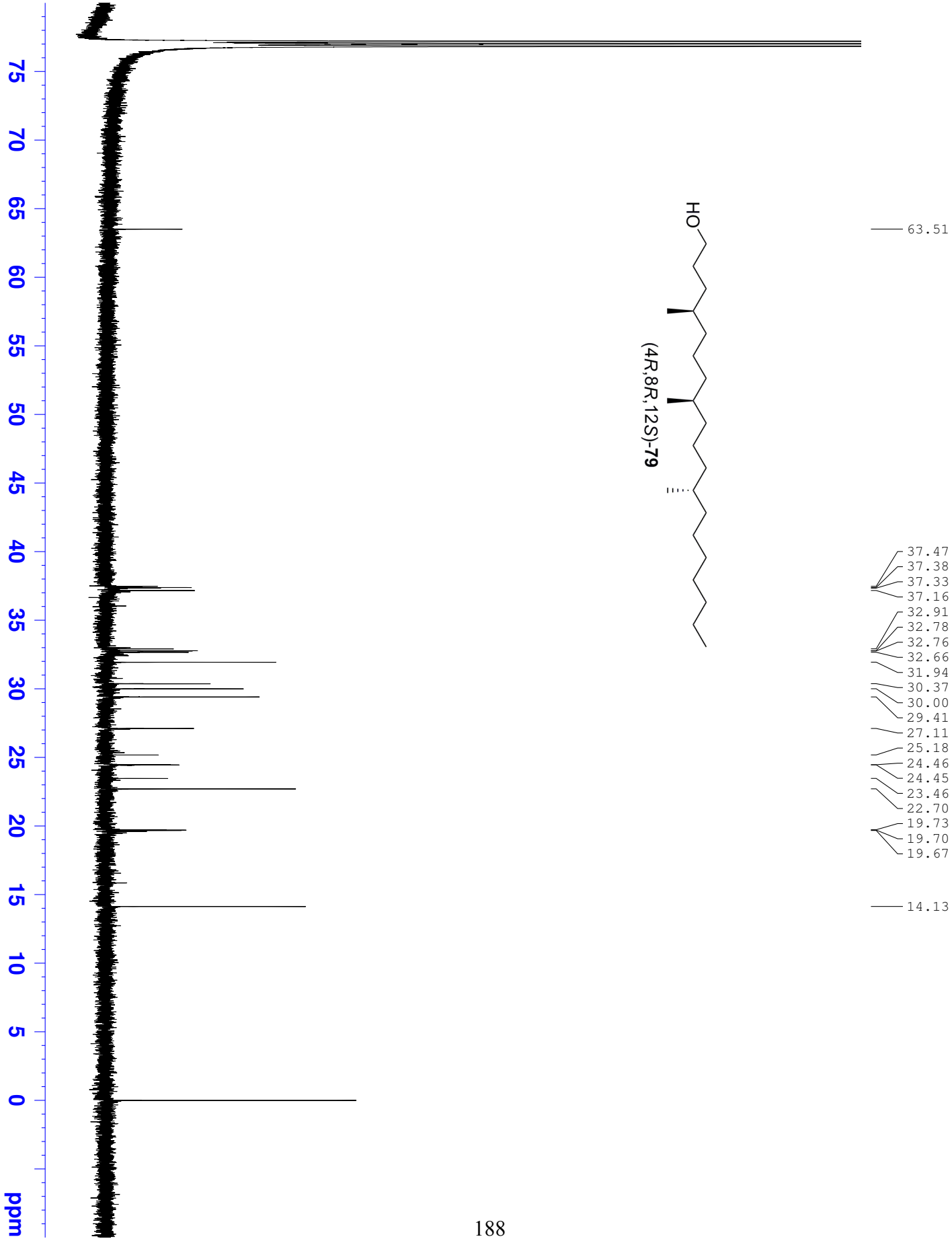
75
70
65
60
55
50
45
40
35
30
25
20
15
10
5
0
ppm
HO
(4R,8R,12S)-79
63.51
37.47
37.38
37.33
37.16
32.91
32.78
32.76
32.66
31.94
30.37
30.00
29.41
27.11
25.18
24.46
24.45
23.46
22.70
19.73
19.70
19.67
14.13

BIBLIOGRAPHY

1. Luo, Z.; Zhang, Q.; Oderaotoshi, Y.; Curran, D. P., Fluorous Mixture Synthesis: A Fluorous-Tagging Strategy for the Synthesis and Separation of Mixtures of Organic Compounds. *Science* **2001**, *291*, 1766-1769.
2. Curran, D. P., Fluorous Chemistry in Pittsburgh: 1996-2008. *J. Fluorine Chem.* **2008**, *129*, 898-902.
3. Euerby, M.; McKeown, A. P.; Petersson, P., Chromatographic Classification and Comparison of Commercially Available Perfluorinated Stationary Phases for Reverse-Phase Liquid Chromatography using Principle Component analysis. *J. Sep. Sci* **2003**, *26*, 295-306.
4. Berendsen, G. E.; Pikaart, K. A.; de Galan, L.; Olieman, C., (Heptadecafluorodecyl)-demethylsilyl Bonded Phase for Reversed-Phase Liquid Chromatography. *Anal. Chem.* **1980**, *53*, 1990-1993.
5. Billiet, H. A. H.; Schoenmakers, P. J.; de Galan, L., Retention and Selectivity Characteristics of a Non-Polar Perfluorinated Stationary Phase for Liquid Chromatography. *J. Chrom.* **1981**, *218*, 443-454.
6. Josien, H.; Ko, S.-B.; Bom, D.; Curran, D. P., A General synthetic Approach to the (20*S*)-Camptothecin Family of Antitumor Agents by a Regiocontrolled Cascade Radical Cyclization of Aryl isonitriles. *Chem. Eur. J* **1998**, *4* (67-83).
7. (a) Yang, F.; Newsome, J. J.; Curran, D. P., Structure Assignment of Lagunapyrone B by Fluorous Mixture Synthesis of Four Candidate Stereoisomers. *J. Am. Chem. Soc.* **2006**, *128*, 14200-14205; (b) Wilcox, C. S.; Gudipati, V.; Lu, H.; Turkyilmaz, S.; Curran, D. P., Solution-Phase Mixture Synthesis with Double Separation Tagging: Double Demixing of a Single Mixture Provides a Stereoisomer Library of 16 Individual Murisolins. *Angew. Chem. Int. Ed.* **2005**, *44*, 6938-6940; (c) Curran, D. P.; Zhang, Q.; Richard, C.; Lu, H.; Gudipati, V.; Wilcox, C. S., Total Synthesis of a 28-Member Stereoisomer Library of Murisolins. *J. Am. Chem. Soc.* **2006**, *128*, 9561-9578; (d) Curran, D. P.; Moura-Lett, G.; Pohlman, M., Solution-Phase Mixture synthesis with Fluorous Tagging En Route: Total Synthesis of an Eight Member stereoisomer Libraryof Passifloricins. *Angew. Chem. Int. Ed.* **2006**, *45*, 2423-2426.
8. Dandapani, S.; Jeske, M.; Curran, D. P., Synthesis of All 16 Stereoisomers of Pinesaw Fly Sex Pheromones-Tools and Tactics for Solving Problems in Fluorous Mixture Synthesis. *J. Org. Chem.* **2005**, *70*, 9447-9462.
9. (a) Curran, D. P.; Sinha, M. K.; Zhang, K.; Sabatini, J. J.; Cho, D.-H., Binary Fluorous Tagging: Fluorous Mixture Synthesis of a Sixteen Stereoisomer Library of Macrosphelides A and E and Correction of the Structure of Macrosphelide D. *Nature Chem.* **2011**; (b) Sui, B.; Yeh, E. A.-H.; Curran, D. P., Assigment of the Structure of Petrocortyne a by Mixture Syntheses of

Four Candidate Stereoisomers. *J. Org. Chem.* **2010**, *75*, 2942-2954; (c) Moretti, J.; Wang, X.; Curran, D. P., SCH725674. **2012**.
10. Jung, W.-H.; Guyenne, S.; Riesco-Fagundo, C.; Mancuso, J.; Nakamura, S.; Curran, D. P., Confirmation of the Stereostructure of (+)-Cytostatin by Fluorous Mixture Synthesis of Four Candidate Stereoisomers. *Angew. Chem. Int. Ed.* **2008**, *47*, 1130-1133.
11. Wilcox, C. S.; Turkyilmaz, S., Oligomeric Ethylene Glycols as Sorting Tags for Parallel and Combinatorial Mixture Synthesis. *Tetrahedron Lett* **2005**, *46*, 1827-1829.
12. Gladysz, J. A.; Curran, D. P.; Horvath, I. T., *Handbook of Fluorous Chemistry*. Wiley-VCH: 2004.
13. (a) Nakamura, Y.; Mori, K., Pheromone Synthesis, CXCVIII Synthesis of (1*S*,2*S*,6*S*,10*R*)- and (1*S*,2*R*,6*R*,10*R*)-1,2,6,10-Tetramethyldodecyl Propanoate, the Components of the Sex Pheromone of the Pine Sawfly. *Eur. J. Org. Chem.* **1999**, 2175-2182; (b) Dowd, P.; Hershline, R.; Ham, S. W.; Naganathan, S., Mechanism of Action of Vitamin K. *Nat. Prod. Rep.* **1994**, *11*, 251-264; (c) Holt, A. A.; Morley, H. V., A Proposed Structure for Chlorophyll-*d*. *Can. J. Chem.* **1959**, *37*, 507-514; (d) Moody, D. B.; Ulrichs, T.; Muhlecker, W.; Ypung, D. C.; Gurcha, S. S.; Grant, E.; Rosat, J.-P.; Brenner, M. B.; Costello, C. E.; Bersa, G. S.; Porcelli, S. A., CD1c-Mediated T-cell Recognition of Isoprenoid Glycolipid in *Mycobacterium tuberculosis* Infection. *Nature* **2000**, *404*, 884-888; (e) Bergel, F.; Jacob, A.; Todd, A. R.; Work, T. S., Studies on Vitamin E. Part IV. Synthetic Experiments in the Coumaran and Chroman Series. The Structure of the Tocopherols. *J. Chem. Soc.* **1938**, 1375-1382.
14. Hofius, D.; Sonnewald, U., Vitamin E Biosynthesis: Biochemistry Meets Cell Biology. *Trends Plant Sci* **2003**, *8*, 6-8.
15. Huo, S.; Negishi, E.-I., A Convenient and Asymmetric Protocol for the Synthesis of Natural Products Containing Chiral Alkyl Chains via Zr-Catalyzed Asymmetric Carboalumnination of Alkenes. Synthesis of Phytol and Vitamins E and K. *Org. Lett.* **2001**, *3*, 3253-3256.
16. (a) Still, W. C.; Darst, K. P., Remote Asymmetric Induction. A Stereoselective Approach to Acyclic Diols via Cyclic Hydroboration. *J. Am. Chem. Soc.* **1980**, *102*, 7385-7387; (b) Cohen, N.; Scott, C. G.; Neukom, C.; Lopresti, R. J.; Weber, G.; Saucy, G., Total synthesis of All Eight Stereoisomers of α-Tocopheryl Acetate. Determination of Their Diastereoisomeric and Enantiomeric Purity by Gas Chromatography. *Helv. Chim. Acta* **1981**, *64*, 1158-1173.
17. Cohen, N.; Lopresti, R. J.; Neukom, C., Studies on the Total Synthesis of (2*R*,4'*R*,8'*R*)-α-Tocopherol (Vitamin E). Stereospecific Cyclizations Leading to Optically Active Chromans. *J. Org. Chem.* **1981**, *46*, 2445-2450.
18. Bonrath, W.; Netscher, T., Catalytic Processes in Vitamin Synthesis and Production. *Appl. Catal., A* **2005**, *280*, 55-73.
19. (a) Brownstein, S.; Burton, G. W.; Hughes, L.; Ingold, K. U., Chiral Effects on the ^{13}C Resonances of α-Tocopherol and Related Compounds. a Novel Illustration of Newman's "Rule of Six". *J. Org. Chem.* **1989**, *54*, 560-569; (b) Matsuo, M.; Urano, S., ^{13}C NMR Spectra of Tocopherols and 2,2-Dimethylchromanols. *Tetrahedron* **1975**, *32*, 229-231; (c) Goodman, R. A.; Oldfield, E.; Allerhand, A., Assignments in the Natural-Abundance Carbon-13 Nuclear Magnetic Resonance Spectrum of Chlorophyll a and a Study of Segmental Motion in Neat Phytol. *J. Am. Chem. Soc.* **1973**, *95*, 7553-7558.
20. Bremer, W.; Vogel, F. G. M., Determination of the Enantiomeric Purity of α-Tocopherol by ^{13}C NMR Spectroscopy. *Org. Magn. Res.* **1980**, *14*, 155-156.

21. Zhang, T.; Zhang, Y. Z.; Tao, J. S., Antibacterial Constituents from *Stemona sessilifolia*. *J. Asian Nat. Prod. Res* **2007**, *9*,479-485.
22. Crich, D.; Dudkin, V., Efficient, Diastereoselective chemical synthesis of a *β*-Mannopyranosyl Phosphoisoprenoid. *Org. Lett.* **2000**, *2*, 3941-3943.
23. Moody, D. B.; Besra, G. S.; Wilson, I. A.; Prorcelli, S. A., The Molecular Basis of CD1-Mediated Presentation of Lipid Antigens. *Immuno. Rev.* **1999**, *172*, 285-296.
24. Matsunaga, I.; Bhatt, A.; Young, D. C.; Cheng, T. Y.; Eyles, S. J.; Besra, G. S.; Briken, V.; Porcelli, S. A.; Costello, C. E.; Jacobs, W. R. J.; Moody, D. B., Mycobacterium tuberculosis pks 12 Produces a Novel Polyketide Presented by CD1c to T-cells. *J. Exp. Med.* **2004**, *200*, 1559-1569.
25. van Summeren, R. P.; Moody, D. B.; Feringa, B. L.; Minnaard, A. J., Total Synthesis of Enantiopure *β*-D-Mannosyl Phosphomycoketides from *Mycobacterium tuberculosis*. *J. Am. Chem. Soc.* **2006**, *128*, 4546-4547.
26. Des Mazery, R.; Pullez, M.; Lopez, F.; Harutyunyan, S. R.; Minnaard, A. J.; Feringa, B. L., An Iterative Catalytic Route to Enantiopure deoxypropionate Subunits: Asymmetric conjugate Addition of Grignard Reagents to *α,β*-Unsaturated Thioesters. *J. Am. Chem. Soc.* **2005**, *127*, 9966-9967.
27. Blackmore, P. R.; Cole, W. J.; Kocienski, P. J.; Morley, A., A Stereoselective Synthesis of *trans*-1,2-Disubstituted Alkenes Based on the Condensation of Aldehyde with Metallated 1-Phenyl-1*H*-tetrazol-5-yl Sulfones. *Synlett* **1998**, 26-28.
28. Scharf, L.; Li, N.-S.; Hawk, A. J.; Garzon, D.; Zhang, T.; Fox, L. M.; Kazen, A. R.; Shah, S.; Haddadian, E. J.; Gumperz, J. E.; Saghatelian, A.; Faraldo-Gomez, J. D.; Meredith, S. C.; Piccirilli, J. A.; Adams, E. J., The 2.5 A Structure of CD1c in Complex with a Mycobacterial Lipid REveals an Open Groove Idealy Suited for Diverse Antigen Presentation. *Immunity* **2010**, *33*, 853-862.
29. de Jong, A.; Arce, E. C.; Cheng, T. Y.; van Summeren, R. P.; Feringa, B. L.; Dudkin, V.; Crich, D.; Matsunaga, I.; Minnaard, A. J.; Moody, D. B., CD1c Presentation of Synthetic Glycolipid Antigens with Foreign Alkyl Branching Motifs. *Chem. Biol.* **2007**, *14*, 1232-1242.
30. Kumli, E., Postdoctoral Report (unpublished). **2009**.
31. Brown, H. C.; Bhat, K. S., Enantiomeric (*Z*)- and (*E*)-Crotyldiisopinocampheylboranes. Synthesis an High Optical Purity of All Four Possible Stereoisomers of *β*-Methylhomoallyl Alcohols. *J. Am. Chem. Soc.* **1986**, *108*, 293-294.
32. Chatterjee, A. K.; Choi, T.-L.; Sanders, D. P.; Grubbs, R. H., A General Model for Selectivity in Olefin Cross Metathesis. *J. Am. Chem. Soc.* **2003**, *125*, 11360-11370.
33. (a) Tschugaeff, L., Ueber das Thujen, ein neues bicyclisches Terpen. *Ber. Dtsch. Chem. Ges.* **1990,** *33*, 3118-3126; (b) Paquette, L. A.; Roberts, R. A.; Drtina, G. J., Total Synthesis of (-)-Silphiperfol-6-ene and (-)-5-Oxosilphiperfol-6-ene. *J. Am. Chem. Soc.* **1984**, *106*, 6690-6693.
34. Krishnamurthy, S., Rapid Reduction of Alkyl Tosylates with Lithium Triethylborohydride. A Convenient and Advantageous Procedure for the Deoxygenation of Simple and Hindered Alcohols. Comparison of Various Hydride Reagents. *J. Organometal. Chem.* **1978**, *156*, 171-181.
35. Robins, M. J.; Wilson, J. S., Smooth and Efficient Deoxygenation of Secondary Alcohols. A General Procedure for the Conversion of Ribonucleosides to 2'-Deoxynucleosides *J. Am. Chem. Soc.* **1980**, *103*, 932-933.
36. Barton, D. H. R.; McCombie, S. W., A New Method for the Deoxygenation of Secondary Alcohols. *J. chem. Soc. Perkin Trans. I* **1975**, 1574-1585.

37. Roush, W. R.; Ando, K.; Powers, D. B.; Palkowitz, A. D.; Halterman, R. L., Asymmetric Synthesis Using Diisopropyl Tartrate Modified (*E*)- and (*Z*)-Crotylboronates: Preparation of the Chiral Crotylboronates and Reactions with Achiral Aldehydes. *J. Am. Chem. Soc.* **1990**, *112*, 6339-6348.
38. Hoye, T. R.; Jeffrey, C. S.; Shao, F., Mosher Ester Analysis for the Determination of Absolute Configuration of Stereogenic (Chiral) Carbinol Carbons. *Nat. Proto.* **2007**, *2*, 2451-2458.
39. Breit, B.; Seiche, W., Hydrogen Bonding as a Construction element for Bidentate Donor Ligands in Homogeneous Catalysis: Regioselective Hydroformylation of Terminal alkenes. *J. Am. Chem. Soc.* **2003**, *125*, 6608-6609.
40. Le Stang, S.; Meier, R.; Rocaboy, C.; Gladysz, J. A., Convenient Syntheses of Fluorous Phenol of the Formula $HOC_6H_{5-n}((CH_2)_3(CF_2)_7CF_3)_n$ (n = 1, 2) and the Corresponding Triarylphosphites. *J. Fluorine Chem.* **2003**, *119*, 141-149.
41. Ueng, S.-H.; Fensterbank, L.; Lacote, E.; Malacria, M.; Curran, D. P., Radical Deoxygenation of Xanthates and Related Functional Groups with New Minimalist N-Heterocyclic Carbene Boranes. *Org. Lett.* **2010**, *12*, 3002-3005.
42. Traficante, D. D.; Nemeth, G. A., A New and Improved Apodization Function for Resolution Enhancement in NMR Spectroscopy. *J. Magn. Res.* **1986**, *71*, 237-245.
43. Pangborn, A. B.; Giardello, M. A.; Grubbs, R. H.; Rosen, R. K.; Timmers, F. J., Safe and Convenient Procedure for Solvent Purification. *Organometallics* **1996**, *15*, 1518-1520.